Personalizing Anti-Cancer Treatment from Genetic and Pharmacokinetic Perspective

Het personaliseren van de behandeling tegen kanker vanuit genetisch en farmacokinetisch oogpunt

Sander Bins

Personalizing Anti-Cancer Treatment from Genetic and Pharmacokinetic Perspective

Het personaliseren van de behandeling tegen kanker vanuit genetisch en farmacokinetisch

oogpunt

Proefschrift

ter verkrijging van de graad van doctor aan de

Erasmus Universiteit Rotterdam

op gezag van de

rector magnificus

Prof.dr. H.A.P. Pols

en volgens besluit van het College voor Promoties.

De openbare verdediging zal plaatsvinden op

Woensdag 15 februari 2017 om 13.30 uur

Sander Bins

geboren te *Voorburg*

Erasmus University Rotterdam

Promotiecommissie

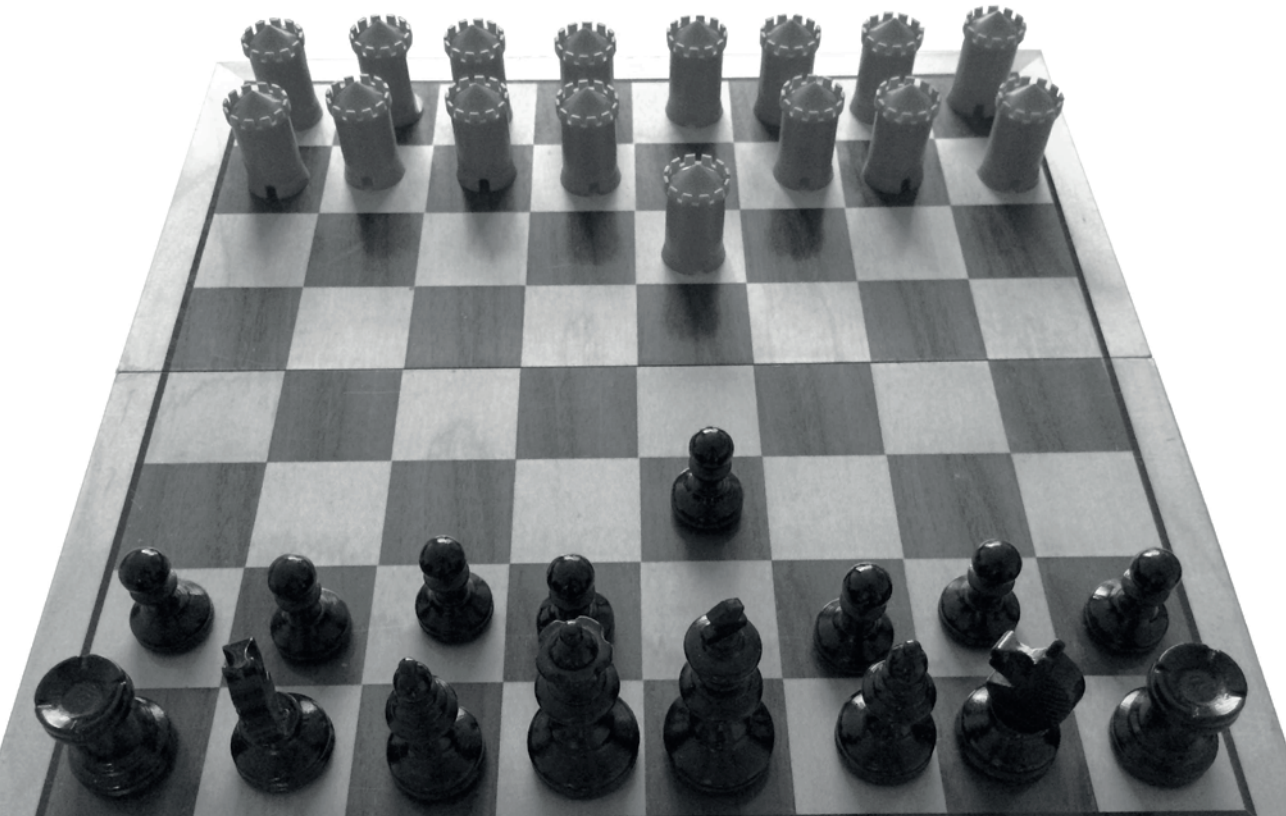|	
Promotoren:	Prof.dr. S. Sleijfer
	Prof.dr. A.H.J. Mathijssen
Overige leden:	Prof.dr. R.H.N. van Schaik
	Prof.dr. A.D.R. Huitema
	Prof.dr. E.E. Voest

Hoe verder men keek,
hoe groter het leek.
J.A. Deelder

# Contents

CHAPTER 1

Introduction

Cancer treatment has been subject of discussion for centuries. Surgery was already practiced (unsuccessfully) back in ancient Egypt,[1] but until recent ages every type of cancer was deemed incurable, if detected at all. Whereas methods of surgery and radiotherapy were evolving in a revolutionary way during the 19th and early 20th century, systemic anti-cancer treatment only found its way into the clinic in the second half of the previous century. After World War I, the myelotoxic effect of mustard gas was noticed and translated into the first chemotherapy: nitrogen mustard.[2] Since then, many other systemic anti-cancer agents have been developed for the treatment of many different types of cancer. The first group of patients that benefited from systemic anti-cancer treatment were those with hematological cancers. Nowadays, many leukemia and lymphoma patients can even be cured by systemic treatment sometimes combined with radiotherapy. However, except for patients with germline tumors and for the use in adjuvant or neoadjuvant setting, systemic therapies still rarely cure patients with solid tumors. This indicates that, despite all progress that has been made, there is much to win in this field of medicine.

Although there is still much to be learned, the biological behavior of tumors has been scrutinized in parallel to the advent of chemotherapy. Since the 1950s, many researchers have examined cancer cells and have – successfully – found ways to stop these cells from proliferating. One of the earliest examples of the translation of increasing biological understanding into anti-cancer drugs is the group of fluoropyrimidines.[3] Basic research had shown that rat hepatoma cells take up much more uracil than other (healthy) tissue. By attaching the toxic atom fluorine to an uracil base, resulting in 5-fluorouracil (5-FU), the cytostatic effects of this drug are predominantly, but not exclusively, localized in cancer cells. Despite its age, 5-FU is currently still standard of care for the treatment of several cancer types.

Accordingly, the increasing biological knowledge has led to the discovery of many other ways to kill cancer cells. Hormones appeared to stimulate cancer cell growth, which could be stopped by inhibiting this hormonal signaling, e.g. with the famous selective estrogen receptor modulator tamoxifen. Similarly, many other (non-hormonal) signaling pathways have been identified. Currently, a number of genes have been described that, when mutated or overexpressed, cause either activation of proliferative signaling (proto-

oncogenes) or inhibition of anti-proliferative signaling (tumor suppressor genes). A schematic description of these processes is depicted in **Figure 1**.
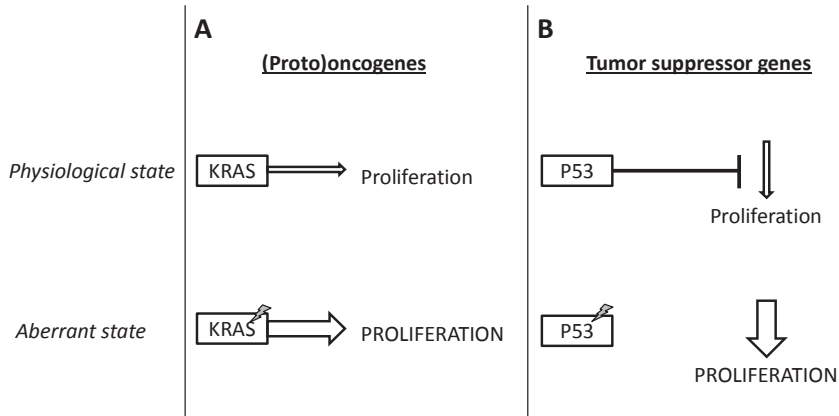
Figure 1. *A schematic depiction of oncogenes and tumor suppressor genes. (**A**) Proto-oncogenes are physiologically involved in the normal process of cell cycle regulation. Mutated proto-oncogenes can become oncogenes and become constitutively activated, which leads to continuous proliferative signaling. (**B**) Tumor suppressor genes are physiologically involved in suppressing cell proliferation. When mutated, they can lose their suppressive function, which leads to increased proliferative signaling.*

Just as for the anti-hormonal agents, drugs are being developed to specifically target these aberrant proliferative signals. This has resulted broad spectrum of targeted anti-cancer drugs with different mechanisms of decreasing intracellular signaling: tyrosine kinase inhibitors (TKIs) prevent the phosphorylation of intracellular proteins, monoclonal antibodies (mABs) target extracellular receptors that initiate the intracellular signaling, and there are many other examples such as drugs that inhibit mammalian target of rapamycin (mTOR-inhibitors).

Precision Medicine

The first – and still the most impressive – example of a targeted anti-cancer agent is the TKI imatinib. In 1996, imatinib was found to inhibit the growth of chronic myelogenous leukemia (CML) cells that contained the *BCR-ABL* translocation.[4] Patients with *BCR-ABL-*

positive leukemia now have considerably increased chances of long term survival: 83% of patient remains recurrence-free after 5 years of systemic treatment.[5] Similarly, patients with gastrointestinal stromal tumors (GIST) that harbor a mutation in a specific proto-oncogene, *KIT*, live substantially longer when treated with imatinib (median overall survival (OS) > 50 months)[6] than when treated with conventional chemotherapy (median OS in doxorubicin treated patients was only 9 months).[7] For decades, cancers were categorized by their histological features. Recently, however, insight into the biology of cancer (which stimuli cause cancer cells to proliferate) has increased rapidly.[8, 9] Many tumors appear to exhibit unrestrained proliferative signaling, initiated by a "driver" mutation. Following the example of imatinib, these proliferative signals are being targeted by the increasing number of available targeted agents. By complementing cancer diagnostics with molecular tumor cell characteristics, such as the presence of (potential) driver mutations, systemic treatment can be allocated much more specific to the patients that truly benefit from it. This specification of the diagnostic process is referred to as "precision medicine" or as "personalized medicine." With a rapidly growing number of drugs to target the proliferative signaling pathways, precision medicine is thought to ultimately result in playing chess with cancer: each step cancer makes to proliferate is ideally counteracted by reversing that step with a specific drug. Within that context, the Dutch Center for Personalized Cancer Treatment (CPCT) was formed, in which many oncology centers currently collaborate. The CPCT investigates intratumoral genetic aberrations that are predictive for clinical outcome of existing systemic therapies. Since the molecular characteristics of tumors can change over time (and space),[10] tumor biopsies are obtained from a metastatic lesion, which is likely to represent the most actual – and therefore the most malignant – status of the tumor. Subsequently, the DNA of these tumors is analyzed using next-generation sequencing (NGS) platforms and compared to treatment outcome, i.e. tumor response and survival. Before collecting tumor biopsies on a large scale, safety of the biopsy procedures and feasibility of the DNA extraction should be assured. These aspects are described in **Chapter 2**.

Although the arsenal of available therapies has increased drastically, drugs need to be invented to target newly discovered oncogenic pathways. Originally, phase I trials were designed to assess the safety of drugs during their first clinical application, and to

identify the optimal dose for further study in phase II and III setting. The early phase clinical research, however, is also subject to the era of precision medicine and patient stratification is increasingly being based upon molecular profile of the tumor, even in phase I studies where safety is the primary endpoint.[11] That way, endpoints biological mechanisms, such as changes in protein expression or phosphorylation, can already be integrated in this setting in order to optimize the efficiency of drug development. Even treatment effect is being assessed earlier during treatment. Since overall survival (OS), the most solid endpoint for treatment effect, will take much longer to investigate than the other phase I endpoints, alternatives are sought to determine treatment effect at an earlier time point. In **Chapter 3**, a cohort of everolimus treated patients was used to investigate if a novel volumetric surrogate endpoint, i.e. the time to progression (TTP) ratio, is a better parameter for detecting clinical benefit in early phase research.

Pharmacokinetics

Treatment effect is not only a matter of hitting the right target. It is equally important to hit the target with sufficient strength. One can envision that (too) low drug concentrations in the systemic circulation may lead to insufficient drug exposure in the tumor and, consequently, to treatment failure. *Vice versa*, (too) high systemic concentrations increase the risk of causing excessive harm to healthy tissue. Currently, for many anti-cancer drugs, especially cytostatic agents, the administered dose is based on body surface area (BSA), which is deduced from a patient's height and weight. The lack of rationale to correct the dose for BSA is described in **Chapter 4**. Over the last years, research has focused increasingly on individual characteristics that influence a patient's exposure to the drug, such as activity of drug metabolizing enzymes and drug transporters. The function of these enzymes and transporters can be influenced by a variety of factors: their function can be inhibited and induced by concomitantly administered drugs ("drug-drug interactions"),[12] by germline genetic polymorphisms in the encoding genes ("pharmacogenetics"),[13] or by more trivial factors such as organ function.[14] When the elimination of a drug is slowed down due to inhibition of an efflux transporter, the drug will accumulate within the systemic circulation and both tumor and healthy tissue will be exposed increasingly to it.

The increased exposure might lead to a better anti-cancer effect, but also to more side effects. *Vice versa*, reduced exposure may cause a drug to be less effective. This illustrates the importance of quantifying the influence that different factors have on drug exposure, especially in drugs with a wide interindividual variability (IIV) in exposure, such as the TKI sorafenib that is used for the treatment of hepatocellular carcinoma (HCC), renal cell carcinoma (RCC) and differentiated thyroid cancer (DTC). Once the individual factors that cause these interindividual differences in pharmacokinetics (PK) are characterized, the dose of sorafenib can be adjusted for those factors. That is another form of precision medicine, by which patients ideally experience optimal anti-cancer effects and suffer as little as possible from the side effects of a drug. Early steps in characterizing the factors that influence sorafenib PK are described in this thesis. In **Chapter 5**, the efflux transporter OATP1B was inhibited – both genetically and chemically – in order to find out if the hepatobiliary efflux of sorafenib's metabolite sorafenib-glucuronide is influenced by this process. Since this study only assessed the pharmacokinetics of this TKI, the clinical effects of OATP1B inhibition were evaluated in **Chapter 6**, where the association between single nucleotide polymorphisms (SNPs) in the genes encoding for OATP1B (*SLCO1B*) and the clinical outcome was tested retrospectively in sorafenib treated patients.

Changes in exposure over time

Drug exposure is not a constant, as many of the factors mentioned above change over time: concomitant medication can be added or stopped during treatment, but also renal or hepatic function can deteriorate. Even without these conditions changing, systemic drug exposure can change over time. Systemic imatinib exposure, for example, decreases by 30% after three months of treatment.[15] At first, this was attributed to decreased imatinib absorption from the intestine due to change in drug transporter activity,[15] but in an alternative explanation it was suggested that decreased inflammatory state would lead to decreased presence of alpha-1 acid glycoprotein (AGP, an acute phase protein to which imatinib binds predominantly in the systemic circulation) and hence would facilitate increased clearance of imatinib.[16] In **Chapter 7**, imatinib treated patients were followed for 1 year after imatinib treatment start in order to prospectively assess the course of AGP

1

concentrations during this period and the correlation between AGP levels and imatinib pharmacokinetics (PK).

Therapeutic drug monitoring (TDM)

Based on the variability in exposure, it has become common to monitor systemic drug concentrations in other fields of medicine, e.g. infectious diseases or psychiatry.[17, 18] If drug concentrations are too low and patients are unlikely to benefit from treatment, the dose can be increased in order to optimize the treatment effect. *Vice versa*, too high drug concentrations might lead to severe toxicity on the long term, which could be prevented by decreasing the dose early during treatment. In oncology, however, TDM has not found its way into clinical practice yet, although many anti-cancer drugs lend themselves to TDM.[19] Imatinib concentrations treatment were retrospectively found to be correlated with tumor response in patients with gastrointestinal stromal tumor (GIST)[20] and in patients with chronic myeloid leukemia (CML).[21] For 5-FU, similar results have been found.[22] Pazopanib is another TKI, for which the relationship between systemic exposure and treatment outcome has been described.[23] In **Chapter 8**, it was evaluated if it was feasible to increase exposure by increasing dose in pazopanib treated patients that have too low exposure on the original dose of 800 mg daily. Additionally, several methods to measure the concentration, i.e. by blood withdrawal and by dried blood spot (DBS), were compared in the same study (**Chapter 9**).

REFERENCES

1. Cotlar AM, Dubose JJ, Rose DM. History of surgery for breast cancer: radical to the sublime. Curr Surg. 2003;60(3):329-37

2. Gilman A. The initial clinical trial of nitrogen mustard. Am J Surg. 1963;105:574-8

3. Heidelberger C, Chaudhuri NK, Danneberg P, Mooren D, Griesbach L, Duschinsky R, et al. Fluorinated pyrimidines, a new class of tumour-inhibitory compounds. Nature. 1957;179(4561):663-6

4. Druker BJ, Tamura S, Buchdunger E, Ohno S, Segal GM, Fanning S, et al. Effects of a selective inhibitor of the Abl tyrosine kinase on the growth of Bcr-Abl positive cells. Nat Med. 1996;2(5):561-6

5. Druker BJ, Guilhot F, O'Brien SG, Gathmann I, Kantarjian H, Gattermann N, et al. Five-year follow-up of patients receiving imatinib for chronic myeloid leukemia. N Engl J Med. 2006;355(23):2408-17

6. Blanke CD, Rankin C, Demetri GD, Ryan CW, von Mehren M, Benjamin RS, et al. Phase III randomized, intergroup trial assessing imatinib mesylate at two dose levels in patients with unresectable or metastatic gastrointestinal stromal tumors expressing the kit receptor tyrosine kinase: S0033. J Clin Oncol. 2008;26(4):626-32

7. Verweij J, Casali PG, Zalcberg J, LeCesne A, Reichardt P, Blay J-Y, et al. Progression-free survival in gastrointestinal stromal tumours with high-dose imatinib: randomised trial. The Lancet. 2004;364(9440):1127-34

8. Hanahan D, Weinberg RA. The hallmarks of cancer. Cell. 2000;100(1):57-70

9. Hanahan D, Weinberg RA. Hallmarks of cancer: the next generation. Cell. 2011;144(5):646-74

10. Gerlinger M, Rowan AJ, Horswell S, Larkin J, Endesfelder D, Gronroos E, et al. Intratumor heterogeneity and branched evolution revealed by multiregion sequencing. N Engl J Med. 2012;366(10):883-92

11. Bins S, Schellens JH, Voest EE, Sleijfer S. Geneesmiddelenonderzoek in de oncologie; vorderingen in het genoomtijdperk. Ned Tijdschr Geneeskd. 2014;158:A6801

12. van Leeuwen RW, van Gelder T, Mathijssen RH, Jansman FG. Drug-drug interactions with tyrosine-kinase inhibitors: a clinical perspective. Lancet Oncol. 2014;15(8):e315-26

13. Mathijssen RH, Marsh S, Karlsson MO, Xie R, Baker SD, Verweij J, et al. Irinotecan pathway genotype analysis to predict pharmacokinetics. Clin Cancer Res. 2003;9(9):3246-53

14. Calvert AH, Newell DR, Gumbrell LA, O'Reilly S, Burnell M, Boxall FE, et al. Carboplatin dosage: prospective evaluation of a simple formula based on renal function. J Clin Oncol. 1989;7(11):1748-56

15. Eechoute K, Fransson MN, Reyners AK, de Jong FA, Sparreboom A, van der Graaf WT, et al. A long-term prospective population pharmacokinetic study on imatinib plasma concentrations in GIST patients. Clin Cancer Res. 2012;18(20):5780-7

16. Chatelut E, Gandia P, Gotta V, Widmer N. Long-term prospective population PK study in GIST patients--letter. Clin Cancer Res. 2013;19(4):949

17. Welty TE, Copa AK. Impact of vancomycin therapeutic drug monitoring on patient care. Ann Pharmacother. 1994;28(12):1335-9

18. Sproule B. Lithium in Bipolar Disorder. Clinical Pharmacokinetics. 2002;41(9):639-60

19. Yu H, Steeghs N, Nijenhuis CM, Schellens JH, Beijnen JH, Huitema AD. Practical guidelines for therapeutic drug monitoring of anticancer tyrosine kinase inhibitors: focus on the pharmacokinetic targets. Clin Pharmacokinet. 2014;53(4):305-25

20. Demetri GD, Wang Y, Wehrle E, Racine A, Nikolova Z, Blanke CD, et al. Imatinib plasma levels are correlated with clinical benefit in patients with unresectable/metastatic gastrointestinal stromal tumors. J Clin Oncol. 2009;27(19):3141-7

21. Picard S, Titier K, Etienne G, Teilhet E, Ducint D, Bernard MA, et al. Trough imatinib plasma levels are associated with both cytogenetic and molecular responses to standard-dose imatinib in chronic myeloid leukemia. Blood. 2007;109(8):3496-9

22. Lee JJ, Beumer JH, Chu E. Therapeutic drug monitoring of 5-fluorouracil. Cancer Chemother Pharmacol. 2016

23. Suttle AB, Ball HA, Molimard M, Hutson TE, Carpenter C, Rajagopalan D, et al. Relationships between pazopanib exposure and clinical safety and efficacy in patients with advanced renal cell carcinoma. Br J Cancer. 2014;111(10):1909-1

Implementation of a Multicenter Biobanking Collaboration for Next-Generation Sequencing-Based Biomarker Discovery Based on Fresh Frozen Pretreatment Tumor Tissue Biopsies

Sander Bins, Geert A. Cirkel, Christa G. Gadellaa – van Hooijdonk, Fleur Weeber, Isaac J. Nijman, Annette H. Bruggink, Paul J. van Diest, Stefan M. Willems, Wouter B. Veldhuis, Michel M. van den Heuvel, Rob J. de Knegt, Marco J. Koudijs, Erik van Werkhoven, Ron H.J. Mathijssen, Edwin Cuppen, Stefan Sleijfer, Jan H.M. Schellens, Emile E. Voest, Marlies H.G. Langenberg, Maja J.A. de Jonge, Neeltje Steeghs, Martijn P. Lolkema
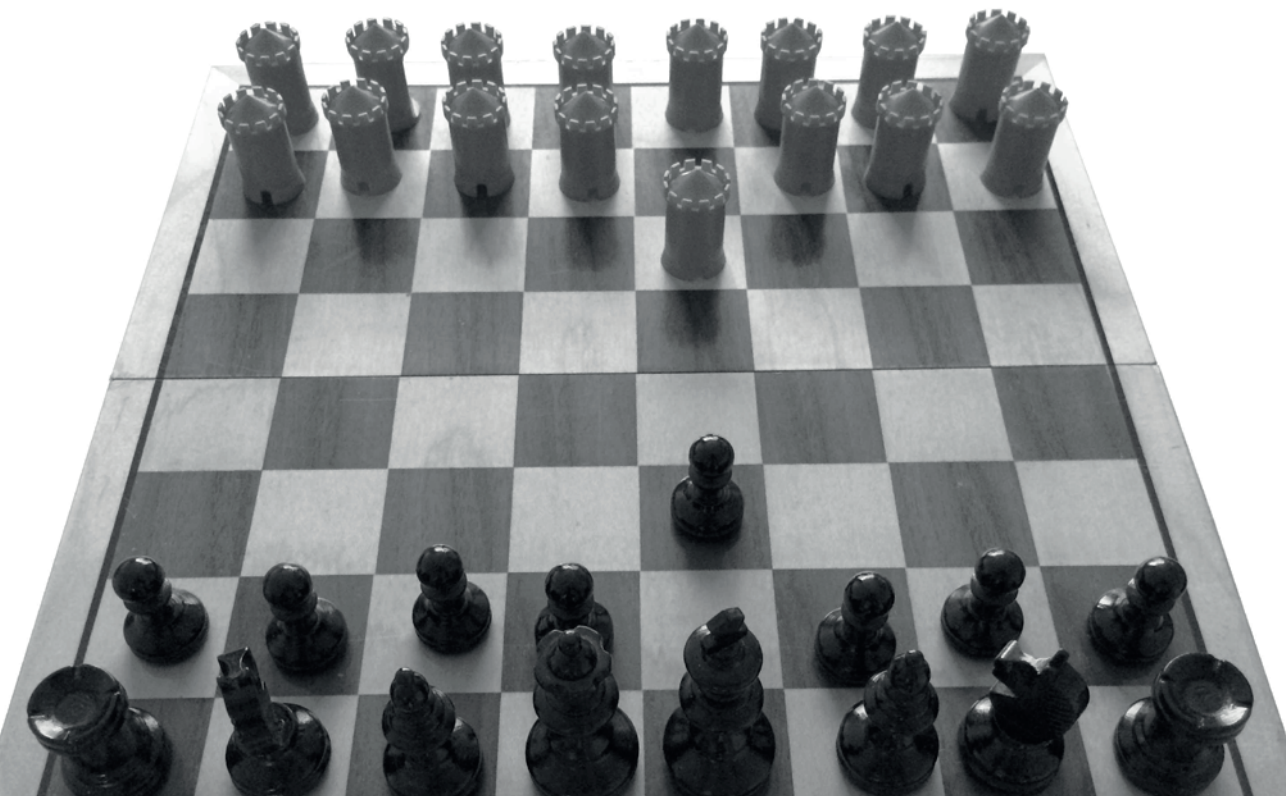
ABSTRACT

Background. The discovery of novel biomarkers that predict treatment response in advanced cancer patients requires acquisition of high-quality tumor samples. As cancer evolves over time, tissue is ideally obtained before the start of each treatment. Preferably, samples are freshly frozen to allow analysis by next-generation DNA/RNA sequencing (NGS) but also for making other emerging systematic techniques such as proteomics and metabolomics possible. Here, we describe the first 469 image-guided biopsies collected in a large collaboration in the Netherlands (Center for Personalized Cancer Treatment) and show the utility of these specimens for NGS analysis.

Patients and methods. Image-guided tumor biopsies were performed in advanced cancer patients. Samples were fresh frozen, vital tumor cellularity was estimated, and DNA was isolated after macrodissection of tumor-rich areas. Safety of the image-guided biopsy procedures was assessed by reporting of serious adverse events within 14 days after the biopsy procedure.

Results. Biopsy procedures were generally well tolerated. Major complications occurred in 2.1%, most frequently consisting of pain. In 7.3% of the percutaneous lung biopsies, pneumothorax requiring drainage occurred. The majority of samples (81%) contained a vital tumor percentage of at least 30%, from which at least 500 ng DNA could be isolated in 91%. Given our preset criteria, 74% of samples were of sufficient quality for biomarker discovery. The NGS results in this cohort were in line with those in other groups.

Conclusion. Image-guided biopsy procedures for biomarker discovery to enable personalized cancer treatment are safe and feasible and yield a highly valuable biobank.

Implications for Practice. This study shows that it is safe to perform image-guided biopsy procedures to obtain fresh frozen tumor samples and that it is feasible to use these biopsies for biomarker discovery purposes in a Dutch multicenter collaboration. From the majority of the samples, sufficient DNA could be yielded to perform next-generation sequencing. These results indicate that the way is paved for consortia to prospectively collect fresh frozen tumor tissue.

2

INTRODUCTION

In oncology, the prediction of treatment outcome remains an important issue. The number of available treatments steadily increases and re-emphasizes our need for guidance on which treatment to choose for a specific patient. Hypothesis-driven biomarkers have been successful: For example, BRAF mutations in melanoma predict response to BRAF inhibitors.[1] However, other effective treatments such as immune checkpoint blockers and novel targeted treatments often lack obvious hypothesis-driven biomarkers. Therefore, unbiased, large-scale approaches such as next-generation DNA/RNA sequencing (NGS), proteomics, and metabolomics may improve the search for more and better predictive biomarkers. To enable the use of these large- scale technologies on clinical samples, it is essential to start the systematic collection of well annotated tissue samples. Because snap freezing is considered the most optimal preservation method for nucleic acids as well as proteins and metabolites, this should be the preferred way clinical samples intended for current and future biomarker discovery are processed.

One major issue in biomarker discovery remains the heterogeneity of tumors. Genetic heterogeneity has been described extensively, and this heterogeneity spans both temporal and spatial differences.[2-5] Consequently, any biomarker discovery study should try to minimize the time elapsing between sampling and treatment and document the sampling site. Moreover, imaging and pathology studies have shown extensive intralesional heterogeneity with respect to important features such as angiogenesis, oxygen supply, energy consumption, and stromal content.[6-8] This heterogeneity will cause a baseline variability despite any effort to homogenize the sampling time and location. Thus, obtaining a large enough sample size to average out our baseline variation is required for the detection of true differences. The actual sample size needed to detect a meaningful difference remains an elusive matter. However, despite all these potential factors that may cause failure to find novel biomarker profiles, there is an increasing number of successful examples of biomarker detection using NGS, including a study that showed that novel T-cell epitopes predict efficacy of immunotherapy, in which the authors were able to detect a meaningful difference in a sample of 11 responders and 14 nonresponders.[9] Therefore, collecting materials from patients who undergo specified

treatments could yield interesting results even when only limited patient numbers are included, given the proper preservation of such materials.

Any large-scale technology that uses unbiased data collection suffers from difficulty in analysis because of the amount of data generated. This problem needs to be addressed at the start of any sample collection project. For NGS-based DNA sequencing the collection of adequate germline samples is essential for the detection of somatic genetic alteration. Also, sampling multiple times from the same patient allows detection of resistance mechanisms.[10-12] Thus any protocol should encourage repetitive sampling.

In the Netherlands, all large oncology centers, including the nine academic centers, are now collaborating in the Center for Personalized Cancer Treatment (CPCT). The CPCT has set up a pipeline for the collection of fresh frozen tumor tissue and for storage in a central biobank. In parallel, all relevant clinical data are recorded in an electronic case record form and can be linked to the results of the tests performed on the tumor material. The primary objective of this biobanking effort is to analyze the individual cancer genome in advanced cancer patients to develop future predictors for response to systemic treatment. Here, we show that it is feasible to set up such a multicenter initiative by presenting the safety of the first 469 image-guided tumor biopsy procedures and by providing the DNA sequencing results of a selected set of 73 biopsy specimens.

PATIENTS AND METHODS

Study Design

To obtain research-related biopsies from advanced cancer patients without curative treatment options, the institutional review board of the participating centers approved a protocol. An important characteristic of the protocol was that it allowed the recruitment of patients with all solid tumor types and multiple treatment protocols. Therefore, it was called the "umbrella" biopsy protocol (NCT01855477). This umbrella protocol was a prospective multicenter trial protocol in which biopsies are obtained to perform next-generation sequencing on fresh frozen biopsy specimens to allow for biomarker detection as well as exploratory biomarker discovery. Patients did not receive systemic treatment as part of this protocol itself. Patients participated in the umbrella protocol and received

systemic treatment, either standard of care or experimental treatment, within a different protocol.

Within the umbrella protocol a baseline biopsy procedure was performed, and clinical data were collected, including radiological response data. The protocol allowed for multiple biopsy procedures at different time points to document changes in genetic profiles upon treatment. Study related procedures were (a) screening procedures to ascertain eligibility and safety of the biopsy procedure, (b) biopsy procedures, and (c) a blood draw to determine germline DNA. The umbrella protocol defined radiological tumor assessments within 8 to 12 weeks after the start of the first initiated treatment after baseline biopsy. The study was conducted in accordance with the latest versions of the Declaration of Helsinki and Good Clinical Practice guidelines.

Patient Selection

All patients provided written informed consent before any of the study-related procedures. Patients aged ≥18 years with a locally advanced or metastatic solid tumor without curative treatment options were eligible for inclusion. Patients were eligible only if systemic treatment according to standard of care or with experimental anticancer agents was planned. Eligible patients had an Eastern Cooperative Oncology Group performance status of 0 (asymptomatic) to 2, measurable lesions according to Response Evaluation Criteria in Solid Tumors,[13] and adequate renal and hepatic functions. Patients with a history of bleeding disorders or bleeding complications, using anticoagulant medication in which discontinuation of anticoagulants was unadvisable, and patients with a contraindication for lidocaine and, if applicable, midazolam or phentanyl (or their derivatives) were excluded. Biopsy of a locally advanced or metastatic lesion had to be considered safe according to the intervening physician.

Blood Sample Collection and Processing

Tumor-matched blood samples were collected to determine patient's germline variation. This information was used to differentiate between somatic and germline mutations in the tumor and was specifically not used to detect cancer predisposition. Venous blood was

collected in K2EDTA tubes. Blood samples were shipped at room temperature to the central core facility of the CPCT for subsequent processing.

Biopsy Procedure

Percutaneous biopsy procedures were performed under ultrasound or computed tomographic guidance after local anesthesia (and in incidental cases under conscious sedation). Whether a guiding needle was used mainly depended on tumor localization and on the preference of the individual physician. We aimed to retrieve two to four core biopsy specimens, preferably with at least an 18-gauge biopsy needle. If appropriate, a gastroenterologist performed an endoscopic (ultrasound) guided procedure using a 19-gauge endoscopic ultrasound histology needle under sedation with midazolam and opioids (phentanyl) for pain relief. When we suspected possible complications with patients, we used ultrasound or computed tomography (CT) to check for major complications (e.g., pneumothorax or initial bleeding complications).

Biopsy Sample Processing

Biopsy specimens were labeled and snap-frozen directly after the biopsy procedure. Subsequently, the specimens were stored at -80°C until they were shipped on dry ice to the central core facility of the CPCT.

Histological Assessment

From each biopsy, 4-mm frozen sections were cut and stained for hematoxylin and eosin. A dedicated pathologist (S.M.W. or P.J.D.) performed histological assessment to confirm the presence of tumor tissue as well as the percentage of tumor cells based on the quantity of nuclei and tumor cell vitality. Tissue morphology was comparable to frozen sections and allowed for reliable confirmation of the presence of cancer. Obvious tumor-rich islands within the sections were marked to obtain an optimal tumor cellularity and quality and to facilitate macrodissection, during which regions of interest were scraped off with a scalpel and collected in phosphate-buffered saline solution. Only when the percentage of vital tumor cells was at least 30%, we proceeded to DNA isolation after macrodissection of indicated areas.

DNA Isolation

DNA was isolated from 500 mL of whole blood and from approximately five macrodissected 20-mm sections using the NorDiag Arrow machine (Isogen Life Science, De Meern, The Netherlands, http://www.isogen-lifescience.com) for isolation and purification of the DNA. DNA extraction was performed in batches (1 to 12 samples per run) using 230 mL of lysis buffer and 20 mL of proteinase K and comprised two washing steps with a final elution volume of 100 mL, according to the manufacturer's protocol. DNA quantity was measured with the Qubit 2.0 fluorometer (Thermo Fisher Scientific Life Sciences, Waltham, MA, http://www.thermofisher.com). Depending on DNA quantity, the protocol was repeated on additional tissue sections to aim for a DNA quantity of at least 500 ng of DNA.DNA was stored at220°C until sequencing was performed.

Safety Evaluation

Observation after the biopsy procedure was performed according to local protocols. No observation was required for patients undergoing superficial tumor biopsies (e.g., biopsy of a subcutaneous lesion or low-risk biopsy of a superficial lymph node). After a percutaneous lung biopsy, a chest x-ray was routinely performed after 1 to 4 hours, depending on local protocols, which in some cases required overnight hospitalization. After all other biopsy procedures, patients were clinically observed for 1 to 4 hours.

Biopsy procedures of individual patients were included in the safety evaluation if specimens for research purposes had been retrieved. All major complications, defined as any adverse events grade 3 or higher related to the biopsy procedure, and all serious adverse events (SAE) occurring within 14 days after tumor biopsy, were registered prospectively. Adverse events were graded according to the National Cancer Institute Common Terminology Criteria for Adverse Events (version 4).[14] An SAE was defined in the protocol as any complication that resulted in death, was life threatening, required prolonged hospitalization, resulted in persistent or significant disability or incapacity, or was a congenital anomaly or birth defect. Clinical observation or hospitalization to facilitate biopsy procedures was not considered a criterion for seriousness. Special attention was paid to the occurrence of bleeding complications and to pneumothorax

after transthoracic biopsy. Pneumothorax and hematothorax are treated invasively at grade 2 and were therefore registered at that grade or higher.

Feasibility

Within the umbrella protocol, retrieval of research specimens for biomarker analyses could be combined with a biopsy procedure for diagnostic assessment. All the image-guided biopsy procedures during which research specimens were retrieved were evaluable for quantification of vital tumor cellularity. Sequencing was performed if DNA yield was at least 500 ng. Performing extended sequencing on paired blood samples (germline DNA) allowed for filtering for true somatic mutations in tumor samples.

DNA Sequencing

Two different platforms have been used for DNA sequencing, that is, a targeted panel analysis using SOLiD sequencing and exome sequencing analysis using Illumina sequencing.

For SOLiD, single nucleotide variants and insertions or deletions (INDELs) were detected by targeted sequencing of a designed "cancer mini-genome" consisting of 1,977 cancer genes (**Supplementary Table S1**). Barcoded fragment libraries were generated from 2 mg of isolated DNA from tumor and control samples, as described previously.[15] Pools of libraries were enriched for 1,977 cancer-related genes (cancer mini-genome[16] using SureSelect technology [Agilent, Santa Clara, CA, http://www.agilent.com/home]). Enriched libraries were sequenced on a SOLiD 5500xl instrument, according to the manufacturer's protocol. Reads were mapped on the human genome (GRCh37) by using Burrows-Wheeler Aligner (BWA)[17] with the following parameters: -c –l 25 –k 2 –n 10. Variant calling was done using a custom pipeline identifying variants with at least10 coverage, an allele frequency of 15%, and multiple (>2) occurrences in the seed (the first 25 base pairs [bp] most accurately mapped part of the read), as well as support from independent reads (>3). All variant positions identified were subsequently genotyped in the raw datasets of all samples using SAMtools mpileup (SourceForge.net, http://samtools.sourceforge.net/mpileup.shtml) to ensure the presence or absence of

possible low-frequency variants. To identify somatic mutations, we excluded all variants identified in both tumor and blood from further analysis.

The Illumina data were processed with an in-house developed pipeline (version 1.2.1) (https://github.com/CuppenResearch/IAP), including GATK v3.2.2,[18] according to the best- practices guidelines.[19] Briefly, we mapped the pairs withBWA-MEMv0.7.5a,[17] marked duplicates, merged lanes, and realigned INDELs. Base recalibration did not improve our exome results, so this step was skipped. Next, GATK Haplotype caller was used to call single nucleotide polymorphisms (SNPs) and INDELs. Variants are flagged as PASS only if they do not meet the following criteria: QD < 2.0, MQ < 40.0, FS > 60.0, HaplotypeScore > 13.0, MQRankSum < -12.5, ReadPosRankSum < -8.0, snpclusters ≥ 3 in 35 bp. For INDELs: QD < 2.0, FS >200.0, ReadPosRankSum < -20.0. Effect predictions and annotation were added using snpEFF[20] and dbNSFP.[21] Somatic mutation is determined by providing the reference and tumor sequencing data to the following algorithms: Strelka v1.0.14,[22] Varscan v2.3.7,[23] and Freebayes v0.9.20.[24] High-confident variants are determined by the tool-filtering steps and merged to a single .vcf file.

Statistical Analysis

All baseline patient characteristics, image-guided biopsy procedure characteristics, and other described analyses were performed using descriptive statistics (Microsoft Excel 2010; Microsoft, Redmond, WA, https://www.microsoft.com/en-us). Tumor cellularity and DNA yield were recorded as continuous variables but were grouped (on the basis of our preset criteria) to allow for descriptive analysis.

RESULTS

Baseline Characteristics

From August 17, 2011, until December 31, 2013, a total of 500 patients signed informed consent and were included in the study. In 50 patients, the biopsy procedure was not performed, because the procedure was not deemed safe or because of clinical progression before the planned biopsy. In Table 1, baseline characteristics are depicted for the 450 biopsied patients, of which the majority had been diagnosed with breast cancer, lung cancer, colorectal cancer, or melanoma.

Biopsy Procedures

In order to be evaluable for this study, patients had to be biopsied at least once before the start of designated treatment. We attempted to obtain other biopsies during or directly after treatment. Multiple biopsies for study purposes were performed in 44 patients, that is, two biopsies in 37 patients, three biopsies in 5 patients, and four biopsies in 2 patients. Of the 503 biopsy procedures in this study, 469 were performed under image guidance of ultrasonography, CT scan, or endoscopy (**Figure 1**, **Table 2**). Most image-guided biopsies were performed on the liver (n 5 185; 39%). Other abdominal organs (n 5 94; 20%) and intrathoracic organs (n 5 56; 12%) were also biopsied frequently. Superficial lesions such as cutaneous, subcutaneous, and soft tissue lesions were biopsied in 120 procedures (26%) and osseous lesions in 14 (3%).

Table 1. Baseline characteristics.

		Biopsied patients N=450		Sequenced biopsies N=73	
Age	*mean (SD)*	59	(11)	58	(11)
Sex	*Male*	239	(53%)	37	(51%)
	Female	211	(47%)	36	(49%)
Primary tumor	*GI: CRC*	99	(22%)	16	(22%)
	Lung cancer	61	(14%)	3	(4%)
	Breast cancer	49	(11%)	5	(7%)
	Melanoma	44	(10%)	16	(22%)
	Hepatobiliary cancer	37	(8%)	6	(8%)
	GI: other	32	(7%)	7	(10%)
	Gynecological cancer	31	(7%)	5	(7%)
	GU cancer	31	(7%)	2	(3%)
	Other	27	(6%)	6	(8%)
	Sarcoma	26	(6%)	4	(5%)
	Head / neck cancer	13	(3%)	3	(4%)

*Abbreviations: CRC, colorectal cancer; GI, gastrointestinal tract; GU, genitourinary tract.*

2

Table 2. Biopsy characteristics.

Characteristics	Image-guided biopsies N=469	
Biopsy timing		
- **Baseline**	419	(89%)
- **On-/post-treatment**	50	(11%)
Biopsy localization		
- **Abdominal: liver**	185	(39%)
- **Abdominal: other**	94	(20%)
- **Superficial**[a]	120	(26%)
- **Thoracic**[b]	56	(12%)
- **Bone**	14	(3%)
Imaging modality		
- **CT-scan**	101	(22%)
- **Ultrasonography**	360	(77%)
- **Endoscopy**[c]	8	(2%)

a. Superficial lesions include all subcutaneous tumors, superficial lymph nodes and breast tumors.

b. Thoracic lesions include pulmonary tumors, pleural tumors, intrathoracic lymph nodes and thymic tumors.

c. Endoscopy was performed as gastroscopy (N=5), colonoscopy (N=1), bronchoscopy (N=1) or endoscopic ultrasonography (N=1).
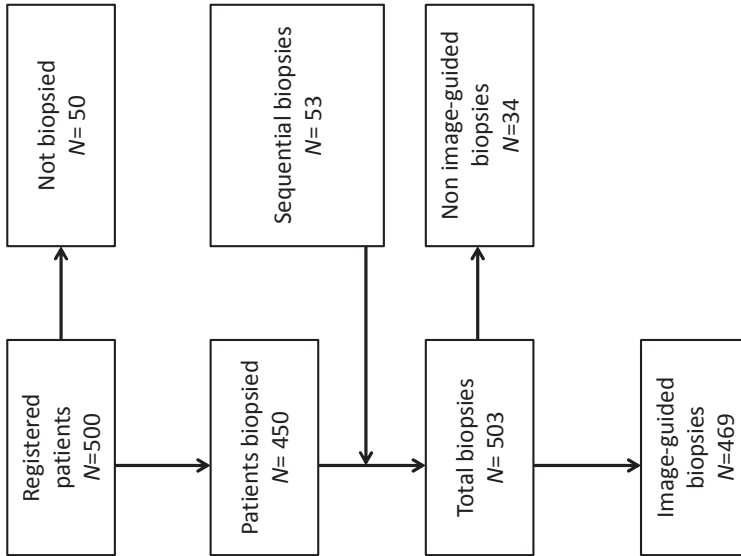
Figure 1. Study flowchart.

Treatment Details

Of all biopsied patients, 324 (72%) were subsequently treated with systemic therapy. The majority of these patients were treated with targeted agents (Table 3).

Table 3. Treatment details of all biopsied patients.

Details	Subjects *N*=450	
Treatment		
Classical chemotherapy	83	(18%)
Phase I drug(s)	76	(17%)
Everolimus	51	(11%)
VEGF TKI (sunitinib / sorafenib / pazopanib)	37	(8%)
Monoclonal antibody	26	(6%)
Vemurafenib	23	(5%)
Anti-hormonal therapy	16	(4%)
Other TKI	12	(3%)
No treatment started	126	(28%)
Treatment duration (months)		
Observations	301	
Median (range)	1.91	(0.00-20.24)
Median (IQR)	1.91	(0.92-3.88)
Lost to follow up	23	
Response at first evaluation		
Complete response (CR)	1	(0%)
Partial response (PR)	39	(13%)
Stable disease (SD)	129	(43%)
Progressive disease (PD)	110	(37%)
Not evaluable	2	(1%)
Not done	12	(4%)
Lost to follow up	8	(3%)

Abbreviations: IQR, interquartile range; TKI, tyrosine kinase inhibitor; VEGF, vascular endothelial growth factor.

Safety

Adverse events occurred after 10 image-guided biopsy procedures (2.1%; Table 4). Four tients experienced grade 3 pain, one patient had grade 3 hypertension, and one patient

experienced grade 3 vasovagal reaction. Of the 41 patients who underwent percutaneous CT-guided lung biopsy, three patients (7.3%) suffered from pneumothorax, for which drainage was indicated (grade 3 in two patients and grade 2 in one patient). Grade 2 pleural hemorrhage was observed once after a CT-guided liver biopsy of a metastatic lesion that was situated directly subdiaphragmatic. In this case, drainage was required, but treatment was not delayed.

Table 4. Adverse events.

Adverse event	Grade	Related to biopsy	Biopsied organ	Duration of hospitalization
Pain	3	Definite	Abdomen (US-guided)	NA
Pain	3	Definite	Liver (US-guided)	Hours*
Pain	3	Definite	Para-vertebral mass (US-guided)	NA
Pain	3	Possible	Liver (US-guided)	Days
Vasovagal reaction	3	Definite	Liver (US-guided)	NA
Hypertension	3	Possible	Abdomen (US-guided)	Hours*
Pneumothorax	3	Definite	Lung (CT-guided)	Days
Pneumothorax	3	Definite	Lung (CT-guided)	Days
Pneumothorax	2	Definite	Lung (CT-guided)	Days
Pleural hemorrhage	2	Definite	Liver (CT-guided)	Days

Abbreviations: CT, computed tomography; NA, not applicable; US, ultrasonography.
*Two patients were admitted to the hospital for several hours after the biopsy procedure and were discharged on the same day.

Tumor Cells and DNA Yield

From 20 patients who underwent image-guided biopsies, no samples were sent in for analysis, because all material was used for standard-of-care treatment. In 363 of the remaining 449 image-guided biopsy-retrieved specimens (81%), we found a tumor cell percentage of 30% or more. Of the 86 tumor specimens with an insufficient percentage of

tumor cells, 40 did not contain tumor cells at all. A sufficient amount of DNA (i.e., 500 ng or more) was obtained from 331 of the 363 biopsy specimens containing ≥30% tumor cells. From 14 of these specimens, DNA had to be isolated a second time to retrieve the required amount of DNA. These 331 specimens (74% of the 449 image-guided biopsy-retrieved specimens received at the central core facility) met our preset criteria to perform DNA sequencing. For all three centers individually, the proportion of samples that met the criteria was 70% or higher and did not differ significantly between the centers (p = .77; Chi-square test).

DNA Sequencing

At data cut-off for this analysis, the sequencing results from 73 biopsied specimens were available. DNA data could be retrieved from all specimens. On SOLiD (n554) we sequenced samples for the 1,977-gene panel until a minimum mean coverage of 1503 was reached (mean of 1853). For exome analysis on Illumina (n519) we sequenced reference samples at least ~753 (mean of 953) and tumor ~1503 (mean of 1853). The most frequently mutated genes were TP53, APC, and BRAF (Table 5).

DISCUSSION

With these results we have shown that it is feasible to set up large, multicenter logistics to biobank image-guided retrieved tumor biopsies. In several other retrospective studies, it has been shown that research-related biopsies are safe and feasible.[25–28] Description of large biopsy series have generally reported on comparable frequencies of major complications.[29–31] The incidence of pneumothorax requiring drainage after percutaneous lung biopsies (3 out of 41 biopsied patients) was similar to that described by El-Osta et al.[32] (2 out of 42). Importantly, the additional value of our series is that we have also shown that it is feasible to extract sufficient DNA from the majority of the biopsy specimens to perform analyses such as NGS. Moreover, because all samples are processed at a central location within the CPCT, uniformity of the analyses is ensured. We could retrieve sufficient DNA for NGS from 74% of the image-guided retrieved biopsy specimens. Although this may be too low for a regular diagnostic test, we feel this hit rate justifies

Table 5. Overview of mutated genes categorized by histological origin shown as N (%).

Gene	Total (N=73)	Breast cancer (N=5)	GI cancer; CRC (N=16)	GI cancer; non CRC[a] (N=7)	Gynaecological cancer[b] (N=5)	Head / Neck cancer[c] (N=3)	Hepatobiliary cancer[d] (N=6)	Lung cancer[e] (N=3)	Melanoma (N=16)	Other[f] (N=12)
TP53	**34 (47)**	2 (40)	11 (69)	5 (71)	2 (40)	1 (33)	4 (67)	1 (33)	3 (19)	5 (42)
APC	**15 (21)**	1 (20)	9 (56)	0 (0)	0 (0)	1 (33)	0 (0)	0 (0)	3 (19)	1 (8)
BRAF	**13 (18)**	0 (0)	0 (0)	0 (0)	0 (0)	0 (0)	0 (0)	0 (0)	13 (81)	0 (0)
CCNB3	**12 (16)**	1 (20)	2 (13)	0 (0)	2 (40)	0 (0)	1 (17)	0 (0)	4 (25)	2 (17)
LRP2	**12 (16)**	1 (20)	4 (25)	0 (0)	2 (40)	1 (33)	1 (17)	0 (0)	2 (13)	1 (8)
ATRX	**11 (15)**	1 (20)	1 (6)	0 (0)	1 (20)	0 (0)	1 (17)	0 (0)	5 (31)	2 (17)
CTBP2	**11 (15)**	0 (0)	0 (0)	2 (29)	0 (0)	0 (0)	2 (33)	0 (0)	5 (31)	2 (17)
FAT3	**11 (15)**	1 (20)	2 (13)	2 (29)	1 (20)	0 (0)	1 (17)	0 (0)	3 (19)	1 (8)
KRAS	**11 (15)**	0 (0)	6 (38)	1 (14)	0 (0)	0 (0)	1 (17)	1 (33)	0 (0)	2 (17)
OBSCN	**11 (15)**	1 (20)	0 (0)	0 (0)	2 (40)	0 (0)	2 (33)	0 (0)	4 (25)	2 (17)
PIK3CA	**10 (14)**	3 (60)	2 (13)	1 (14)	2 (40)	0 (0)	0 (0)	0 (0)	1 (6)	1 (8)

a) Esophageal cancer (N=3), stomach cancer (N=2) and small intestine cancer (N=2).
b) Cervical cancer (N=2), endometrial cancer (N=2) and ovarian cancer (N=1).
c) Laryngeal cancer (N=1), oral cavity cancer (N=1) and pharyngeal cancer (N=1).
d) Liver cancer (N=3) and pancreatic cancer (N=3).
e) Non-small cell lung cancer (N=2) and other lung cancer (N=1).
f) Thyroid cancer (N=1), soft tissue sarcoma (N=4), kidney cancer (N=2) and cancer of unknown primary (N=5).

Abbreviations: CRC, colorectal cancer; GI, gastrointestinal.

2

systematic tissue collection in this manner, because similar proportions have been reported in other series[26] and because this hit rate is therefore likely to represent the true potential of image-guided tumor biopsies. For the specimens that did not meet the criteria for DNA sequencing, we found that 86 of the 118 specimens contained less than 30% tumor cells. Retrospectively, we cannot discern whether this low tumor cell percentage is due to issues with the biopsy procedure or due to intratumoral aspects, such as heterogeneity. As sequencing techniques advance, specimens with lower tumor cell percentage can probably be sequenced in the future, but especially in these specimens it will remain challenging to determine the clinical relevance of infrequent aberrations. The DNA sequencing data for the first 73 biopsy specimens are largely concordant with the results from the Cancer Genome Atlas (TCGA).[33] Alterations in *TP53*, *APC*, *KRAS*, and *PIK3CA* were among the most frequently found genomic aberrations across all tumor types. The higher incidence of *PTEN* and *VHL* in the TCGA set and of *BRAF* in our set is likely to be caused by the difference in tumor types between the two sets: The TCGA set contains glioblastoma multiforme samples and many samples, relatively, from gynecological and kidney cancers, whereas our set contains a large number of melanoma samples. By sequencing germline DNA as a reference for the intratumoral findings, we were bound to detect hereditary mutations, as had been foretold almost a decade ago.[34] The way these findings have been handled in our consortium has been published separately.[35] By establishing a multi-institutional pipeline for large-scale collection of fresh frozen tumor material, we have shown that it is possible for consortia to prospectively collect high-quality fresh frozen tumor tissue. In our collaboration, we have set up a unique framework in which tumor biopsies are obtained prior to standard-of-care systemic treatment and in which these biopsies are stored in a way that enables us to perform not only NGS, but also many other analyses on RNA, protein, epigenetic processes, or even metabolite concentrations if sufficient tissue remains. Because the biopsy specimens are obtained just before the start of the treatment, we are able to capture the most accurate status of genetic and metabolic processes within a tumor. The process of obtaining fresh frozen samples is seemingly simple but requires significant investment when introduced into the clinical setting. The effort we describe is meaningful if intended to serve as a discovery tool. Although many groups have shown that NGS and

other molecular techniques such as RNA sequencing are possible from formalin-fixed, paraffin-embedded (FFPE) tissue samples,[36] there are still discordances between RNA sequencing results from FFPE and fresh frozen tissue,[37] and our experience is that NGS results from fresh frozen tissue are more consistent. However, the logistical process needed to implement our protocol in itself represents added value for discovery purposes and large-scale biobanking.

Patient accrual is one of the major issues in gathering biopsies in the context of a clinical study in which there is no direct benefit for an individual patient. Both the willingness of patients and the reluctance of the treating physician to ask their patients for research biopsies play a role here. This is a common phenomenon in the process of acquiring research biopsies and has recently been described elsewhere.[38] Consequently, many of the early-phase clinical trials that include mandatory biopsies fail to report on biomarker analysis.[39,40] Despite the scarcity of adequately collected tumor material, many tumor biopsies are still collected in small initiatives or by industry studies, looking predominantly at only *RAS*, *RAF*, or the *ERBB* family.[41] An alternative would be to identify predictive markers in preclinical model systems, but here the major discrepancies between pharmacologic drug responses for identical cell lines in the two largest pharmacogenomics cell line studies suggest that preclinical studies often lack predictive power.[42] Thus, current and future clinical research should be aimed at collecting tumor tissue and at correlating molecular data to clinical outcome to identify true predictive biomarkers. In this study we have shown that it is feasible to perform next-generation sequencing on fresh frozen biopsies for biomarker discovery in a multi-institutional setting. Additionally, we have confirmed that acquiring fresh frozen tumor biopsies under image guidance is safe in advanced cancer patients.

REFERENCES

1. Flaherty KT, Puzanov I, Kim KB, Ribas A, McArthur GA, Sosman JA, et al. Inhibition of mutated, activated BRAF in metastatic melanoma. N Engl J Med. 2010;363(9):809-19

2. Hoogstraat M, de Pagter MS, Cirkel GA, van Roosmalen MJ, Harkins TT, Duran K, et al. Genomic and transcriptomic plasticity in treatment-naive ovarian cancer. Genome Res. 2014;24(2):200-11

3. Alizadeh AA, Aranda V, Bardelli A, Blanpain C, Bock C, Borowski C, et al. Toward understanding and exploiting tumor heterogeneity. Nat Med. 2015;21(8):846-53

4. Gerlinger M, Rowan AJ, Horswell S, Larkin J, Endesfelder D, Gronroos E, et al. Intratumor heterogeneity and branched evolution revealed by multiregion sequencing. N Engl J Med. 2012;366(10):883-92

5. McGranahan N, Swanton C. Biological and therapeutic impact of intratumor heterogeneity in cancer evolution. Cancer Cell. 2015;27(1):15-26

6. Nakajima EC, Laymon C, Oborski M, Hou W, Wang L, Grandis JR, et al. Quantifying Metabolic Heterogeneity in Head and Neck Tumors in Real Time: 2-DG Uptake Is Highest in Hypoxic Tumor Regions. PLoS One. 2014;9(8):e102452

7. Hatt M, Majdoub M, Vallières M, Tixier F, Le Rest CC, Groheux D, et al. 18F-FDG PET Uptake Characterization Through Texture Analysis: Investigating the Complementary Nature of Heterogeneity and Functional Tumor Volume in a Multi–Cancer Site Patient Cohort. Journal of Nuclear Medicine. 2015;56(1):38-44.

8. Picchio M, Beck R, Haubner R, Seidl S, Machulla H-J, Johnson TD, et al. Intratumoral Spatial Distribution of Hypoxia and Angiogenesis Assessed by 18F-FAZA and 125I-Gluco-RGD Autoradiography. Journal of Nuclear Medicine. 2008;49(4):597-605

9. Snyder A, Makarov V, Merghoub T, Yuan J, Zaretsky JM, Desrichard A, et al. Genetic basis for clinical response to CTLA-4 blockade in melanoma. N Engl J Med. 2014;371(23):2189-99

10. Hoogstraat M, Gadellaa-van Hooijdonk CG, Ubink I, Besselink NJ, Pieterse M, Veldhuis W, et al. Detailed imaging and genetic analysis reveal a secondary BRAF(L505H) resistance mutation and extensive intrapatient heterogeneity in metastatic BRAF mutant melanoma patients treated with vemurafenib. Pigment Cell Melanoma Res. 2015;28(3):318-23

11. Romano E, Pradervand S, Paillusson A, Weber J, Harshman K, Muehlethaler K, et al. Identification of Multiple Mechanisms of Resistance to Vemurafenib in a Patient with BRAFV600E-Mutated Cutaneous Melanoma Successfully Rechallenged after Progression. Clinical Cancer Research. 2013;19(20):5749-57

12. Kemper K, Krijgsman O, Cornelissen-Steijger P, Shahrabi A, Weeber F, Song JY, et al. Intra- and inter-tumor heterogeneity in a vemurafenib-resistant melanoma patient and derived xenografts. EMBO Mol Med. 2015;7(9):1104-18

13. Eisenhauer EA, Therasse P, Bogaerts J, Schwartz LH, Sargent D, Ford R, et al. New response evaluation criteria in solid tumours: revised RECIST guideline (version 1.1). Eur J Cancer. 2009;45(2):228-47

14. National Cancer Institute. Common Terminology Criteria for Adverse Events v4.0. NCI, NIH, DHHS. May 29, 2009. NIH publication # 09-7473

15. Harakalova M, Mokry M, Hrdlickova B, Renkens I, Duran K, van Roekel H, et al. Multiplexed array-based and in-solution genomic enrichment for flexible and cost-effective targeted next-generation sequencing. Nat Protoc. 2011;6(12):1870-86

16. Vermaat JS, Nijman IJ, Koudijs MJ, Gerritse FL, Scherer SJ, Mokry M, et al. Primary colorectal cancers and their subsequent hepatic metastases are genetically different: implications for selection of patients for targeted treatment. Clin Cancer Res. 2012;18(3):688-99

17. Li H, Durbin R. Fast and accurate short read alignment with Burrows-Wheeler transform. Bioinformatics. 2009;25(14):1754-60

18. McKenna A, Hanna M, Banks E, Sivachenko A, Cibulskis K, Kernytsky A, et al. The Genome Analysis Toolkit: a MapReduce framework for analyzing next-generation DNA sequencing data. Genome Res. 2010;20(9):1297-303

19. Van der Auwera GA, Carneiro MO, Hartl C, Poplin R, Del Angel G, Levy-Moonshine A, et al. From FastQ data to high confidence variant calls: the Genome Analysis Toolkit best practices pipeline. Curr Protoc Bioinformatics. 2013;11(1110):11 0 1- 0 33

2

20. Cingolani P, Platts A, Wang le L, Coon M, Nguyen T, Wang L, et al. A program for annotating and predicting the effects of single nucleotide polymorphisms, SnpEff: SNPs in the genome of Drosophila melanogaster strain w1118; iso-2; iso-3. Fly (Austin). 2012;6(2):80-92

21. Liu X, Jian X, Boerwinkle E. dbNSFP v2.0: a database of human non-synonymous SNVs and their functional predictions and annotations. Hum Mutat. 2013;34(9):E2393-402

22. Saunders CT, Wong WS, Swamy S, Becq J, Murray LJ, Cheetham RK. Strelka: accurate somatic small-variant calling from sequenced tumor-normal sample pairs. Bioinformatics. 2012;28(14):1811-7

23. Koboldt DC, Zhang Q, Larson DE, Shen D, McLellan MD, Lin L, et al. VarScan 2: somatic mutation and copy number alteration discovery in cancer by exome sequencing. Genome Res. 2012;22(3):568-76

24. Garrison E, Marth G. Haplotype-based variant detection from short-read sequencing. arXiv preprint arXiv:12073907. 2012

25. Dowlati A, Haaga J, Remick SC, Spiro TP, Gerson SL, Liu L, et al. Sequential tumor biopsies in early phase clinical trials of anticancer agents for pharmacodynamic evaluation. Clin Cancer Res. 2001;7(10):2971-6

26. Gomez-Roca CA, Lacroix L, Massard C, De Baere T, Deschamps F, Pramod R, et al. Sequential research-related biopsies in phase I trials: acceptance, feasibility and safety. Ann Oncol. 2012;23(5):1301-6

27. Lee JM, Hays JL, Noonan AM, Squires J, Minasian L, Annunziata C, et al. Feasibility and safety of sequential research-related tumor core biopsies in clinical trials. Cancer. 2013;119(7):1357-64

28. Tran B, Brown AM, Bedard PL, Winquist E, Goss GD, Hotte SJ, et al. Feasibility of real time next generation sequencing of cancer genes linked to drug response: results from a clinical trial. Int J Cancer. 2013;132(7):1547-55

29. Giorgio A, Tarantino L, de Stefano G, Francica G, Esposito F, Perrotta A, et al. Complications after interventional sonography of focal liver lesions: a 22-year single-center experience. J Ultrasound Med. 2003;22(2):193-205

30. Atwell TD, Smith RL, Hesley GK, Callstrom MR, Schleck CD, Harmsen WS, et al. Incidence of bleeding after 15,181 percutaneous biopsies and the role of aspirin. AJR Am J Roentgenol. 2010;194(3):784-9

31. McGill DB, Rakela J, Zinsmeister AR, Ott BJ. A 21-year experience with major hemorrhage after percutaneous liver biopsy. Gastroenterology. 1990;99(5):1396-400

32. El-Osta H, Hong D, Wheler J, Fu S, Naing A, Falchook G, et al. Outcomes of research biopsies in phase I clinical trials: the MD anderson cancer center experience. Oncologist. 2011;16(9):1292-8

33. Kandoth C, McLellan MD, Vandin F, Ye K, Niu B, Lu C, et al. Mutational landscape and significance across 12 major cancer types. Nature. 2013;502(7471):333-9

34. McGuire AL, Caulfield T, Cho MK. Research ethics and the challenge of whole-genome sequencing. Nat Rev Genet. 2008;9(2):152-6

35. Bijlsma RM, Bredenoord AL, Gadellaa-Hooijdonk CG, Lolkema MP, Sleijfer S, Voest EE, et al. Unsolicited findings of next-generation sequencing for tumor analysis within a Dutch consortium: clinical daily practice reconsidered. Eur J Hum Genet. 2016.

36. Mittempergher L, de Ronde JJ, Nieuwland M, Kerkhoven RM, Simon I, Rutgers EJ, et al. Gene expression profiles from formalin fixed paraffin embedded breast cancer tissue are largely comparable to fresh frozen matched tissue. PLoS One. 2011;6(2):e17163

37. Hedegaard J, Thorsen K, Lund MK, Hein AM, Hamilton-Dutoit SJ, Vang S, et al. Next-generation sequencing of RNA and DNA isolated from paired fresh-frozen and formalin-fixed paraffin-embedded samples of human cancer and normal tissue. PLoS One. 2014;9(5):e98187

38. Seah DS, Scott S, Guo H, Najita J, Lederman R, Frank E, et al. Variation in the attitudes of medical oncologists toward research biopsies in patients with metastatic breast cancer. Oncologist. 2015;20(9):992-1000

39. Freeman GA, Kimmelman J. Publication and reporting conduct for pharmacodynamic analyses of tumor tissue in early-phase oncology trials. Clin Cancer Res. 2012;18(23):6478-84

40. Sweis RF, Drazer MW, Ratain MJ. Analysis of Impact of Post-Treatment Biopsies in Phase I Clinical Trials. Journal of Clinical Oncology. 2016;34(4):369-74

41. Roper N, Stensland KD, Hendricks R, Galsky MD. The landscape of precision cancer medicine clinical trials in the United States. Cancer Treat Rev. 2015;41(5):385-90

42. Haibe-Kains B, El-Hachem N, Birkbak NJ, Jin AC, Beck AH, Aerts HJ, et al. Inconsistency in large pharmacogenomic studies. Nature. 2013;504(7480):389-93

Supplementary Table S1. SureSelect design CPCT capture kit > 1977 genes (update september 2011).

AAK1	AL117209.2	ARRB2	BID	CAB39	CCNA2
AATK	ALK	ASAP1	BIRC2	CAB39L	CCNB1
ABCA1	ALKBH1	ASCC1	BIRC3	CABC1	CCNB2
ABL1	ALKBH2	ASH1L	BIRC5	CACYBP	CCNB3
ABL2	ALKBH3	ASH2L	BLK	CAD	CCND1
AC005726.6	ALMS1	ASPSCR1	BLM	CALM1	CCND2
AC005756.1	ALPK1	ASXL1	BMP1	CALM2	CCND3
AC008735.15	ALPK2	ATF1	BMP10	CALM3	CCNE1
AC012652.1	ALPK3	ATF2	BMP15	CALML3	CCNE2
AC013461.1	AMH	ATF4	BMP2	CALML5	CCNG1
AC021106.1	AMHR2	ATM	BMP2K	CALML6	CCNG2
AC068353.1	ANAPC1	ATP5S	BMP4	CAMK1	CCNH
AC107883.1	ANAPC10	ATP8B1	BMP5	CAMK1D	CCR3
AC113191.2	ANAPC11	ATR	BMP6	CAMK1G	CCR7
AC114947.1	ANAPC13	ATRX	BMP7	CAMK2A	CCRK
AC130454.2	ANAPC2	AURKA	BMP8A	CAMK2B	CD109
ACTR2	ANAPC4	AURKB	BMP8B	CAMK2D	CD14
ACVR1	ANAPC5	AURKC	BMPR1A	CAMK2G	CD248
ACVR1B	ANAPC7	AXIN1	BMPR1B	CAMK4	CD40
ACVR1C	ANGPTL4	AXIN2	BMPR2	CAMKK1	CD47
ACVR2A	ANK1	AXL	BMX	CAMKK2	CD82
ACVR2B	ANK2	B9D1	BOC	CAMKV	CDC14A
ACVRL1	ANKK1	BACH1	BRAF	CAMP	CDC14B
AD000671.3	ANKRD29	BAD	BRCA1	CAPG	CDC16
ADAM17	AP000654.1	BAG2	BRCA2	CAPN1	CDC20
ADAM29	AP003355.2	BAI1	BRD2	CAPN2	CDC23
ADAMTS15	APAF1	BAI3	BRD3	CARD9	CDC25A
ADAMTS18	APC	BAIAP2	BRD4	CARM1	CDC25B
ADAMTSL3	APC2	BAP1	BRDT	CARS	CDC25C
ADCK1	APH1A	BARD1	BRIP1	CASK	CDC26
ADCK2	APPL1	BAX	BRSK1	CASP1	CDC27
ADCK4	AR	BBC3	BRSK2	CASP10	CDC2L5
ADCK5	ARAF	BBS2	BTC	CASP2	CDC2L6
ADORA1	AREG	BBS4	BTK	CASP3	CDC42
ADRBK1	AREGB	BBS5	BTRC	CASP4	CDC42BPA
ADRBK2	ARFRP1	BBS7	BUB1	CASP5	CDC42BPB
AGK	ARID1A	BBS9	BUB1B	CASP6	CDC42BPG
AIFM1	ARIH2	BCKDK	BUB3	CASP7	CDC45L
AIFM2	ARL13B	BCL2	C10orf104	CASP8	CDC6
AIM1	ARL4C	BCL2L1	C10orf137	CASP9	CDC7
AIMP2	ARL6	BCL2L11	C13orf34	CBL	CDC73
AIP	ARNT	BCL2L14	C14orf153	CBLB	CDCA8
AKAP4	ARNT2	BCL2L2	C16orf53	CBLC	CDH1
AKT1	ARPC3	BCL6	C17orf106	CCBE1	CDH20
AKT1S1	ARPC4	BCL9	C8ORF4	CCDC6	CDH3
AKT2	ARPC5	BCR	C9orf100	CCDC99	CDK1
AKT3	ARRB1	BDNF	C9orf96	CCNA1	CDK10

2

CDK11A	CLK2	CTNNBIP1	DLL1	EDA	EPHB6
CDK17	CLK3	CUBN	DLL3	EEF2K	EPS8
CDK2	CLK4	CUL1	DLL4	EFNB1	ERBB2
CDK4	CLSPN	CUL2	DMAP1	EFNB2	ERBB3
CDK5	CLSTN1	CXCL12	DMPK	EGF	ERBB4
CDK6	CLTC	CXCR4	DNAH11	EGFL6	ERC2
CDK7	CLUAP1	CXCR7	DNAH5	EGFR	ERCC1
CDK8	CNKSR1	CXXC4	DNAH9	EGLN1	ERCC2
CDK9	CNKSR2	CYCS	DNAI1	EGLN2	ERCC3
CDKL1	CNTN4	CYLD	DNLZ	EGLN3	ERCC4
CDKL2	CNTN6	CYS1	DOT1L	EGR1	ERCC5
CDKL3	COL14A1	DAAM1	DPP3	EHMT1	ERCC6
CDKL4	COL1A1	DAAM2	DPP4	EHMT2	ERCC6L
CDKL5	COL4A1	DAPK1	DSCAML1	EI24	EREG
CDKN1A	COL4A2	DAPK2	DSTYK	EIF2AK1	ERGIC3
CDKN1B	COL4A4	DAPK3	DTX1	EIF2AK2	ERN1
CDKN1C	COL4A6	DARC	DTX2	EIF2AK3	ERN2
CDKN2A	COMP	DAXX	DTX3	EIF2AK4	ERO1L
CDKN2B	COX7A2L	DBF4	DTX3L	EIF2B5	ESCO2
CDKN2C	CREB1	DCC	DTX4	EIF3J	ESPL1
CDKN2D	CREB3L2	DCLK1	DUSP1	EIF4A2	ESR1
CDON	CREBBP	DCLK2	DUSP10	EIF4B	ETFA
CDT1	CRK	DCLK3	DUSP14	EIF4E	ETS1
CEBPA	CRKL	DCN	DUSP16	EIF4E1B	EVL
CENPA	CRKRS	DDB2	DUSP2	EIF4E2	EWSR1
CENPE	CRLF2	DDIT3	DUSP3	EIF4EBP1	EXO1
CEP290	CSF1	DDIT4	DUSP4	ELF3	EXOC4
CER1	CSF1R	DDR1	DUSP5	ELF4	EXOC7
CERK	CSF2RA	DDR1	DUSP6	ELK1	EXOG
CFL2	CSF2RB	DDR2	DUSP7	ELK3	EXT1
CFLAR	CSF3R	DDX23	DUSP8	ELK4	EXT2
CHD3	CSK	DFFA	DUSP9	EML4	EYA4
CHD5	CSMD1	DFFB	DVL1	ENDOD1	EZH1
CHD8	CSMD3	DGKA	DVL2	ENDOG	EZH2
CHEK1	CSNK1A1	DGKB	DVL3	EP300	FADD
CHEK2	CSNK1A1L	DGKD	DYRK1A	EPAS1	FAM123B
CHIC2	CSNK1D	DGKE	DYRK1B	EPCAM	FAM20C
CHL1	CSNK1E	DGKG	DYRK2	EPHA1	FANCA
CHRD	CSNK1G1	DGKH	DYRK3	EPHA10	FANCC
CHRM1	CSNK1G2	DGKI	DYRK4	EPHA2	FANCD2
CHUK	CSNK1G3	DGKQ	E2F1	EPHA3	FANCE
CIB2	CSNK2A1	DGKZ	E2F2	EPHA4	FANCF
CIC	CSNK2A2	DHH	E2F3	EPHA5	FANCG
CIR1	CSNK2B	DIABLO	E2F4	EPHA6	FARP1
CIT	CTBP1	DIP2C	E2F5	EPHA7	FARP2
CITED1	CTBP2	DKK1	E2F6	EPHA8	FAS
CKS1B	CTNNA1	DKK2	E2F7	EPHB1	FASLG
CLDN1	CTNNA2	DKK3	E2F8	EPHB2	FASN
CLIP1	CTNNA3	DKK4	E4F1	EPHB3	FASTK
CLK1	CTNNB1	DLK1	ECSIT	EPHB4	FAT3

FBXL14	FOXL2	GRAP2	HIPK4	IKBKB	ITPK1
FBXW11	FOXM1	GRB10	HIST1H1B	IKBKE	ITPKA
FBXW7	FOXO1	GRB2	HK1	IKBKG	ITPKB
FER	FOXO3	GRK1	HK2	IL12RB1	ITPKC
FES	FOXO4	GRK4	HK3	IL18BP	ITPR2
FGF1	FRAT1	GRK5	HNF1A	IL1R1	JAG1
FGF10	FRAT2	GRK6	HNF1B	IL1R2	JAG2
FGF11	FRK	GRK7	HNRNPH2	IL1RAP	JAK1
FGF12	FRZB	GSG2	HRAS	IL3RA	JAK2
FGF13	FST	GSK3A	HSF4	IL6	JAK3
FGF14	FTO	GSK3B	HSP90AA1	IL6ST	JARID2
FGF16	FYB	GSTP1	HSP90AB1	IL8	JHDM1D
FGF17	FYN	GSX2	HSP90B1	ILK	JMJD1C
FGF18	FZD1	GTSE1	HSPA1A	INCENP	JMJD4
FGF19	FZD10	GUCY1A2	HSPA1B	INHBA	JMJD5
FGF2	FZD2	GUCY2C	HSPA1L	INHBB	JMJD6
FGF20	FZD3	GUCY2D	HSPA2	INHBC	JMJD7-
FGF21	FZD4	GUCY2F	HSPA6	INHBE	PLA2G4B
FGF22	FZD5	GYS1	HSPA8	INPP4A	JMJD8
FGF23	FZD6	GYS2	HSPB1	INPP5D	JUN
FGF3	FZD7	H2AFX	HSPB8	INPP5K	JUNB
FGF4	FZD8	H2AFY2	HUNK	INPPL1	JUND
FGF5	FZD9	HABP4	ICAM1	INS	JUP
FGF6	FZR1	HAPLN1	ICAM2	INSR	KALRN
FGF7	GAB1	HAT1	ICAM3	INSRR	KAT2A
FGF8	GABRA6	HAUS3	ICAM4	INVS	KAT2B
FGF9	GADD45A	HBEGF	ICK	IP6K1	KAT5
FGFR1	GADD45B	HBXIP	ID1	IP6K2	KCNE1
FGFR2	GADD45G	HCK	ID2	IP6K3	KDM1A
FGFR3	GAK	HDAC1	ID3	IPMK	KDM1B
FGFR4	GALNS	HDAC10	ID4	IPPK	KDM2A
FGR	GAS1	HDAC11	IDH1	IQCB1	KDM2B
FH	GATA1	HDAC2	IDH2	IQGAP2	KDM3A
FIGF	GATA2	HDAC3	IDUA	IRAK1	KDM3B
FKBP1A	GATA3	HDAC4	IFNG	IRAK2	KDM4A
FLCN	GCK	HDAC5	IFT172	IRAK3	KDM4B
FLNA	GDF5	HDAC6	IFT57	IRAK4	KDM4C
FLNB	GDF6	HDAC7	IFT81	IRF3	KDM4D
FLNC	GDF7	HDAC8	IFT88	IRS1	KDM4DL
FLOT1	GDNF	HDAC9	IGF1	IRS2	KDM5A
FLOT2	GLI1	HES1	IGF1R	IRS4	KDM5B
FLT1	GLI2	HES5	IGF2	ITCH	KDM5C
FLT3	GLI3	HGF	IGF2R	ITGA2	KDM5D
FLT3LG	GMNN	HHIP	IGFBP1	ITGA2B	KDM6A
FLT4	GMPS	HIF1A	IGFBP2	ITGA3	KDM6B
FN1	GNA12	HIF1AN	IGFBP3	ITGA6	KDR
FOS	GNAQ	HIF3A	IGFBP4	ITGAE	KIAA1468
FOSL1	GNAS	HIPK1	IGFBP5	ITGAV	KIF11
FOXC1	GNG12	HIPK2	IHH	ITGB1	KIF15
FOXC2	GPR141	HIPK3	IKBKAP	ITK	KIF1B

KIF2C	LRP2BP	MAPK1	MEF2C	MYD88	NKX3-1
KIF3A	LRP5	MAPK10	MELK	MYLK	NLK
KIF3B	LRP6	MAPK11	MEN1	MYLK2	NODAL
KIFAP3	LRRC50	MAPK12	MERTK	MYLK3	NOG
KISS1	LRRC6	MAPK13	MET	MYLK4	NOS2
KIT	LRRK1	MAPK14	MFSD4	MYO18B	NOS3
KITLG	LRRK2	MAPK15	MGMT	MYO3A	NOSIP
KLC3	LTBP1	MAPK3	MGST1	MYO3B	NOSTRIN
KLHL4	LTK	MAPK4	MINK1	MYST1	NOTCH1
KLK3	LYN	MAPK6	MITF	MYST2	NOTCH2
KNTC1	LZTS2	MAPK7	MKKS	MYST3	NOTCH2NL
KRAS	MACC1	MAPK8	MKNK1	MYST4	NOTCH3
KREMEN1	MAD1L1	MAPK8IP1	MKNK2	MYT1	NOTCH4
KREMEN2	MAD2L1	MAPK8IP2	MKRN2	NBN	NPHP1
KRT20	MAD2L1BP	MAPK8IP3	MKS1	NCK1	NPHP3
KRT71	MAD2L2	MAPK9	MLH1	NCK2	NPHP4
KRT73	MAK	MAPKAPK2	MLH3	NCOA4	NPM1
KRTCAP2	MAML1	MAPKAPK3	MLKL	NCOR1	NPR1
KRTCAP3	MAML2	MAPKAPK5	MLL	NCOR2	NPR2
KSR1	MAML3	MAPKSP1	MLL2	NCSTN	NR4A1
KSR2	MAP2	MAPRE1	MLL3	NDC80	NRAS
L3MBTL	MAP2K1	MAPRE3	MLL5	NDP	NRBP1
LAMA1	MAP2K2	MAPT	MLST8	NDUFV3	NRBP2
LAMA2	MAP2K3	MARK1	MMP1	NEDD9	NRG1
LAMA3	MAP2K4	MARK2	MMP2	NEK1	NRG2
LAMA4	MAP2K5	MARK3	MMP7	NEK10	NRG3
LAMA5	MAP2K6	MARK4	MMP9	NEK11	NRG4
LAMB1	MAP2K7	MAST1	MOS	NEK2	NRK
LAMB2	MAP3K1	MAST2	MPL	NEK3	NSD1
LAMB3	MAP3K10	MAST3	MRAS	NEK4	NTF3
LAMB4	MAP3K11	MAST4	MRE11A	NEK5	NTF4
LAMC1	MAP3K12	MASTL	MSH2	NEK6	NTHL1
LAMC2	MAP3K13	MATK	MSH3	NEK7	NTRK1
LAMC3	MAP3K14	MAX	MSH6	NEK8	NTRK2
LATS1	MAP3K15	MBIP	MSN	NEK9	NTRK3
LATS2	MAP3K2	MCC	MST1	NF1	NUAK1
LCK	MAP3K3	MCF2L2	MST1R	NF2	NUAK2
LEF1	MAP3K4	MCL1	MTAP	NFAT5	NUF2
LEFTY1	MAP3K5	MCM2	MTOR	NFATC1	NUMA1
LEFTY2	MAP3K6	MCM3	MUC1	NFATC2	NUMB
LFNG	MAP3K7	MCM4	MUSK	NFATC3	NUMBL
LGR5	MAP3K7IP1	MCM5	MUTYH	NFATC4	NUP98
LGR6	MAP3K7IP2	MCM6	MVP	NFKB1	OBSCN
LIMK1	MAP3K8	MCM7	MXD1	NFKB2	ODC1
LIMK2	MAP3K9	MCM8	MXI1	NFKBIA	OFD1
LMTK2	MAP4K1	MDM2	MYC	NFKBIE	OGG1
LMTK3	MAP4K2	MDM4	MYCBP2	NGF	OPRM1
LNX1	MAP4K3	MECOM	MYCL1	NKD1	ORC1L
LRDD	MAP4K4	MED12	MYCN	NKD2	ORC2L
LRP2	MAP4K5	MED12L	MYCNOS	NKX2-1	ORC3L

ORC4L	PDK4	PIP5K1A	PPM1A	PRKCD	PTPRS
ORC5L	PDPK1	PIP5K1B	PPM1B	PRKCE	PTPRT
ORC6L	PERP	PIP5K1C	PPM1D	PRKCG	PTPRU
OSR1	PFTK1	PIP5K2A	PPP1CA	PRKCH	PTTG1
OXSR1	PFTK2	PIP5K2B	PPP1CB	PRKCI	PXK
P2RX7	PGF	PIP5KL1	PPP1CC	PRKCQ	PXN
PAK1	PGPEP1	PIPSL	PPP1R13B	PRKCZ	PYGB
PAK2	PHF15	PITX2	PPP1R3A	PRKD1	PYGL
PAK3	PHF16	PIWIL1	PPP1R3B	PRKD2	PYGM
PAK4	PHF17	PKD1	PPP1R3C	PRKD3	PYGO1
PAK6	PHF2	PKD2	PPP1R3D	PRKDC	PYGO2
PAK7	PHF8	PKDCC	PPP2CA	PRKG1	RAB23
PALB2	PHIP	PKHD1	PPP2CB	PRKG2	RAC1
PAPD5	PHKA1	PKLR	PPP2R1A	PRKX	RAC2
PARD3	PHKA2	PKMYT1	PPP2R1B	PRKY	RAC3
PARD6A	PHKB	PKN1	PPP2R5A	PROC	RAD21
PARK2	PHKG1	PKN2	PPP2R5B	PRPF4	RAD50
PARK7	PHKG2	PKN3	PPP2R5C	PRPF4B	RAD51
PARP1	PHLDB2	PKNOX1	PPP2R5D	PSEN1	RAD52
PARP10	PHOX2A	PLA2G2A	PPP2R5E	PSEN2	RAD54L
PARP11	PHOX2B	PLCB1	PPP3CA	PSENEN	RAD9A
PARP12	PI4K2A	PLCB2	PPP3CB	PSKH1	RAD9B
PARP14	PI4K2B	PLCB3	PPP3CC	PSKH2	RAET1E
PARP15	PI4KA	PLCB4	PPP3R1	PSMC4	RAET1L
PARP16	PI4KB	PLCG1	PPP3R2	PSPH	RAF1
PARP3	PIAS1	PLCG2	PPP5C	PTCH1	RAGE
PARP8	PIAS2	PLCXD1	PRCC	PTCH2	RALA
PARP9	PIAS3	PLCXD2	PRDM2	PTCRA	RALB
PASK	PIAS4	PLCXD3	PRDM4	PTEN	RALBP1
PAX8	PIK3C2A	PLCZ1	PRDM6	PTGS2	RALGDS
PBK	PIK3C2B	PLD1	PRDM7	PTK2	RANBP2
PBRM1	PIK3C2G	PLD6	PRDM9	PTK2B	RAP1A
PCBD1	PIK3C3	PLK1	PRICKLE1	PTK6	RAP1B
PCK1	PIK3CA	PLK2	PRICKLE2	PTK7	RAP1GAP
PCK2	PIK3CB	PLK3	PRKAA1	PTN	RAPGEF1
PCNA	PIK3CD	PLK4	PRKAA2	PTPN1	RAPGEF2
PCTK1	PIK3CG	PLXNB3	PRKAB1	PTPN11	RAPGEF3
PCTK3	PIK3R1	PMAIP1	PRKAB2	PTPN13	RAPGEF4
PDE3A	PIK3R2	PML	PRKACA	PTPN14	RARA
PDE3B	PIK3R3	PMS1	PRKACB	PTPN3	RARB
PDE4D	PIK3R4	PMS2	PRKACG	PTPN5	RASA1
PDGFA	PIK3R5	PNCK	PRKAG1	PTPN6	RASA2
PDGFB	PIK3R6	POLS	PRKAG2	PTPN7	RASA3
PDGFRA	PIKFYVE	PORCN	PRKAG3	PTPRA	RASGRF1
PDGFRB	PIM1	POU2F1	PRKAR1A	PTPRD	RASGRF2
PDGFRL	PIM2	PPA1	PRKAR1B	PTPRF	RASGRP1
PDIK1L	PIM3	PPA2	PRKAR2A	PTPRG	RASGRP2
PDK1	PIN4	PPARD	PRKAR2B	PTPRJ	RASGRP3
PDK2	PINK1	PPARG	PRKCA	PTPRN2	RASGRP4
PDK3	PIP4K2C	PPARGC1A	PRKCB	PTPRR	RASSF1

2

RASSF5	RP11-481A12.5	SESN1	SLC2A4	SPINK1	STK32C
RAVER2	RP5-862P8.2	SESN2	SLK	SPINK2	STK33
RAX2	RPA1	SESN3	SMAD1	SPINK4	STK35
RB1	RPA2	SETD1A	SMAD2	SPINK5	STK36
RBBP4	RPA3	SETD1B	SMAD3	SPINK6	STK38
RBBP5	RPA4	SETD2	SMAD4	SPINK7	STK38L
RBBP8	RPGR	SETD3	SMAD5	SPINK8	STK39
RBL1	RPGRIP1	SETD4	SMAD6	SPINK9	STK4
RBL2	RPGRIP1L	SETD5	SMAD7	SPRED1	STK40
RBPJ	RPRM	SETD6	SMAD9	SPTBN2	STMN1
RBPJL	RPS6	SETD7	SMARCA4	SRC	STOML3
RBX1	RPS6KA1	SETD8	SMARCB1	SREBF1	STRADA
RCHY1	RPS6KA2	SETDB1	SMARCD1	SRF	STRADB
REEP5	RPS6KA3	SETDB2	SMARCE1	SRM	STYK1
REL	RPS6KA4	SETMAR	SMC1A	SRMS	SUFU
RELA	RPS6KA5	SFN	SMC1B	SRPK1	SUV39H1
RELB	RPS6KA6	SFRP1	SMC3	SRPK2	SUV39H2
RET	RPS6KB1	SFRP2	SMG1	SRPK3	SUV420H1
RFC1	RPS6KB2	SFRP4	SMO	SSBP1	SUV420H2
RFC2	RPS6KC1	SFRP5	SMURF1	SSBP2	SYK
RFC3	RPS6KL1	SFRS6	SMURF2	SSH1	SYMPK
RFC4	RPTOR	SGCB	SMYD1	SSH2	TAF1
RFC5	RRAS	SGK1	SMYD2	SSSCA1	TAF1L
RFNG	RRAS2	SGK2	SMYD3	SSTR1	TAOK1
RFWD2	RRM1	SGK3	SMYD4	SSTR2	TAOK2
RFX2	RRM2	SGOL1	SMYD5	SSTR3	TAOK3
RHEB	RRM2B	SGOL2	SNAI1	SSTR4	TBCK
RHO	RSPO1	SH2B2	SNAI2	SSTR5	TBK1
RHOA	RUNX1	SH2D2A	SNRK	ST13	TBL1X
RHOC	RUNX1T1	SH2D7	SNTB1	STAG1	TBL1XR1
RHOQ	RUVBL1	SHC1	SNW1	STAG2	TBL1Y
RICTOR	RXRA	SHC2	SNX25	STAM	TBX22
RIOK1	RXRB	SHC3	SNX4	STAT1	TBX3
RIOK2	RXRG	SHC4	SOCS1	STAT3	TCEB1
RIOK3	RYK	SHFM1	SOCS2	STAT5A	TCEB2
RIPK1	SBK1	SHH	SOCS3	STAT5B	TCEB3
RIPK2	SBK2	SHISA5	SOCS4	STAT6	TCF3
RIPK3	SCEL	SHOX	SORBS1	STEAP3	TCF4
RIPK4	SCYL1	SIAH1	SOS1	STK10	TCF7
RMI1	SCYL2	SIK1	SOS2	STK11	TCF7L1
RNASEL	SCYL3	SIK2	SOST	STK16	TCF7L2
RNF213	SDCCAG1	SIK3	SOX17	STK17A	TEC
RNF220	SDHB	SIN3A	SP1	STK17B	TECTA
ROCK1	SDHD	SIN3B	SPAG5	STK19	TEK
ROCK2	SEC31A	SIX4	SPC24	STK24	TESK1
ROR1	SENP2	SKP1	SPC25	STK25	TESK2
ROR2	SEPT9	SKP2	SPEG	STK3	TEX14
ROS1	SERPINB5	SLC26A1	SPHK1	STK31	TFDP1
RP11-330H6.5	SERPINE1	SLC29A1	SPHK2	STK32A	TFDP2
		SLC2A1	SPI1	STK32B	TFE3

TFG	TNFRSF1A	TRAF3	TTN	VEGFB	WNT5B
TGFA	TNFRSF1B	TRAF3IP2	TWF1	VEGFC	WNT6
TGFB1	TNFRSF8	TRAF4	TWIST1	VHL	WNT7A
TGFB2	TNFSF10	TRAF5	TXK	VHLL	WNT7B
TGFB3	TNFSF12	TRAF6	TYK2	VPS16	WNT8A
TGFBR1	TNIK	TRIB1	TYMS	VRK1	WNT8B
TGFBR2	TNK1	TRIB2	TYRO3	VRK2	WNT9A
TGM3	TNK2	TRIB3	UBE2B	VRK3	WNT9B
THBS1	TNKS	TRIM24	UBE2C	WASF2	WRN
THBS2	TNKS2	TRIM28	UBR5	WASL	WT1
THBS3	TNNI3K	TRIM33	UCK2	WDR75	WTAP
THBS4	TOE1	TRIM77	UHMK1	WEE1	XIAP
TICAM1	TOP1	TRIO	UHRF2	WEE2	XPA
TIE1	TOP2A	TRIP10	ULK1	WHSC1	XPC
TIPARP	TOP2B	TRPM6	ULK2	WHSC1L1	XPNPEP3
TIRAP	TOP3B	TRPM7	ULK3	WIF1	XPO1
TLE1	TOPBP1	TRRAP	ULK4	WISP1	XRCC1
TLK1	TOPORS	TSC1	UMPS	WIT1	XRCC3
TLK2	TP53	TSC2	UPF1	WNK1	YES1
TLL1	TP53AIP1	TSHR	UQCRC2	WNK2	YME1L1
TLR1	TP53BP1	TSPAN8	USP17L2	WNK3	YSK4
TLR2	TP53BP2	TSPYL2	USP24	WNK4	ZAP70
TLR3	TP53I3	TSPYL5	USP28	WNT1	ZBTB16
TLR4	TP53RK	TSSK1B	USP33	WNT10A	ZBTB17
TLR5	TP63	TSSK2	USP39	WNT10B	ZEB2
TLR9	TP73	TSSK3	USP9X	WNT11	ZFYVE16
TMEM67	TPM3	TSSK4	UTY	WNT16	ZFYVE9
TNF	TPR	TSSK6	VANGL1	WNT2	ZIC2
TNFAIP3	TPTE2P1	TTBK1	VANGL2	WNT2B	ZMAT3
TNFRSF10A	TPX2	TTBK2	VAV2	WNT3	ZNF217
TNFRSF10B	TRADD	TTC8	VAV3	WNT3A	ZNF668
TNFRSF10C	TRAF1	TTK	VBP1	WNT4	ZNF703
TNFRSF10D	TRAF2	TTLL3	VEGFA	WNT5A	ZYX

The time to progression ratio: a new individualized volumetric parameter for the early detection of clinical benefit of targeted therapies

Geert A. Cirkel, Fleur Weeber, Sander Bins, Christa G. Gadellaa – van Hooijdonk, Erik van Werkhoven, Stefan M. Willems, Marijn van Stralen, Wouter B. Veldhuis, Inge Ubink, Neeltje Steeghs, Maja J.A. de Jonge, Marlies H.G. Langenberg, Jan H.M. Schellens, Stefan Sleijfer, Martijn P. Lolkema, Emile E. Voest
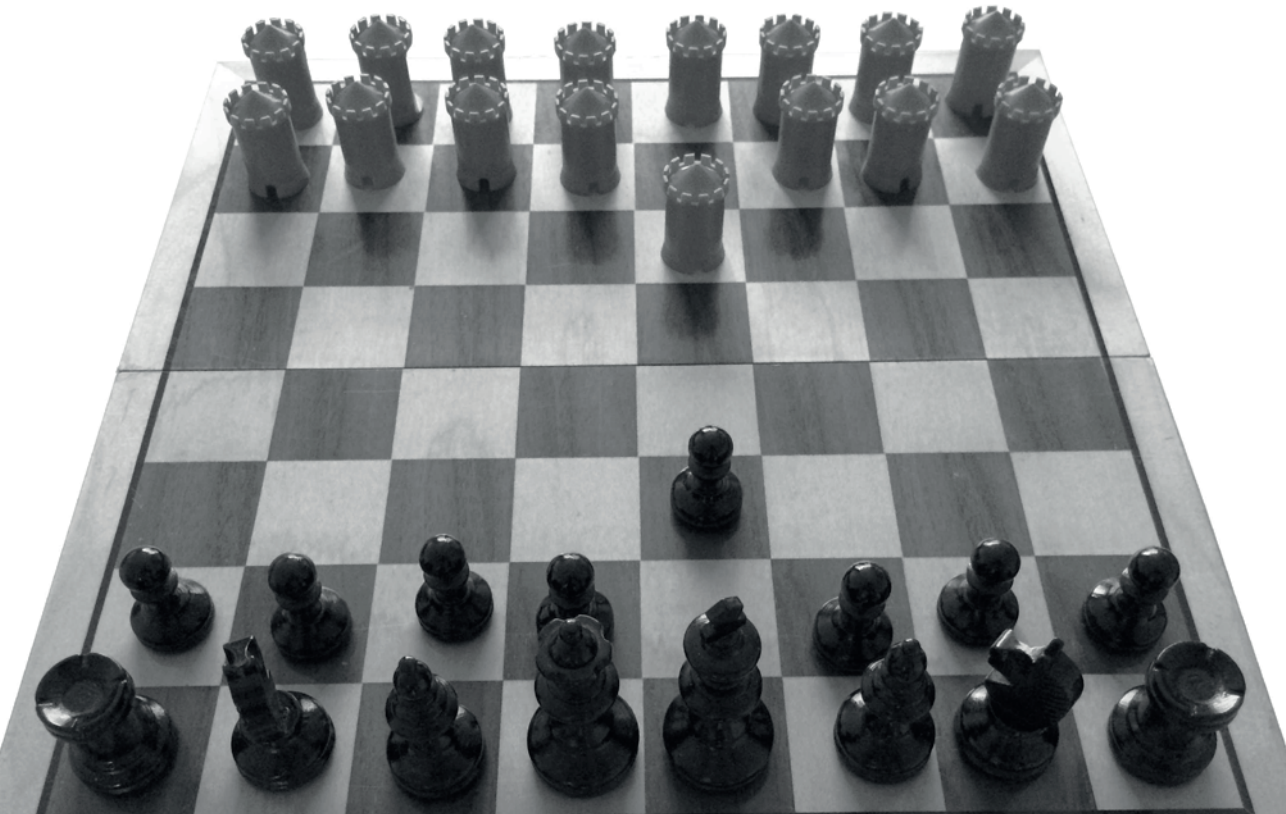
ABSTRACT

Background. Early signs of efficacy are critical in drug development. Response Evaluation Criteria in Solid Tumors (RECIST) are commonly used to determine the efficacy of anti-cancer therapy in clinical trials. RECIST, however, emphasizes the value of tumor shrinkage, while many targeted agents induce prolonged tumor growth arrest. This limits its use for the detection of treatment efficacy for these more cytostatic regimens. Therefore, we designed an individualized variant of a time to progression (TTP) end point based on prospective volumetric measurements and an intra-patient control, the TTP ratio.

Patients and methods. Patients with any metastatic malignancy, without regular treatment options, were treated with the mTOR inhibitor everolimus. Treatment response was determined using both RECIST and the TTP ratio. The TTP ratio was defined as the volumetric pretreatment TTP divided by the volumetric on-treatment TTP. A patient was classified as a responder if the TTP ratio was <0.7. Consistency and reproducibility of volumetric measurements were determined.

Results. Seventy-three patients were included of whom 59 started treatment. A TTP ratio could be established in 73% (n = 43) of the treated patients. The inter-observer agreement for volumetric progression was 0.78 (95% confidence interval 0.70–0.87) (Krippendorff's α-coefficient). According to RECIST, 35 patients (59%) had stable disease (SD) and 1 patient demonstrated a partial response (PR), whereas only 21 patients (36%) met the prespecified criteria for treatment efficacy according to the TTP ratio. Treatment response according to both the TTP ratio and RECIST (SD + PR) correlated with overall survival (OS) [P(log-rank) < 0.001]. The TTP ratio, however, was also able to differentiate which patients had a better OS within the RECIST SD group [P(log-rank) = 0.0496].

Conclusion. The TTP ratio had a high inter-observer agreement, correlated with OS and identified which patients within the RECIST SD group had a longer OS.

3

INTRODUCTION

Early signs of clinical activity are important in the decision to further develop new drugs. At present, Response Evaluation Criteria in Solid Tumors 1.1 (RECIST)-based parameters such as the response rate (RR) or progression-free survival (PFS) are standard to determine drug efficacy in early clinical trials.[1] The introduction of targeted and immunomodulatory agents, however, has intensified the debate on the validity of these commonly used endpoints in clinical trials.[2] Although RR reliably measures significant tumor progression and regression, it lacks the capability to detect growth rate reduction, which may be of great clinical value. This is an important limitation because targeted agents often exert a more cytostatic effect than chemotherapy, resulting in delayed growth rather than objective tumor regression.[3] Patients with indolent growing tumors will end up in the stable disease (SD) group, obscuring the distinction between a slow natural course of disease and treatment effect. The value of PFS in single-arm studies is also adversely affected by inter-tumor variation in the natural growth rate. A drug-induced decrease in growth rate will not be detected without knowledge of the intrinsic growth rate. Using only RR or PFS as an efficacy end point in early-phase clinical trials may therefore lead to wrongful interpretation of the results with all untoward consequences.[4]

These limitations of RECIST emphasize the need for a reliable parameter of clinical benefit that corrects for growth characteristics of the individual patient's tumor. Such a parameter will not only improve detection of drug efficacy but also support drug development in early clinical trials. Here, we introduce and evaluate a new personalized response parameter to measure the efficacy of targeted therapy: the time to progression (TTP) ratio (**Figure 1**). The TTP ratio prospectively compares volumetric tumor growth off and on treatment and therefore serves as an intra-patient control for natural tumor growth rate.

METHODS

Patients

Patients with any advanced malignancy, who progressed on their previous treatment and had no regular systemic treatment options left, were eligible for inclusion. Key eligibility criteria included an age of 18 years or older; Eastern Cooperative Oncology Group (ECOG)

performance status of ≤2; volumetrically measurable disease; feasibility of histologic tumor biopsy; and adequate hepatic, renal and hematologic function.

Study Regulatory Compliance

The protocol (ClinicalTrials.gov identifier NCT01566279) was approved by the ethical review board of The Netherlands Cancer Institute and complied with the Declaration of Helsinki, Dutch law and Good Clinical Practice. All patients provided written informed consent before study-related procedures.
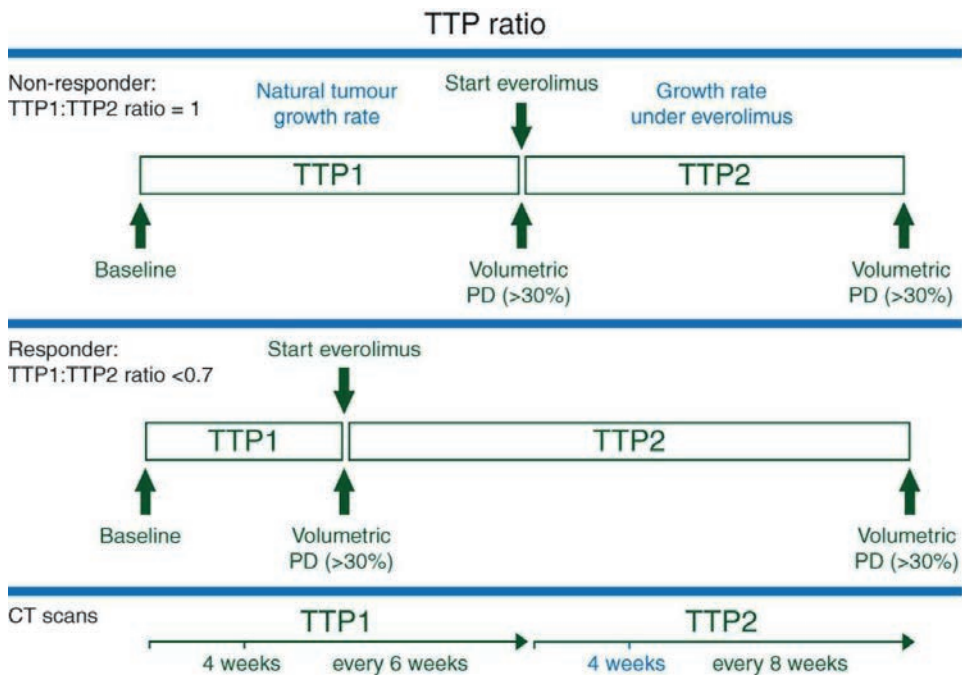
Figure 1. TTP ratio.
The TTP1 ratio is used to determine treatment efficacy in this study. If everolimus is beneficial for an individual patient, the time to progression under treatment (TTP2) is longer than the time to progression without treatment (TTP1). If the ratio of TTP1:TTP2 is <0.7, the patient is classified as a responder. In this figure, an example is given of a non-responder and responder. In the case of a >30% volumetric increase or new lesions on CT, the patient is classified as having progressive disease. The timing of CT evaluations has also been incorporated in this figure. The CT evaluation at 4 weeks in TTP2 will be done only if a patient is progressive at the first evaluation in TTP1.

3

Study Design

The CPCT-03 study was an open-label, prospective, single-arm, multicenter intervention study. Study objectives included biomarker identification using RECIST and TTP ratio, evaluating the TTP ratio as a marker for treatment efficacy, and determining PFS, overall survival (OS) and Disease Control Rate (DCR) as defined by RECIST. Patients were accrued at the Netherlands Cancer Institute, UMC Utrecht Cancer Center and Erasmus MC Cancer Institute Rotterdam.

Treatment

All patients received everolimus 10 mg once daily, orally, on a continuous basis until disease progression according to RECIST. Dose reductions to 5 mg once daily and 5 mg every other day were allowed. A third dose reduction, or treatment interruption of more than 3 weeks, was not allowed.

Efficacy Assessments

After study inclusion, the time to an either ≥30% volumetric increase in target lesions or the development of new lesions was determined in a prospective manner, before the treatment with everolimus. This period was called time to progression 1 (TTP1) and represented the natural tumor growth rate. In TTP1, tumor assessments were carried out at baseline, 4 weeks after baseline and every 6 weeks subsequently. In the case of obvious clinical progression during TTP1, a computed tomography (CT) scan was carried out immediately. Subsequently, treatment with everolimus was started and patients were again followed until a ≥30% volumetric increase in target lesions or the development of new lesions. This was called time to progression 2 (TTP2) and represented the growth speed of the tumor under treatment. In TTP2, tumor assessments were carried out every 8 weeks until progressive disease, according to RECIST, was observed. The only exception was patients who were already progressive in TTP1 at 4 weeks, they had their first on-treatment scan at 4 weeks. The TTP ratio was calculated by dividing TTP1 by TTP2. A patient was classified as a responder if the TTP ratio was <0.7. The 0.7 cut-off for response was based on the PFS ratio of Von Hoff et al.[5] Von Hoff et al. divided TTP2 by TTP1 (in

contrast to TTP1 by TTP2) and used a threshold of >1.33 for response, which corresponds to 0.75 for our TTP ratio. They determined TTP1 under the previous treatment, whereas here it is determined without treatment and the more stringent cut-off 0.7 was chosen.

All tumor assessments were carried out using CT and sent to a central facility. Volumetric measurements were carried out using semiautomatic software (EncoreUnFoie, v5.0, Image Sciences, UMC Utrecht, the Netherlands, 2012). All CT scans were measured by at least two independent observers (GAC, FW, CGMG-H, IU) using the same set of target lesions. At study entry, volumetrically measurable target lesions were selected in adherence to RECIST guidelines.[1] A lesion was considered volumetrically measurable if its borders could be delimited on every single CT scan slice. Volumetric measurements were carried out by manually contouring the lesion on all axial slices. Subsequently, the volume of each individual lesion was calculated automatically (**Supplementary Figure S1**). The percent change in volume was calculated for the sum of volumes. If there was no consensus on the presence or absence of volumetric progressive disease, a third observer was consulted. An increase of 30% since nadir or more in the cumulative volume of target lesions or appearance of new lesions was considered PD. The 30% cut-off was chosen based on the work of van Kessel et al.[6], who found that for individual observers, 95% of all repeated lesion measurements fell within the limit of −28.6% and 30.4%. Patients were also evaluated according to the conventional RECIST during the TTP2 period. For all TTP ratio assessable patients, the PFS ratio as described by Von Hoff et al.[5] was also determined to enable comparison with the TTP ratio. The PFS ratio uses TTP on the most recent line of treatment as an intra-patient control.

Evaluability of Patients

Patients were not evaluable for TTP ratio if they did not complete the TTP1 period or if they had a protocol violation, lost their volumetric measurability or stopped treatment due to reasons other than PD [with the exception of patients that had already passed the threshold of response (<0.7)]. Patients were evaluable for RECIST if treatment response was determined on at least one CT.

Statistical Analyses

The majority of analyses were carried out using SPSS Statistics version 22 (IBM). Baseline data were reported with descriptive statistics. PFS and OS curves were constructed using the Kaplan–Meier technique, and analyzed using a log-rank test. Numbers of target lesions were compared using a paired t-test. A Spearman correlation was used to analyze the relation between TTP1 and TTP ratio, TTP1 and the wash-out period of the previous treatment, and baseline tumor volume and percentage change. Inter-observer variability was calculated using R version 3.2.0 (www.r-project.org) with Krippendorff's α-coefficient.

Table 1.

Demographic or clinical characteristic	Patients (*N*)	%
No. of patients	73	
Sex		
Male	29	39.7
Age, years		
Mean	59	
Range	31–79	
WHO PS		
0	21	28.8
1	42	57.5
2	2	2.7
Missing	8	11.0
Primary tumor		
Colorectal	23	31.5
NET	9	12.3
Esophageal	5	6.8
Breast	4	5.5
NSCLC	4	5.5
Ovarian	3	4.1
Bladder	3	4.1
Sarcoma	3	4.1
Cervical	2	2.7
Head and neck	2	2.7
Renal cell	2	2.7
Unknown origin	2	2.7

Demographic or clinical Characteristic	Patients (*N*)	%
Time since initial diagnosis		
≤6 months	6	8.2
>6 months to ≤2 years	27	37.0
>2 to ≤5 years	23	31.5
>5 years	17	23.3
No. of organs involved		
1	13	17.8
2	17	23.3
>2	38	52.1
Unknown	5	6.8
Prior treatment		
Chemotherapy	68	93.1
Targeted therapy	27	37.0
Hormone therapy	9	12.3
Immunotherapy	0	—
Radiotherapy	38	52.1

Abbreviations: NET, neuroendocrine tumor; NSCLC, non-small cell lung cancer; WHO PS, World Health Organisation Performance Score.

RESULTS

Study Population

Seventy-three patients were included between 15 August 2012 and 23 April 2014 (**Supplementary Figure S2**). Fifty-nine patients started treatment with everolimus. Reasons for drop-out during TTP1 included clinical deterioration (n = 8), initiation of other treatment (n = 2), toxicity from a previous treatment (n = 1), screen failure (n = 1) or withdrawal of informed consent (n = 1). Baseline patient characteristics are depicted in **Table 1**.

TTP Ratio Versus RECIST

To compare the TTP ratio and RECIST, we evaluated several factors, including number of target lesions, concordance of change and response classification. Forty-three (73%) patients reached TTP2 and were evaluable for efficacy using the TTP ratio. Fifty-one (86%) patients were evaluable using RECIST. Reasons for non-evaluability according to TTP ratio included protocol violation (n = 1), loss of volumetric measurability (n = 3) and stop of treatment due to reasons other than PD (n = 12). Patients were not evaluable for RECIST when treatment response was not determined (n = 8). Because not all lesions can be measured volumetrically, we compared the number of target lesions used for RECIST and volumetric measurements. Within patients evaluable for both methods, fewer lesions were selected as target lesions for volumetric measurements [mean 2.5 (±1.0 SD)] compared with RECIST [mean 3.0 (±1.2 SD)]. This difference was statistically significant (P < 0.001, paired t-test). Volumetric and RECIST measurements were concordant in measuring either tumor growth or regression in 79% of cases (**Supplementary Figure S3**).

Using standard RECIST, most patients were classified as having SD (59%, Table 2). Twenty-five percent of patients were classified as progressive (PD) and one patient had a partial response (PR). Using the TTP ratio, 36% of patients were classified as responders and 37% as non-responders. The RECIST SD cohort could be split in 20 TTP ratio responders and 8 non-responders.

TTP Ratio As an Efficacy End Point

To evaluate the consistency of measuring volumetric progressive disease, the inter-observer agreement was calculated using Krippendorff's α-coefficient. The inter-observer agreement was 0.78 [95% confidence interval (CI) 0.70–0.87] with 199 evaluated scans. Baseline tumor volume was not correlated to the percentage of change in target lesions (P = 0.413, Spearman). TTP1 was not correlated to TTP ratio (P = 0.551, Spearman) or the wash-out period of the previous treatment (P = 0.251, Spearman).

3
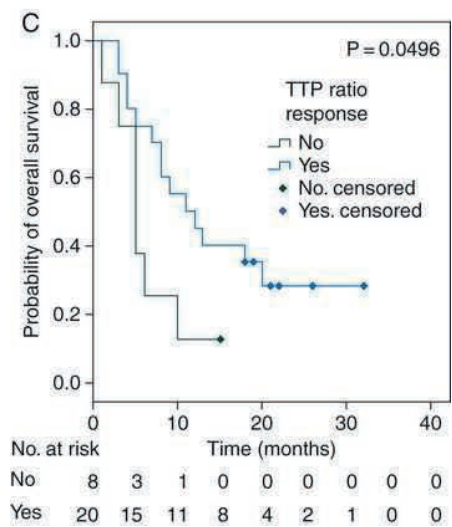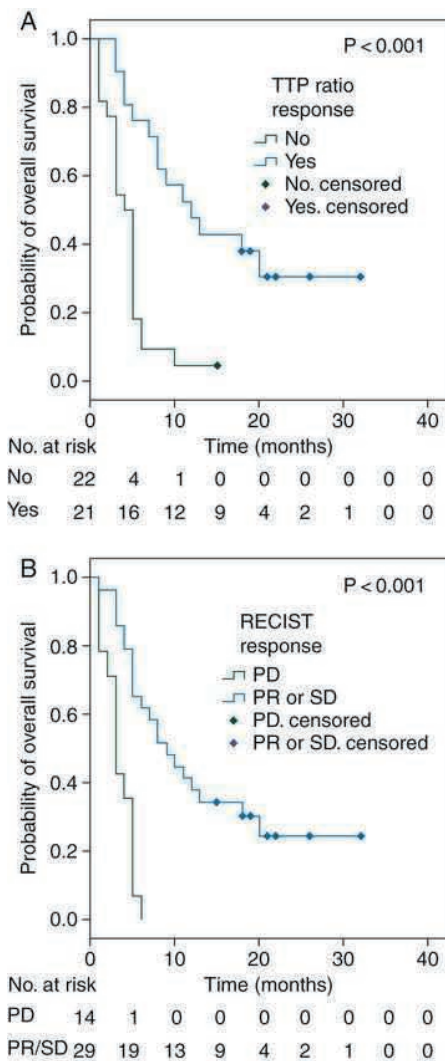
Figure 2. Correlation of outcome measures to OS. *(A) TTP ratio correlated with OS in the TTP ratio evaluable cohort, (B) PR and SD according to RECIST also correlated with OS in the TTP ratio evaluable cohort, (C) response according to TTP ratio within the SD cohort (n = 28) correlated to OS.*

To explore the predictive value of outcome according to TTP ratio, we analyzed its relation with OS in the TTP ratio evaluable cohort (n = 43). **Figure 2A** shows OS of responders versus non-responders according to TTP ratio. A significant difference in OS between responders [median 12 months (95% CI 6.0–18.0)] and non-responders [median 4 months (95% CI 2.9–5.1)] was observed [P(log-rank) < 0.001]. There was also a significant difference in OS between the RECIST SD and PR patients versus the PD patients in the same cohort [P(log-rank) < 0.001, **Figure 2B**]. Because a large proportion of the RECIST SD population were TTP ratio responders, we carried out a separate analysis within the RECIST SD cohort to evaluate if TTP ratio response was correlated to OS within this subgroup (n = 28). The median OS was significantly longer in the TTP ratio responder group [median 11 months (95% CI 4.4–17.6)] than in the non-responder group [median 5 months (95% CI 3.2–6.8)] [P(log-rank) = 0.0496, **Figure 2C**]. PFS ratio response also correlated to OS [P(log-rank) = 0.008]. However, in contrast to the TTP ratio, response according to PFS ratio was not correlated to OS in the RECIST SD cohort [P(log-rank) = 0.311].

Efficacy of Everolimus

Within this study, we also evaluated the efficacy of everolimus according to both end points among different tumor types (**Table 2**). Individual TTP times and ratios are shown in **Supplementary Figure S4**. According to RECIST, high disease control rates (PR + SD) were observed for breast (75%) and esophageal (80%) cancer, including a PR for esophageal cancer. Both tumor types also had a high rate of responders according to the TTP ratio: 60% for esophageal cancer and 75% for breast cancer.

All TTP ratio evaluable breast cancers and esophageal adenocarcinomas had a short TTP1 and a response according to the TTP ratio. The squamous cell esophageal carcinomas included a patient with a long TTP1 and response according to the TTP ratio (this patient also had a RECIST PR). The second patient was not evaluable for response according to the TTP ratio. RECIST response was SD. On CT, however, necrosis of the lung metastases was observed (**Supplementary Figure S5**).

The majority of patients stopped treatment due to PD (n = 35). Other reasons to stop treatment were adverse events (AEs) (n = 7); toxicity (n = 3); patient refusal (n = 1); clinical deterioration (n = 1); death (n = 1); other (n = 7). At the time of analysis, four patients were still on treatment. AEs are summarized in **Table 3**.

Table 2. Efficacy of everolimus.

	All patients (*n* = 59)	Colorectal (*n* = 17)	Neuro-endocrine (*n* = 9)	Esophageal (*n* = 5)	Breast (*n* = 4)
TTP ratio (*n*, %)					
Response (<0.7)	21 (36%)	5 (29%)	2 (22%)	3 (60%)	3 (75%)
Non-response (≥0.7)	22 (37%)	10 (59%)	2 (22%)	0 (—)	0 (—)
Unknown	16 (27%)	2 (12%)	5 (56%)	2 (40%)	1 (25%)
Best response (*n*, %)					
CR	0 (—)	0 (—)	0 (—)	0 (—)	0 (—)
PR	1 (2%)	0 (—)	0 (—)	1 (20%)	0 (—)
SD	35 (59%)	8 (47%)	6 (67%)	3 (60%)	3 (75%)
PD	15 (25%)	8 (47%)	1 (11%)	1 (20%)	0 (—)
Unknown	8 (14%)	1 (6%)	2 (22%)	0 (—)	1 (25%)
Disease control rate	**36 (61%)**	**8 (47%)**	**6 (67%)**	**4 (80%)**	**4 (75%)**
PFS					
Events (*n*, %)	45 (62%)	14 (82%)	3 (33%)	4 (80%)	3 (75%)
Median, months	2	2	15	3	1
95% CI	1.2–2.8	1.5–2.5	0–39.2	0.5–5.5	0–6.2
OS					
Events (*n*, %)	50 (85%)	17 (100%)	6 (67%)	4 (80%)	4 (100%)
Median, months	5	5	17	3	4
95% CI	4.3–5.7	4.0–6.0	0–34.5	0–6.2	0–9.9

Abbreviations: CR, complete response; OS, overall survival; PD, progressive disease; PFS, progression free survival; PR, partial response; TTP ratio, time to progression ratio.

Table 3. Adverse events.

Adverse event	All grades, *N*(%)	Grade 3/4, *N*(%)
Y-GT increased	16 (26.7%)	1 (1.7%)
AF increased	8 (13.3%)	1 (1.7%)
Fatigue	6 (10%)	1 (1.7%)
Anemia	5 (8.3%)	1 (1.7%)
Dyspnea	5 (8.3%)	5 (8.3%)
Hyperglycemia	5 (8.3%)	0 (-)
Fever	4 (6.7%)	4 (6.7%)
AST increased	3 (5%)	0 (-)
Trombocytopenia	3 (5%)	0 (-)

DISCUSSION

The results of our study suggest that the TTP ratio has additional value when determining the clinical benefit of targeted therapies in early-phase clinical studies. In this phase I population, both TTP ratio and RECIST correlated to OS. However, TTP ratio was also able to differentiate within the RECIST SD group which patients had a longer OS, which could be interpreted as a sign of clinical benefit. TTP ratio measurements were highly reproducible among observers in this study. If validated in other cohorts, this provides an opportunity to determine whether patients classified as having SD actually experienced clinical benefit, and gives more insight as to which patient groups benefit from treatment. Ultimately, we believe the TTP ratio could support drug development by improved detection of early signs of clinical activity.

Furthermore, TTP ratio as an outcome measure was able to detect the efficacy of everolimus in breast and esophageal cancer. Previous studies show that everolimus combined with exemestane is active in breast cancer. However, the beneficial effect of everolimus for esophageal cancer patients has never been fully explored. Early phase studies by Werner et al.[7] and Wainberg et al.[8] report low RRs and a large SD population. Because it remains unclear if patients with SD actually benefit from treatment, further studies were discontinued. Our data, however, suggest that we were able to evaluate whether patients within the SD group indeed had a drug-attributable decrease in tumor growth rate. For all esophageal cancer patients in this study (n = 5), this was, in fact, the case. Despite their heavily pretreated status, these patients seemed to benefit from treatment with everolimus. Taking into account small patient numbers, these results may spark an interest to further investigate everolimus in esophageal cancer.

Despite the advantages discussed above, using the TTP ratio as an end point in clinical studies also has several limitations. First, it has been a laborious effort to perform volumetric measurements (in duplicate) of each CT scan. Volumetric measurements are, and will remain, time-consuming procedures until robust and reliable fully automatic software is developed. Secondly, the wait-and-see period to assess natural growth rate initially raised concerns with physicians and patients. Eight patients (11%) were not able to

start treatment due to clinical deterioration during the waiting period. Percentagewise, this is comparable to the early drop-out rate in large phase I cohorts.[9] In this regard, it is important to realize that participants in this study had no other treatment options besides best supportive care or phase I study participation, with a small chance of treatment success, possible suboptimal dosing and unknown toxicity profiles. A wait-and-see approach is also not necessarily disadvantageous. In this study, six patients had a TTP1 of >100 days. These patients had no strict indication to start treatment immediately and their quality of life was not negatively affected by treatment-related AEs during their waiting period. In addition, a first follow-up CT taking place at 4 weeks ensured early detection of highly progressive tumors with a low threshold to start treatment because a volumetric increase of 30% equals a much smaller increase in diameter.[6] Altogether we feel that the aforementioned considerations legitimate the design of this study and exploratory end point. We cannot exclude the possibility of pseudoprogression in some patients. When adopting the TTP ratio to evaluate the efficacy of treatments that can result in pseudoprogression, we recommend a similar approach as the Immune-Related Response Criteria, namely performing a consecutive CT after 4 weeks to confirm PD.

Previous studies have also recognized the limitations of on-treatment RECIST for targeted therapies and several alternative end points have been explored[4,5,10,11] such as the tumor growth rate (TGR), by Ferté et al.,[11] which compared tumor growth rate on-treatment and before treatment. They compared TGR and RECIST in a large cohort of renal cancer patients treated with sorafenib or everolimus and found that it facilitated detection of early signs of efficacy and was associated with PFS and OS. However, growth rate before treatment was determined retrospectively in the wash-out period, making it a less reliable end point. Another example is the PFS ratio by Von Hoff et al. where PFS according to RECIST was compared with PFS on the previous treatment.[5] Although an intra-patient control is used, the success of the previous treatment is a major determinant of efficacy of the treatment of interest. Although PFS ratio also correlated to OS, PFS ratio was not able to differentiate within the RECIST SD group which patients had a longer OS. The TTP ratio, in contrast to the aforementioned examples, is thus far the only efficacy end point in

which natural growth rate (via intra-patient control) was prospectively determined and which correlated to OS in the RECIST SD group.

To summarize, we believe that measuring clinical benefit according to TTP ratio is of additional value to standard RECIST measurements when determining the efficacy of targeted therapeutics in early-phase clinical studies as it (i) corrects for the natural growth rate of the tumor, (ii) corresponds well with OS in a phase I population of patients, (iii) is able to differentiate which patients had a longer OS within the SD cohort, (iv) shows high inter-observer agreement and (v) is able to identify potential patient groups (i.e. esophageal cancer) that might benefit from treatment. Our findings warrant further exploration and validation of this approach as it could greatly facilitate early detection of drug efficacy and thereby support drug development.

REFERENCES

1. Eisenhauer EA, Therasse P, Bogaerts J, Schwartz LH, Sargent D, Ford R, et al. New response evaluation criteria in solid tumours: revised RECIST guideline (version 1.1). Eur J Cancer. 2009;45(2):228-47

2. Sleijfer S, Wagner AJ. The challenge of choosing appropriate end points in single-arm phase II studies of rare diseases. J Clin Oncol. 2012;30(9):896-8

3. Ratain MJ, Eckhardt SG. Phase II studies of modern drugs directed against new targets: if you are fazed, too, then resist RECIST. J Clin Oncol. 2004;22(22):4442-5

4. Dhani N, Tu D, Sargent DJ, Seymour L, Moore MJ. Alternate endpoints for screening phase II studies. Clin Cancer Res. 2009;15(6):1873-82

5. Von Hoff DD, Stephenson JJ, Jr., Rosen P, Loesch DM, Borad MJ, Anthony S, et al. Pilot study using molecular profiling of patients' tumors to find potential targets and select treatments for their refractory cancers. J Clin Oncol. 2010;28(33):4877-83

6. van Kessel CS, van Leeuwen MS, Witteveen PO, Kwee TC, Verkooijen HM, van Hillegersberg R. Semi-automatic software increases CT measurement accuracy but not response classification of colorectal liver metastases after chemotherapy. Eur J Radiol. 2012;81(10):2543-9

7. Werner D, Atmaca A, Pauligk C, Pustowka A, Jager E, Al-Batran SE. Phase I study of everolimus and mitomycin C for patients with metastatic esophagogastric adenocarcinoma. Cancer Med. 2013;2(3):325-33

8. Wainberg ZA, Soares HP, Patel R, DiCarlo B, Park DJ, Liem A, et al. Phase II trial of everolimus in patients with refractory metastatic adenocarcinoma of the esophagus, gastroesophageal junction and stomach: possible role for predictive biomarkers. Cancer Chemother Pharmacol. 2015;76(1):61-7

9. Olmos D, A'Hern R P, Marsoni S, Morales R, Gomez-Roca C, Verweij J, et al. Patient selection for oncology phase I trials: a multi-institutional study of prognostic factors. J Clin Oncol. 2012;30(9):996-1004

10. Ferte C, Fernandez M, Hollebecque A, Koscielny S, Levy A, Massard C, et al. Tumor growth rate is an early indicator of antitumor drug activity in phase I clinical trials. Clin Cancer Res. 2014;20(1):246-52

11. Ferte C, Koscielny S, Albiges L, Rocher L, Soria JC, Iacovelli R, et al. Tumor growth rate provides useful information to evaluate sorafenib and everolimus treatment in metastatic renal cell carcinoma patients: an integrated analysis of the TARGET and RECORD phase 3 trial data. Eur Urol. 2014;65(4):713-20

3

SUPPLEMENTARY FIGURES
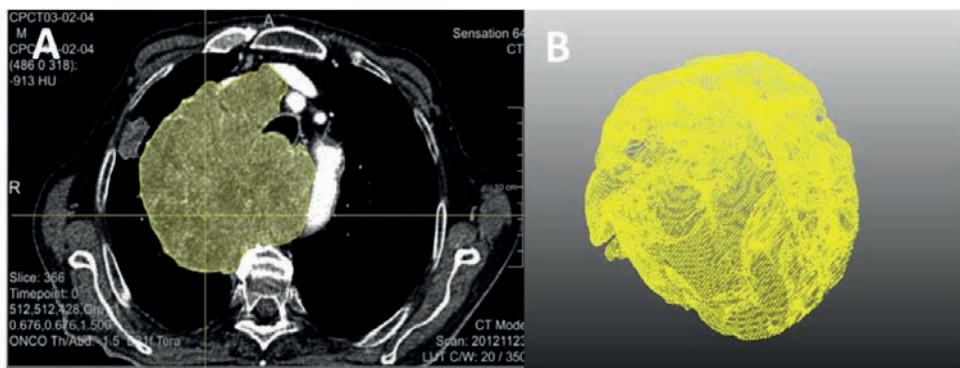
Supplementary Figure 1. Semi-automated volumetric measurements. *A) this figure demonstrates the delineation of the tumor on one CT slice. After delineating the tumor on every single CT slice, you get figure B and the volume is calculated automatically by the computer.*
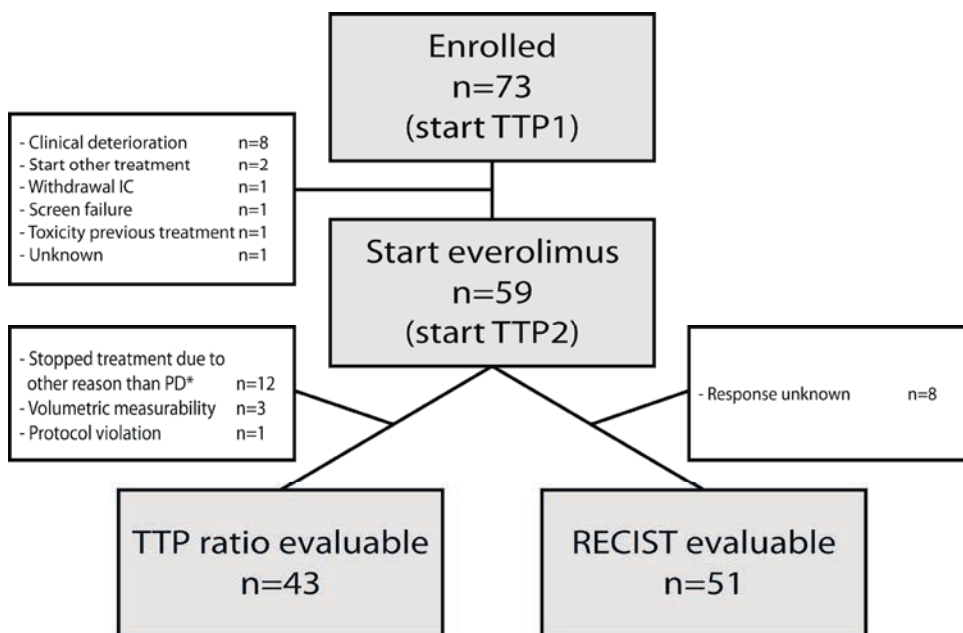
Supplementary Figure 2. Evaluability of patients. *This figure describes the evaluability of patients for the analyses included in this study. The flowchart demonstrates how many of the patients are evaluable for RECIST response and response according to the TTP ratio. A single patient can be evaluable in both cohorts. *Patients are non-evaluable for TTP ratio if they stopped treatment due to reasons other than PD, with the exception of patients that surpassed the threshold for response (<0.7) during follow-up. Abbreviations: IC, Informed Consent; PD, Progressive Disease; TTP1, Time To Progression 1; TTP2, Time To Progression 2.*
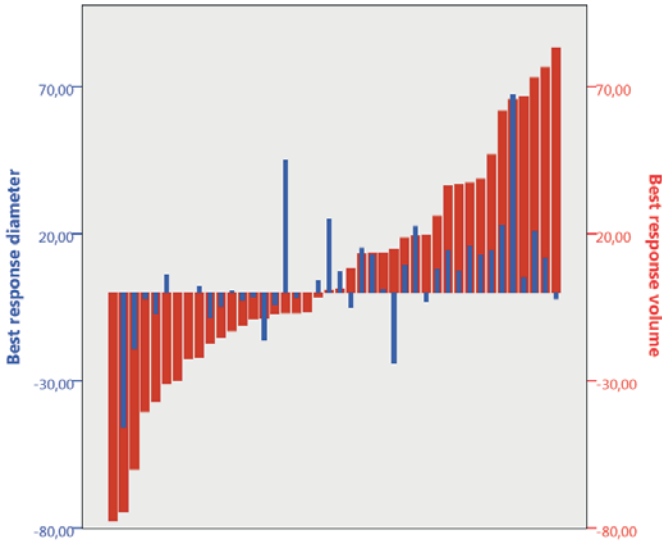
Supplementary Figure 3. Waterfall plot volumetric and RECIST best response. *This figure shows the best response as measured volumetrically (red bar) and by diameter (blue bar) for all patients that were evaluable for both outcomes. Absence of the blue bar means that no change has been detected. Using volumetric measurements, change in tumor size is more easily detected. Both outcome measures are highly concordant in reporting either a decrease or increase in tumor size.*
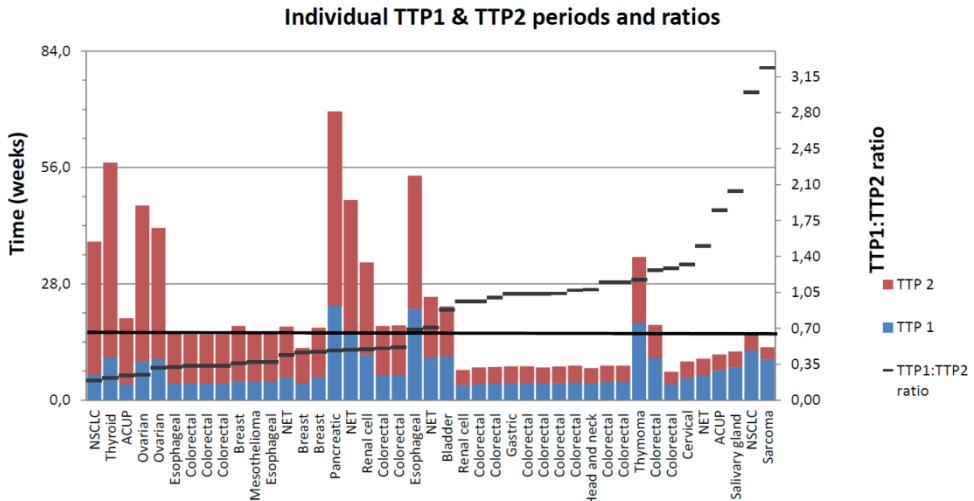
Supplementary Figure 4. Individual TTP1 & TTP2 periods and ratios. *This figure portrays the time to progression pre-treatment (blue bar) and on-treatment (red bar) for individual patients in weeks on the left y-axis. The right y-axis and black stripes represent the TTP ratio.*
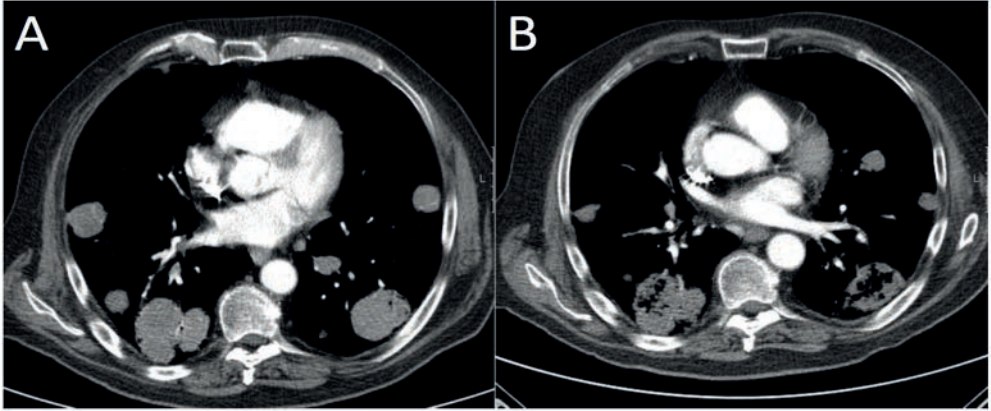
Supplementary Figure 5. CT scan pre- and post-everolimus. *A) pre-treatment scan, B) post-treatment scan which shows substantial necrosis of the lung metastases.*

Conventional dosing of anticancer agents: precisely wrong or just inaccurate?

Sander Bins, Mark J. Ratain, Ron H.J. Mathijssen

Interindividual variability (IIV) in the pharmacokinetics of anticancer drugs is influenced by a wide variety of factors, including body composition, organ function, genetics, and environmental elements.[1] Unfortunately, the body surface area (BSA)–based dosing strategy adjusts only for height and weight and is therefore unlikely to be sufficient to (safely) dose agents with a narrow therapeutic window. Moreover, this approach is conceptually invalid and should be replaced by better alternatives based on fundamental principles of clinical pharmacology.

History

Dose adjustments for BSA acquired their role in oncology in a rather controversial way. In 1958, Donald Pinkel concluded that the maximum tolerable dose of a few cytostatic agents appeared to be quite comparable among different animal species, including humans (both young and adult) if corrected for BSA.[2] The BSA range in his study was huge (from 0.0075 m^2 in mice to 1.85 m^2 in humans). In accordance with this finding and the hypothesis that the most important pharmacological processes are related to body size, the starting dose in oncology phase I studies was thereafter based on BSA.[3] Something remarkable happened: this correction for BSA in early clinical trials was simply generalized to standard-of-care dosing of anticancer drugs in adults, without any additional evidence that this extrapolation was valid. In the decades that followed, the original 1916 formula by Du Bois and Du Bois[4] was modified and simplified by others (i.e., Mosteller[5] in 1987), but the principle remained the same. Even though this almost antique formula was based on the body compositions of (only) nine randomly chosen people, the correlation between all these formulas is strikingly high,[1] making these formulas interchangeable.

Evidence-based dosing?

Although BSA-adjusted dosing has been widely utilized in oncology for decades, there has been extensive criticism of this approach. For many agents (e.g., epirubicin, cisplatin, and irinotecan), studies have demonstrated that this approach has little or no value in achieving the goal of reducing the IIV in exposure.[6] For some drugs (e.g., paclitaxel), a correction for BSA may lead to reduced variability in clearance,[6,7] and BSA is often a significant covariate in population pharmacokinetic models. However,

statistical significance is not necessarily associated with clinical relevance. To clarify this, we took a representative data set of 270 cancer patients treated with paclitaxel chemotherapy, with the pharmacokinetic parameters estimated from a population pharmacokinetic model.[8] This modeling procedure is thought to deliver the most reliable pharmacokinetic data. Following current daily practice, all patients were dosed using BSA. If the BSA for these patients is plotted against paclitaxel clearance, the coefficient of variation is still over 30% (**Figure 1**). If we look at patients with a mean BSA of 1.8 m2, clearance may differ threefold within this subset. In addition, as shown earlier, BSA is not related to paclitaxel toxicity, especially myelosuppression.[9] So, even for drugs like paclitaxel for which correction for BSA has the potential to reduce the IIV, the value of BSA in its dosing strategy is limited and should therefore be seriously questioned. In other words, despite its ability to lower the IIV of some drugs, BSA does not provide enough improvement in IIV to be used as the sole correction factor in dosing strategies.

Another problem with BSA-based dosing is that it leads to a false sense of security. Calculating a dose on the basis of BSA will generate a very precise dose. For instance, for a patient 161 cm tall and weighing 54.7 kg who receives a drug dose of 75 mg/m2, a dose of 117.31 mg (Mosteller[5]) will be displayed on the calculator. Although this dose is very precise, this precision is relevant only if it is also accurate. Unfortunately, the calculation of BSA is not as accurate as we would wish. In an obese population, it was found that the original formula underestimated BSA by 2.7% and 4.5% in males and females, respectively.[10] Precision without accuracy has no medical value.

Practical considerations for choosing a dosing strategy

For newer drugs, particularly those given orally, the concept of BSA-based dosing has already been abandoned, and the starting dose is the same (fixed) for all patients. Because both BSA-adjusted dosing and fixed dosing are strategies with many imperfections, one should balance their workability. Fixed dosing comes with many practical advantages over BSA-adjusted dosing. First, the risk of prescription errors is smaller if there is only one dose to prescribe. A recent French study showed that prescription errors accounted for more than 90% of all errors in dosing chemotherapy, and that, if not discovered in time,

such errors may lead to serious overdosing issues, which in turn could cause potentially life-threatening damage.[11] As a result of the current practice of electronically prescribing anticancer drugs, oncologists are no longer required to calculate a dose because it is automatically generated in many systems. However, this could potentially increase the risk of prescription errors because physicians may fail to recognize their own errors. Furthermore, administration of (oral) drugs by patients themselves is simplified by maintaining only one dose that applies to all patients. This could enhance compliance and will also lead to a reduction in (self-)administration errors. Moreover, it is not always easy to round doses to the nearest strength of available pills. Consequently, many patients are handed a dose of—for example—capecitabine that differs from the calculated dose according to their BSA. Deviating from the calculated dose introduces yet another error.
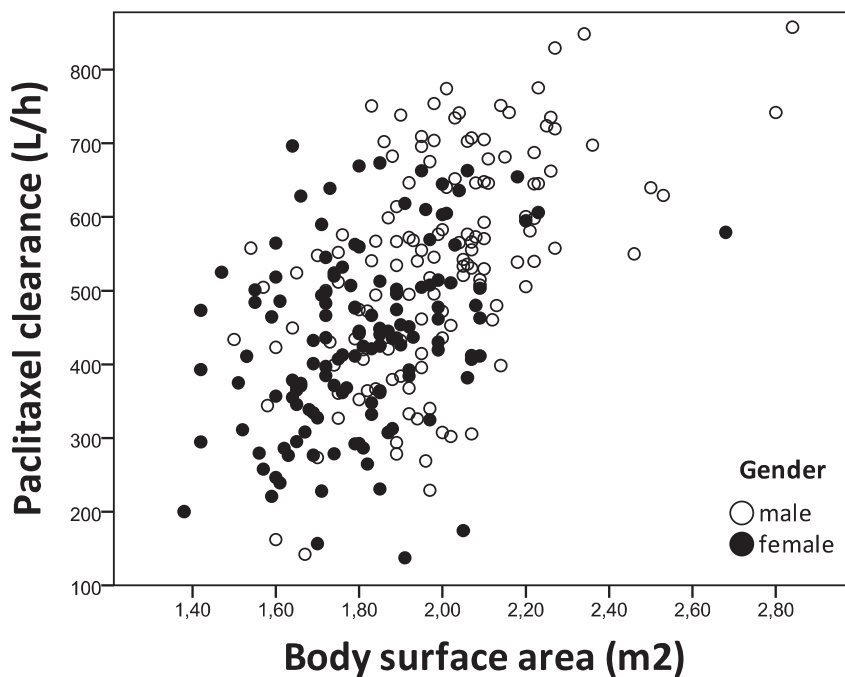
Figure 1. *Relationship between body surface area (x-axis) and the clearance of paclitaxel (based on unbound plasma concentrations) in 270 cancer patients (139 men and 131 women). Raw data were obtained from a recent clinical study.8 The mean clearance ±SD in this group was 488 l/h ± 149 l/h, and the coefficient of variation (CV) was 30.6%. Clearance was significantly higher in male patients (open circles) than in female patients (closed circles) (541 l/h ± 154 l/h; CV 28.5% vs. 432 l/h ± 141 l/h; CV32.7%, respectively; P < 0.001).*

Finally, several parties will benefit from a fixed-dosing strategy. The most obvious benefit concerns the preparation of parenteral drugs for administration, as single-dose vials could be used for all patients (absent any need for dose reduction). This would reduce preparation time and avoid the waste of partial vials.

Some critics say fixed dosing is not realistic because patients with extremely low or high BSAs will be overdosed or underdosed if no correction is made for body size. Therefore, another interesting alternative dosing strategy for BSA was introduced by Plumridge and Sewell.[12] They divided their patients into a few groups (based on a range of BSAs), and all patients within a group received the same dose (**Figure 2**). This dose was based on the mean BSA in that group. This dosing strategy, called dose banding, seems to combine the advantages of both fixed dosing and BSA-based dosing because only a limited number of standard doses (e.g., three or five) need to be available, and patients with extreme body-size measures will receive a dose more adjusted to their body size than the overall mean. A recent study with six cytostatic agents showed that the IIV for dose banding is comparable to that for BSA-based dosing.[13]
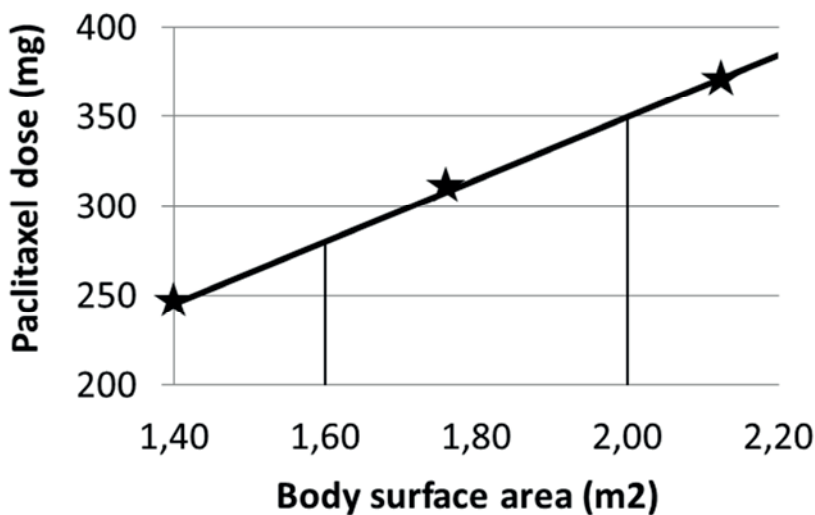
Figure 2. Example of dose banding for paclitaxel, originally dosed at 175 mg/m^2.
The population has been divided into three (arbitrarily chosen) categories (BSA <1.60 m^2, 1.60–2.00 m^2, and >2.00 m^2). In each category, the dose is set on the BSA-adjusted dose for the mean BSA of that category. This leads, after rounding, to three fixed doses of 260, 315, and 370 mg, respectively (indicated by stars). Because the large majority of patients will fall into the middle category, only a small minority receive the low or high fixed dose.

Rational alternatives to BSA

Figure 1 shows clearly that BSA-based dosing is a misconception for dosing paclitaxel chemotherapy. From this figure we also see that clearances differ significantly between men and women (despite the widely overlapping range); nonetheless, in clinical practice we do not distinguish men and women in dosing paclitaxel. If we are truly willing to improve our treatment by personalizing therapies, we should take the crucial step of implementing factors other than body size in our dosing regimens. These factors can be categorized as intrinsic (e.g., age, sex), genetic (e.g., variation in drug-metabolizing enzymes and transporters), and environmental (smoking, comedication, alternative medicine) and are likely to have a much larger influence on IIV than BSA does.[1] Oral drugs are even less likely to be impacted by BSA, given the additional factors of adherence, concomitant food intake, increased risk of drug–drug interactions, and variability in absorption and first-pass metabolism.

When looking for better and more rational options in dosing anticancer drugs, it is important to create a good starting dose. For some drugs, pharmacogenetic differences may help to prevent toxic doses for subgroups of patients (e.g., TPMT genotyping before dosing 6-mercaptopurine). However, any predictive test will have limited accuracy. Alternative phenotyping procedures are in development that might be more accurate than other approaches, with dosing of subsequent cycles based on observed plasma concentrations and toxicities.

Implementation of alternative dosing strategies

Dosing strategies remain a controversial issue in oncology. There are many opinions regarding the ideal way to maximize the likelihood of benefit while minimizing the risk of excessive toxicity. It is unlikely that BSA-based dosing will have the same role in the future that it has today.

Regrettably, despite the coming era of personalized medicine, the majority of the factors influencing the disposition of these agents are not yet taken into account by today's applied dosing strategies. From a practical, ethical, and financial point of view, randomized trials of dosing strategies are unlikely to be conducted. Therefore, we propose the following strategy:

1. For marketed drugs, continue using BSA-based dosing if supported by data. If not, then dose banding is recommended, with adjustment for other important parameters (e.g., food, comedication, smoking, certain genotypes).

2. For investigational drugs, BSA (and weight) should be utilized only if pharmacokinetically or clinically relevant.

Application of this strategy might result in implementation of a more accurate way of dosing anticancer agents in the short term. Nevertheless, practical disadvantages should always be regarded carefully before implementation because the potential obstacles might otherwise outweigh the benefits of this strategy.

One final thought: what if we were currently using another dosing strategy instead of BSA-based dosing? Would the current evidence convince the vast majority of prescribers to switch to BSA-based dosing, or would it be viewed as not worth the effort?

REFERENCES

1. Mathijssen RH, de Jong FA, Loos WJ, van der Bol JM, Verweij J, Sparreboom A. Flat-fixed dosing versus body surface area based dosing of anticancer drugs in adults: does it make a difference? The oncologist. 2007;12(8):913-23

2. Pinkel D. The use of body surface area as a criterion of drug dosage in cancer chemotherapy. Cancer Res. 1958;18(7):853-6

3. Sawyer M, Ratain MJ. Body surface area as a determinant of pharmacokinetics and drug dosing. Investigational new drugs. 2001;19(2):171-7

4. Du Bois D, Du Bois E. Clinical calorimetry: Tenth paper a formula to estimate the approximate surface area if height and weight be known. Arch Intern Med. 1916;17:863-71.

5. Mosteller RD. Simplified calculation of body-surface area. N Engl J Med. 1987;317(17):1098

6. Baker SD, Verweij J, Rowinsky EK, Donehower RC, Schellens JH, Grochow LB, et al. Role of body surface area in dosing of investigational anticancer agents in adults, 1991-2001. J Natl Cancer Inst. 2002;94(24):1883-8

7. Smorenburg CH, Sparreboom A, Bontenbal M, Stoter G, Nooter K, Verweij J. Randomized cross-over evaluation of body-surface area-based dosing versus flat-fixed dosing of paclitaxel. Journal of clinical oncology : official journal of the American Society of Clinical Oncology. 2003;21(2):197-202

8. de Graan AJ, Elens L, Smid M, Martens JW, Sparreboom A, Nieuweboer AJ, et al. A pharmacogenetic predictive model for paclitaxel clearance based on the DMET platform. Clin Cancer Res. 2013;19(18):5210-7

9. Miller AA, Rosner GL, Egorin MJ, Hollis D, Lichtman SM, Ratain MJ. Prospective evaluation of body surface area as a determinant of paclitaxel pharmacokinetics and pharmacodynamics in women with solid tumors: Cancer and Leukemia Group B Study 9763. Clin Cancer Res. 2004;10(24):8325-31

10. Verbraecken J, Van de Heyning P, De Backer W, Van Gaal L. Body surface area in normal-weight, overweight, and obese adults. A comparison study. Metabolism. 2006;55(4):515-24.

11. Ranchon F, Salles G, Spath HM, Schwiertz V, Vantard N, Parat S, et al. Chemotherapeutic errors in hospitalised cancer patients: attributable damage and extra costs. BMC Cancer. 2011;11:478

12. Plumridge RJ, Sewell GJ. Dose-banding of cytotoxic drugs: a new concept in cancer chemotherapy. Am J Health Syst Pharm. 2001;58(18):1760-4

13. Chatelut E, White-Koning ML, Mathijssen RH, Puisset F, Baker SD, Sparreboom A. Dose banding as an alternative to body surface area-based dosing of chemotherapeutic agents. Br J Cancer. 2012;107(7):1100-6

Influence of OATP1B1 Function on the Disposition of Sorafenib-β-D-Glucuronide

Sander Bins, Leni van Doorn, Mitch A. Phelps, Alice A. Gibson, Shuiying Hu, Lie Li, Aksana Vasilyeva, Guoqing Du, Paul Hamberg, Ferry A.L.M. Eskens, Peter de Bruijn, Alex Sparreboom, Ron H.J. Mathijssen and Sharyn D. Baker
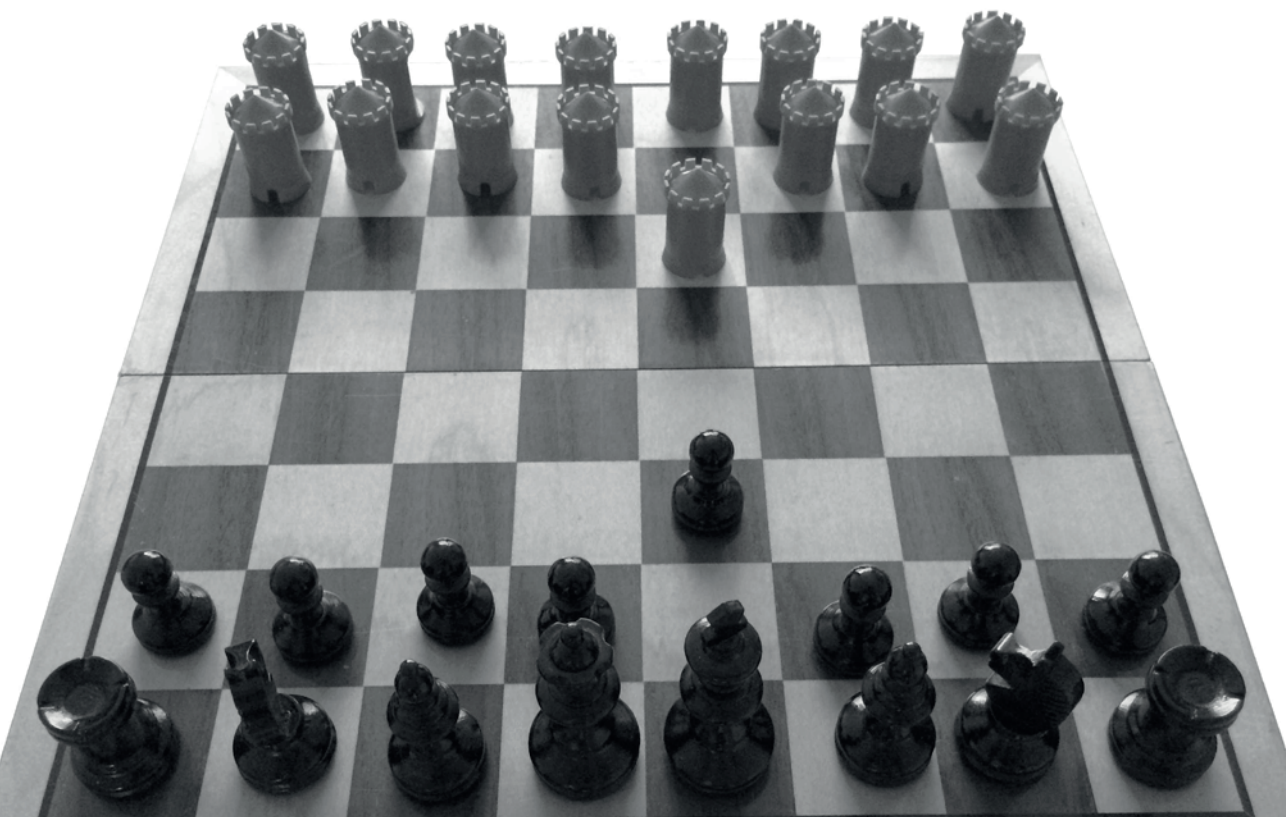
ABSTRACT

Sorafenib undergoes extensive UGT1A9-mediated formation of sorafenib-β-D-glucuronide (SG). This metabolite can be extruded into bile by ABCC2 or follow a liver-to-blood shuttling loop via ABCC3-mediated efflux into the systemic circulation and subsequent uptake in neighboring hepatocytes by OATP1B-type transporters. We assessed SG uptake in OATP1B1, Oatp1b2 and/or ABCC2 transfected cells in the presence and absence of rifampin. The effect of rifampin on the pharmacokinetics of sorafenib and its metabolites was measured in Oatp1b2 knock-out (KO) and wildtype (WT) mice, as well as in 9 sorafenib treated patients in a randomized cross-over trial. The in vitro transport of SG by human OATP1B1 and its murine equivalent Oatp1b2 was potently inhibited by rifampin. In mice, rifampin increased plasma levels of SG 15-fold, but not in Oatp1b2-KO animals. In human subjects on a chronic sorafenib regimen, rifampin acutely more than doubled exposure to SG (P<0.001). We show impaired OATP1B-type transport leads to systemic accumulation of SG. In view of the dominant role of SG in the enterohepatic recirculation of sorafenib, prolonged OATP1B inhibition by co-medication or by an inherited genetic predisposition may lead to reduced plasma levels of sorafenib, and consequently a diminished therapeutic efficacy.

INTRODUCTION

The multikinase inhibitor sorafenib is used as a chemotherapeutic agent in the treatment of multiple malignant diseases, including cancers of the liver, kidney, and thyroid.[1-3] The pharmacokinetic properties of sorafenib are characterized by up to 90% variation in oral exposure between patients receiving the same therapeutic regimen.[4] The high degree of interindividual pharmacokinetic variability observed with sorafenib has important toxicological ramifications. For example, it was recently demonstrated that levels of sorafenib in plasma are correlated with the incidence of skin rash,[5] with dose reduction and study withdrawal due to adverse effects [6], and with the development of severe adverse reactions.[7]

The mechanisms underlying the unpredictable pharmacokinetic profile of sorafenib remain largely unexplained. After oral administration, sorafenib enters hepatocytes by incompletely defined mechanisms,[8, 9] and then undergoes CYP3A4-mediated oxidation[10, 11] and UGT1A9-mediated glucuronidation.[11] A mass balance study of oral sorafenib in humans has shown that 15% of the dose was eliminated as sorafenib-β-D-glucuronide (SG), compared to less than 5% as oxidative metabolites. Interestingly, SG was not detectable in feces, which may be due to its instability in the presence of bacterial glucuronidases present in the gut.[12] Therefore, it has been suggested that the actual contribution of glucuronidation to sorafenib elimination may have been underestimated in the mass balance study,[9] and that, because of its effective secretion into bile,[13] the appearance of SG in the systemic circulation represents an overshoot mechanism that poorly reflects the actual extent of its formation. These observations suggest that a critical determinant of sorafenib's pharmacokinetic variability with possible consequences for clinical management may be associated with differential expression and function of SG transporters regulating its distribution and elimination.[14]

After its formation, SG is secreted into the bile through a process mediated by the ATP-binding cassette efflux transporter ABCC2 (MRP2).[13] Under normal physiologic conditions, a fraction of the hepatocellular SG is secreted back into the blood stream by ABCC3 (MRP3), from where it can be taken up again into downstream hepatocytes via the uptake carrier OATP1B1 (Oatp1b2 in mice) (**Figure 1**).[13] This liver-to-blood shuttling loop called hepatocyte-hopping, may prevent saturation of ABCC2-mediated biliary secretion of

endogenous and xenobiotic glucuronides in upstream hepatocytes, thereby ensuring their efficient biliary elimination and hepatocyte detoxification. Once secreted into bile, SG enters the intestinal lumen where it serves as a substrate for a bacterial β-glucuronidase that produces sorafenib, which subsequently undergoes intestinal absorption and then reenters the systemic circulation.[13] In the current proof-of-concept study, we tested the hypothesis that the hepatocyte hopping of SG can be interrupted by a clinical OATP1B1-mediated drug-drug interaction based on the expectation that inhibition of a hepatic uptake mechanism will lead to acute increases in levels of SG in plasma.

METHODS

Cell lines and chemicals

A model of OATP1B1-expressing cells was created by transfecting HEK293 cells with the pIRES2-EGFP vector (Clontech) containing *SLCO1B1* cDNA. Similarly, HEK293 cells were transfected with the pDream2.1/MCS vector (GenScript) containing *Slco1b2* cDNA. The HEK293 (ATCC® CRL¬1573™) cell line was obtained from ATCC (American Type Culture Collection). This cell line was exclusively used to study drug transport, and was not authenticated by the authors. All stable cell lines were selected and maintained in DMEM supplemented with 10% FBS and G418 sulfate (500-1,000 µg/mL; AG Scientific) at 37ºC under 5% CO_2.

Sorafenib and rifampin were obtained from Chemie Tek. General tritium-labeled sorafenib (specific activity, >1 Ci/mmol; radiochemical purity, >97.1%) was custom made by Moravek Biochemicals, and [³H]estradiol-17β-D-glucuronide (E2G; specific activity, 50.1 Ci/mmol; radiochemical purity, 99.0%), a positive control substrate for OATP1B1 and Oatp1b2, was obtained from American Radiolabeled Chemicals.
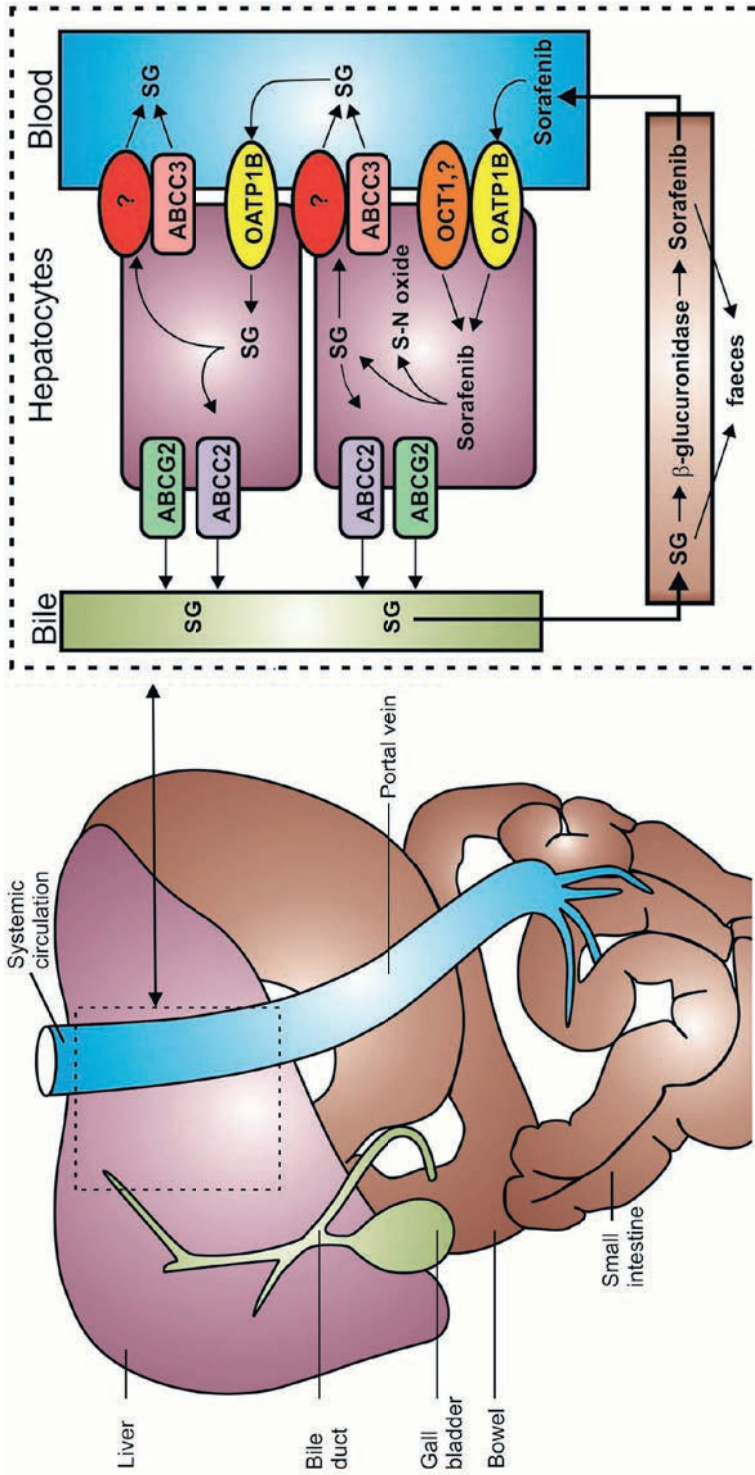
Figure 1. Hepatocyte hopping and recirculation of sorafenib-β-D-glucuronide. *After oral administration, sorafenib enters the hepatocytes by incompletely defined transporters mechanisms, including OATP1B-type carriers and OCT1, and undergoes ABCG2-mediated biliary secretion, CYP3A4-mediated metabolism to sorafenib-N-oxide (S-N-oxide), or UGT1A9- mediated glucuronidation to form sorafenib-β-D-glucuronide (SG). After conjugation, SG is extensively secreted into the bile by a process that is mainly mediated by ABCC2. Under physiological conditions, a fraction of the intracellular SG is secreted by ABCC3 and at least one other transporter back to the blood, from where it can be taken up again into downstream hepatocytes via OATP1B-type carriers. This secretion-and-reuptake loop may prevent the saturation of ABCC2-mediated biliary excretion in the upstream hepatocytes, thereby ensuring efficient biliary elimination and hepatocyte detoxification. Once secreted into bile, SG enters the intestinal lumen where it can either be excreted or serve as a substrate for an as yet unknown bacterial 6-glucuronidase that produces sorafenib, which is subsequently undergoing intestinal absorption and re-enters the systemic circulation.*

5

Uptake studies

Cells were seeded in 6-well plates in phenol red-free DMEM media containing 10% FBS, and were incubated at 37°C for 24 hours. Cells were then washed with warm PBS and incubated with sorafenib or SG in phenol-free DMEM media (without FBS and supplements) at 37°C. Uptake and inhibition studies were performed as outlined in detail elsewhere.[13] The experiment was terminated by placing cells on ice and washing twice with ice-cold PBS. Cells were collected and centrifuged at 1050 r.p.m. for 5 min at 4°C. The cell pellet was lysed in 1 N NaOH by vortex-mixing, incubated at 4°C overnight, and then the solution was neutralized with 2 M HCl. Total protein was measured using a Pierce BCA Protein Assay Kit (Thermo Scientific) and total protein content was quantified using a Biotek µQuant microplate spectrophotometer. Intracellular drug concentrations were determined in the remaining cell lysate by liquid scintillation counting using a LS 6500 Multipurpose Scintillation Counter (Beckman). The experiments were performed in triplicate. Intracellular concentrations of SG were measured by liquid chromatography-tandem mass spectrometry (LC-MS/MS), as described previously.[11]

Transcellular transport

MDCKII cells were transduced with pIRES2 construct containing CFP-ABCC2-V5, GFP-OAT1B1-FLAG, or GFP-OATP1B1-FLAG/CFP-ABCC2-V5 (**Figure 2**). The MDCKII (ATCC® CRL¬2936™) cell line was obtained from ATCC (American Type Culture Collection). This cell line was exclusively used to study drug transport, and was not authenticated by the authors. Transport of SG (1 µM) was performed in 6-well plates (Corning), as described.[11] Trans-epithelial electrical resistance was measured to confirm the integrity of cell monolayers.
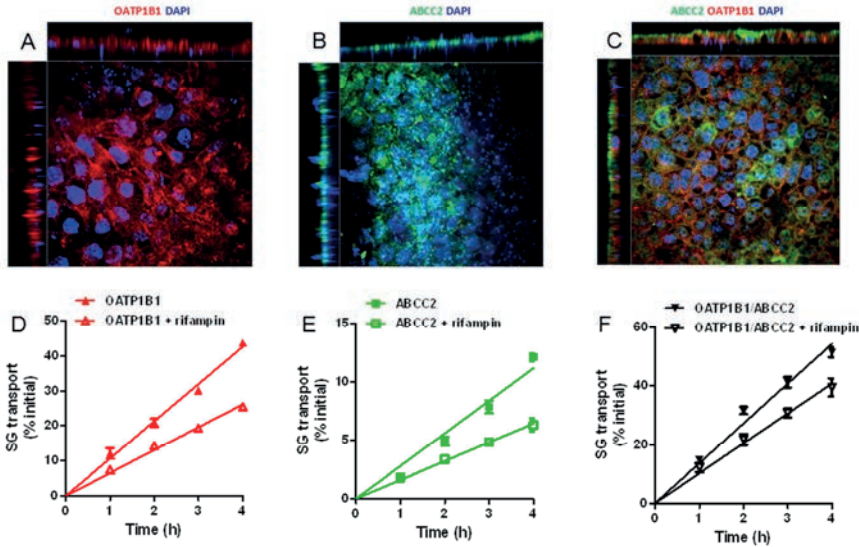
Figure 2. Transcellular transport of SG in transfected MDCKII cells.
*MDCKII cells were stably transduced with pIRES2-GFP-OATP1B1-FLAG (**A**), pIRES2-CFP-ABCC2-V5 (**B**), or both (**C**). Cells were stained with antibodies against FLAG (red; OATP1B1), V5 (green; ABCC2), or both. Panels on top and left sides of the images represent x-z and y-z projections and represent slide to coverslip image where OATP1B1 is visualized on the basolateral membrane and ABCC2 on the apical membrane. Basolateral-to apical transcellular transport of SG in these cells is shown for OATP1B1 (**D**), ABCC2 (**E**), or both (**F**) in the presence or absence of rifampin. Cells were incubated with SG (1 μM) at t=0 then 50-μL aliquots were taken at 1, 2, 3, and 4 hours from the compartment opposite to where the drug was added. Data are expressed as percent of the initial SG concentration, and symbols represent mean ± SE (error bars) of at least 3 replicate experiments.*

Immunofluorescence

MDCKII cells transduced with CFP-ABCC2-V5 and/or GFP-SLCO1B1-FLAG were seeded at 2×10^5 cells/well into 6-transwell plates. When they have reached about 90% confluence, cells were washed with ice-cold PBS, fixed with 4% paraformaldehyde-PBS, permeabilized with 0.1% TritonX-100-PBS and incubated in 3% BSA-PBS blocking buffer. Then, cells were stained with either anti-V5 (Sigma-Aldrich) or anti-FLAG M2 (Sigma-Aldrich) followed by staining with Alexa488 and Alex568 (Life Technologies), respectively, along with DAPI (Invitrogen) to stain the nuclei. Transwell membranes were cut out and placed on a slide, covered with a coverslip, and sealed. Imaging was done using a Marianas spinning disk confocal (SDC) imaging system (Intelligent Imaging Innovations/3i) based on AxioObserver

Z1 inverted microscope (Carl Zeiss MicroImaging). Images were acquired with Zeiss Plan-Apochromat 63× 1.4 NA DIC objective and Evolve 512 EMCCD camera (Photometrics) using SlideBook 5 software (3i).

Murine pharmacokinetics

Eight female mice knockout for Oatp1b2 [Oatp1b2(-/-)] and eight age-matched wild-type mice on a DBA1/lacJ background were bred in-house. Mice were housed in a temperature-controlled environment with a 12-hour light cycle and given a standard diet and water *ad libitum*. Experiments were approved by the Institutional Animal Care and Use Committee.

Sorafenib was formulated in 50% Cremophor EL (Sigma Aldrich) and 50% ethanol, and diluted 1:4 (vol/vol) with deionized water immediately before administration by oral gavage at a dose of 10 mg/kg. Mice were fasted for 3 hours before and during the study, with unrestricted access to drinking water. In four Oatp1b2(-/-) and in four wild-type mice, rifampin (20 mg/kg) was administered intravenously 5 minutes prior to the oral sorafenib administration. At select time points, blood samples (30 μL each) were taken from individual mice at 0.25, 0.5, and 1.5 h from the submandibular vein using a lancet, and at 3, and 4.5 h from the retro-orbital venous plexus using a capillary. A final blood draw was obtained at 7.5 h by a cardiac puncture using a syringe and needle. For sampling via retro-orbital bleeding, mice were anesthetized under 1-5% isoflurane through inhalation, and blood was collected using a heparinized capillary tube. The total blood volume collected during the procedure from each mouse was 150 μL. All blood samples were centrifuged at 3000 × g for 5 min, and plasma was separated and stored at -80°C until analysis. At the terminal time points, liver samples were immediately collected and flash-frozen on dry ice. Liver specimens were stored at -80°C until further processing. Plasma and liver concentrations of sorafenib, sorafenib-N-oxide, and SG were determined by LC-MS/MS, as described previously.[11] Pharmacokinetic parameters were calculated using WinNonlin 6.3 software (Pharsight).

Clinical studies

Patients were enrolled and received standard of care treatment with sorafenib in an open-label randomized cross-over trial. The principle inclusion criteria were: age ≥18 years, confirmed diagnosis of cancer, WHO performance score 0-1, and adequate organ function. Also, patients had to be on steady state of sorafenib, which we had defined as at least 14 days treatment at the same sorafenib dose. The major exclusion criteria were prior liver transplantation, contra-indications for any of the study drugs, and use of any co-medication or supplement that can interact with the study drugs. The sample size of the study was determined to be 9 in order to detect a difference of 239 ng/mL (25%) in steady state exposure to SG in the presence of rifampin, with a significance level of 0.05, power of 0.8, and an estimated SD of the difference between two measurements in one patient of 223 ng/mL (unpublished data). Between August 2013 and March 2015, 9 evaluable patients with hepatocellular carcinoma were included in the clinical study, of which 8 were male and 1 was female. Their mean age was 71 years (range, 62-79) and all patients had WHO performance score 1. Patients were randomized by minimization using the web based application Trial Online Process (TOP). Patient characteristics were entered in TOP by one of the investigators and the patient's trial number and randomization arm were then sent to all investigators in an automatic email from TOP. Four patients were randomized to receive rifampin during the first sampling period and 5 were randomized to rifampin during the second period. The administered sorafenib (Nexavar®; Bayer, the Netherlands) dose was 200 mg BID for 5 patients and 400 mg BID for 4 patients. The study was approved by the institutional review board (Protocol number, MEC 2013-194), and registered in the Dutch Trial Registry (www.trialregister.nl; number NTR4110). All patients provided written informed consent, and the study was conducted in accordance with Good Clinical Practice guidelines and the Declaration of Helsinki (59th WMA General Assembly, Seoul, Republic of Korea, October 2008).

Subjects were admitted to the hospital for two separate days of blood sampling: once with prior rifampin administration and once without. Days of blood sampling were separated by a period of 9 days. Patients were randomized to receive rifampin either in advance of the first or the second sampling period. Rifampin was taken without food as 600 mg tablets (Rifadin®; Sanofi-Aventis, the Netherlands) on the day before and on the

day of sampling at 8 AM, exactly one hour before sorafenib administration. Two and a half hours after sorafenib intake, midazolam (2.5 mg; Actavis, the Netherlands) was administrated intravenously as a probe for CYP3A4 activity.[15] During both hospitalizations, blood samples (6 mL each) for the determination of sorafenib and metabolite levels were collected just before the administration of sorafenib, and 2, 4 and 7.5 hours after the administration of sorafenib. Samples were prepared by centrifugation at 1,200 *g* for 5 minutes to obtain plasma, which was stored at -80°C until analysis. Concentrations of midazolam and its metabolites were measured in three plasma samples taken 2, 4 and 6 hours after midazolam administration during both sample periods. The midazolam samples were centrifuged and stored as described above. WinNonlin 6.3 (Pharsight) was used for calculating pharmacokinetic parameters.

Patients were seen in the outpatient clinic on a weekly basis for clinical examination, laboratory tests, and to evaluate possible side effects. Skin toxicity and diarrhea were managed according to local guidelines. Adverse events were registered according to the National Cancer Institute's CTCAE version 4.03. During the study, dose changes of sorafenib and the use of co-medication that influences CYP3A4 function were not allowed.

Statistical analysis

Pharmacokinetic data are presented as geometric mean and 95% confidence interval. No statistical analyses have been performed on the cell line and murine experiments, since these experiments were replicated less than five times each and these results should therefore be regarded as exploratory. In patients that received sorafenib 200 mg BID, AUCs and absolute concentrations were corrected towards a 400 mg BID dose, i.e. all parameters were doubled, as sorafenib has been described to exhibit linear pharmacokinetics.[16] Statistical analysis was performed using GraphPad Prism 5.0 (GraphPad Software). Geometric means of the pharmacokinetic parameters were compared using two-sided paired t-tests, and *P*<0.05 was considered statistically significant.

RESULTS

Influence of rifampin on SG transport in vitro

Experiments were initially carried out with HEK293 cells expressing OATP1B1 or its murine equivalent Oatp1b2 using the recommended model substrate estradiol-17β-glucuronide (E2G),[17] and the clinically-relevant OATP1B-type transporter inhibitor rifampin.[18] Following a 15-min incubation period, E2G uptake by human OATP1B1 and mouse Oatp1b2 was strongly inhibited by a pre-incubation with rifampin (30 μM) (**Figure 3A-B**). Since rifampin-mediated inhibition of OATP1B1 can be substrate-dependent, with up to 12-fold variation in IC50 values,[19] we next used SG as a test substrate in the same models. Similar to E2G, the intracellular uptake of SG by both OATP1B1 and Oatp1b2 was efficiently inhibited by rifampin (**Figure 3A-B**), and this process was dependent on the rifampin concentration (**Figure 3C**). The resulting IC50 values of approximately 1 μM for both OATP1B1 and Oatp1b2 were similar to those reported previously for uptake inhibition by rifampin of other substrates.[20] As measured plasma levels of rifampin after an oral dose of 600 mg reach >7 μM,[21] the intrinsic likelihood of an OATP1B1-mediated pharmacokinetic drug-drug interaction between rifampin and SG is high.

Because rifampin is also a known inhibitor of various ABC transporters,[22] and can influence the transport of SG in inside-out vesicles expressing ABCC2,[13] we next evaluated the influence of rifampin on the flux of SG in MDCKII cells engineered to overexpress OATP1B1, ABCC2, or both OATP1B1 and ABCC2 (**Figure 2**). Transfection of OATP1B1 (basolaterally localized) into MDCKII cells significantly increased the basal-to-apical transport of SG, and this translocation was diminished in the presence of rifampin (**Figure 2D**). However, the basal-to-apical flux of SG was not substantially enhanced by co-transfection of ABCC2 (apically localized), and not further reduced by rifampin in cells expressing both OATP1B1 and ABCC2 (**Figure 2D**). This suggests that rifampin can be utilized for *in vivo* studies as a bona fide inhibitor of SG transport by OATP1B-type carriers.
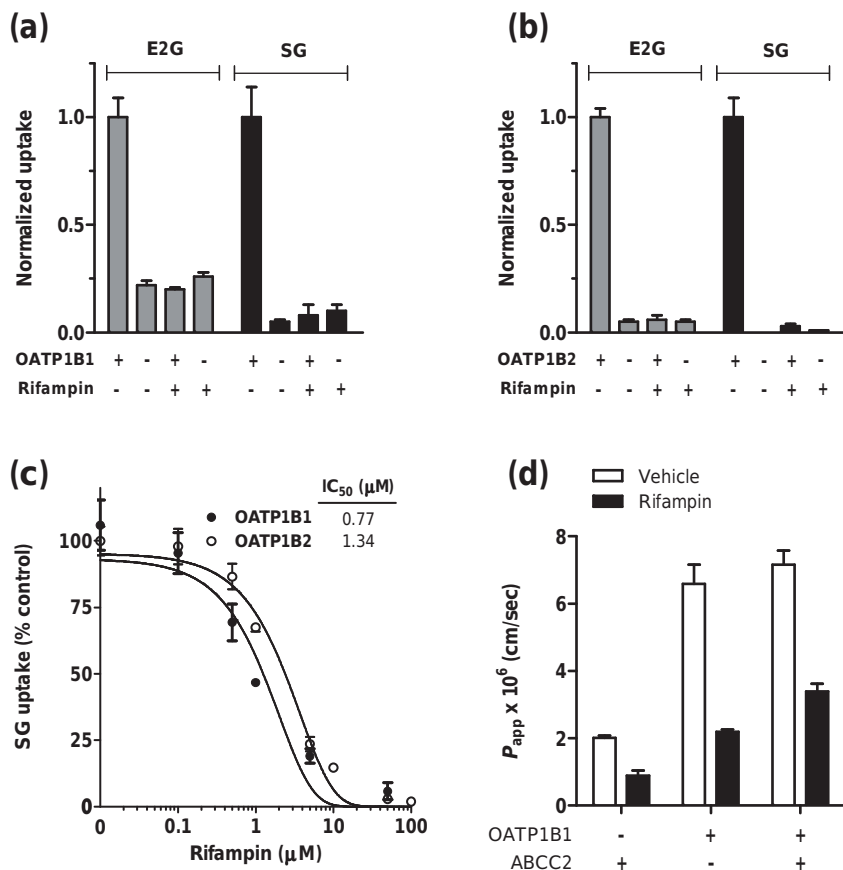
Figure 3. Transport of SG by OATP1B-type transporters.

*Transport of estradiol-17β-glucuronide (E2G; 0.1 µM) and sorafenib-β-D-glucuronide (SG; 10 µM) in HEK293 cells engineered to overexpress OATP1B1 (**a**) or OATP1B2 (**b**) with or without rifampin (20 µM). All results are normalized to the transport rate in OATP1B transfected cells without rifampin, i.e. the experiments with unrestricted OATP1B effect, which were 4.77 pmol/mg protein (OATP1B1) and 26.73 pmol/mg protein (OATP1B2) in 15 minutes for E2G, and 57.46 pmol/mg protein (OATP1B1) and 770.17 pmol/mg protein (OATP1B2) in 15 minutes for SG. (**c**) Inhibition of OATP1B1 or OATP1B2-mediated transport of SG (10 µM) by different concentrations of rifampin (0-100 µM). Data are normalized to the relative uptake without rifampin, i.e. when the function of OATP1B is unrestricted, and represent the mean ± SE from 3-4 independent experiments (9-12 replicates). (**d**) Transcellular transport of SG in MDCKII cells expressing OATP1B1 and/or ABCC2. Cells were incubated with SG (1 µM), and 50-µl aliquots were taken at 1, 2, 3, and 4 hours from the compartment opposite to where the drug was added, in the presence or absence of rifampin (100 µM). Data are expressed as transporter-mediated apparent permeability coefficient (P_{app}) for the basolateral to apical direction (B-to-A). Data represent the mean ± SE (at least 3 replicates).*
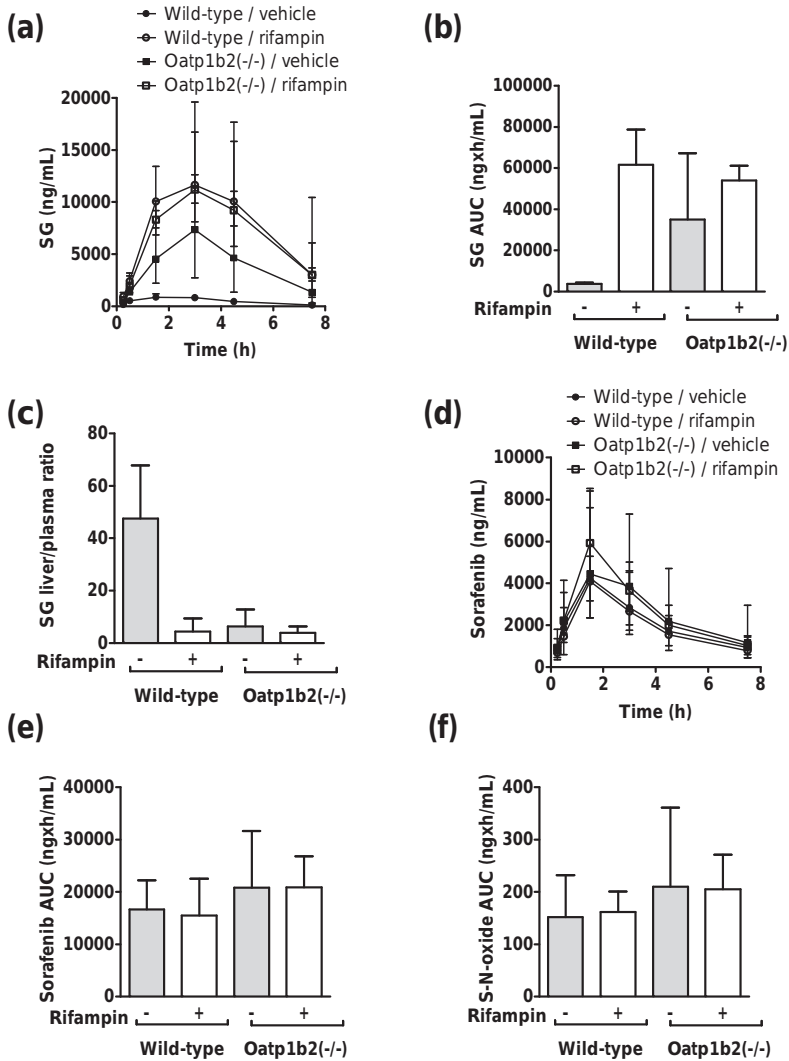
Figure 4. Pharmacokinetics of sorafenib and SG in wild-type and Oatp1b2(-/-) mice.
Plasma concentration-time profiles of SG (a) and sorafenib (d) in wild-type mice and Oatp1b2(-/-) mice in the presence and absence of rifampin pretreatment. Corresponding area under the plasma concentration-time curves (AUCs) of SG, sorafenib, and sorafenib-N-oxide (S-N-oxide) are shown in (b), (e), and (f). Sorafenib was administered orally at a dose of 10 mg/kg with or without pretreatment with rifampin (20 mg/kg). Livers were taken at 7.5 h after sorafenib administration (n=4 per group), with results expressed as the liver-to-plasma concentration ratio of SG (c). Concentrations in liver were normalized to corresponding concentrations in plasma. All data represent the geometric mean and the 95% confidence interval.

Table 1. Sorafenib pharmacokinetic parameters in mice.*

Parameter	Wild-type		Oatp1b2(-/-)	
	With rifampin (n=4)	Without rifampin (n=4)	With rifampin (n=4)	Without rifampin (n=4)
Sorafenib				
C_{max} (ng/mL)	4,089 (3,163-5,285)	4,238 (2,357-7,623)	5,926 (4,120-8,524)	4,884 (3,172-7,519)
AUC (ng×h/mL)	15,001 (9,495-23,701)	16,318 (11,302-23,560)	20,570 (15,035-28,142)	19,903 (11,298-35,060)
SG				
C_{max} (ng/mL)	12,748 (9,010-18,037)	880 (678-1,142)	11,180 (9,892-12,634)	7,746 (3,375-17,776)
AUC (ng×h/mL)	60,735 (45,157-81,687)	3,972 (3,316-4,758)	53,870 (47,349-61,289)	31,373 (19,371-50,811)
Sorafenib N-oxide				
C_{max} (ng/mL)	29 (22-37)	29 (18-46)	38 (28-51)	38 (18-81)
AUC (ng×h/mL)	160 (124-208)	145 (83-253)	203 (151-272)	192 (87-427)

Sorafenib was administered by oral gavage at a dose of 10 mg/kg. Rifampin was administered intravenously at a dose of 20 mg/kg, 5 minutes in advance of sorafenib administration.

*Values represent geometric mean with 95% confidence interval in parenthesis.

Abbreviations: AUC, area under the plasma concentration-time curve; C_{max}, peak plasma concentration; SG, sorafenib-β-D-glucuronide.

Effects of rifampin on SG disposition in mice

The *in vivo* role of rifampin (20 mg/kg) in the transport of SG was next evaluated in wild-type mice and Oatp1b2-deficient [Oatp1b2(-/-)] littermates receiving a single oral dose of sorafenib (10 mg/kg). This experiment was based on the expectation that the systemic exposure to SG would increase by rifampin in an Oatp1b2-dependent manner, as predicted from our *in vitro* transport experiments. In line with our previous findings,[9] Oatp1b2-deficiency in mice was associated with a substantially increased systemic exposure to SG (**Figure 4**; **Table 1**).

The liver-to-plasma ratio of SG was reduced by approximately 90% in wild-type mice pre-treated with rifampin, and similar to that observed in Oatp1b2(-/-) mice receiving sorafenib either alone or when given in combination with rifampin (**Figure 4C**). Oatp1b2-deficiency and/or rifampin pre-treatment did not substantially affect the plasma levels of sorafenib parent drug or of its primary oxidated metabolite sorafenib-N-oxide (**Figure 4D-F**). This observation is consistent with our previous finding that sorafenib itself is not a transported substrate of Oatp1b2,[9] and with the contention that the applied single dose of rifampin is unlikely to have artificially influenced other enzymes and transporters of relevance to the disposition of sorafenib or SG.

Effects of rifampin on SG disposition in humans

We next assessed the influence of pre-treatment with rifampin (two daily oral doses of 600 mg) on the pharmacokinetics of SG in human subjects receiving oral sorafenib at steady-state using an open-label randomized cross-over design. As predicted from the murine pharmacokinetic studies, we found that concomitant rifampin administration resulted in acute, statistically significant increases in the systemic exposure to SG (32,479 ng×h/mL *versus* 14,646 ng×h/mL; $P<0.001$) (**Figure 5A**; **Table 2**), and this was independent of the randomization sequence (**Figure 5B**).
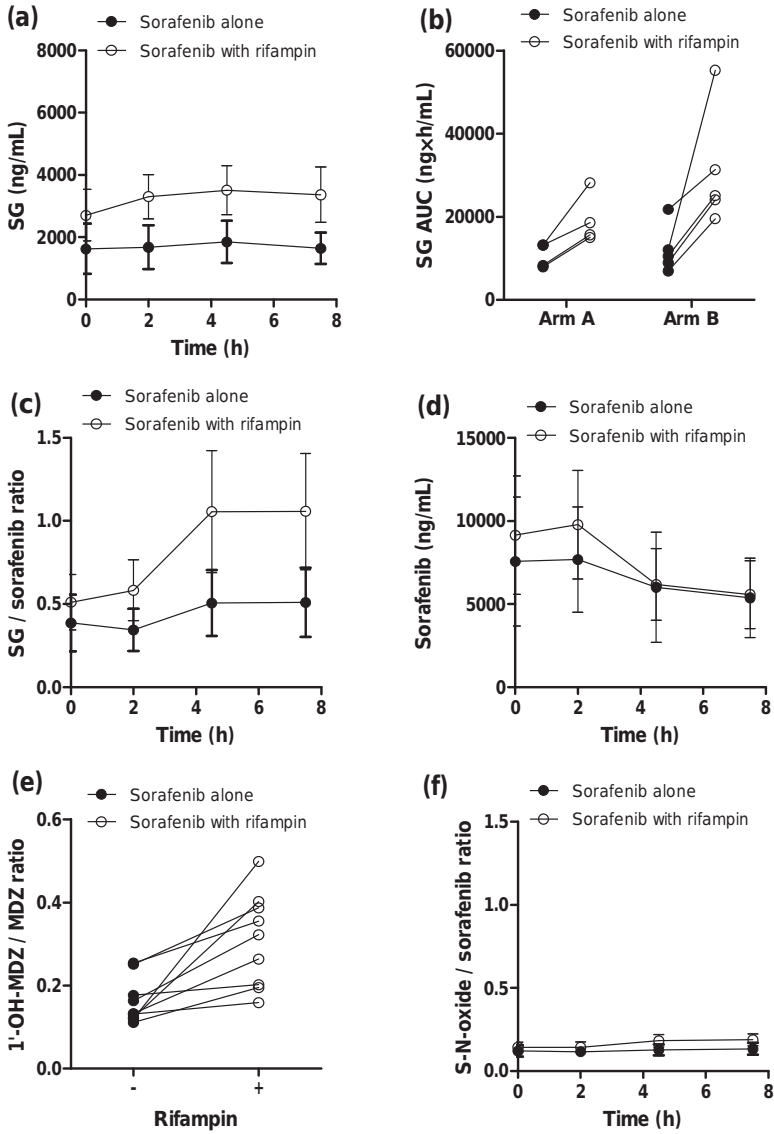
Figure 5. Influence of rifampin on the pharmacokinetics of sorafenib in humans.

Plasma concentration-time profiles of SG (a) and sorafenib (d) in patients with hepatocellular carcinoma in the presence and absence of rifampin pretreatment. The corresponding area under the plasma concentration-time curve (AUC) of SG is shown as a function of the randomization sequence of the cross-over trial (b). The metabolic ratios for SG to sorafenib, 1'-hydroxy-midazolam (1'-OH-MDZ) to midazolam (MDZ) and sorafenib-N-oxide (S-N-oxide) to sorafenib are shown in (c), (e), and (f), respectively. All data represent the geometric mean and the 95% confidence interval.

Table 2. Sorafenib pharmacokinetic parameters in humans.*

Parameter	With rifampin (n=9)	Without rifampin (n=9)	Ratio**	P-value
Sorafenib				
C_{max} (ng/mL)	9,761 (7,085-13,447)	7,786 (5,384-11,261)	1.25 (0.93-1.69)	0.07
AUC (ng×h/mL)	44,214 (32,509-60,132)	38,017 (27,282-52,976)	1.16 (0.80-1.70)	0.25
SG				
C_{max} (ng/mL)	5,374 (3,877-7,447)	2,561 (1,839-3,567)	2.10 (1.41-3.12)	<0.001
AUC (ng×h/mL)	32,479 (23,421-45,040)	14,646 (10,484-20,459)	2.22 (1.52-3.24)	<0.001
Sorafenib N-oxide				
C_{max} (ng/mL)	1,464 (1,037-2,065)	919 (563-1,501)	1.59 (1.01-2.52)	0.03
AUC (ng×h/mL)	7,074 (4,957-10,093)	4,489 (2,851-7,068)	1.58 (0.97-2.56)	0.04

Sorafenib was administered orally at a dose of 200 mg BID or 400 mg BID. Rifampin was administered orally at a dose of 600 mg.
Values represent geometric mean with 95% confidence interval in parenthesis.
***With rifampin / without rifampin.*
Abbreviations: AUC, area under the plasma concentration-time curve; C_{max} peak plasma concentration; SG, sorafenib-β-D-glucuronide.

5

The mean metabolic ratios of SG to sorafenib in the studied patient cohort were also significantly increased during rifampin administration (**Figure 5C**). No statistically significant differences were observed in the pharmacokinetic parameter estimates of sorafenib (**Figure 5D**). Although the mean ratio between 1'-hydroxymidazolam and midazolam, used as a measure of CYP3A4 activity changes,[23] was approximately 2 times higher after rifampin intake (*P*=0.005; **Figure 5E**), the extent of sorafenib-N-oxide formation was not different between treatment cycles (**Figure 5F**). During the course of the clinical study, no toxicities were observed that could be attributed to rifampin or midazolam. In one patient, bilirubin levels in plasma were elevated from 14 to 29 μM (upper limit of normal, 16 μM) on the second day of rifampin intake, but bilirubin levels normalized to baseline within 2 days.

DISCUSSION

This study shows that acute inhibition of the hepatic uptake transporter OATP1B1 by rifampin results in a substantial pharmacokinetic interaction with SG at steady-state in human subjects receiving oral sorafenib. This finding not only emphasizes the need to consider hepatic handling of xenobiotic glucuronides in the design of pharmacokinetic drug-drug interaction studies of agents that undergo extensive Phase II conjugation, but also has potentially direct clinical relevance for the chemotherapeutic treatment with sorafenib.

It was previously suggested based on *in vitro* microsomal studies that the most prominent pathway of sorafenib elimination consists of CYP3A4-mediated metabolism leading to the formation of sorafenib-N-oxide and several other metabolites.[8] This finding suggested that sorafenib was potentially subject to a host of CYP3A4-mediated drug interactions with commonly co-prescribed medications.[24] Here, the AUCs of the CYP3A4-mediated metabolites of midazolam and sorafenib were nearly 2 times higher after rifampin, but – to a smaller extent – this was also true for sorafenib. As the ratio of sorafenib-N-oxide to sorafenib did not change between both cycles, the interaction of rifampin on sorafenib-N-oxide formation does not seem to be relevant. Additionally, the prototypical CYP3A4 inhibitor ketoconazole has been demonstrated to have no influence on the pharmacokinetics of sorafenib in healthy male volunteers after single-dose

sorafenib administration, suggesting that the fraction of sorafenib that is metabolized by the Phase I oxidative pathway is low.[12] However, although clinical data suggest that sorafenib glucuronidation accounts for only 15% of the dose, it is likely that this percentage is grossly underestimated,[13] and may be increased further if the competing CYP3A4-mediated pathway is inhibited.[12] The long-term clinical implications of such pharmacokinetic drug-drug interaction remain unstudied.

The use of rifampin as an OATP1B1 inhibitor in our studies was based on considerations published elsewhere.[18] The relatively strong impact of rifampin on SG levels in mice (>9-fold increase) compared with humans (~2-fold) likely reflects a differential direct influence of rifampin on the uptake of sorafenib itself into hepatocytes, which process is partially dependent on OATP1B-type transporters in humans but appears of less relevance in mice.[9] In addition, SG is known to undergo substantial renal excretion in humans but not in mice,[13] and the possible presence of a rifampin-insensitive escape mechanism in the kidney may result in shunting of SG to urine when OATP1B1 function in humans is impaired.

It should also be pointed out that, although acute exposure to rifampin inhibits OATP1B1,[25] extended daily administration of rifampin may induce enzymes and transporters of putative relevance to sorafenib. For example, exposure to rifampin for 5 days or more dramatically increased the clearance of the CYP3A4 substrate drugs midazolam,[26] alfentanil,[27] and erythromycin.[28] Several recent studies have evaluated the effects of acute and extended exposure to rifampin on CYP3A4 activity in the same individuals. For example, rifampin 600 mg given once daily for 1-2 doses (acute exposure) and for 6.5 days (extended exposure) changed the systemic exposure to bosentan, a dual OATP1B1 and CYP3A4 substrate drug, by +500% and -58%, respectively.[29] If induction of enzymes occurs, it is likely that rifampin exposure for 5 days or more is required to cause a clinically-relevant, induced CYP3A4 phenotype. Because CYP3A4 induction seems to play only a modest role here, the present observations with sorafenib in conjunction with acute exposure to rifampin may not be extrapolated to the situation where the agent is co-administered with rifampin for an extended period of time or have relevance to a scenario in which other OATP1B1-interfering medications are co-prescribed with sorafenib.

Interestingly, administered at a dose of 600 mg once daily for 5 days with a single oral dose of sorafenib in healthy volunteers, rifampin was previously found to cause a 37% decrease in the mean systemic exposure to sorafenib.[30] The causal connection of this observation with altered CYP3A4 activity, however, remains uncertain and other plausible mechanisms could contribute to the reported observations. For example, prolonged exposure to rifampin can significantly upregulate OATP1B1 and ABCC2 in primary hepatocytes,[31] and can induce *UGT1A9* mRNA and UGT1A9 activity in human subjects after 6 days of exposure to a once daily dose of 600 mg.[32] Interestingly, prolonged treatment with rifampin may also affect the hepatic expression and function of the uptake transporter OCT1,[33] which has been proposed as a possible hepatic uptake carrier of sorafenib.[8, 34] However, this may not be of concern clinically, since recent studies in mice with a hepatic OCT1-deficiency indicate this transporter plays only a relatively minor role in the overall elimination of sorafenib.[35]

The potential clinical ramifications of the hepatocyte-hopping phenomenon of SG and the impact of interference in this process with transporter inhibitors such as rifampin requires additional investigation. For example, it should be examined if excessive systemic accumulation of SG leads to adverse events, as is the case with morphine-6-glucuronide.[36] This is further emphasized by the fact that single nucleotide polymorphisms in *SLCO1B1* are associated with the risk of sorafenib toxicity.[37] On the other hand, future research should be aimed at the consequences of reduced biliary SG excretion on the maintenance of systemic sorafenib exposure: sorafenib undergoes enterohepatic recirculation[38] following bacterial β-glucuronidase-mediated de-conjugation of SG within the intestinal lumen,[39] and interference of this de-conjugation by neomycin treatment decreases the systemic exposure to sorafenib by more than 50% (Nexavar package insert). It can be envisaged that interference of the biliary excretion of SG by inhibition of OATP1B1-mediated uptake into hepatocytes could potentially lead to diminished enterohepatic recycling of sorafenib and, ultimately, a reduced systemic exposure to the pharmacologically active species. A similar phenomenon has been recently reported for mycophenolate mofetil, an immune-suppressive drug that, like sorafenib, undergoes extensive glucuronidation. In this case, a cohort of renal transplant patients with an inherited genotype associated with decreased OATP1B1 function had reduced circulating

levels of the active moiety, mycophenolic acid, and a concomitant increase in the levels of its glucuronide metabolite, presumably due to a disturbance in enterohepatic cycling.[40] Although phenotypes similar to those reported for mycophenolate mofetil were not observed with sorafenib, it should be pointed out that our current study was neither designed nor statistically powered to observe effects of rifampin treatment on parent drug levels, despite the fact that we administered rifampin a day longer than recommended by the International Transporter Consortium[18] in order to be able to observe the maximal effect on parent drug levels. It is also conceivable that direct inhibition of OATP1B1-mediated transport of sorafenib by rifampin in the studied patient population, in addition to an independent inhibitory effect of rifampin on SG transport by OATP1B1, could have masked an influence on enterohepatic recirculation.

Overall, our findings signify an important contribution of OATP1B1 in the elimination of sorafenib in humans, whereby compromised OATP1B1 function leads to systemic SG accumulation, of which the clinical relevance needs to be assessed. The OATP1B1-related excretion of SG seems to take place via a sinusoidal liver-blood shuttling loop. As the design of this study was not suitable to detect the influence of OATP1B1 inhibition on sorafenib exposure, the theory for lower systemic sorafenib exposure after prolonged OATP1B1 inhibition still cannot be rejected, with important potential ramifications illustrated by the established exposure-toxicity relationships. We expect that the current observations with sorafenib may have relevance to other kinase inhibitors undergoing Phase II conjugation through glucuronidation (**Table 3**). Therefore, the effects of prolonged OATP1B1 inhibiting factors, e.g. clarithromycin[41] and ramipiril,[20] on the pharmacokinetics of glucuronidated drugs should be assessed. Until then, we suggest that caution is warranted if such drugs have to be administered together with agents that potently inhibit OATP1B-type transporters.

Table 3. Kinase inhibitors undergoing glucuronidation.

Compound	Target	Enzyme(s)	Ref.
ASP015K	JAK1/3	N/a	[42]
Apatinib	VEGFR2	UGT2B7, 1A4	[43]
Axitinib	VEGFR1-3	UGT1A1, 1A3, 1A9	[44, 45]
BMS-690514	pan-ErbB	UGT2B4, 2B7	[46]
Briciclib	Cyclin D1	N/a	[47]
Cediranib	VEGFR2	UGT1A4	[48]
Dasatinib	BCR/ABL	N/a	[49]
Flavopiridol	CDK	UGT1A9	[50]
Flumatinib	BCR/ABL	N/a	[51]
Fostamatinib	SYP	N/a	[52]
JNJ-10198409	PDGFR	N/a	[53]
MDC-1016	RAS	N/a	[54]
NU7026	DNA-PKcs	N/a	[55]
OTS167	MELK	UGT1A1, 1A3	[56]
PKI-166	EGFR	N/a	[57]
Regorafenib	Multikinase	UGT1A9	[14]
Ruxolitinib	JAK1/2	N/a	[58]
Sapitinib	Pan-ErbB	N/a	[59]
Sorafenib	Multikinase	UGT1A9	[11]
Tanzisertib	JNK	UGT1A1, 1A4, 1A10, 2B4	[60, 61]
Trametinib	MEK	N/a	[62]
Vandetanib	VEGFR2	N/a	[63]

Abbreviation: N/a, not available.

REFERENCES

1. Escudier B, Eisen T, Stadler WM, Szczylik C, Oudard S, Siebels M, et al. Sorafenib in advanced clear-cell renal-cell carcinoma. N Engl J Med. 2007;356(2):125-34

2. Brose MS, Nutting CM, Jarzab B, Elisei R, Siena S, Bastholt L, et al. Sorafenib in radioactive iodine-refractory, locally advanced or metastatic differentiated thyroid cancer: a randomised, double-blind, phase 3 trial. Lancet. 2014;384(9940):319-28

3. Llovet JM, Ricci S, Mazzaferro V, Hilgard P, Gane E, Blanc JF, et al. Sorafenib in advanced hepatocellular carcinoma. N Engl J Med. 2008;359(4):378-90

4. Strumberg D, Clark JW, Awada A, Moore MJ, Richly H, Hendlisz A, et al. Safety, pharmacokinetics, and preliminary antitumor activity of sorafenib: a review of four phase I trials in patients with advanced refractory solid tumors. Oncologist. 2007;12(4):426-37

5. Kuczynski EA, Lee CR, Man S, Chen E, Kerbel RS. Effects of Sorafenib Dose on Acquired Reversible Resistance and Toxicity in Hepatocellular Carcinoma. Cancer research. 2015;75(12):2510-9

6. Shimada M, Okawa H, Kondo Y, Maejima T, Kataoka Y, Hisamichi K, et al. Monitoring Serum Levels of Sorafenib and Its N-Oxide Is Essential for Long-Term Sorafenib Treatment of Patients with Hepatocellular Carcinoma. Tohoku J Exp Med. 2015;237(3):173-82

7. Fucile C, Marenco S, Bazzica M, Zuccoli ML, Lantieri F, Robbiano L, et al. Measurement of sorafenib plasma concentration by high-performance liquid chromatography in patients with advanced hepatocellular carcinoma: is it useful the application in clinical practice? A pilot study. Med Oncol. 2015;32(1):335

8. Swift B, Nebot N, Lee JK, Han T, Proctor WR, Thakker DR, et al. Sorafenib hepatobiliary disposition: mechanisms of hepatic uptake and disposition of generated metabolites. Drug Metab Dispos. 2013;41(6):1179-86

9. Zimmerman EI, Hu S, Roberts JL, Gibson AA, Orwick SJ, Li L, et al. Contribution of OATP1B1 and OATP1B3 to the disposition of sorafenib and sorafenib-glucuronide. Clin Cancer Res. 2013;19(6):1458-66

10. Ghassabian S, Rawling T, Zhou F, Doddareddy MR, Tattam BN, Hibbs DE, et al. Role of human CYP3A4 in the biotransformation of sorafenib to its major oxidized metabolites. Biochem Pharmacol. 2012;84(2):215-23

11. Zimmerman EI, Roberts JL, Li L, Finkelstein D, Gibson A, Chaudhry AS, et al. Ontogeny and sorafenib metabolism. Clin Cancer Res. 2012;18(20):5788-95

12. Lathia C, Lettieri J, Cihon F, Gallentine M, Radtke M, Sundaresan P. Lack of effect of ketoconazole-mediated CYP3A inhibition on sorafenib clinical pharmacokinetics. Cancer Chemother Pharmacol. 2006;57(5):685-92

13. Vasilyeva A, Durmus S, Li L, Wagenaar E, Hu S, Gibson AA, et al. Hepatocellular Shuttling and Recirculation of Sorafenib-Glucuronide Is Dependent on Abcc2, Abcc3, and Oatp1a/1b. Cancer Res. 2015;75(13):2729-36

14. Tlemsani C, Huillard O, Arrondeau J, Boudou-Rouquette P, Cessot A, Blanchet B, et al. Effect of glucuronidation on transport and tissue accumulation of tyrosine kinase inhibitors: consequences for the clinical management of sorafenib and regorafenib. Expert opinion on drug metabolism & toxicology. 2015;11(5):785-94

15. Mathijssen RH, van Schaik RH. Genotyping and phenotyping cytochrome P450: perspectives for cancer treatment. Eur J Cancer. 2006;42(2):141-8

16. Di Gion P, Kanefendt F, Lindauer A, Scheffler M, Doroshyenko O, Fuhr U, et al. Clinical pharmacokinetics of tyrosine kinase inhibitors: focus on pyrimidines, pyridines and pyrroles. Clinical pharmacokinetics. 2011;50(9):551-603

17. Izumi S, Nozaki Y, Maeda K, Komori T, Takenaka O, Kusuhara H, et al. Investigation of the impact of substrate selection on in vitro organic anion transporting polypeptide 1B1 inhibition profiles for the prediction of drug-drug interactions. Drug Metab Dispos. 2015;43(2):235-47

18. International Transporter Consortium, Giacomini KM, Huang SM, Tweedie DJ, Benet LZ, Brouwer KL, et al. Membrane transporters in drug development. Nat Rev Drug Discov. 2010;9(3):215-36

19. Izumi S, Nozaki Y, Komori T, Maeda K, Takenaka O, Kusano K, et al. Substrate-dependent inhibition of organic anion transporting polypeptide 1B1: comparative analysis with prototypical probe substrates

estradiol-17beta-glucuronide, estrone-3-sulfate, and sulfobromophthalein. Drug Metab Dispos. 2013;41(10):1859-66

20. Gui C, Obaidat A, Chaguturu R, Hagenbuch B. Development of a cell-based high-throughput assay to screen for inhibitors of organic anion transporting polypeptides 1B1 and 1B3. Curr Chem Genomics. 2010;4:1-8

21. Choi MK, Jin QR, Choi YL, Ahn SH, Bae MA, Song IS. Inhibitory effects of ketoconazole and rifampin on OAT1 and OATP1B1 transport activities: considerations on drug-drug interactions. Biopharmaceutics & drug disposition. 2011;32(3):175-84

22. Cui Y, Konig J, Keppler D. Vectorial transport by double-transfected cells expressing the human uptake transporter SLC21A8 and the apical export pump ABCC2. Mol Pharmacol. 2001;60(5):934-43

23. Kloth JS, Klumpen HJ, Yu H, Eechoute K, Samer CF, Kam BL, et al. Predictive value of CYP3A and ABCB1 phenotyping probes for the pharmacokinetics of sunitinib: the ClearSun study. Clinical pharmacokinetics. 2014;53(3):261-9

24. Bowlin SJ, Xia F, Wang W, Robinson KD, Stanek EJ. Twelve-month frequency of drug-metabolizing enzyme and transporter-based drug-drug interaction potential in patients receiving oral enzyme-targeted kinase inhibitor antineoplastic agents. Mayo Clinic proceedings. 2013;88(2):139-48

25. Lau YY, Huang Y, Frassetto L, Benet LZ. effect of OATP1B transporter inhibition on the pharmacokinetics of atorvastatin in healthy volunteers. Clinical pharmacology and therapeutics. 2007;81(2):194-204

26. Backman JT, Olkkola KT, Neuvonen PJ. Rifampin drastically reduces plasma concentrations and effects of oral midazolam. Clinical pharmacology and therapeutics. 1996;59(1):7-13

27. Kharasch ED, Russell M, Mautz D, Thummel KE, Kunze KL, Bowdle A, et al. The role of cytochrome P450 3A4 in alfentanil clearance. Implications for interindividual variability in disposition and perioperative drug interactions. Anesthesiology. 1997;87(1):36-50

28. Paine MF, Wagner DA, Hoffmaster KA, Watkins PB. Cytochrome P450 3A4 and P-glycoprotein mediate the interaction between an oral erythromycin breath test and rifampin. Clinical pharmacology and therapeutics. 2002;72(5):524-35

29. van Giersbergen PL, Treiber A, Schneiter R, Dietrich H, Dingemanse J. Inhibitory and inductive effects of rifampin on the pharmacokinetics of bosentan in healthy subjects. Clinical pharmacology and therapeutics. 2007;81(3):414-9

30. Keating GM, Santoro A. Sorafenib: a review of its use in advanced hepatocellular carcinoma. Drugs. 2009;69(2):223-40

31. Williamson B, Dooley KE, Zhang Y, Back DJ, Owen A. Induction of influx and efflux transporters and cytochrome P450 3A4 in primary human hepatocytes by rifampin, rifabutin, and rifapentine. Antimicrob Agents Chemother. 2013;57(12):6366-9

32. Pang X, Zhang Y, Gao R, Zhong K, Zhong D, Chen X. Effects of rifampin and ketoconazole on pharmacokinetics of morinidazole in healthy chinese subjects. Antimicrob Agents Chemother. 2014;58(10):5987-93

33. Cho SK, Yoon JS, Lee MG, Lee DH, Lim LA, Park K, et al. Rifampin enhances the glucose-lowering effect of metformin and increases OCT1 mRNA levels in healthy participants. Clinical pharmacology and therapeutics. 2011;89(3):416-21

34. Herraez E, Lozano E, Macias RI, Vaquero J, Bujanda L, Banales JM, et al. Expression of SLC22A1 variants may affect the response of hepatocellular carcinoma and cholangiocarcinoma to sorafenib. Hepatology. 2013;58(3):1065-73

35. Neul C, Baker SD, Sparreboom A, Schaeffeler E, Schwab M, Nies AT. Cellular uptake of sorafenib into hepatocellular carcinoma cells is independent of human organic cation transporter 1 (OCT1). Naunyn-Schmied Arch Pharmacol. 2015;388(S1):S23

36. Tiseo PJ, Thaler HT, Lapin J, Inturrisi CE, Portenoy RK, Foley KM. Morphine-6-glucuronide concentrations and opioid-related side effects: a survey in cancer patients. Pain. 1995;61(1):47-54

37. Bins S, Lenting A, El Bouazzaoui S, van Doorn L, Oomen-de Hoop E, Eskens FA, et al. Polymorphisms in SLCO1B1 and UGT1A1 are associated with sorafenib-induced toxicity. Pharmacogenomics. 2016;17(14):1483-90

38. Jain L, Woo S, Gardner ER, Dahut WL, Kohn EC, Kummar S, et al. Population pharmacokinetic analysis of sorafenib in patients with solid tumours. Br J Clin Pharmacol. 2011;72(2):294-305

39. Hilger RA, Richly H, Grubert M, Kredtke S, Thyssen D, Eberhardt W, et al. Pharmacokinetics of sorafenib in patients with renal impairment undergoing hemodialysis. Int J Clin Pharmacol Ther. 2009;47(1):61-4.

40. Picard N, Yee SW, Woillard JB, Lebranchu Y, Le Meur Y, Giacomini KM, et al. The role of organic anion-transporting polypeptides and their common genetic variants in mycophenolic acid pharmacokinetics. Clinical pharmacology and therapeutics. 2010;87(1):100-8

41. Hirano M, Maeda K, Shitara Y, Sugiyama Y. Drug-drug interaction between pitavastatin and various drugs via OATP1B1. Drug Metab Dispos. 2006;34(7):1229-36

42. Nakada N, Oda K. Identification and characterization of metabolites of ASP015K, a novel oral Janus kinase inhibitor, in rats, chimeric mice with humanized liver, and humans. Xenobiotica. 2015;45:757-765

43. Ding J, et al. Metabolism and pharmacokinetics of novel selective vascular endothelial growth factor receptor-2 inhibitor apatinib in humans. Drug Metab. Dispos. 2013;41:1195-1210

44. Smith BJ, et al. Pharmacokinetics, metabolism, and excretion of [14C]axitinib, a vascular endothelial growth factor receptor tyrosine kinase inhibitor, in humans. Drug Metab. Dispos. 2014;42:918-931

45. Zientek MA, et al. In vitro kinetic characterization of axitinib metabolism. Drug Metab. Dispos. 2016;44(1):102-14

46. Hong H, et al. In vitro characterization of the metabolic pathways and cytochrome P450 inhibition and induction potential of BMS-690514, an ErbB/vascular endothelial growth factor receptor inhibitor. Drug Metab. Dispos. 2011;39:1658-1667

47. Cho SY, et al. Determination of the glucuronide metabolite of ON 013100, a benzylstyrylsulfone antineoplastic drug, in colon cancer cells using LC/MS/MS. J. Pharm. Biomed. Anal. 2013;75:138-144

48. Schulz-Utermoehl T, et al. In vitro hepatic metabolism of cediranib, a potent vascular endothelial growth factor tyrosine kinase inhibitor: interspecies comparison and human enzymology. Drug Metab. Dispos. 2010;38:1688-1697

49. Christopher LJ, et al. Metabolism and disposition of dasatinib after oral administration to humans. Drug Metab. Dispos. 2008;36:1357-1364

50. Hagenauer B, et al. In vitro glucuronidation of the cyclin-dependent kinase inhibitor flavopiridol by rat and human liver microsomes: involvement of UDP-glucuronosyltransferases 1A1 and 1A9. Drug Metab. Dispos. 2001;29:407-414

51. Gong A, Chen X, Deng P, Zhong D. Metabolism of flumatinib, a novel antineoplastic tyrosine kinase inhibitor, in chronic myelogenous leukemia patients. Drug Metab. Dispos. 2010;38:1328-1340

52. Martin P, Oliver S, Gillen M, Marbury T, Millson D. Pharmacokinetic properties of fostamatinib in patients with renal or hepatic impairment: results from 2 phase I clinical studies. Clin. Ther. 2015;37(12):2823-36

53. Yan Z. et al. N-glucuronidation of the platelet-derived growth factor receptor tyrosine kinase inhibitor 6,7-(dimethoxy-2,4-dihydroindeno[1,2-C]pyrazol-3-yl)-(3-fluoro-phenyl)-amine by human UDP-glucuronosyltransferases. Drug Metab. Dispos. 2006;34:748-755

54. Mackenzie GG, et al. A novel Ras inhibitor (MDC-1016) reduces human pancreatic tumor growth in mice. Neoplasia. 2013;15:1184-1195

55. Nutley BP, et al. Preclinical pharmacokinetics and metabolism of a novel prototype DNA-PK inhibitor NU7026. Br. J. Cancer. 2015;93:1011-1018

56. Ramirez J, Mirkov S, House LK, Ratain MJ. Glucuronidation of OTS167 in humans Is catalyzed by UDP-glucuronosyltransferases UGT1A1, UGT1A3, UGT1A8, and UGT1A10. Drug Metab. Dispos. 2015;43:928-935

57. Takada T, Weiss HM, Kretz O, Gross G, Sugiyama Y. Hepatic transport of PKI166, an epidermal growth factor receptor kinase inhibitor of the pyrrolo-pyrimidine class, and its main metabolite, ACU154. Drug Metab. Dispos. 2004;32:1272-1278

58. Shilling AD, et al. Metabolism, excretion, and pharmacokinetics of [14C]INCB018424, a selective Janus tyrosine kinase 1/2 inhibitor, in humans. Drug Metab. Dispos. 2010;38:2023-2031

59. Ballard P, et al. Metabolic disposition of AZD8931, an oral equipotent inhibitor of EGFR, HER2 and HER3 signalling, in rat, dog and man. Xenobiotica. 2014;44:1083-1098

60. Atsriku C, Hoffmann M, Moghaddam M, Kumar G, Surapaneni S. In vitro metabolism of a novel JNK inhibitor tanzisertib: interspecies differences in oxido-reduction and characterization of enzymes involved in metabolism. Xenobiotica. 2015;45:465-480

5

61. Atsriku C, Hoffmann M, Ye Y, Kumar G, Surapaneni S. Metabolism and disposition of a potent and selective JNK inhibitor [14C]tanzisertib following oral administration to rats, dogs and humans. Xenobiotica. 2015;45:428-441

62. Ho MY, et al. Trametinib, a first-in-class oral MEK inhibitor mass balance study with limited enrollment of two male subjects with advanced cancers. Xenobiotica. 2014;44:352-368

63. Martin P, et al. Pharmacokinetics of vandetanib: three phase I studies in healthy subjects. Clin Ther. 2012;34(1):221-37

Polymorphisms in SLCO1B1 and UGT1A1 are associated with sorafenib-induced toxicity

Sander Bins, Anne Lenting, Samira el Bouazzaoui, Leni van Doorn, Esther Oomen – de Hoop, Ferry A.L.M. Eskens, Ron H.N. van Schaik, Ron H.J. Mathijssen

ABSTRACT

Aim. Sorafenib-treated patients display a substantial variation in the incidence of toxicity. We aimed to investigate the association of genetic polymorphisms with observed toxicity on sorafenib.

Patients & methods. We genotyped 114 patients that were treated with sorafenib at the Erasmus MC Cancer Institute, the Netherlands, for *SLCO1B1*, *SLCO1B3*, *ABCC2*, *ABCG2*, *UGT1A1* and *UGT1A9*.

Results. The *UGT1A1* (rs8175347) polymorphism was associated with hyperbilirubinemia and treatment interruption. Polymorphisms in *SLCO1B1* (rs2306283, rs4149056) were associated with diarrhea and thrombocytopenia, respectively. None of the investigated polymorphisms was associated with overall or progression-free survival in hepatocellular cancer patients.

Conclusion. Polymorphisms in *SLCO1B1* and *UGT1A1* are associated with several different sorafenib side effects.

INTRODUCTION

Sorafenib, a tyrosine kinase inhibitor (TKI), is currently approved for the treatment of unresectable or metastatic hepatocellular carcinoma (HCC), renal cell carcinoma (RCC) and iodine-refractory differentiated thyroid cancer.[1-3] Like other TKIs, sorafenib shows a wide variation in toxicity, which cannot be predicted for individual patients. The most common sorafenib-induced adverse events include hand–foot skin reaction (HFSR), diarrhea, hypertension and liver function disorders. These adverse events may lead to dose reductions (26%) or treatment discontinuation (38%).[1] In addition, these side effects have at least partly been related to sorafenib pharmacokinetics (PK), which show large inter-individual variability on its own.[4-6]
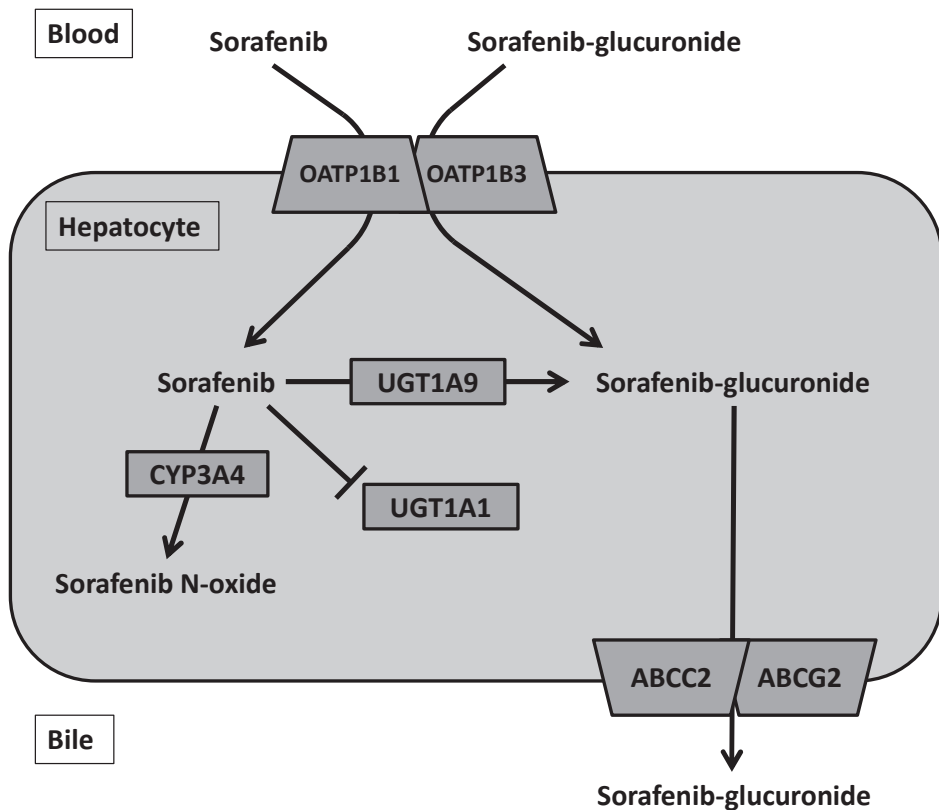
Figure 1. Important proteins regarding hepatic disposition and effect of sorafenib and its major metabolites.

Although little is known about factors that induce this inter-individual variability in sorafenib exposure, many pharmacokinetic processes have already been described in detail.[7] Sorafenib is primarily metabolized in the liver and undergoes both UGT1A9-mediated glucuronidation and CYP3A4-mediated oxidation.[8] Different membrane transporters (e.g., OATP1B1, ABCC2; **Figure 1**) are responsible for hepatocellular uptake and efflux of sorafenib and its metabolites.[7] Theoretically, differences in function of these proteins may lead to altered systemic sorafenib exposure, for example, due to co-medication or genetic variation. Systemic sorafenib exposure is known to correlate with certain toxicities, such as hypertension and HFSR.[5,9] Moreover, multiple studies have identified SNPs in a variety of genes to be associated with sorafenib toxicity. OATP1B1 and OATP1B3, major influx transporters for both sorafenib and sorafenib-glucuronide, have predominantly been investigated in patients treated with irinotecan, which is glucuronidated and distributed by OATP1B (*SLCO1B*) in a similar fashion as sorafenib. Homozygous polymorphisms in *SLCO1B1* 388A>G have been associated with longer progression-free survival (PFS) in irinotecan treated non-small cell lung cancer patients and also with more grade 3 diarrhea.[10,11] Another polymorphism, *SLCO1B1* 521T>C, leads to decreased transporter activity and consequently to increased exposure of the irinotecan metabolite SN-38, which might explain the higher incidence of neutropenia in patients with this polymorphism.[10,11] SNPs in *SLCO1B3* have been investigated scarcely, but the 334T>G polymorphism has been associated with decreased plasma concentrations of mycophenolic acid, which has a similar pattern of hepatobiliary disposition as sorafenib.[12] The efflux transporters ABCC2 and ABCG2 are involved in the biliary secretion of several anticancer drugs. For sorafenib, patients with the *ABCC2* -24CC genotype were at higher risk of skin rash than those with the computed tomography (CT) genotype.[13] Besides, reduced risk of neutropenia and diarrhea was associated with *ABCC2* -24CT for irinotecan.[11] Reports on PFS in patients with the -24TT genotype showed contradictory results.[11,14] For imatinib, neither trough levels nor response were found to be affected by this SNP.[15] The *ABCG2* 421C>A polymorphism has been associated with increased risk of developing diarrhea and higher 5-year PFS rate for a variety of TKIs.[16,17] UGT1A9 is involved in the metabolism of sorafenib and patients with the -2152C>T polymorphism have a higher risk of diarrhea.[19] UGT1A1 is not identified in sorafenib metabolism, but its

function is inhibited by sorafenib. Patients with at least one *UGT1A1* -53TA6>TA7 allele (*UGT1A1*28*) have increased plasma bilirubin concentrations.[19] For irinotecan, *UGT1A1* -53TA7 carriers have an increased risk of neutropenia and diarrhea and a reduced PFS.[11,20–21]

Here, we aimed to investigate whether these pharmacogenetic polymorphisms are correlated with the observed clinical toxicity of sorafenib in a relatively large cohort of patients exposed to this TKI.

PATIENTS & METHODS

Study design

In this retrospective study, we analyzed 114 patients treated with sorafenib between 2006 and 2016 at the Erasmus MC Cancer Institute. We included patients from whom whole blood for DNA analysis was collected (local ethics board study number MEC 02.1002). Patient charts were reviewed to record demographic and clinical information, in other words, age, gender, ethnicity, Eastern Cooperative Oncology Group (ECOG)-performance status, tumor type, prior treatment and sorafenib dose changes.

Adverse events were registered during the entire treatment period and graded according to the National Cancer Institute Common Terminology Criteria for Adverse Events (NCI-CTCAE) v4.0. HFSR, diarrhea, hyperbilirubinemia, cytopenias, increased liver enzymes, rash, hypertension and any toxicity were recorded as end point if ≥grade 3, except for HFSR, which was also recorded if ≥grade 2. Additionally, the maximum bilirubin level during the first 2 months of treatment was compared with total bilirubin at baseline and acute hyperbilirubinemia was defined as a ≥100% increase in blood bilirubin concentrations during these 2 months. In case of treatment interruption, dose reduction or treatment discontinuation, all details were recorded.

PFS was defined as time from start of sorafenib treatment to date of radiological or clear clinical progression. Patients who did not have progressive disease, were censored for PFS at the time of last follow-up, at start of next treatment or at date of death. Overall survival

(OS) was defined as time from start of sorafenib treatment to date of death, or date at which patients were last known to be alive.

SNP selection

We identified eight potentially functional polymorphisms in six genes involved in the PK of sorafenib. These polymorphisms were selected based on previously reported research into clinically relevant associations. The genes and the selected polymorphisms are listed in **Table 1**. Although CYP3A4 is involved in sorafenib metabolism, *CYP3A4* polymorphisms were not included, because the only clinically relevant SNP, in other words, *CYP3A4*22* (rs35599367), leads to impaired protein function and CYP3A4 inhibition has previously been shown not to influence sorafenib exposure.[22–25]

DNA isolation

Four hundred microliters of whole-blood specimens collected in EDTA tubes were extracted on the MagNAPure Compact instrument (Roche Diagnostics GmbH, Germany) using the Nucleic Acid Isolation Kit I (Roche Diagnostics GmbH, Germany) and a final elution volume of 200 µl.

Table 1. Investigated single nucleotide polymorphisms.

Gene	Rs-number	Variant	Allele	WW	WM	MM	MAF
SLCO1B1	rs2306283	388A>G	*1B	39	51	24	43%
	rs4149056	521T>C	*5	85	25	4	14%
SLCO1B3	rs4149117	334T>G		5	32	77	18%
ABCC2	rs717620	-24C>T		82	30	2	15%
ABCG2	rs2231142	421C>A		95	17	2	9%
UGT1A1	rs8175347	-53TA6>TA7	*28	53	46*	14	33%
UGT1A9	rs17868320	-2152C>T		104	10	0	4%
	rs6714486	-275T>A		103	11	0	5%

*One patient harbored a TA5/TA6 genotype, which was categorized as a heterozygous variant.
Abbreviations: MAF, minor allele frequency; MM, mutant - mutant; WM, wild type - mutant; WW, wild type - wild type.*

Taqman genotyping

The *SLCO1B1* 388A>G and 521T>C, *SLCO1B3* 334T>G, *ABCC2* -24C>T, *ABCG2* 421C>A, *UGT1A9* -2152C>T and -275T>A genotyping was done using predesigned Drug Metabolism Enzymes Taqman allelic discrimination assays on the Life Technologies Taqman 7500 system (Applied Biosystems, Life Technologies Europe BV, Bleiswijk, The Netherlands). The assay IDs are listed in **Table 1**. Each assay consisted of two allele-specific minor groove binding probes, labeled with the fluorescent dyes VIC and FAM. PCRs were performed in a reaction volume of 10 µl, containing assay-specific primers, allele-specific Taqman minor groove binding probes, Abgene Absolute QPCR Rox Mix (Thermo Scientific, Life Technologies Europe BV, Bleiswijk, The Netherlands) and genomic DNA (20 ng). The thermal profile consists of 40 cycles of denaturation at 95°C for 20 s and annealing at 92°C for 3 s and extension at 60°C for 30 s. Genotypes were scored by measuring allele-specific fluorescence using the 7500 software v2.3 for allelic discrimination (Applied Biosystems).

LightCycler

The real-time PCR assay was developed on the LightCycler 2.0 instrument (Roche Diagnostics GmbH, Mannheim, Germany). The primers and fluorescence resonance energy transfer hybridization probes were analyte-specific reagents from Roche Molecular Diagnostics targeting the UGT1A1 gene. The PCR assay was performed using the LC FastStart DNA master hybridization probe kit (Roche Diagnostics GmbH). The total volume per reaction mixture was 21 µl (20 µl of master mix plus 1 µl of extracted nucleic acid 10 ng/µl). PCR amplification with real-time detection was performed using the following cycling parameters: one-template denaturing cycle at 95°C for 10 min, followed by 45 amplification cycles at 95°C for 0 s, 60°C for 10 s and 72°C for 15 s. Following amplification, a melting curve analysis was performed by measuring the fluorescent signal during the following cycling parameters: 95°C for 30 s, 45°C for 30 s and 70°C for 0 s, with a transition of 0.2°C/s. Following a second melting curve analysis was performed by measuring the fluorescent signal during the following cycling parameters: 95°C for 30 s, 45°C for 30 s and 70°C for 0 s, with a transition of 0.1°C/s. Finally a cooling down step was performed at 40°C for 30 min. Positive results were detected at 640 nm and using the melting curve-Tm

6

calling analysis. Wild-type TA6 peaked at about 55°C. Heterozygous TA (6)/TA (7) patients peaked at about 55 and 59°C, and the variant TA7 peaked at about 59°C.

Statistical analysis

The distribution of genotypes was tested for Hardy–Weinberg equilibrium using the Chi-square test. Polymorphisms with a minor allele frequency <1% were not analyzed. Polymorphisms within a single gene were tested for linkage disequilibrium (LD) in the European population in reference haplotypes from Phase III of the 1000 Genomes Project using LDlink.[26] The limit for LD was set at $R^2 > 0.8$. In Utah Residents from north and west Europe (CEU population), the polymorphisms in *UGT1A9* met the criteria for LD ($R^2 = 0.94$) and the polymorphisms in SLCO1B1 were not correlated ($R^2 = 0.14$). Therefore, the polymorphisms in *UGT1A9* were further analyzed as haplotype. The selected polymorphisms and haplotype were fitted and the most appropriate model was selected. As for the dominant and recessive model, the polymorphisms and haplotype were tested against the toxicity end points using the Chi-square test or Fisher's exact test, while logistic regression analysis was applied for the multiplicative and additive model[27] If an end point occurred in more than 20 patients, candidate genetic variables with $p \leq 0.1$ were selected for the multiple logistic regression analysis with toxicity as depending variable. All multivariable analyses corrected for age, gender and ECOG performance status. PFS and OS were estimated in patients with HCC by the Kaplan–Meier method, and the log-rank test was used for univariable survival analysis. If all groups in the model contained more than ten patients, multivariable survival analysis was considered. All statistical analyses were performed using SPSS version 21 software (SPSS, IL, USA). A two-sided $p < 0.05$ was considered significant. In view of the exploratory nature of this study, no correction for multiple testing was applied.

RESULTS

Patients & treatment

Between 2006 and 2016, 114 sorafenib-treated patients provided blood samples for pharmacogenetic analysis. Baseline patient characteristics are depicted in **Table 2**. Fifty-five patients (48%) started sorafenib at 400 mg b.i.d., 57 patients (50%) started at 200 mg

b.i.d. and two patients (2%) started at 600 mg. In the latter two groups, the dose was increased to 400 mg b.i.d. by adding 200 mg to the daily dose every 2 weeks, if deemed safe and feasible. Any drug-related toxicity ≥grade 3 occurred in 76 patients (67%): 39 patients had elevated liver enzymes (34%), 14 had hyperbilirubinemia (12%), ten had hypertension (9%), nine had diarrhea (8%), nine had HFSR (8%), nine had rash (8%) and nine had thrombocytopenia (8%). Grade 2 HFSR occurred in 36 patient (32%). Dose at start of treatment (200 vs 400 mg b.i.d.) was not significantly associated with incidence of toxicity ≥grade 3, although hyperbilirubinemia was observed significantly more frequent in the group started at 200 mg b.i.d. (p = 0.016, Fisher's exact test). At data cut-off on 1 March 2016, eight patients were still treated with sorafenib, whereas the other patients had stopped treatment due to progressive disease (PD; n = 63; 55%), toxicity (n = 33; 29%), both PD and toxicity (n = 8; 7%) or other reasons (n = 2; 2%). During treatment, in 50 patients both dose reduction and interruption was pursued (44%), dose reduction alone was pursued in 13 patients (11%) and dose interruption alone in eight patients (7%).

6

Table 2. Baseline patient characteristics.

Characteristics	Patients (n=114)
Gender	
Male	89 (78%)
Female	25 (22%)
Age **(years)**	
mean (± SD)	63 (± 11)
Primary tumor	
Hepatocellular carcinoma (HCC)	99 (87%)
Renal cell cancer (RCC)	14 (12%)
Desmoid fibromatosis	1 (1%)
WHO-score	
0	20 (18%)
1	90 (79%)
2	4 (4%)
Ethnicity	
Caucasian	104 (91%)
Black	3 (3%)
Asian	5 (4%)
Combination	2 (2%)

Table 3. Selection of the significant associations of SNPs with toxicity endpoints. .

Endpoint	Factor	Genotype	Univariable OR (95% CI)	p	Multivariable OR (95% CI)	p
Ethnicity other than Caucasian	SLCO1B1 388A>G	GG vs AA + AG	11.941 (2.804-50.852)	<0.001†		
	SLCO1B3 334T>G	TG + GG vs TT	0.119 (0.017-0.817)	0.012†		
	ABCC2 -24C>T	CT + TT vs CC	4.500 (1.177-17.199)	0.019†		
Any toxicity	Age				1.008 (0.967-1.050)	0.721
	Gender				1.902 (0.639-5.657)	0.248
	ECOG-performance				1.210 (0.481-3.042)	0.685
	UGT1A1 53TA6>TA7	Other vs TA6-TA6	1.952 (0.885-4.305)	0.084	2.002 (0.902-4.446)	0.088
Diarrhea	Age					
	Gender					
	ECOG-performance					
	SLCO1B1 388A>G	AG + GG vs AA	0.125 (0.025-0.636)	0.007†		
	ABCC2 -24C>T	CT + TT vs CC	0.890 (0.825-0.961)	0.059†		
Acute hyperbilirubinemia*	Age				1.003 (0.963-1.044)	0.885
	Gender				0.728 (0.255-2.079)	0.553
	ECOG-performance				1.125 (0.442-2.864)	0.805
	SLCO1B1 388A>G	AA → AG → GG‡	0.580 (0.340-0.987)	0.045	0.693 (0.394-1.220)	0.204
	UGT1A1 53TA6>TA7	TA7-TA7 vs other	6.519 (1.706-24.902)	0.003†	5.413 (1.362-21.513)	0.016
Hyperbilirubinemia	Age					
	Gender					
	ECOG-performance					
	SLCO1B1 388A>G	AG + GG vs AA	1.230 (1.103-1.370)	0.002†		
Thrombocytopenia	Age					
	Gender					
	ECOG-performance					
	SLCO1B1 521T>C	CT + CC vs TT	4.219 (1.049-16.962)	0.045†		
Elevated liver enzymes	Age				0.983 (0.944-1.022)	0.384
	Gender				0.836 (0.296-2.358)	0.735
	ECOG-performance				1.097 (0.416-2.889)	0.852
	ABCG2 421C>A	CA + AA vs CC	0.307 (0.084-1.129)	0.070†	0.317 (0.085-1.183)	0.087

Endpoint	Factor	Genotype	Univariable		Multivariable	
			OR (95% CI)	***p***	**OR (95% CI)**	***p***
Rash	Age					
	Gender					
	ECOG-performance					
	SLCO1B1 388A>G	GG *vs* AA + AG	3,400 (0,837-13,817)	0.091†		
Treatment interruption	Age				1.007 (0.968-1.047)	0.726
	Gender				0.914 (0.340-2.458)	0.858
	ECOG-performance				0.854 (0.346-2.110)	0.733
	UGT1A1 53TA6>TA7	Other *vs* TA6-TA6	3.330 (1.531-7.245)	0.002	3.397 (1.553-7.430)	0.002

*Acute hyperbilirubinemia was defined as a ≥100% increase in blood bilirubin concentrations during the first two months.

† Fisher's exact test was used here. All other p-values for the univariable analyses were calculated using the chi-square test.

‡ Arrows indicate a multiplicative model.

6

Association of pharmacogenetic polymorphisms with toxicity

The results of the genotyping analyses are depicted in **Table 1**. The polymorphisms that met our preset criteria for association with the end points in univariable analysis were entered in the multivariable logistic regression (**Table 3**). For any toxicity ≥grade 3, no association was found with the polymorphisms in multivariable analysis. This was also the case for elevated liver enzymes. Hyperbilirubinemia, thrombocytopenia, diarrhea and rash occurred in less than 20 patients and were therefore not considered for multivariable analysis. Hypertension, HFSR ≥grade 3 and HFSR ≥grade 2 were not associated with any of the polymorphisms in univariable analysis. The presence of at least one mutant *UGT1A1* allele was associated with 3.4-fold higher odds of interrupting treatment (p = 0.002), whereas the homozygous variant was associated with over fivefold higher odds of acute hyperbilirubinemia (p = 0.016). In univariable analysis, polymorphisms in *SLCO1B1* were also related to the incidence toxicity: at least one mutant allele at codon 388 was associated with almost eightfold lower odds of developing diarrhea (p = 0.007) and at least one C allele at codon 521 was associated with 4.2-fold higher odds of thrombocytopenia (p = 0.045). Between HCC patients and the other patients the incidence of acute hyperbilirubinemia (41 vs 40%, respectively; p = 0.917), of hyperbilirubinemia (14 vs 0%, respectively; p = 0.209) and of thrombocytopenia (9 vs 0%, respectively; p = 0.224) did not differ significantly. Other liver enzymes were elevated more frequently in HCC patients (38%) than in patients with RCC or desmoid fibromatosis (7%; p = 0.018).

Association of pharmacogenetic polymorphisms with survival

None of the SNPs were associated to PFS for HCC in univariable analysis. For OS, the recessive *ABCC2* and *ABCG2* models seemed associated, but both models had only two patients in the homozygous affected group and were therefore excluded.

DISCUSSION

In this study, we have found new associations between genetic polymorphisms in genes encoding for drug transporters and various kinds of well-recognized sorafenib toxicity. Earlier genotyping efforts in sorafenib-treated patients have predominantly focused on genes related to pharmacodynamics, for example, *VEGF* and *VEGFR2* .[9,28–29] Up till now,

genetic polymorphisms in *ABCC2*, *UGT1A1* and *UGT1A9* have been associated with sorafenib-induced toxicity.[13,18–19] In our population, the significant association between polymorphisms in *ABCC2* and *UGT1A9* and toxicity could not be confirmed, but we did find that patients carrying a homozygous *UGT1A1* -53 TA7 repeat (rs8175347) were at an increased odds for a more than twofold – and therefore clinically relevant – increase of bilirubin concentrations during the first 2 months of treatment. Any toxicity ≥grade 3 also occurred twice as often in patients with at least one mutant *UGT1A1* -53 allele, although this was not statistically significant (p = 0.088). Furthermore, patients with at least one mutant allele at this position had their treatment interrupted significantly more often in our series, which is likely to be caused (partly) by the higher incidence of acute hyperbilirubinemia. This phenomenon was described in a case report, in which a sorafenib-treated patient with one mutant allele had a marked unconjugated hyperbilirubinemia.[30] This has also been described before for several other drugs, like atazanavir and nilotinib.[31,32] Unfortunately, we were unable to differentiate conjugated from unconjugated hyperbilirubinemia due to the retrospective character of this study. As systemic accumulation of unconjugated bilirubin is essentially benign, it may be useful for clinicians to be aware of *UGT1A1*28* status in order to adequately consider sorafenib therapy in case of hyperbilirubinemia.

Diarrhea and thrombocytopenia occurred significantly more often in patients with at least one mutant allele in *SLCO1B1*. The presence of a mutant G allele at codon 388 (rs2306283), which leads to OATP1B1 activation,[33] was associated with much lower odds of diarrhea than the wild-type genotype. On the other hand, patients with at least one mutant C allele at codon 521 (rs4149056), which is known to reduce OATP1B1 activity,[33] had significantly higher odds of developing thrombocytopenia. The OATP1B1 transporter, encoded for by *SLCO1B1*, is known to mediate hepatic transport of sorafenib-glucuronide,[7] but is possibly also involved in transport of unconjugated sorafenib.[34] Our findings suggest that systemic concentrations of sorafenib or its glucuronide are highly dependent of OATP1B1 activity. Higher OATP1B1 activity and the subsequent higher hepatic clearance of the drug, for example, for **1B*, leads to lower systemic exposure and therefore less toxicity (diarrhea) and vice versa for **5* and thrombocytopenia. As for the unconjugated

bilirubin, we do not have pharmacokinetic data from these patients at our disposal and therefore cannot substantiate this theory with pharmacokinetic evidence. Still, our findings are similar to those in studies with other drugs like irinotecan[10,11] or pravastatin.[35] Hence the scenario sketched above may not only be plausible, but also relevant since OATP1B1 function can also be altered by co-medication.[8]

To provide definite proof of these retrospective observations, a prospective study, including PK and additional unconjugated bilirubin analysis, should be pursued. We were limited in registering low grade toxicity, which was not reported structurally in the patient records. On the other hand, clinically relevant adverse events are reported in a standardized way and therefore it is unlikely that we have missed important toxicity in our dataset. Finally, some of the end points we used, in other words, thrombocytopenia, hyperbilirubinemia and elevated liver enzymes, can also manifest as a symptom of advanced HCC. In our population however, only the latter occurred significantly more often in HCC patients. Therefore, the potential bias caused by differences in primary tumor seems to be limited.

Conclusion

We have observed that genetic polymorphisms in *SLCO1B1* (rs2306283 and rs4149056) are associated with sorafenib-induced toxicity. Future fundamental research has to be aimed at discovering whether sorafenib itself or its metabolite sorafenib-glucuronide is being accumulated and causes toxicity. Additionally, we have confirmed that *UGT1A1*28* (rs8175347) is associated with acute hyperbilirubinemia, which causes physicians to interrupt treatment significantly more frequent.

REFERENCES

1. Llovet JM, Ricci S, Mazzaferro V, Hilgard P, Gane E, Blanc JF, et al. Sorafenib in advanced hepatocellular carcinoma. N Engl J Med. 2008;359(4):378-90

2. Cheng AL, Kang YK, Chen Z, Tsao CJ, Qin S, Kim JS, et al. Efficacy and safety of sorafenib in patients in the Asia-Pacific region with advanced hepatocellular carcinoma: a phase III randomised, double-blind, placebo-controlled trial. Lancet Oncol. 2009;10(1):25-34

3. Escudier B, Eisen T, Stadler WM, Szczylik C, Oudard S, Staehler M, et al. Sorafenib for treatment of renal cell carcinoma: Final efficacy and safety results of the phase III treatment approaches in renal cancer global evaluation trial. J Clin Oncol. 2009;27(20):3312-8

4. Shimada M, Okawa H, Kondo Y, Maejima T, Kataoka Y, Hisamichi K, et al. Monitoring Serum Levels of Sorafenib and Its N-Oxide Is Essential for Long-Term Sorafenib Treatment of Patients with Hepatocellular Carcinoma. Tohoku J Exp Med. 2015;237(3):173-82

5. Fukudo M, Ito T, Mizuno T, Shinsako K, Hatano E, Uemoto S, et al. Exposure-toxicity relationship of sorafenib in Japanese patients with renal cell carcinoma and hepatocellular carcinoma. Clin Pharmacokinet. 2014;53(2):185-96

6. Fucile C, Marenco S, Bazzica M, Zuccoli ML, Lantieri F, Robbiano L, et al. Measurement of sorafenib plasma concentration by high-performance liquid chromatography in patients with advanced hepatocellular carcinoma: is it useful the application in clinical practice? A pilot study. Med Oncol. 2015;32(1):335

7. Vasilyeva A, Durmus S, Li L, Wagenaar E, Hu S, Gibson AA, et al. Hepatocellular Shuttling and Recirculation of Sorafenib-Glucuronide Is Dependent on Abcc2, Abcc3, and Oatp1a/1b. Cancer Res. 2015;75(13):2729-36

8. Bins S, Van Doorn L, Gibson A, Hu S, Li L, Vasilyeva A, et al. 305 Influencing sorafenib disposition by blocking hepatocellular sorafenib-glucuronide uptake with rifampin in mice and humans. European Journal of Cancer. 2015;51:S56

9. Jain L, Sissung TM, Danesi R, Kohn EC, Dahut WL, Kummar S, et al. Hypertension and hand-foot skin reactions related to VEGFR2 genotype and improved clinical outcome following bevacizumab and sorafenib. J Exp Clin Cancer Res. 2010;29:95

10. Han JY, Lim HS, Shin ES, Yoo YK, Park YH, Lee JE, et al. Influence of the organic anion-transporting polypeptide 1B1 (OATP1B1) polymorphisms on irinotecan-pharmacokinetics and clinical outcome of patients with advanced non-small cell lung cancer. Lung Cancer. 2008;59(1):69-75

11. Teft WA, Welch S, Lenehan J, Parfitt J, Choi YH, Winquist E, et al. OATP1B1 and tumour OATP1B3 modulate exposure, toxicity, and survival after irinotecan-based chemotherapy. Br J Cancer. 2015;112(5):857-65

12. Picard N, Yee SW, Woillard JB, Lebranchu Y, Le Meur Y, Giacomini KM, et al. The role of organic anion-transporting polypeptides and their common genetic variants in mycophenolic acid pharmacokinetics. Clin Pharmacol Ther. 2010;87(1):100-8

13. Tsuchiya N, Narita S, Inoue T, Hasunuma N, Numakura K, Horikawa Y, et al. Risk factors for sorafenib-induced high-grade skin rash in Japanese patients with advanced renal cell carcinoma. Anticancer Drugs. 2013;24(3):310-4

14. Han JY, Lim HS, Yoo YK, Shin ES, Park YH, Lee SY, et al. Associations of ABCB1, ABCC2, and ABCG2 polymorphisms with irinotecan-pharmacokinetics and clinical outcome in patients with advanced non-small cell lung cancer. Cancer. 2007;110(1):138-47

15. Eechoute K, Sparreboom A, Burger H, Franke RM, Schiavon G, Verweij J, et al. Drug transporters and imatinib treatment: implications for clinical practice. Clin Cancer Res. 2011;17(3):406-15

16. Cusatis G, Gregorc V, Li J, Spreafico A, Ingersoll RG, Verweij J, et al. Pharmacogenetics of ABCG2 and adverse reactions to gefitinib. J Natl Cancer Inst. 2006;98(23):1739-42

17. Koo DH, Ryu MH, Ryoo BY, Beck MY, Na YS, Shin JG, et al. Association of ABCG2 polymorphism with clinical efficacy of imatinib in patients with gastrointestinal stromal tumor. Cancer Chemother Pharmacol. 2015;75(1):173-82

18. Boudou-Rouquette P, Narjoz C, Golmard JL, Thomas-Schoemann A, Mir O, Taieb F, et al. Early sorafenib-induced toxicity is associated with drug exposure and UGT1A9 genetic polymorphism in patients with solid tumors: a preliminary study. PLoS One. 2012;7(8):e42875

6

19. Peer CJ, Sissung TM, Kim A, Jain L, Woo S, Gardner ER, et al. Sorafenib is an inhibitor of UGT1A1 but is metabolized by UGT1A9: implications of genetic variants on pharmacokinetics and hyperbilirubinemia. Clin Cancer Res. 2012;18(7):2099-107

20. Liu X, Cheng D, Kuang Q, Liu G, Xu W. Association of UGT1A1*28 polymorphisms with irinotecan-induced toxicities in colorectal cancer: a meta-analysis in Caucasians. Pharmacogenomics J. 2014;14(2):120-9

21. de Jong FA, de Jonge MJ, Verweij J, Mathijssen RH. Role of pharmacogenetics in irinotecan therapy. Cancer Lett. 2006;234(1):90-106

22. Zimmerman EI, Roberts JL, Li L, Finkelstein D, Gibson A, Chaudhry AS, et al. Ontogeny and sorafenib metabolism. Clin Cancer Res. 2012;18(20):5788-95

23. Ghassabian S, Rawling T, Zhou F, Doddareddy MR, Tattam BN, Hibbs DE, et al. Role of human CYP3A4 in the biotransformation of sorafenib to its major oxidized metabolites. Biochem Pharmacol. 2012;84(2):215-23

24. Elens L, van Gelder T, Hesselink DA, Haufroid V, van Schaik RH. CYP3A4*22: promising newly identified CYP3A4 variant allele for personalizing pharmacotherapy. Pharmacogenomics. 2013;14(1):47-62

25. Lathia C, Lettieri J, Cihon F, Gallentine M, Radtke M, Sundaresan P. Lack of effect of ketoconazole-mediated CYP3A inhibition on sorafenib clinical pharmacokinetics. Cancer Chemother Pharmacol. 2006;57(5):685-92

26. Machiela MJ, Chanock SJ. LDlink: a web-based application for exploring population-specific haplotype structure and linking correlated alleles of possible functional variants. Bioinformatics. 2015;31(21):3555-7

27. Lewis CM. Genetic association studies: design, analysis and interpretation. Brief Bioinform. 2002;3(2):146-53

28. Lee JH, Chung YH, Kim JA, Shim JH, Lee D, Lee HC, et al. Genetic predisposition of hand-foot skin reaction after sorafenib therapy in patients with hepatocellular carcinoma. Cancer. 2013;119(1):136-42

29. Qin C, Cao Q, Li P, Wang S, Wang J, Wang M, et al. The influence of genetic variants of sorafenib on clinical outcomes and toxic effects in patients with advanced renal cell carcinoma. Sci Rep. 2016;6:20089

30. Meza-Junco J, Chu QS, Christensen O, Rajagopalan P, Das S, Stefanyschyn R, et al. UGT1A1 polymorphism and hyperbilirubinemia in a patient who received sorafenib. Cancer Chemother Pharmacol. 2009;65(1):1-4

31. Culley CL, Kiang TK, Gilchrist SE, Ensom MH. Effect of the UGT1A1*28 allele on unconjugated hyperbilirubinemia in HIV-positive patients receiving Atazanavir: a systematic review. Ann Pharmacother. 2013;47(4):561-72

32. Shibata T, Minami Y, Mitsuma A, Morita S, Inada-Inoue M, Oguri T, et al. Association between severe toxicity of nilotinib and UGT1A1 polymorphisms in Japanese patients with chronic myelogenous leukemia. Int J Clin Oncol. 2014;19(2):391-6

33. Ieiri I, Higuchi S, Sugiyama Y. Genetic polymorphisms of uptake (OATP1B1, 1B3) and efflux (MRP2, BCRP) transporters: implications for inter-individual differences in the pharmacokinetics and pharmacodynamics of statins and other clinically relevant drugs. Expert Opin Drug Metab Toxicol. 2009;5(7):703-29

34. Swift B, Nebot N, Lee JK, Han T, Proctor WR, Thakker DR, et al. Sorafenib hepatobiliary disposition: mechanisms of hepatic uptake and disposition of generated metabolites. Drug Metab Dispos. 2013;41(6):1179-86

35. Kivisto KT, Niemi M. Influence of drug transporter polymorphisms on pravastatin pharmacokinetics in humans. Pharm Res. 2007;24(2):239-47

Analysis in GIST Patients on the Role of Alpha-1 Acid Glycoprotein in Imatinib Exposure

Sander Bins, Karel Eechoute, Jacqueline S.L. Kloth, Femke M. de Man, Astrid W. Oosten, Peter de Bruijn, Stefan Sleijfer, Ron H.J. Mathijssen
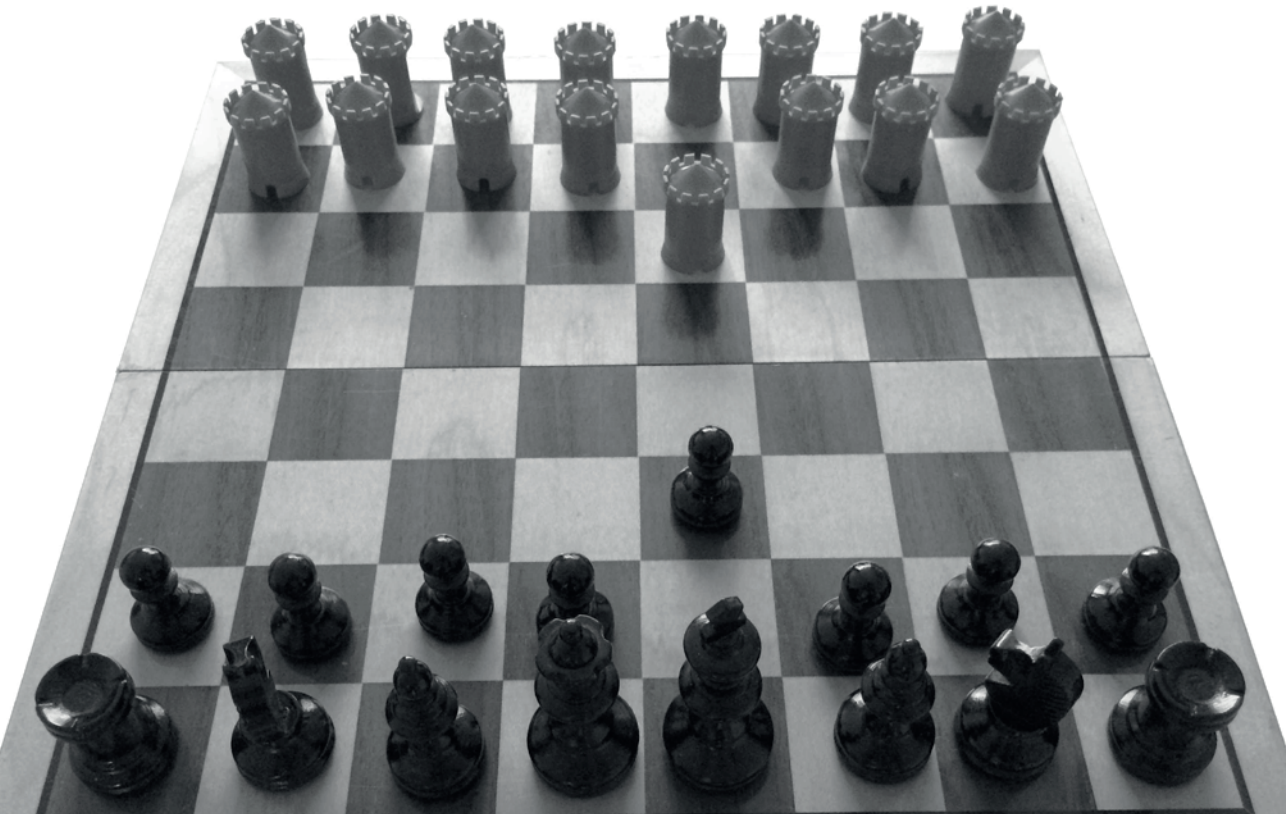
ABSTRACT

Background. For imatinib, a relationship between systemic exposure and clinical outcome has been suggested. Importantly, imatinib concentrations are not stable and decrease over time, for which several mechanisms have been suggested. In this study, we investigated if a decrease in alpha-1 acid glycoprotein (AGP) is the main cause of the lowering in imatinib exposure over time.

Methods. We prospectively measured imatinib trough concentration (C_{min}) values in 28 patients with gastrointestinal stromal tumours, at 1, 3 and 12 months after the start of imatinib treatment. At the same time points, AGP levels were measured.

Results. Overall, imatinib C_{min} and AGP levels were correlated ($R^2 = 0.656$; $P < 0.001$). However, AGP levels did not fluctuate significantly over time, nor did the change in AGP levels correlate with the change in the imatinib C_{min}.

Conclusion. We showed that systemic AGP levels are not likely to be a key player in the decrease in systemic imatinib exposure over time. As long as intra-individual changes in imatinib exposure remain unexplained, researchers should standardize the sampling times for imatinib in order to be able to assess the clinical applicability of therapeutic drug monitoring.

BACKGROUND

Imatinib is one of the first tyrosine kinase inhibitors (TKIs) for which therapeutic drug monitoring (TDM) is deemed suitable in the treatment of both chronic myeloid leukaemia (CML) and gastrointestinal stromal tumours (GISTs). In CML, higher imatinib exposure has been found in patients with a treatment response,[1-4] and imatinib trough concentration (C_{min}) values above 1000 ng/mL have been found to be predictive of higher response rates.[1,2] For GIST, the target imatinib C_{min} has been established in a phase II study, in which patients with an imatinib C_{min} in the lowest quartile (i.e. below 1100 ng/mL) had significantly worse progression-free survival (PFS), and it was suggested that this concentration should serve as a target C_{min}.[5] Studies conducted in the context of routine care have shown that more than half of imatinib-treated patients do not reach that C_{min}.[6–8] In these studies performed in daily practice, the C_{min} was measured more than 3 months after the start of treatment, whereas in the study describing the threshold of 1100 ng/mL, the imatinib C_{min} was established after 4 weeks of treatment. Meanwhile, it has been shown that imatinib clearance increases—and systemic concentrations therefore decrease—during the first 3 months of treatment.[9,10] Hence, it could be expected upfront that an even larger proportion of patients than the 25 % in the phase II study would have a C_{min} below 1100 ng/mL when it was determined later than 3 months after the start of treatment, and doubts have been raised as to whether this threshold set at a time when systemic exposure has not yet stabilized is indeed the appropriate target imatinib C_{min} in patients with GIST.[11] Accordingly, in one of the more recent retrospective studies in GIST patients, a threshold of 760 ng/mL led to better prediction of the outcome.[8] In the same study population, however, the median PFS was longer for patients with a C_{min} >1100 ng/mL than for those with a C_{min} >760 ng/mL (67 versus 56 months).[8]

Several mechanisms have been suggested to account for the reduction in systemic imatinib concentrations over time, the first being decreased absorption.[9] Alternatively, Chatelut et al.[12] proposed that systemic imatinib exposure decreases because of increased clearance rather than because of decreased absorption. As imatinib is predominantly bound to the acute-phase protein alpha-1 acid glycoprotein (AGP),[13-15] a reduction in AGP over time would lead to less protein-bound imatinib and therefore a larger proportion of free imatinib that could be metabolized or excreted.[12] According to

this theory, it is assumed that a decrease in the tumour burden leads to a reduced inflammatory syndrome, which in turn causes lowering of AGP levels. The finding that changes in AGP levels over time correlate well with changes in imatinib concentrations seems to back this mechanism.[16] However, these data were analysed in retrospect and, more importantly, they were not collected in a structured manner, as imatinib concentrations and AGP levels were measured at separate time points. Additionally, AGP levels and imatinib concentrations were not assessed synchronously in that study. To firmly establish the influence of AGP levels on blood imatinib concentrations, this study aimed to prospectively assess the correlation between imatinib C_{min} values and AGP levels.

METHODS

Patients

Adult patients with GIST in whom commencement of imatinib treatment was planned were eligible for inclusion in this study. The exclusion criteria were prior imatinib treatment within 3 months prior to the start of the study, major surgery within 2 weeks prior to the start of the study, use of potent cytochrome P450 (CYP) 3A inhibitors or inducers, and inability to give or understand informed consent. The study protocol was approved by the local institutional review board (protocol number MEC13-203). All procedures performed in this study were in accordance with the ethical standards of the institutional and/or national research committee and with the 1964 Helsinki Declaration and its later amendments or comparable ethical standards. Written informed consent was obtained from all individual participants included in the study.

Study Procedures

Pharmacokinetic sampling was performed at 1, 3 and 12 months after the start of imatinib treatment. At each time point, two blood samples were collected in addition to the standard-of-care blood draw at scheduled outpatient visits. The first sample was collected in a glass tube containing lithium heparin as an anticoagulant, and was used to quantify the concentrations of imatinib and its main metabolite, CGP74588. This sample was processed to plasma within 30 minutes by centrifugation for 15 min at 2500×g (4 °C). Next, the plasma was transferred to polypropylene tubes and stored at −70 °C until the

time of analysis at the Laboratory of Translational Pharmacology, Erasmus MC Cancer Institute (Rotterdam, the Netherlands). The methods used for quantification of imatinib and CGP74588 concentrations have been described previously.[17] The second sample was collected in a serum-separating tube and processed to serum. Serum AGP levels were measured using an immunoturbidimetric assay on a Cobas Integra 800 (Roche Diagnostics GmbH, Mannheim, Germany) in accordance with the instructions of the manufacturer. Briefly, serum AGP was agglutinated with a polyclonal goat-antihuman AGP antibody. The amount of agglutination of the antigen–antibody complex was measured turbidimetrically.

Statistical Considerations

At least 24 patients had to be included to identify a rho value of 0.55 in a two-sided test with alpha = 0.05 and power = 0.8. Correlation was tested using Pearson's correlation, equality of two means was tested using t tests and equality of more than two means was tested using one-way analysis of variance (ANOVA). P values <0.05 were considered statistically significant. Descriptive statistics were performed using IBM SPSS Statistics version 21 software (SPSS, Chicago, IL, USA). All other statistical analyses were performed using GraphPad Prism 5.0 software (GraphPad Software, La Jolla, CA, USA).

RESULTS

Baseline

Between April 2013 and March 2015, 35 patients signed informed consent and were included in the study. Four patients were not evaluable because they stopped imatinib treatment within 3 months and therefore did not provide repetitive pharmacokinetic samples. In another three patients, only one C_{min} value was available because the patients had taken imatinib prior to the other sampling time points or because they had an imatinib concentration below the limit of quantification (<20.0 ng/mL). The baseline characteristics of the 28 evaluable patients are depicted in **Table 1**. Eight of the evaluable patients stopped treatment before the final sampling time point because of progressive disease (n = 3), cessation of neoadjuvant treatment (n = 4) or toxicity (n = 1).

AGP Levels and Imatinib Concentrations

A total of 73 imatinib trough concentration samples were obtained. In 69 cases, a blood sample for measurement of the AGP level was collected synchronically. The mean values of AGP, imatinib and CGP74588 at each time point are depicted in **Table 2**. At any of the three time points, the AGP levels in the five patients treated in the adjuvant setting did not differ significantly from those in the patients treated in the neoadjuvant or palliative settings (**Figure 1a**).

Table 1. Baseline patient characteristics.

Characteristics		Patients (n=28)
Age at start	Years	69 (36-85)
Gender	- Male	16 (57%)
	- Female	12 (43%)
WHO performance	- 0	12 (43%)
	- 1	13 (46%)
	- 2	1 (4%)
	- Unknown	2 (7%)
c-KIT mutation	- Wildtype	5 (18%)
	- Exon 9	6 (21%)
	- Exon 11	12 (43%)
	- Exon 13	3 (11%)
	- Unknown	2 (7%)
Treatment setting	- Neoadjuvant	11 (39%)
	- Adjuvant	5 (18%)
	- Palliative	12 (43%)
Dose at start	- 300 mg QD	1 (4%)
	- 400 mg QD	26 (93%)
	- 800 mg QD	1 (4%)

All values are presented as n (%) *or as* mean (SD).

(a)

AGP concentrations at day 30 (white), day 90 (striped) and day 365 (grey)
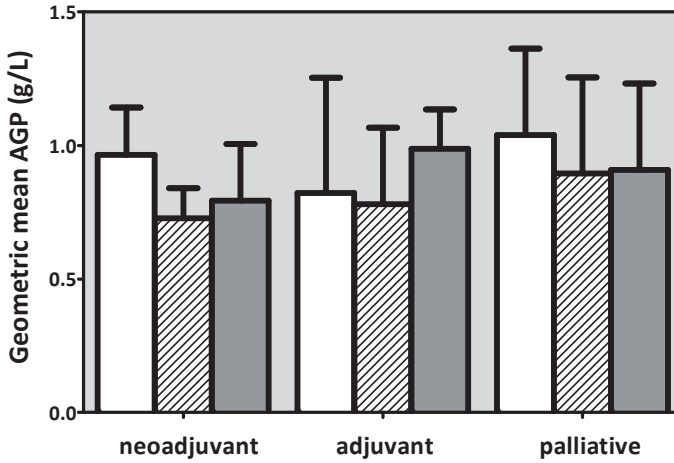
(b)

Course of imatinib (black bars) and AGP (white bars)
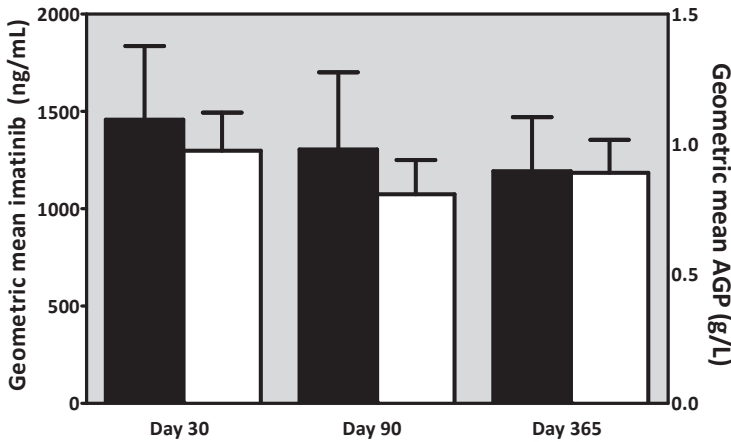
Figure 1. *(a) Geometric means of the AGP concentrations at 30 days (white bars), 90 days (striped bars), and 365 days (dotted bars) from treatment start, for each treatment setting. (b) Geometric means of imatinib trough concentrations (black bars) and AGP (white bars) at each of the time points. The error bars represent the 95% confidence intervals.*

AGP Versus Imatinib

Overall, AGP levels were significantly correlated with imatinib concentrations (R^2 = 0.656; P < 0.001; **Figure 2**) and with the sum of imatinib and CGP74588 concentrations (R^2 = 0.667; P < 0.001). The correlation between imatinib concentrations and AGP levels was less strong in the 25 samples that were taken at the first time point after 30 days (R^2 = 0.526; P < 0.001; **Figure 3**) in comparison with the correlations assessed at the two later time points. The absolute difference in AGP levels between time points 1 and 2 was also significantly correlated with the absolute difference in imatinib concentrations between time points 1 and 2 (R^2 = 0.381; P = 0.002) and between time points 1 and 3 (R^2 = 0.355; P = 0.03). The relative differences in AGP levels and imatinib concentrations between time points were not significantly correlated. The geometric mean AGP levels did not differ significantly between the three time points (P = 0.141; **Figure 1b**).

Table 2. Analyses of the samples obtained at the different time points.

	Time point 1 (n=25)	Time point 2 (n=25)	Time point 3 (n=19)	Total (n=69)
Actual time since start imatinib *(days)*	30 (3)	97 (30)	364 (20)	
AGP *(g/L)*	0.97 (0.85-1.10)	0.81 (0.69-0.94)	0.89 (0.78-1.00)	0.89 (0.82-0.96)
Imatinib *(ng/mL)*	1,457 (1,155-1,838)	1,305 (1,001-1,702)	1,193 (967-1,472)	1,325 (1,158-1,516)
CGP74588 *(ng/mL)*	308 (247-384)	265 (205-343)	231 (179-299)	270 (235-309)
Imatinib + CGP74588 *(ng/mL)*	1,777 (1,420-2,224)	1,578 (1,217-2,047)	1,439 (1,165-1,777)	1,606 (1,407-1,833)
Correlation between imatinib and AGP	0.526 (p<0.001)	0.839 (p<0.001)	0.411 (p=0.003)	0.656 (p<0.001)

The three time points represent the 3 moments at which sampling was scheduled according to protocol, i.e. 30 days, 90 days, and 365 days after start of treatment. Correlations are depicted as r^2 (p-value). Units of time are presented as mean (SD). All other values are presented as geometric mean (95% confidence interval).
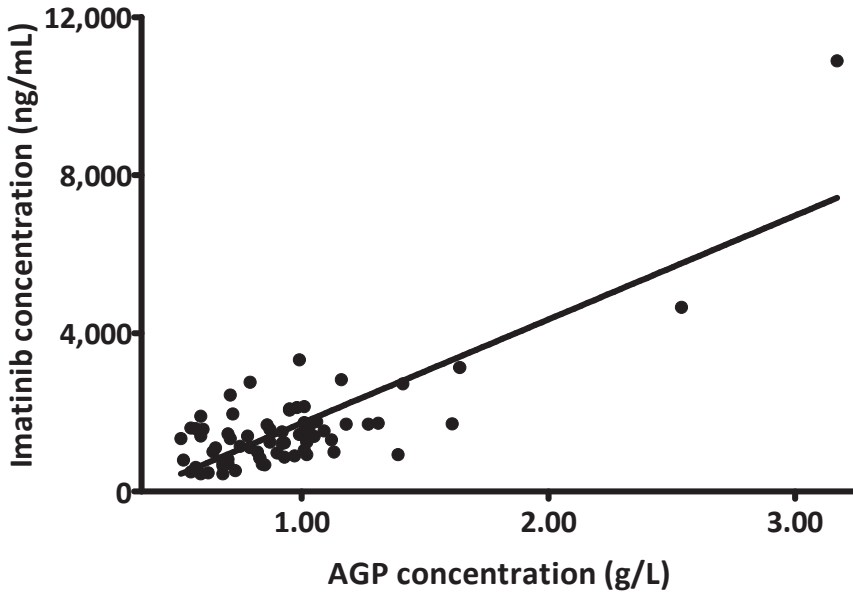
Figure 2. Correlation between imatinib and AGP in all samples (n=69).

7
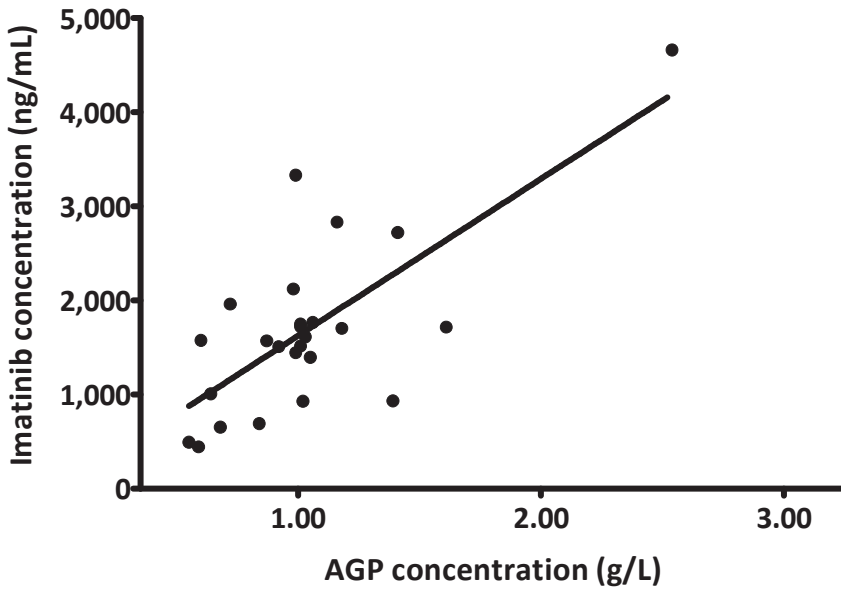
Figure 3. Correlation between imatinib and AGP at day 30 (n=25).

DISCUSSION

In this prospective setting, imatinib pharmacokinetics were closely correlated with systemic AGP levels when all samples obtained at the three different time points were considered together (R^2 = 0.656; P < 0.001). Although—at first sight—this appeared to be in line with the hypothesis that the increase in imatinib clearance is due to reduced systemic AGP levels,[14,16] the differences in AGP levels and imatinib C_{min} values between the time points were less strongly correlated. Moreover, the argument that AGP decreases during treatment and thereby contributes to increased imatinib clearance over time[12] did not seem to hold true, as we did not find substantial reductions in AGP levels during treatment (P = 0.141; **Figure 1**). Patients treated in the adjuvant setting even had a gradual increase in AGP levels, which contradicted the theory that AGP levels are initially elevated because of an inflammatory syndrome directly after tumour surgery and decline over time when the surgery effects resolve.[12] Even though the decrease in imatinib concentrations was not as large as those published previously, the implication of our current findings is that the role of systemic AGP levels in the reduced systemic imatinib exposure over time is relatively small and that other factors, e.g. reduced bioavailability, likely have larger influences on systemic exposure. Still, AGP might seriously interfere with imatinib exposure in vivo, as extravascular AGP affects imatinib pharmacokinetics beyond the systemic circulation,[15] and preclinical research has shown that the pharmacodynamic effects of imatinib are reduced in the presence of AGP.[18-20] Nonetheless, it remains questionable whether these extravascular effects can be used to determine the optimal dose for individual patients.

Unfortunately, the available evidence for individualized imatinib dosing in GIST patients is currently not robust, hampering assessment of the clinical relevance of TDM in GIST. Imatinib C_{min} values measured at different time points during treatment have previously been related to the clinical outcome.[5,8] Also, as mentioned previously, because of the decrease in systemic imatinib concentrations over time, target C_{min} values after 1 month cannot be extrapolated into a dosing algorithm for the entire treatment period. Although it has been proposed that TDM be performed only after imatinib pharmacokinetics have stabilized after 3 months of treatment,[11] whether or not an individual with GIST receives

the proper treatment and dose would ideally become visible much earlier during treatment. For example, by using fludeoxyglucose (18F) [18F-FDG] positron emission tomography [PET] as early as a few days after the start of treatment, it is possible to know whether or not a GIST patient is responding to treatment.[21] Either way, TDM in imatinib treatment can reach its full potential only when sampling times are standardized between research groups.[22] The sampling schedule employed in the current study could serve as a blueprint for larger studies because it incorporated C_{min} values at 1 month and at later time points, enabling assessment of long-term pharmacokinetic targets, which could subsequently be compared with the established target at 1 month. Alternatively, long-term pharmacokinetic targets could be derived from the target C_{min} at 1 month, using a formula that corrects for the parameters that contribute to the decrease in imatinib exposure. However, as the biological mechanism of this decreased exposure seems to be complex and multifactorial, the latter option to determine long-term pharmacokinetic targets is not likely to be computed soon. In parallel, other challenges in making TDM clinically usable will be to integrate the dosing range (300–800 mg daily) and the possible options in the case of insufficient concentrations (dose escalation or a treatment switch), but these are secondary to standardization of the sampling time points. Last, but certainly not least, it remains to be proven that imatinib TDM in GIST really translates into a better outcome in terms of either less toxicity or better anti-tumour effects.

Conclusion

We found that systemic AGP levels are not likely to be a key player in the decrease of systemic imatinib exposure over time. We believe that TDM is a very potent tool to improve personalized imatinib treatment, but it can flourish only if researchers ensure that their results are obtained in a standardized way.

REFERENCES

1. Larson RA, Druker BJ, Guilhot F, O'Brien SG, Riviere GJ, Krahnke T, et al. Imatinib pharmacokinetics and its correlation with response and safety in chronic-phase chronic myeloid leukemia: a subanalysis of the IRIS study. Blood. 2008;111(8):4022-8

2. Picard S, Titier K, Etienne G, Teilhet E, Ducint D, Bernard MA, et al. Trough imatinib plasma levels are associated with both cytogenetic and molecular responses to standard-dose imatinib in chronic myeloid leukemia. Blood. 2007;109(8):3496-9

3. Ishikawa Y, Kiyoi H, Watanabe K, Miyamura K, Nakano Y, Kitamura K, et al. Trough plasma concentration of imatinib reflects BCR-ABL kinase inhibitory activity and clinical response in chronic-phase chronic myeloid leukemia: a report from the BINGO study. Cancer Sci. 2010;101(10):2186-92

4. Zhong JS, Meng FY, Xu D, Zhou HS, Dai M. Correlation between imatinib trough concentration and efficacy in Chinese chronic myelocytic leukemia patients. Acta Haematol. 2012;127(4):221-7

5. Demetri GD, Wang Y, Wehrle E, Racine A, Nikolova Z, Blanke CD, et al. Imatinib plasma levels are correlated with clinical benefit in patients with unresectable/metastatic gastrointestinal stromal tumors. J Clin Oncol. 2009;27(19):3141-7

6. Yoo C, Ryu M-H, Ryoo B-Y, Beck MY, Chang H-M, Lee J-L, et al. Changes in imatinib plasma trough level during long-term treatment of patients with advanced gastrointestinal stromal tumors: correlation between changes in covariates and imatinib exposure. Investigational New Drugs. 2011;30(4):1703-8

7. Lankheet NA, Knapen LM, Schellens JH, Beijnen JH, Steeghs N, Huitema AD. Plasma concentrations of tyrosine kinase inhibitors imatinib, erlotinib, and sunitinib in routine clinical outpatient cancer care. Ther Drug Monit. 2014;36(3):326-34

8. Bouchet S, Poulette S, Titier K, Moore N, Lassalle R, Abouelfath A, et al. Relationship between imatinib trough concentration and outcomes in the treatment of advanced gastrointestinal stromal tumours in a real-life setting. Eur J Cancer. 2016;57:31-8

9. Eechoute K, Fransson MN, Reyners AK, de Jong FA, Sparreboom A, van der Graaf WT, et al. A long-term prospective population pharmacokinetic study on imatinib plasma concentrations in GIST patients. Clin Cancer Res. 2012;18(20):5780-7

10. Judson I, Ma P, Peng B, Verweij J, Racine A, di Paola ED, et al. Imatinib pharmacokinetics in patients with gastrointestinal stromal tumour: a retrospective population pharmacokinetic study over time. EORTC Soft Tissue and Bone Sarcoma Group. Cancer Chemother Pharmacol. 2005;55(4):379-86

11. Judson I. Therapeutic drug monitoring of imatinib--new data strengthen the case. Clin Cancer Res. 2012;18(20):5517-9

12. Chatelut E, Gandia P, Gotta V, Widmer N. Long-term Prospective Population PK Study in GIST Patients--Letter. Clin Cancer Res. 2013;19(4):949

13. Gambacorti-Passerini C, le Coutre P, Zucchetti M, D'Incalci M. Binding of imatinib by alpha(1)-acid glycoprotein. Blood. 2002;100(1):367-8; author reply 8-9

14. Widmer N, Decosterd LA, Csajka C, Leyvraz S, Duchosal MA, Rosselet A, et al. Population pharmacokinetics of imatinib and the role of alpha-acid glycoprotein. Br J Clin Pharmacol. 2006;62(1):97-112

15. Zsila F, Fitos I, Bencze G, Keri G, Orfi L. Determination of human serum alpha1-acid glycoprotein and albumin binding of various marketed and preclinical kinase inhibitors. Curr Med Chem. 2009;16(16):1964-77

16. Mathijssen RH, de Bruijn P, Eechoute K, Sparreboom A. Long-term Prospective Population PK Study in GIST Patients--Response. Clin Cancer Res. 2013;19(4):950

17. Schiavon G, Eechoute K, Mathijssen RH, de Bruijn P, van der Bol JM, Verweij J, et al. Biliary excretion of imatinib and its active metabolite CGP74588 during severe hepatic dysfunction. J Clin Pharmacol. 2012;52(7):1115-20

18. Beckmann S, Long T, Scheld C, Geyer R, Caffrey CR, Grevelding CG. Serum albumin and alpha-1 acid glycoprotein impede the killing of Schistosoma mansoni by the tyrosine kinase inhibitor Imatinib. Int J Parasitol Drugs Drug Resist. 2014;4(3):287-95

19. Gambacorti-Passerini C, Barni R, le Coutre P, Zucchetti M, Cabrita G, Cleris L, et al. Role of alpha1 acid glycoprotein in the in vivo resistance of human BCR-ABL(+) leukemic cells to the abl inhibitor STI571. J Natl Cancer Inst. 2000;92(20):1641-50

20. Larghero J, Leguay T, Mourah S, Madelaine-Chambrin I, Taksin AL, Raffoux E, et al. Relationship between elevated levels of the alpha 1 acid glycoprotein in chronic myelogenous leukemia in blast crisis and pharmacological resistance to imatinib (Gleevec) in vitro and in vivo. Biochem Pharmacol. 2003;66(10):1907-13

21. Van den Abbeele AD, Gatsonis C, de Vries DJ, Melenevsky Y, Szot-Barnes A, Yap JT, et al. ACRIN 6665/RTOG 0132 phase II trial of neoadjuvant imatinib mesylate for operable malignant gastrointestinal stromal tumor: monitoring with 18F-FDG PET and correlation with genotype and GLUT4 expression. J Nucl Med. 2012;53(4):567-74

22. Yu H, Steeghs N, Nijenhuis CM, Schellens JH, Beijnen JH, Huitema AD. Practical guidelines for therapeutic drug monitoring of anticancer tyrosine kinase inhibitors: focus on the pharmacokinetic targets. Clin Pharmacokinet. 2014;53(4):305-25
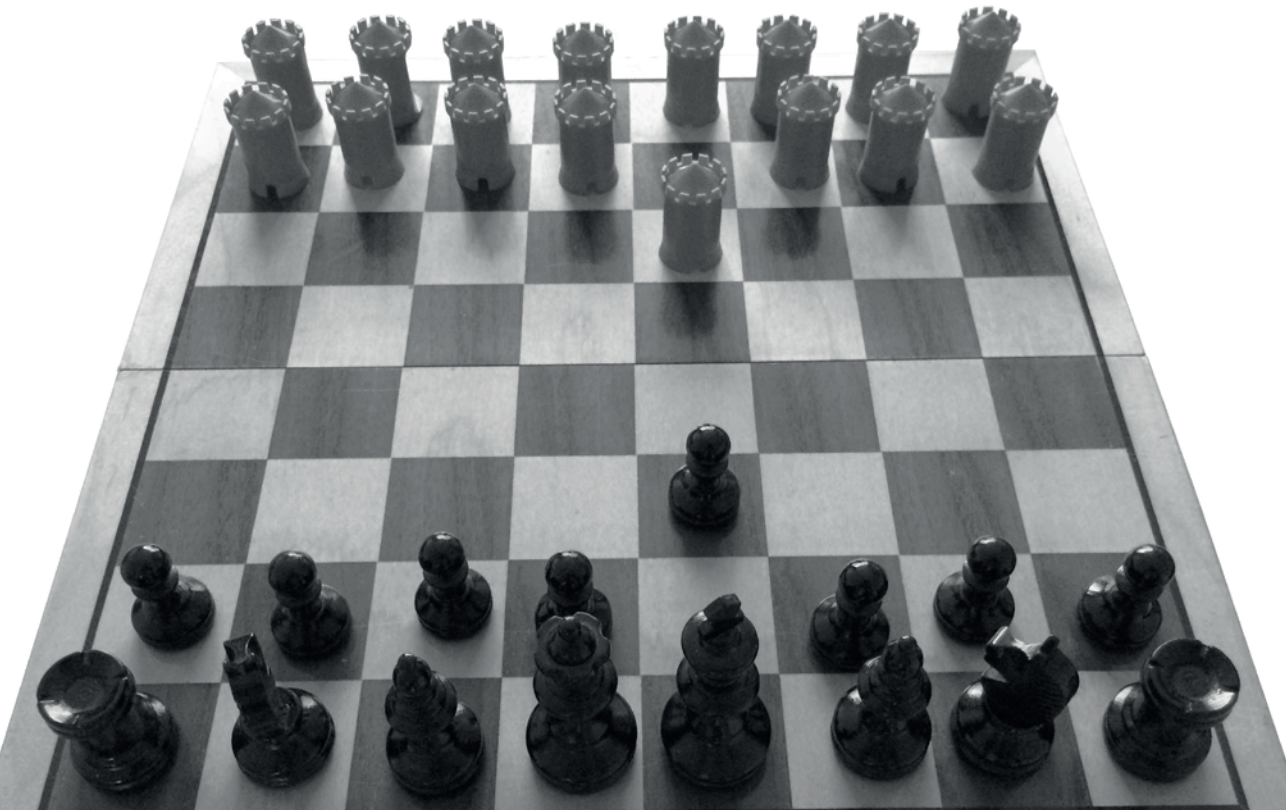
7

Individualized pazopanib dosing: a prospective feasibility study in cancer patients

Sander Bins,* Remy B. Verheijen,* Ron H.J. Mathijssen, Martijn P. Lolkema, Leni van Doorn, Jan H.M. Schellens, Jos H. Beijnen, Marlies H.G. Langenberg, Alwin D.R. Huitema, Neeltje Steeghs
* Both authors contributed equally

ABSTRACT

Purpose. Pazopanib is a tyrosine kinase inhibitor approved for the treatment of renal cell carcinoma and soft tissue sarcoma. Retrospective analyses have shown that an increased median PFS and tumor shrinkage appears in patients with higher plasma trough levels (C_{min}). Therefore, patients with low C_{min} might benefit from pharmacokinetically-guided individualized dosing.

Experimental Design. We conducted a prospective multicenter trial in 30 patients with advanced solid tumors. Pazopanib C_{min} was measured weekly by LC-MS/MS. At week 3, 5 and 7 the pazopanib dose was increased if the measured C_{min} was <20 mg/L and toxicity was < grade 3.

Results. In total, 17 patients had at least one C_{min} <20 mg/L at week 3, 5 and 7. Of these, 10 were successfully treated with a pharmacokinetically-guided dose escalation, leading to daily dosages ranging from 1000 to 1800 mg daily. C_{min} in these patients increased significantly from 13.2 (38.0%) mg/L (mean (CV%)) to 22.9 mg/L (44.9%). Thirteen patients had all C_{min} levels {greater than or equal to}20 mg/L. Of these, nine patients with a high C_{min} of 51.3 mg/L (45.1%) experienced {greater than or equal to} grade 3 toxicity and subsequently required a dose reduction to 600 or 400 mg daily, yet in these patients C_{min} remained above the threshold at 28.2 mg/L (25.3%).

Conclusions. A pharmacokinetically-guided individualized dosing algorithm was successfully applied and evaluated. The dosing algorithm led to patients being treated at dosages ranging from 400 to 1800 mg daily. Further studies are needed to show a benefit of individualized dosing on clinical outcomes such as progression free survival.

INTRODUCTION

Pazopanib is a tyrosine kinase inhibitor targeting VEGFR-1,2,3, PDGFR α/β, FGFR and c-Kit.[1] Pazopanib increased progression free survival (PFS) from 4.2 to 9.2 months in renal cell carcinoma (RCC) and from 1.6 to 4.6 months in soft tissue sarcoma (STS) compared to placebo.[2,3]

A retrospective analysis in 177 RCC patients by Suttle et al. showed an increased tumor shrinkage and longer PFS in patients with plasma trough levels (C_{min}) ≥20.5 mg/L compared to patients with a C_{min} below this threshold (4). Median PFS was found to be 50.2 weeks in patients with higher pazopanib C_{min} versus 19.6 weeks in patients with lower C_{min}. Median tumor shrinkage was 37.9% in the high versus 6.9% in the low exposure group. No further increase in PFS or tumor shrinkage was found above a pazopanib plasma concentration of 20.5 mg/L.

This threshold for efficacy seems to be in accordance with preclinical data showing optimal VEGFR2 inhibition by pazopanib in vivo at a concentration ≥17.5 mg/L (40 µmol/L) in mouse models.[5] Additionally, in the phase I trial hypertension, a pharmacodynamic biomarker for response to anti-angiogenic agents, correlated with C_{24h} values above 15 mg/L at day 22.[6] Plasma concentrations were also correlated with radiographic response in a phase II study of patients with progressive, radioiodine-refractory, metastatic differentiated thyroid cancers treated with pazopanib.[7] The above indicates that efficacy of pazopanib is strongly associated with pharmacokinetic (PK) exposure in many tumor types. Pazopanib PK shows significant inter-individual variability in plasma exposure[6,8,9] and may be affected by various factors, such as concomitant medication (e.g. drugs increasing gastric pH or inhibiting/inducing CYP3A4), intake of food, patient compliance and (exact) time of tablet ingestion and blood sampling.[9–12]

Despite the large variability in exposure, pazopanib is currently still administered at a fixed dose of 800 mg daily. This may however result in suboptimal treatment in a subset of patients who have a low C_{min}. In a retrospective analysis performed by the manufacturer of pazopanib, 20% of patients had a C_{min} below 20.5 mg/L and might have had benefit from an increased dose.[4] The feasibility of PK-guided dosing has already been shown in prospective clinical trials for tamoxifen[13] and another tyrosine kinase inhibitor with similar properties, sunitinib.[14] Therefore, we now conducted a prospective feasibility trial to investigate whether the dose of pazopanib could be safely increased in patients who have a low C_{min} on the fixed

8

800 mg dose of pazopanib and whether this led to increased drug exposure, without intolerable toxicity.

MATERIALS AND METHODS

Patient population

Cancer patients for whom pazopanib was considered standard of care, or for whom no remaining standard treatment options were available, were eligible for enrollment. Patients also had to be at least 18 years of age, had to have a WHO performance score of 0 or 1, needed to have evaluable disease according to RECIST 1.1 and also had to have an adequate organ function at baseline defined as: absolute neutrophil count ≥ 1.5×10^9/L, hemoglobin ≥ 5.6 mmol/L, platelets ≥ 100×10^9/L, prothrombin time or international normalized ratio ≤ 1.2x ULN, activated partial thromboplastin time ≤ 1.2x ULN, total bilirubin ≤ 1.5x ULN, alanine amino transferase and aspartate aminotransferase ≤ 2.5x ULN, serum creatinine ≤ 133 µmol/L or, if >133 µmol/L a calculated creatinine clearance of 30 to 50 mL/min, urinary protein (on dipstick) <2 + or <1 gram in 24-hour urine.

Exclusion criteria were: corrected QT interval (QTc) > 480 milliseconds, history of any relevant cardiovascular conditions, cerebrovascular accidents, transient ischemic attack, pulmonary embolisms or untreated deep venous thrombosis (DVT) within the past 6 months, poorly controlled hypertension (defined as systolic blood pressure (SBP) of ≥140 mmHg or diastolic blood pressure (DBP) of ≥ 90mmHg), clinically significant gastrointestinal abnormalities that might increase the risk for gastrointestinal bleeding, major surgery or trauma within 28 days prior to first pazopanib dose, evidence of active bleeding or bleeding diathesis, known endobronchial lesions and/or lesions infiltrating major pulmonary vessels, recent hemoptysis within 8 weeks before the first dose, any anti-cancer therapy within 14 days or five half-lives of the previous anti-cancer drug (whichever was longer) prior to first pazopanib dose, any ongoing toxicity from prior anti-cancer therapy that was grade >1 and/or that was progressing in severity, except for alopecia.

Pharmacokinetically guided dosing

All patients started at the approved pazopanib dose of 800 mg once daily (QD). Plasma samples for C_{min} measurements were collected weekly in the first 8 weeks of pazopanib treatment and every 4 weeks thereafter. Pazopanib concentrations were measured using a validated LC-

MS/MS assay. A 10 µL plasma aliquot was used, to which 500 µL of methanol containing $^{13}C,^{2}H_{3}$-pazopanib as internal standard and 500 µL of 10 mM ammonium hydroxide in water were added. This solution was then centrifuged at 15.000 rpm and 5 µL of the supernatant was injected into the LC-MS/MS system (LC-system from Agilent Technologies (Santa Clara, CA) and API3000 MS by AB Sciex (Framingham, MA). Elution was performed using an isocratic gradient of 45% 10 mM ammonium hydroxide in water and 55% methanol on a Gemini C18 column, 2.0 x 50 mm, 5 µm by Phenomenex (Torrance, CA). This assay was validated and fulfilled all requirements of the FDA and EMA guidelines for bioanalytical method validation. C_{min} results were reported to the treating physician within 1 week.

At week 3, day 1 (Day 15); week 5, day 1 (Day 29) and week 7, day 1 (Day 43), the dose could be adapted, based on the measured C_{min} collected a week earlier and observed toxicity was graded according to the National Cancer Institute's Common Terminology Criteria for Adverse Events (NCI-CTCAE v4.02). The target exposure for efficacy used during this trial was a $C_{min} \geq 20.0$ mg/L. Patients with a $C_{min} < 15.0$ mg/L received a dose increase of 400 mg daily in the absence of $\geq$ grade 2 toxicity or 200 mg daily when experiencing grade 2 toxicity, but not $\geq$ grade 3 adverse events (AEs). Patients with a C_{min} of 15.0-19.9 mg/L received a 200 mg dose increase if toxicity was below grade 3. No patients would be treated above the prespecified dose limit of 2,000 mg QD, as this was the highest dose previously tested in humans.[6] In case of severe ($\geq$ grade 3) treatment related toxicity the dose was lowered by 1 dose level, or to the previous dose level in case of an earlier dose increment.

Safety assessments

Recording of AEs, physical examination, hematology and blood chemistry assessments were performed weekly during the first 8 weeks and monthly thereafter. The incidence, severity, start and end dates of all serious AEs (SAEs) and of non-serious AEs related to pazopanib were recorded.

Efficacy assessments

CT-scan and/or MRI-scans were performed every 8 weeks after initiation of therapy until documented disease progression according to the Response Evaluation Criteria in Solid Tumors (RECIST) version 1.1. Data on best response and time to progression was collected.

8

Statistical methods

All statistical analyses were performed in R version 3.2.2.[15] For exposure-response relationships the mean of all measured C_{min} levels for each patient during the entire treatment period (from start of treatment to discontinuation) was used as the measure of pazopanib exposure. For the purpose of exposure-toxicity relationships, the C_{min} measurement closest to the first presentation of the toxicity was used. Unless otherwise specified, hypotheses were tested using a two-sided independent sample t-test. P-values <0.05 were considered significant.

Study Conduct and registry

This trial was conducted in accordance with the World Medical Organization declaration of Helsinki, compliant with Good Clinical Practice and approved by the Medical Ethics Committee of the each participating medical centers. All patients provided written informed consent before enrollment. This trial was registered in the EudraCT database (2013-001567-24) and the Netherlands Trial Registry (NTR3967).

RESULTS

Patient population

A total of 30 patients were included from September 2013 until March 2014 in 3 Dutch cancer centers. Characteristics of included patients are shown in **Table 1**. Tumor types of included patients were soft tissue sarcoma (n=7), colorectal carcinoma (n=6), cancer of unknown primary (n=4), neuroendocrine carcinoma (n=2), thymus carcinoid, hepatocellular carcinoma, ovarian carcinoma, mesothelioma, esophageal carcinoma, meningeoma, perivascular epithelial tumor, renal cell carcinoma, choroidal melanoma, endometrial carcinoma and cholangiocarcinoma (all n=1). All patients received at least one dose of pazopanib, underwent at least one C_{min} measurement and were eligible for PK evaluation. Median study follow up was 34 weeks.

Pharmacokinetic guided dosing

Based on treatment outcome patients were divided into four groups, see **Figure 1**. Patients who had at least one C_{min} below 20.0 mg/L at day 15, 29 or 43 were appointed group 1, patients who had all these C_{min} measurement above the target were appointed group 2. Patients who did not experience any toxicity requiring a dose reduction or interruption during

the dose escalation period (the first 8 weeks of treatment) were classified as group a (no severe toxicity), those who did were classed as group b (severe toxicity). Based on this classification the distribution of patients was 10 in group 1a (eligible for a dose escalation), 7 in 1b (no dose escalation possible due to toxicity), 4 in group 2a (adequate C_{min}, no toxicity) and 9 in group 2b (adequate C_{min}, severe toxicity) (**Figure 1**). A full overview of treatment outcomes (C_{min} measurements, dose received and percentage of patients above the C_{min} target) is provided in **Table 2**. Plots of the C_{min} over time per treatment outcome group are shown in **Figure 2**.

Table 1. Demographics of included patients.

Characteristic	Patients (n=30)	
Gender *(n (%))*		
Male	14	(53)
Female	16	(47)
Age *(median (range))*	58	(33– 88)
Steady state C_{min} (mg/L) at 800 mg dose (W2D1) *(mean (CV %))*	30.0	(71.9)
Performance status *(n (%))*		
0	7	(23)
1	23	(77)
Previous lines of systemic therapy *(median (range))*	2	(1-5)
Type *(n(%))*		
Chemotherapy	24	(80)
Targeted therapy	7	(23)
Endocrine therapy	3	(10)
Primary tumor *(n (%))*		
Soft tissue sarcoma	7	(23)
Colorectal carcinoma	6	(20)
Cancer of unknown primary	4	(13)
Neuroendocrine carcinoma	2	(6)
Miscellaneous*	11	(33)

* *Hepatocellular carcinoma, ovarian carcinoma, mesothelioma, esophageal carcinoma, meningeoma, perivascular epithelial tumor, renal cell carcinoma, choroidal melanoma, endometrial carcinoma, cholangiocarcinoma and thymus carcinoid (all n=1).*

8
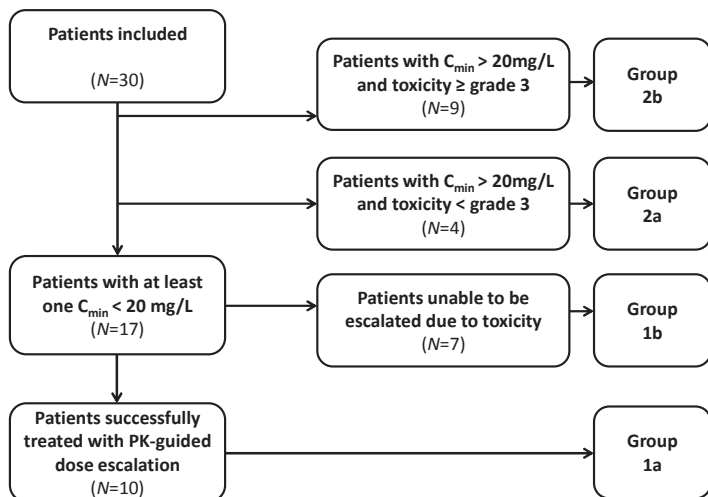
Figure 1a. *Trial outcome flowchart. Toxicity for the purposes of this chart is defined as any adverse event requiring a dose interruption or reduction in the first 8 weeks of treatment. Cmin below or above the target of ≥20.0 mg/L is based on samples from week 2, 4 or 6 as per protocol dose escalations were based on these samples.*
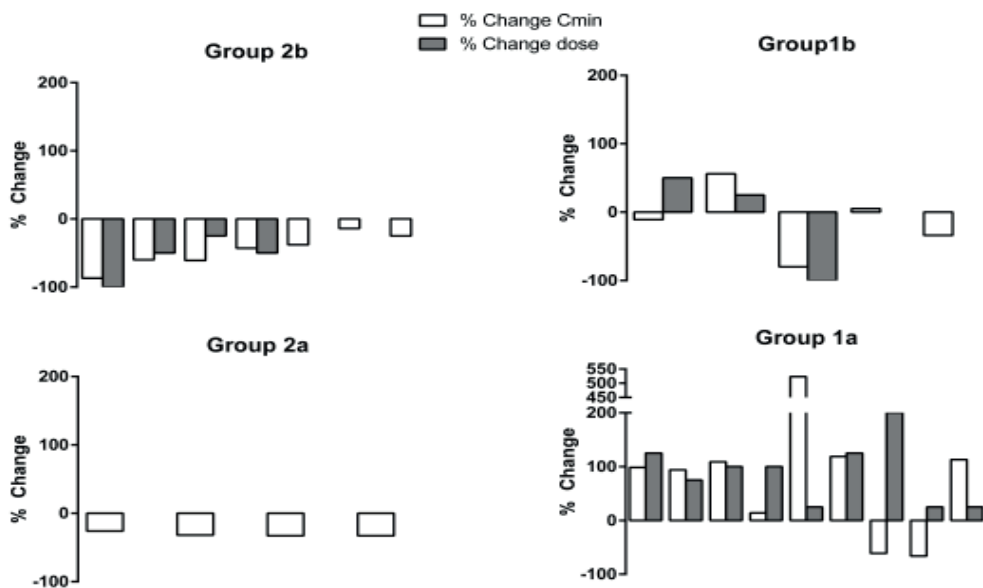
Figure 1b. *Percent change in dose from baseline (steady state at W2D1) to the end of the dose algorithm period (Last dose change (W7D1) and corresponding steady state Cmin W8D1). Grey bars represent % change in pazopanib dose (mg QD) white bars represent % change in pazopanib Cmin (mg/L). Each patient is represented by adjacent bars, plotted per treatment outcome group, only patients evaluable at both week 2 and week 8 are shown.*

**Table 2.** Pazopanib C_{min}, percentage of patients above target and dose per treatment outcome group[‡].

Outcome	Group 1a TOX - C_{min} <20.0 mg/L n = 10	Group 1b TOX + C_{min} <20.0 mg/L n = 7	Group 2a TOX - C_{min} ≥20.0 mg/L n = 4	Group 2b TOX + C_{min} ≥20.0 mg/L n = 9	Total n = 30
	Mean pazopanib C_{min} (mg/L (CV %))				
W2D1	13.2 (38.0)	19.7 (56.6)	37.4 (19.4)	51.3 (45.1)	30.0 (71.9)
W4D1	15.5 (52.8)	16.2 (39.6)	31.8 (8.1)	39.4 (29.5)	24.8 (54.8)
W6D1	19.7 (27.4)	13.3 (39.6)	26.8 (29.2)	33.2 (30.5)	22.8 (43.2)
W8D1	22.9 (44.9)	18.9 (40.5)	25.9 (18.8)	28.2 (25.3)	24.1 (33.9)
	% of pts above the target C_{min} of ≥20.0 mg/L[†]				
W2D1	10.0	42.8	100.0	100	56.7
W4D1	20.0	14.3	100.0	88.6	50.0
W6D1	40.0	14.3	100.0	66.6	50.0
W8D1	40.0	28.6	100.0	55.6	50.0
	Mean daily pazopanib Dose (mg)				
W3D1	1040	933	800	725	893
W5D1	1280	1000	800	667	1000
W7D1	1378	950	800	633	1009

*40% of patients in group 1a achieved the target in week 8. During study follow up, 7 patients in group 1a (70%) achieved target exposure of > 20.0 mg/L within 3 months since start of treatment.

†Patients for whom no C_{min} was available or who discontinued treatment are scored as below the target

‡Toxicity for the purposes of grouping is defined as any adverse event requiring a dose interruption or reduction in the first 8 weeks of treatment. Cmin below or above the target of ≥20.0 mg/L is based on samples from week 2, 4 or 6.

8

Group1a: Group 1a (patients with low drug exposure, and no severe toxicity) consisted of 10 patients who were sustainably treated at an increased dose. The C_{min} in this group increased from 13.2 (CV 38.0%) mg/L in week 2 to 22.9 (CV 44.9%) mg/L in week 8 (p=0.02). Only two patients did not show an increase in C_{min} after the dose escalation. Four patients reached the target at the end of the dose escalation period (week 8) and 7 patients reached the target exposure of ≥20 mg/L within 3 months of treatment. After the last dose escalation (day 43), patients in group 1a were treated at a
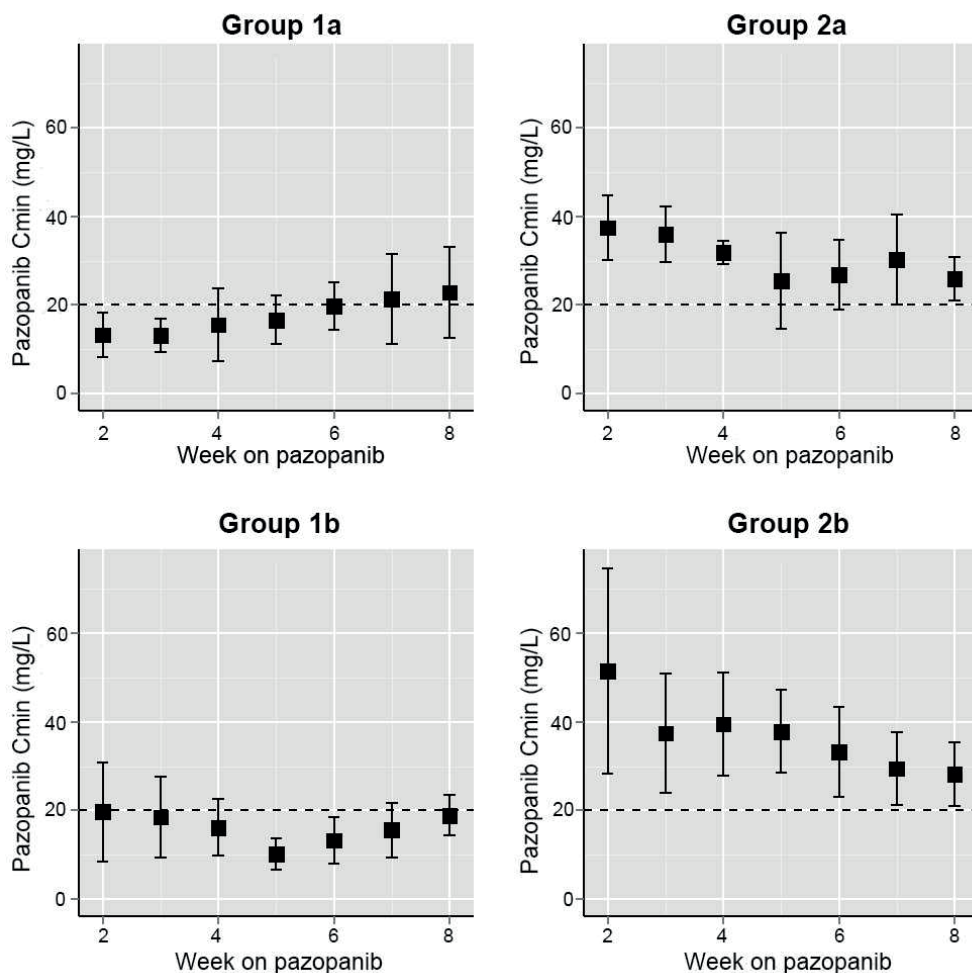
Figure 2. *Pazopanib exposure over time per outcome group (mean Cmin ± standard deviation). The dotted line indicates the threshold of 20 mg/L. Cmin did not change in group 1b (p=0.89). In group 2a and 2b Cmin declined significantly (p=0.04 and 0.04 respectively). Group 1a showed a significant increase in Cmin from 13.2 mg/L to 22.9 mg/L (p=0.02).*

mean dose of 1,378 mg, ranging from 1,000 to 1,800 mg. One patient was treated with 1,800 mg QD for over 33 weeks, with acceptable (<grade 3) toxicity.

Group 1b: Patients in group 1b (patients with low drug exposure, but with toxicity requiring a dose interruption or reduction, n=7) had a stable C_{min} during the dose escalation phase. In this group, one patient could not have a dose escalation because of toxicity (ASAT/ALAT increase) at the prespecified dose escalation moments. Another patient required a dose interruption but could later continue treatment on 800 mg QD. Five patients experienced toxicity after an initial escalation and required a subsequent dose reduction. Four of these five could hereafter be treated successfully until disease progression at a dose of 800 mg (n=3) or 1,000 mg (n=1) daily. One patient discontinued treatment due to toxicity after dose escalation (fatigue, grade 3).Their C_{min} was 19.7 (CV 56.6%) mg/L at week 2 and 18.9 (CV 40.5%) mg/L at week 8 (p=0.89).

Group 2a: Four patients (group 2a, patients with high drug exposure, and no severe toxicity) could be treated on the fixed 800 mg dose with adequate C_{min} without the need for a dose reduction or interruption in the first 8 weeks. Surprisingly, the C_{min} decreased in these patients from 37.4 mg/L (CV 19.4%) at week 2 to 25.9 mg/L (CV 18.8%) at week 8 (p=0.04).

Group 2b: Patients in group 2b (patients with a high drug exposure, but also severe toxicity, n=9) had a decrease in C_{min} from week 2 to week 8 from 51.3 mg/L (CV 45.1%) to 28.2 mg/L CV 25.3%) (p=0.04). The mean dose was reduced from 800 mg to 600 mg in the same interval.

Use of gastric acid reducing agents was discouraged but not prohibited during this trial. Of patients in the low exposure groups 9 (7 in group 1a and 2 in 1b) and in the high exposure groups 4 (all in 2b) used a PPI at any point during treatment. Patients were instructed to take the PPI concomitantly with pazopanib as recommended in the summary of product characteristics.

Adverse events

An overview of the observed AEs related to pazopanib with a frequency of ≥10% is shown in **Table 3**. The most common severe (≥ grade 3) AEs were hypertension, fatigue, ASAT/ALAT increase.

8

Less patients experienced ≥ grade 3 AEs in the low exposure groups (1a and 1b), with 41.2% of patients experiencing at least one ≥ grade 3 AE, compared to 76.9% in the high exposure groups (2a and b). The percentage of patients discontinuing due to toxicity was similar between the high and low exposure groups, 11.8% in 1a plus 1b and 15.4% in 2a plus 2b. Of patients with a high exposure requiring a dose reduction (group 2b, n=9), all but 2 (both cases fatigue grade 3) could be successfully treated at a lower dose until disease progression. Overall, events causing the discontinuation were fatigue (n=3) and ASAT/ALAT increase (n=1). Remarkably, the C_{min} at week 2 appeared higher in patients in group 1 experiencing toxicity (19.7 mg/L versus 13.2 mg/L (p=0.19), respectively) and the same trend was observed in group 2 (37.4 mg/L for patients without toxicity versus 51.3 mg/L for patients with toxicity (p=0.27), respectively).

Patients who experienced fatigue (n=3) or ASAT/ALAT increase (n=2) had a C_{min} (at first presentation of grade 3 toxicity) 51.4 mg/L (range 21.4 - 98.1) and 8.9 mg/L (range 7.3 - 10.5) respectively. Patients with grade 3 hypertension (n=11) had a C_{min} at presentation of 37.3 mg/L (range 7.0 - 76.5) while that patients who experienced grade 2 hypertension (n=10) was 27.8 mg/L (range 16.7 – 43.8).

Efficacy

From 27 patients at least one response evaluation was available. Of these, 3 patients had a partial response (perivascular epithelial tumor, renal cell carcinoma and soft tissue sarcoma, all n=1), 18 had stable disease, and 6 had progressive disease as best response.

The mean of all measured C_{min} levels per patient (from start of treatment to discontinuation) was calculated as a measure of exposure during pazopanib therapy for the purpose of exposure-response relationships. Overall, the average of the mean C_{min} of each patient was 24.4 mg/L (CV 39.1%). In total, 19 patients had a mean C_{min} above and 11 below the target of 20 mg/L. A waterfall plot of the maximum decrease in tumor size from baseline is shown in **Figure 3**. All three patients who had a partial response had a mean C_{min} above the 20 mg/L threshold (with an average of 27.6 mg/L (CV 14.4%). In non-prespecified, exploratory analyses of all evaluable patients (n=27), tumor response was

associated with mean C_{min} of pazopanib. An average change from baseline for patients above and below the PK threshold of -6.49% and +14.6% respectively, (p=0.01). In soft tissue sarcoma patients (n=7), mean change from baseline was -6.01% (n=5) for patients above the threshold and +13.5% for patients below (n=2)(p=0.28). In sarcoma patients PFS was 47.9 weeks (range 8 - 60, n=5) and 11.5 weeks (range 7 - 16, n=2) for patients below the PK threshold (p=0.06, log-rank test).
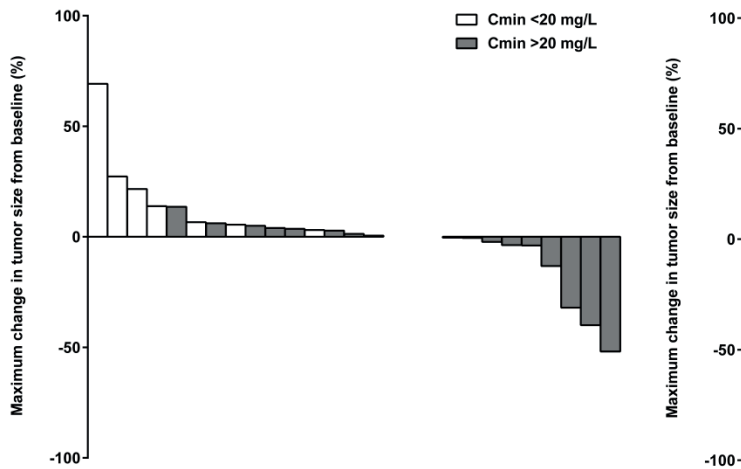
Figure 3. Left panel*: Waterfall plot showing the maximum change in tumor size from baseline in all evaluable patients (n = 27). Grey bars represent patients with a mean Cmin ≥20.0 mg/L (n=17), white bars represent patients with a Cmin <20.0 mg/L (n=10). Mean change from baseline for all evaluable patients (n=27) above and below the PK threshold was -6.49% and +14.6%, (p=0.01).* Right Panel*: Mean change from baseline in soft tissue sarcoma patients (n=7) above and below the PK threshold was -6.01% (n=5) and +13.5% (n=2), (p=0.28).*

Table 3. Toxicity data per outcome group‡, only toxicities related to pazopanib with a frequency of ≥10% are shown.

Any grade	TOX - C_{min} <20.0 mg/L n = 10		TOX + C_{min} <20.0 mg/L n = 7		TOX - C_{min} ≥20.0 mg/L n = 4		TOX + C_{min} ≥20.0 mg/L n = 9		n=30	
	Any grade	Grade ≥3	Any grade	Grade ≥3	Any grade	Grade ≥3	Any grade	Grade ≥3	Any grade	Grade ≥3
Hypertension	4	2*	3	2	1	1*	7	6	15	11
Fatigue	3	0	3	1	1	0	6	2	13	3
Diarrhea	4	1*	4	0	2	0	2	0	12	1
Nausea	2	0	0	0	1	0	6	0	9	0
Rash	2	0	3	1	0	0	3	0	8	1
Hair depigmentation	3	0	2	0	3	0	0	0	8	0
ASAT increase	1	0	2	2	2	0	1	0	6	2
ALAT increase	1	0	2	2	0	0	2	0	5	2
Anorexia	2	0	1	0	0	0	1	0	4	0
Weight loss	1	0	1	0	0	0	2	0	4	0
Dysgeusia	0	0	0	0	2	0	2	0	4	0
Vomiting	1	0	0	0	1	0	2	0	4	0
Edema	0	0	1	0	1	0	1	0	3	0
Proteinuria	1	0	0	0	0	0	2	0	3	0
Dyspnea	1	0	0	0	1	0	1	0	3	0

Data are presented as number patients (n).

*These grade 3 toxicities did not result in a dose reduction or discontinuation or occurred after the 8 week dose escalation period.

‡Toxicity for the purposes of grouping is defined as any adverse event requiring a dose interruption or reduction in the first 8 weeks of treatment. Cmin below or above the target of ≥20.0 mg/L is based on samples from week 2, 4 or 6.

DISCUSSION

We performed a prospective multicenter clinical trial to assess the safety and feasibility of PK-guided individualized dosing of pazopanib in 30 patients with advanced solid tumors. With the PK-guided dosing algorithm, 33.3% of all patients could be treated at a higher dose (1000 – 1800 mg daily) with acceptable toxicity (**Figure 1**). Most of these patients achieved the target C_{min} of 20.0 mg/L within study follow up. Furthermore, overall variability in pazopanib C_{min} was reduced from 71.9% before the dose escalation period to 33.9% thereafter (**Table 2**).

An equal number of patients discontinued treatment in the low C_{min} versus the high C_{min} group and only one patient discontinued treatment after a dose escalation. This suggests PK-guided increasing of the dose does not lead to more severe toxicity or higher rates of treatment discontinuation. Meanwhile, a reduction of the dose in case of very high systemic concentrations, may lead to less toxicity and still maintain therapeutic C_{min} levels (group 2b, **Figure 2**).

High pazopanib exposure seemed predictive of dose reductions for toxicity in patients not eligible for a dose escalation (group 2a en 2b). The C_{min} at week 2 was higher (though not significantly) in the patients that would require a dose reduction (2b) than those who would not (2a), (mean of 51.3 versus 37.4 mg/L, table 2, **Figure 2**). This implies that patients are unlikely to tolerate a very high trough level for a longer period of time and could support strategies to prevent toxicity by implementing dose reduction in patients with C_{min} >50 mg/L, although this is based on limited data.

No clear relations between C_{min} and specific grade ≥ 3 toxicities were found. The most common severe AE was hypertension. This is thought to be related to higher pazopanib exposure;[6] our study found a mean C_{min} at occurrence of hypertension 37.3 and 27.8 mg/L in patients experiencing grade 3 (n=11) and 2 (n=10) hypertension respectively. But this was not significantly higher than the overall mean C_{min}. It might be the case however, that another pharmacokinetic parameter (e.g. C_{max}) may be more appropriate to study exposure-toxicity relationships than C_{min}, the one used in the current trial.

Two patients experienced severe hepatotoxicity, in one case leading to ASAT and ALAT values of over 13 times the upper limit of normal and discontinuation of treatment. This seemed unrelated to high exposure, as the mean C_{min} of these patients (in the sample

8

closest in time to occurrence) was only 8.9 mg/L. This finding is corroborated by a recent study suggesting the mechanism of pazopanib hepatotoxicity may be immunological and therefore unrelated to pazopanib PK or dose.[16]

A significant reduction in pazopanib C_{min} was seen in patients treated continuously at the 800 mg fixed dose (group 2a, **Figure 2**).Though in our trial this group consisted of only a small number of patients, the same effect was observed in a population pharmacokinetic analysis of previously published clinical trials.[17] A time dependent decrease in exposure was also observed for another tyrosine kinase inhibitor, imatinib.[18] For imatinib, upregulation of drug transporters or CYP3A4 have been suggested as possible explanations, which could also be the case for pazopanib as it is a known substrate of both.

In addition to PK-guided dosing of pazopanib other dose individualization strategies could be explored. Pharmacodynamic biomarkers could be used for example, such as interleukin 12 (IL12) or soluble VEGFR2 (sVEGFR2).[19] However given that for pazopanib the relation between C_{min} and PFS was very significant at p=0.0038 and resulted in a remarkable median PFS difference of 32.4 weeks in RCC patients,[4] C_{min} might be a more appropriate biomarker for pazopanib than sVEGFR2 or IL12.

Toxicity based dosing could also be proposed as a dose individualization approach and has been explored previously for erlotinib (using rash), sorafenib and axitinib (both using hypertension).[20–22] A drawback of this strategy is that it, per definition, would lead to more toxicity. The PK-guided approach applied in this trial with pazopanib did not seem to lead to less tolerability.

Another trial was performed to assess PK-guided dosing of pazopanib by De Wit et al.[9] In that trial, pazopanib area under the curve (AUC_{0-24h}) was used as the pharmacokinetic parameter to individualize dosing and a target window of 715-920 mg·h·L^{-1} (corresponding to C_{min} values of 20.5 – 46.0 mg/L) was specified. The primary endpoint of that study in 13 patients was a reduction in variability and, per protocol, only one dose change was allowed. AUC-guided dosing did not significantly reduce inter-patient variability, probably due to intra-patient variability or sampling time issues. Based on this trial the authors concluded it may be more beneficial to target the C_{min} threshold rather than an AUC window.[4,9] In addition, dosing base on C_{min} will also be more practical

to implement in routine care, as it requires just one instead of multiple samples. Moreover, as target inhibition is thought to be concentration dependent, dosing should strive to keep the drug concentration above a certain minimally efficacious concentration during the whole dose interval, which is most accurately reflected by C_{min}.

Most importantly, studies relating pazopanib exposure to response have used C_{min}, rather than AUC, further strengthening the case for C_{min} threshold monitoring.[4,6] Finally, self-sampling approaches facilitated by dried blood spot sampling may further enable the use of PK-guided dosing in routine care and several assays have already been developed for this purpose.[23,24]

The number of patients who had a C_{min} below the target at a moment of possible dose modification was 56.7%, which is markedly higher than the 20% found by Suttle et al.[4] This may partly be explained by the combination of repeated measurements and relatively large intra-individual variability in C_{min}. The large number of patients with low drug exposure may also partially be caused by use of proton pump inhibitors (PPI), which are known to decrease the pH-dependent absorption of pazopanib.[25] 9 patients in the low exposure groups (1a and 1b) used a PPI. The use of gastric-pH increasing agents was discouraged but not prohibited during this trial. On the other hand, it also shows that PK-guided dosing may overcome the problem of pH-limited absorption of pazopanib in patients for whom treatment with PPIs is medically necessary.

A drawback of the current study is that dose modification was limited to three pre-specified time points. If later dose increments would have been allowed, more patients in the low exposure group might have achieved the target threshold. Another limitation is that our study was performed in patients with a wide range of advanced solid tumors. Therefore, a satisfying analysis of the effect of individualized dosing on tumor response or PFS is impossible. Nonetheless, all patients who had a partial response had a C_{min} above the 20.0 mg/L threshold and in a non-prespecified analysis, we found significant association between tumor response (measured as maximum change in tumor size from baseline) and pazopanib C_{min}, which would provide further support for targeting a C_{min} of ≥20.0 mg/L. Interestingly, in a subgroup analysis of STS patients (n=7), a trend toward increased response and longer PFS with higher C_{min} was found. Yet, perhaps due to the small size of this subgroup, these results were not significant.

8

The results of this trial merit further investigation of individualized pazopanib dosing in cancer patients. A similar design to the one that was previously used for axitinib dose titration in RCC patients could be explored.[21,26] As the ideal form of for future studies would be a prospective randomized placebo controlled trial in either STS or RCC patients.

CONCLUSION

In summary, this prospective multicenter trial in patients with advanced solid tumors showed that pazopanib dose could safely be escalated in selected patients with a C_{min} <20.0 mg/L and that pazopanib exposure increased significantly in patients whose dose was escalated based on a low C_{min}. Moreover, a significant association between C_{min} and tumor response was found. The outcomes of this trial support further investigation of individualized pazopanib dosing, using the here described dosing algorithm, ideally in a large prospective randomized clinical trial using PFS or overall survival as an endpoint.

ACKNOWLEDGEMENTS

REFERENCES

1. Hamberg P, Verweij J, Sleijfer S. (Pre-)clinical pharmacology and activity of pazopanib, a novel multikinase angiogenesis inhibitor. Oncologist. 2010;15(6):539-47

2. Sternberg CN, Davis ID, Mardiak J, Szczylik C, Lee E, Wagstaff J, et al. Pazopanib in locally advanced or metastatic renal cell carcinoma: results of a randomized phase III trial. J Clin Oncol. 2010;28(6):1061-8

3. van der Graaf WT, Blay JY, Chawla SP, Kim DW, Bui-Nguyen B, Casali PG, et al. Pazopanib for metastatic soft-tissue sarcoma (PALETTE): a randomised, double-blind, placebo-controlled phase 3 trial. Lancet. 2012;379(9829):1879-86

4. Suttle AB, Ball HA, Molimard M, Hutson TE, Carpenter C, Rajagopalan D, et al. Relationships between pazopanib exposure and clinical safety and efficacy in patients with advanced renal cell carcinoma. Br J Cancer. 2014;111(10):1909-16

5. Kumar R, Knick VB, Rudolph SK, Johnson JH, Crosby RM, Crouthamel MC, et al. Pharmacokinetic-pharmacodynamic correlation from mouse to human with pazopanib, a multikinase angiogenesis inhibitor with potent antitumor and antiangiogenic activity. Mol Cancer Ther. 2007;6(7):2012-21

6. Hurwitz HI, Dowlati A, Saini S, Savage S, Suttle AB, Gibson DM, et al. Phase I trial of pazopanib in patients with advanced cancer. Clin Cancer Res. 2009;15(12):4220-7

7. Bible KC, Suman VJ, Molina JR, Smallridge RC, Maples WJ, Menefee ME, et al. Efficacy of pazopanib in progressive, radioiodine-refractory, metastatic differentiated thyroid cancers: results of a phase 2 consortium study. Lancet Oncol. 2010;11(10):962-72

8. Deng Y, Sychterz C, Suttle AB, Dar MM, Bershas D, Negash K, et al. Bioavailability, metabolism and disposition of oral pazopanib in patients with advanced cancer. Xenobiotica. 2013;43(5):443-53

9. de Wit D, van Erp NP, den Hartigh J, Wolterbeek R, den Hollander-van Deursen M, Labots M, et al. Therapeutic drug monitoring to individualize the dosing of pazopanib: a pharmacokinetic feasibility study. Ther Drug Monit. 2015;37(3):331-8

10. Heath EI, Chiorean EG, Sweeney CJ, Hodge JP, Lager JJ, Forman K, et al. A phase I study of the pharmacokinetic and safety profiles of oral pazopanib with a high-fat or low-fat meal in patients with advanced solid tumors. Clin Pharmacol Ther. 2010;88(6):818-23

11. Tan AR, Gibbon DG, Stein MN, Lindquist D, Edenfield JW, Martin JC, et al. Effects of ketoconazole and esomeprazole on the pharmacokinetics of pazopanib in patients with solid tumors. Cancer Chemother Pharmacol. 2013;71(6):1635-43

12. Xu CF, Xue Z, Bing N, King KS, McCann LA, de Souza PL, et al. Concomitant use of pazopanib and simvastatin increases the risk of transaminase elevations in patients with cancer. Ann Oncol. 2012;23(9):2470-1

13. Fox P, Balleine RL, Lee C, Gao B, Balakrishnar B, Menzies AM, et al. Dose Escalation of Tamoxifen in Patients with Low Endoxifen Level: Evidence for Therapeutic Drug Monitoring-The TADE Study. Clin Cancer Res. 2016;22(13):3164-71

14. Lankheet NA, Kloth JS, Gadellaa-van Hooijdonk CG, Cirkel GA, Mathijssen RH, Lolkema MP, et al. Pharmacokinetically guided sunitinib dosing: a feasibility study in patients with advanced solid tumours. Br J Cancer. 2014;110(10):2441-9

15. R Development Core Team (2011), R: A Language and Environment for Statistical Computing. Vienna, Austria: the R Foundation for Statistical Computing. ISBN: 3-900051-07-0. Available online at http://www.R-project.org/

16. Xu CF, Johnson T, Wang X, Carpenter C, Graves AP, Warren L, et al. HLA-B*57:01 Confers Susceptibility to Pazopanib-Associated Liver Injury in Patients with Cancer. Clin Cancer Res. 2016;22(6):1371-7

17. Yu H, van Erp N, Bins S, Mathijssen RH, Schellens JH, Beijnen JH, et al. Development of a Pharmacokinetic Model to Describe the Complex Pharmacokinetics of Pazopanib in Cancer Patients. Clin Pharmacokinet. 2016 Aug 17 [Epub ahead of print]

18. Eechoute K, Fransson MN, Reyners AK, de Jong FA, Sparreboom A, van der Graaf WT, et al. A long-term prospective population pharmacokinetic study on imatinib plasma concentrations in GIST patients. Clin Cancer Res. 2012;18(20):5780-7

19. Nikolinakos PG, Altorki N, Yankelevitz D, Tran HT, Yan S, Rajagopalan D, et al. Plasma cytokine and angiogenic factor profiling identifies markers associated with tumor shrinkage in early-stage non-small cell lung cancer patients treated with pazopanib. Cancer Res. 2010;70(6):2171-9

8

20. Brahmer JR, Lee JW, Traynor AM, Hidalgo MM, Kolesar JM, Siegfried JM, et al. Dosing to rash: a phase II trial of the first-line erlotinib for patients with advanced non-small-cell lung cancer an Eastern Cooperative Oncology Group Study (E3503). Eur J Cancer. 2014;50(2):302-8

21. Rini BI, Melichar B, Ueda T, Grunwald V, Fishman MN, Arranz JA, et al. Axitinib with or without dose titration for first-line metastatic renal-cell carcinoma: a randomised double-blind phase 2 trial. Lancet Oncol. 2013;14(12):1233-42

22. Karovic S, Wen Y, Karrison TG, Bakris GL, Levine MR, House LK, et al. Sorafenib dose escalation is not uniformly associated with blood pressure elevations in normotensive patients with advanced malignancies. Clin Pharmacol Ther. 2014;96(1):27-35

23. Verheijen RB, Bins S, Thijssen B, Rosing H, Nan L, Schellens JH, et al. Development and clinical validation of an LC-MS/MS method for the quantification of pazopanib in DBS. Bioanalysis. 2016;8(2):123-34

24. de Wit D, den Hartigh J, Gelderblom H, Qian Y, den Hollander M, Verheul H, et al. Dried blood spot analysis for therapeutic drug monitoring of pazopanib. J Clin Pharmacol. 2015;55(12):1344-50

25. van Leeuwen RW, van Gelder T, Mathijssen RH, Jansman FG. Drug-drug interactions with tyrosine-kinase inhibitors: a clinical perspective. Lancet Oncol. 2014;15(8):e315-26

26. Rini BI, Melichar B, Fishman MN, Oya M, Pithavala YK, Chen Y, et al. Axitinib dose titration: analyses of exposure, blood pressure and clinical response from a randomized phase II study in metastatic renal cell carcinoma. Ann Oncol. 2015;26(7):1372-7.

Development and clinical validation of an LC-MS/MS method for the quantification of pazopanib in DBS

Remy B. Verheijen, Sander Bins, Bas Thijssen, Hilde Rosing, Lianda Nan, Jan H.M. Schellens, Ron H.J. Mathijssen, Martijn P. Lolkema, Jos H. Beijnen, Neeltje Steeghs, Alwin D.R. Huitema
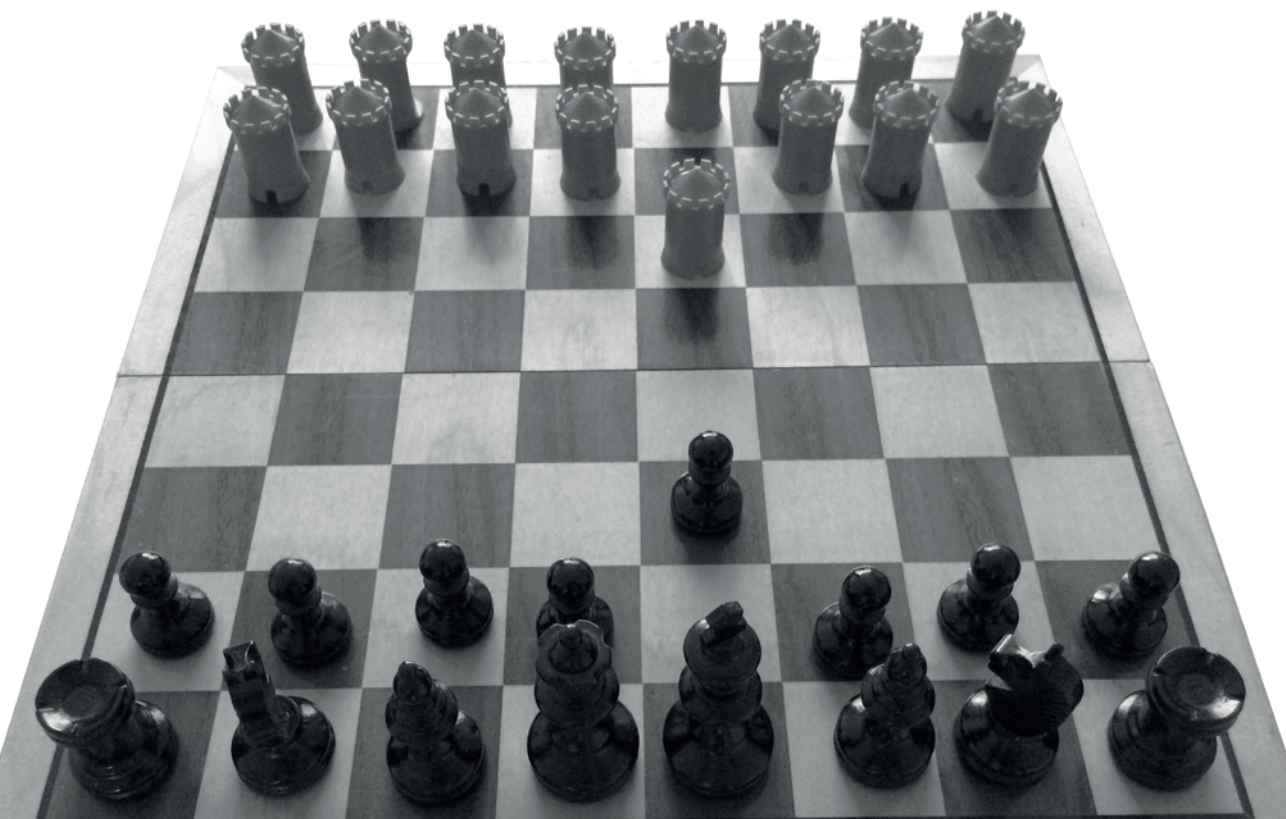
ABSTRACT

Background. Pazopanib is approved for the treatment of renal cell carcinoma and soft tissue sarcoma. Analyses show increased benefit in patients with plasma trough concentrations ≥20.5 µg/ml compared with patients with lower concentrations.

Methods & results. We developed a DBS assay as a patient friendly approach to guide treatment. The method was validated according to US FDA and EMA guidelines and European Bioanalysis Forum recommendations. Influence of spot homogeneity, spot volume and hematocrit were shown to be within acceptable limits. Analysis of paired clinical samples showed a good correlation between the measured plasma and DBS concentrations (R^2 of 0.872).

Conclusion. The method was successfully validated, applied to paired clinical samples and is suitable for application to therapeutic drug monitoring of pazopanib.

BACKGROUND

Pazopanib is an angiogenesis inhibitor targeting the VEGFR-1,2,3, PDGFR α/β, FGFR and the stem cell receptor/c-Kit.[1] Pazopanib has shown efficacy in advanced renal cell carcinoma and soft tissue sarcoma in a fixed dose of 800 mg once daily.[2,3] A recent retrospective analysis of a trial of 177 patients treated with pazopanib showed a markedly increased median progression free survival in patients with (steady-state) plasma trough concentrations (C_{min}) ≥20.5 µg/mL compared with patients with lower C_{min} (50.2 vs 19.6 weeks).[4] In addition, pazopanib shows large interindividual variability in plasma exposure, resulting in a subset of patients at risk of receiving less than optimal exposure.[4–7] Given the established exposure–response relationship and large interindividual variability in exposure, patients might benefit from pharmacokinetically guided dosing, also known as therapeutic drug monitoring

(TDM), based on a measured C_{min}. A quantitative assay is needed to identify patients with a low C_{min} that might benefit from treatment at a higher dose. Several assays to quantify pazopanib in (mouse and human) plasma have been described, both using diode array detection[8] and LC–MS/MS.[9–11] Last year, a review article by Wilhelm et al. discussed the application of DBS to support TDM.[12]. A DBS method would allow patients to take a sample themselves using a simple finger prick. Compared with plasma methods, DBS sampling could be more patient friendly and lead to increased sample stability, limited sample volume, convenient storage and shipping. Additionally DBS methods may be ideally suited to measure C_{min} concentrations, because a blood sample can be obtained at the planned time point by the patients themselves and will not be dependent on the time of the visit to an out-patient clinic. This may be relevant for pazopanib as De Wit et al. found a strong correlation (R^2 of 0.940) between the trough sample (exactly C_{24h}) and pazopanib area under the curve.[7] However, quantification in DBS samples may be more challenging for several reasons. Patients or nurses will need additional training to provide good quality samples and additional validation tests need to be performed, such as the influences of blood hematocrit, spot volume, punch carryover and blood spot homogeneity on analytical outcome.[13] Moreover, a clinical validation study to investigate the relationship between the plasma and DBS concentrations is needed.[14,15] But once a comprehensively validated method is available and patients and nurses are familiar with

the sampling technique, a DBS method will be optimally suited to pharmacokinetically guided dosing of pazopanib. Here, we describe the development, analytical and clinical validation of an LC–MS/MS method for the quantification of pazopanib in DBS.

MATERIALS, METHODS & PATIENTS

Chemicals & reagents

Pazopanib hydrochloride and stable isotopically labeled internal standard (IS) $^{13}C,^2H_3$-pazopanib hydrochloride, with purities as free base of 92.3 and 92.6%, respectively were supplied by GlaxoSmithKline (Zeist, The Netherlands). Formic acid and dimethyl sulfoxide were purchased from Merck (Darmstadt, Germany) and methanol (analytical grade) and water (LC–MS grade) from BioSolve Ltd (Valkenswaard, The Netherlands). Blank human whole K_2EDTA blood was obtained from healthy volunteers and used for preparation of the quality control (QC) samples, calibration standards and matrix blanks.

Stock solutions, calibration standards & quality control samples

Stock solutions of pazopanib (2 mg/mL) were prepared in dimethyl sulfoxide. Working solutions were prepared by dilution from stocks with methanol. The IS stock solution (1 mg/mL) was prepared in methanol. The IS working solution was prepared by further dilution with methanol to a concentration of 0.1 µg/mL. All stock and working solutions were stored at -20°C, the IS working solution at 2–8°C. Calibration standards and QC samples were prepared by spiking 30 µL of the working solutions to 570 µL of control whole blood. Concentrations of 1.00, 3.00, 15.0 and 37.5 µg/mL were used for the QC samples (LLOQ, low, mid and high concentrations, respectively). The concentrations for the calibration standards were: 1.00, 2.00, 5.00, 10.0, 20.0, 30.0, 40.0 and 50.0 µg/mL. From the blanks, calibration standards and QC samples a volume of 15 µL whole blood was spotted on the DBS cards. The blood spots were dried at ambient temperatures (20–25°C) for at least 3 h after which the samples were stored at ambient temperature with desiccant in a sealed foil bag. Hematocrit values of calibration standards and QC samples were not standardized in each run.

Equipment & conditions

Blood was spotted on Whatman™ 903 protein saver cards and punches from these cards were made using a Harris Uni-Core™ 3.0 mm puncher both purchased from GE Healthcare Europe GmbH (Diegem, Belgium). Samples were shaken using an L45 shaker by Labinco (Breda, The Netherlands).

All LC–MS/MS experiments were performed using an 1100 series binary pump, degasser, column oven and autosampler from Agilent Technologies (Santa Clara, CA, USA) and an API3000 triple quadrupole equipped with Turbo ionspray interface operating in positive ion-mode, on Analyst™ software for data analysis from Sciex (Framingham, MA, USA). Mass transitions of precursor and product ions and other MS parameters were optimized. Final settings were: tubro, nebulizer, curtain and collision gases 7 ll/min 7, 8 and 12 au, ion spray voltage 3000 V, ionization temperature 500°C, declustering potential 41 V, collision energy 43 V, collision cell exit and entrance potential 24 V and 10 V. Quantification was performed using the *m/z* 438.2 → *m/z* 357.3 transition for pazopanib and *m/z* 442.2 → *m/z* 361.2 for 13C,2H3-pazopanib (see **Figure 1**).
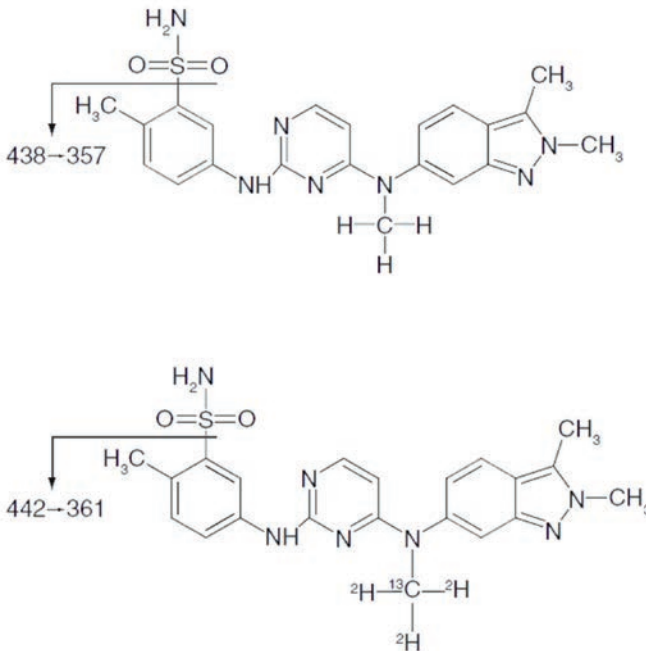
Figure 1. *Chemical structure and proposed mass transition of pazopanib and 13C,2H3-pazopanib.*

Sample preparation

Separation was performed on a Sunfire C18 Column, 2.1 × 50 mm, 5 μm from Waters (Milford, MA, USA) with a Gemini SecurityGuard, 2.0 × 4.0 mm guard column by Phenomenex (Torrance, CA, USA). The column oven was set at 55°C and the tray temperature of the autosampler at 5°C. Elution was achieved by using a gradient of methanol and 0.1% formic acid in water. The gradient started at a flow of 0.4 ml/min at a percentage of 27% methanol, after 1.5 min the gradient was increased to 80% methanol. At 2 min, the flow increased to 0.6 ml/min and at 2.5 min the percentage of methanol was returned to 27% for 1.5 min. The total runtime was 4 min.

On the day of analysis a 3 mm diameter punch was taken from the blood spots and transferred to an eppendorf tube. A total of 50 μL of concentrated formic acid (99%) was added to the spot and the sample was vortex mixed and consequently shaken for 10 min at 1250 rpm. Hereafter, 500 μL of methanol containing the IS (at a concentration of 0.1 μg/mL) was added and the samples were again vortexed and shaken for 10 min at 1250 rpm. After centrifugation at 23100 g, 300 μL of the supernatant was transferred to a clean vial containing 300 μL of water. These vials were then vortex mixed and 5 μL was injected into the LC–MS/MS system.

For plasma samples, a 10 μl aliquot was used, to which 500 μL of IS containing methanol and 500 μL eluent was added. This solution was then centrifuged at 23100 rpm and 5 μL of the supernatant was analyzed by LC–MS/MS.

Validation

The method was validated in accordance with US FDA and EMA guidelines on bioanalytical method validation and Good Laboratory Practices.[16,17] DBS-specific validation tests were performed, as recommended by the European Bioanalysis Forum.[18,19]

Analytical validation

Three separate validation runs were executed on separate days and the following validation parameters were assessed: LLOQ, calibration model, accuracy and precision, dilution integrity, selectivity, instrumentation carryover, matrix effect and recovery.

Linear regression was applied. Nonweighted, 1/x and 1/x2 weighted regression were evaluated (where x equals the peak area ratio). In every run at least 75% of the nonzero standards (including at least one LLOQ and ULOQ) should be within ±15% of the nominal value (or ±20% for the LLOQ), additionally for the LLOQ and ULOQ level at least 50% should meet these criteria. Regression coefficients were calculated in each run.

Accuracy and precision of the method were assessed by injecting five replicates of LLOQ, QC low, mid and high samples in three separate validation runs. Intra- and inter-run accuracy was expressed as the bias in% and intra- and inter-run precision as the coefficient of variation (CV) in%. At each of the QC levels the bias should be within ±15% and the precision should not exceed 15%.

The LLOQ was evaluated in each run using the signal-to-noise ratio expressed as the signal (peak height of the 1.00 µg/ml calibration standard) to the noise (peak height) of a blank sample. This ratio should be at least 5.

Dilution integrity was calculated by analyzing five replicates of samples with a concentration of 100 µg/ml, diluted 10-times with a processed controlled matrix and comparing the measured concentration with the nominal concentration. This bias should be within ±15% and the precision should not exceed 15%.

For selectivity, the effect of endogenous interferences and IS interference were determined. Six different batches of human whole blood were processed both as blanks and spiked at the LLOQ concentration to investigate possible endogenous interferences. Cross analyte interference was assessed by extracting pazopanib without the addition of the IS and by spiking IS separately to a double blank sample (a matrix sample; 3 mm punch from a blood spot without spiking analyte or IS) at the concentration used in the assay. The interference should be less than 20% of the response of the LLOQ of the analyte and less than 5% of the response of the IS.

Instrumentation carryover was tested by injecting two double blank samples after injecting an ULOQ sample in each validation run and expressed as the peak area in the blanks as a percentage of the LLOQ peak area. Carryover was considered acceptable when the response in the first blank at the retention time of the analyte is less than 20% of the response of the LLOQ.

9

The matrix factor (MF) was calculated by dividing the analyte and IS peak area in presence of matrix by the peak area of the analyte and IS in a neat solution, using six different batches of whole blood spiked at both the QC low and QC high concentration. The IS normalized MF was calculated by dividing the MF of pazopanib by the MF of the IS of which the CV was calculated. This CV was considered acceptable if it was less than 15%.

The (sample pretreatment) recovery was determined by comparing peak area of pazopanib in processed validation samples to peak area of pazopanib area in presence of matrix, at QC low and high concentrations in triplicate. No specific requirement for recovery was predefined except that it should be reproducible.

DBS-specific validation

The influence of spot (in)homogeneity, spot volume, blood hematocrit and spot-to-spot carryover was investigated. The spot-to-spot carryover was tested by punching a double blank sample after an ULOQ sample. Carryover was considered acceptable as the response in this blank sample at the retention time of the analyte was ≤20% of the mean (n = 5) response at the LLOQ.

The effect of (in)homogeneity within the blood spot was examined in triplicate by taking punches from the edge of the blood spot and comparing the measured concentration with the nominal concentration, at low and high QC concentrations. The effect of spot volume and blood hematocrit was investigated in triplicate at QC low and QC high concentrations, by spotting a range of volumes on the DBS cards (10, 15, 30 µL). The effect of the hematocrit was determined by preparing batches of whole blood with different hematocrit values in the range from nominally 35 to 50% (tested values: 34.1, 42.4 and 49.7%).

The effect of spot volume, inhomogeneity and hematocrit was considered acceptable if bias and precision were within ±15 and ≤15%, respectively.

Stability

Stability of processed samples stored at nominally 2–8°C and samples on the DBS cards at ambient temperature (in a foil bag with desiccant) was investigated in triplicate at both

low and high QC concentrations. Samples were considered stable if the bias was within ±15% of the nominal concentration and the CV was ≤15%.

Clinical validation

Paired DBS and (venous) plasma samples were obtained from patients with advanced solid tumors treated with pazopanib (n = 30) recruited from three centers (the Netherlands Cancer Institute, Amsterdam, Utrecht University Medical Center, Utrecht and Erasmus MC Cancer Institute, Rotterdam). Doses administered ranged from 400 mg to 1800 mg daily following protocol and within patient adjustments of the dose were possible.[20] The trial was approved by the independent ethics committee of each participating hospital (Dutch Trial Registry; trial identifier NTR3967) and all patients provided written informed consent before enrollment. DBS samples were taken by a finger prick under the supervision of a study nurse and the obtained blood spots were dried at ambient temperatures for at least 3 h, after which the samples were stored with desiccant in a sealed foil bag and sent to the analytical laboratory.

Weighted Deming fit was used to investigate the relationship between the plasma and DBS concentration. Using the observed slope and intercept the plasma concentration were calculated. Bland–Altman plots were made to investigate the bias between the calculated and measured plasma concentrations. These analyses were all performed in R (version 3.0.0).[21]

An arbitrarily selected subset of DBS samples (n = 47) was measured in duplicate (two separate blood spots on the same card, obtained from the same patient at the same date and time) to investigate the variability during the spotting procedure in clinical practice. Another subset of DBS samples was measured in duplicate with one punch of 3 mm and another of 6 mm (n = 51), to assess the effect of punch size in the clinical samples. In this separate analysis the calibration standards and QC samples were also analyzed using a 6 mm punch for the DBS.

RESULTS & DISCUSSION

Analytical validation results

An overview of the validated parameters is shown in **Table 1**. Analytical performance data for pazopanib in DBS are shown in **Table 2**. All tested parameters met their predefined acceptance criteria. As 1/x weighted regression resulted in the lowest total bias this was selected for the calibration model.

Table 1. Summary of validation results.

Parameter	Result
Calibration model	Linear regression coefficients all >0.99
Validated range	1.00–50.0 µg/mL
Overall (in)accuracy	Bias ±4.0%
Inter- and intra-run precision (CV)	≤8.6%
Lower limit of quantification (S/N)	>27
Dilution integrity	Bias ±1.0%, CV 10.7%
Selectivity (endogenous and cross analyte)	≤0.6%
Instrument carryover	0.6% of the LLOQ
IS normalized matrix factor (mean, CV)	1.01, 1.6% (QC low), 0.980, 1.9% (QC high)
Recovery	97.6% (QC low), 103.7% (QC high), CV ≤2.7%
Spot-to-spot carry-over	6.4% of the LLOQ
Blood spot homogeneity	Bias ±3.5%, CV ≤4.6%
Effect of blood spot volume	Bias ±9.5%, CV ≤4.8%
Effect of blood hematocrit	Bias ±14.2%, CV ≤10.2%
Final extract stability (2–8°C)	168 days
DBS stability (ambient temperatures)	398 days

All tested parameters met their predefined criteria (predefined acceptance criteria are mentioned in the text).

Table 2. Analytical performance data for pazopanib in DBS.

Run	Nominal concentration (µg/mL)	Mean measured concentration (µg/mL)	(In)accuracy (%deviation)	Precision (% CV)	Replicates (n)
1	1.01	1.09	8.1	5.6	5
2	1.01	1.02	1.2	5.9	5
3	1.01	1.00	-0.8	6.1	5
Overall	1.01	1.04	2.8	3.7	15
1	3.03	3.04	0.2	5.1	5
2	3.03	2.95	-2.7	5.3	5
3	3.03	3.20	5.7	7.1	5
Overall	3.03	3.06	1.1	3.4	15
1	15.1	15.9	5.0	3.0	5
2	15.1	14.8	-2.3	8.6	5
3	15.1	16.5	9.3	3.8	5
Overall	15.1	15.7	4.0	5.0	15
1	37.9	38.5	1.6	5.8	5
2	37.9	36.6	-3.5	4.9	5
3	37.9	40.3	6.4	3.2	5
Overall	37.9	38.5	1.5	4.4	15

DBS-specific validation results

The spot-to-spot carryover was 6.4% of the mean (n = 5) LLOQ level for pazopanib and 0.0% for $^{13}C,^{2}H_3$-pazopanib. Spot (in)homogeneity resulted in a bias of 3.5 and 2.2% for low and high QC levels with CV percentages of 1.3 and 4.6, respectively.

Data for the effect of spot volume are presented in **Table 3**. The biases for all tested volumes were ≤9.5% of the nominal concentration and the CV was ≤4.8%, indicating that the influence of spot volume was within the requirements.

Results for the influence of hematocrit are shown in **Table 4**. The calibration standards used in the analysis had a hematocrit value of 43.8%. The effect of the hematocrit was within the predefined limits as the mean measured concentration was ≤14.2% of the nominal concentration, with a CV of ≤10.2%.

Table 3. Effect of spot volume on the quantification of pazopanib (n = 3).

Spot volume	QC low bias (%)	CV (%)	QC high bias (%)	CV (%)
10 µL	-9.0	4.7	-5.0	0.7
20 µL	5.2	4.8	-0.7	1.8
30 µL	9.5	3.1	5.5	1.9

Table 4. Effect of blood hematocrit on the quantification of pazopanib (n = 3).

Blood hematocrit	QC low bias (%)	CV (%)	QC high bias (%)	CV (%)
34.1%	-14.2	7.1	-10.0	10.2
42.4%	-4.2	4.4	-7.4	2.4
49.7%	7.4	3.9	1.0	1.3

9

Stability

QC samples at low and high concentrations (n = 3), deviated ≤15% of the nominal concentration after being stored at ambient temperatures (in a foil bag with desiccant) at 398 days. Therefore, pazopanib was considered to be stable for at least 398 days on the DBS cards. Processed samples stored at nominally 2–8°C deviated ≤15% of the nominal concentration and were therefore considered stable at nominally 2–8°C for at least 168 days.

Clinical validation

The method was applied to clinical samples taken approximately 24 h after the last dose (at steady state) from cancer patients treated with pazopanib. In total, 329 paired DBS and plasma samples were obtained from the 30 enrolled patients. Irregular, very large (larger than the printed ring on the DBS card), very small (smaller than the punch diameter) spots were excluded. Samples resulting in concentrations below the LLOQ[15] were also excluded. In total, 221 spots were used for the analysis. As shown in **Figure 2**, a good correlation between the DBS and the plasma concentration was found (R^2 of 0.872 with a slope of 0.709 and an intercept of -0.182).

The plasma concentration was back calculated based on the measured DBS concentration, using [pazopanib$_{calculated\ plasma}$] = ([pazopanib$_{DBS}$] + 0.182) / 0.709. The plotted calculated versus measured plasma concentrations are shown in **Figure 3**. The difference between the calculated and measured plasma concentrations versus the measured plasma concentration is shown in a Bland–Altman plot in **Figure 4**. Back calculated plasma concentrations were within 20% of measured plasma concentrations for 79.2% of the DBS samples.

Correction for patient-specific hematocrit when calculating the plasma concentration (using the formula proposed by Kromdijk et al.[14], [pazopanib$_{calculated\ plasma\ (hmtcrt\ corrected)}$] = [pazopanib$_{DBS}$]/(1-hematocrit)*fraction bound to plasma protein) did not improve the correlation between the calculated and measured plasma concentrations compared with the empirically found Deming regression. The hematocrit values of the patients used for this sub analysis were within the validated range, the mean was 40%, ranging from 36 to 48%.

When used to identify patients above or below the 20 µg/mL threshold the plasma and DBS methods were in agreement in 91.4% of the cases. A Bland–Altman plot of the difference between two spots taken at the same time as a function of the mean of the two measurements is given in **Figure 5**. The Bland–Altman plot showing the deviations of clinical samples punched with both a 3 and a 6 mm diameter punch is shown in **Figure 6**.
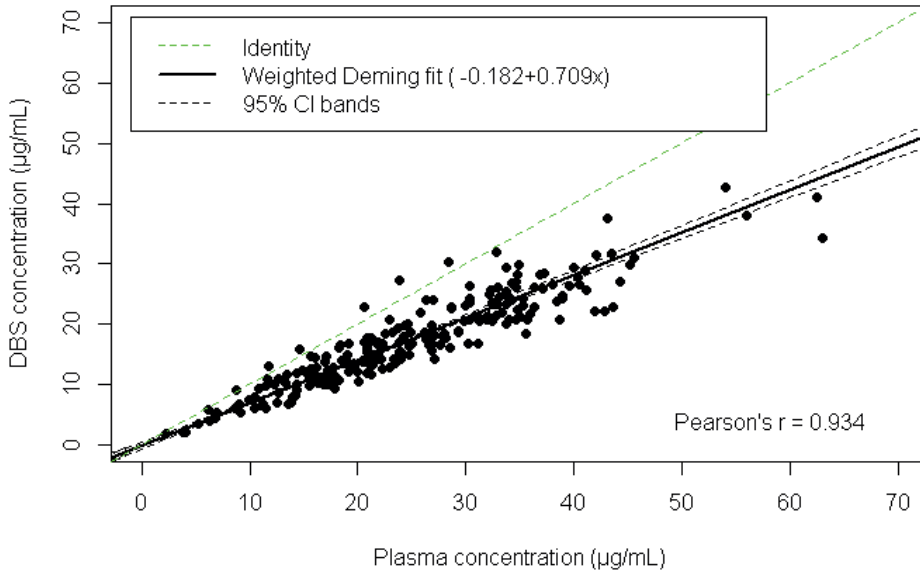
Figure 2. *Measured DBS concentration versus the measured plasma concentration (n= 221). The solid black line represents the weighted Deming fit, the dotted black lines represent the 95% CI of the Deming fit, the green dotted line is the line of unity.*
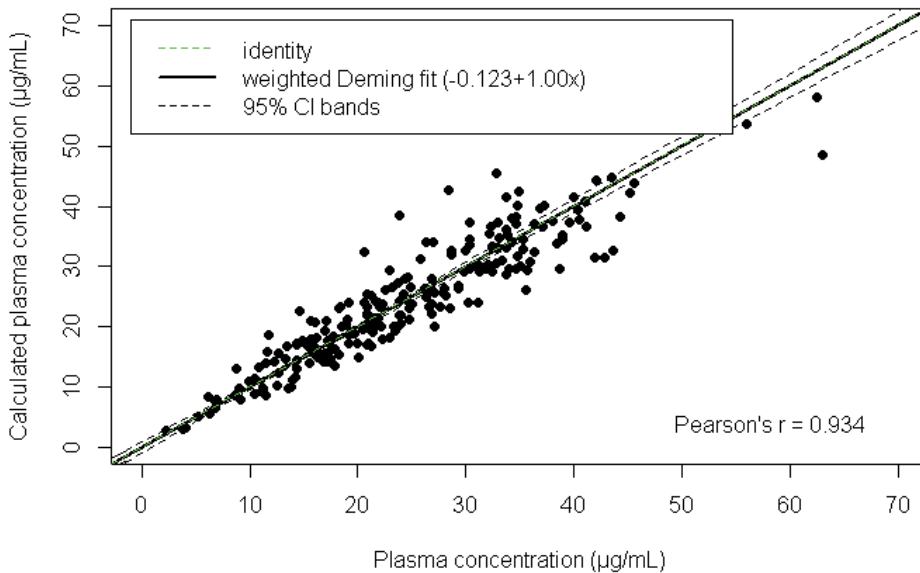
Figure 3. *Calculated plasma versus the measured plasma concentration (n = 221).*
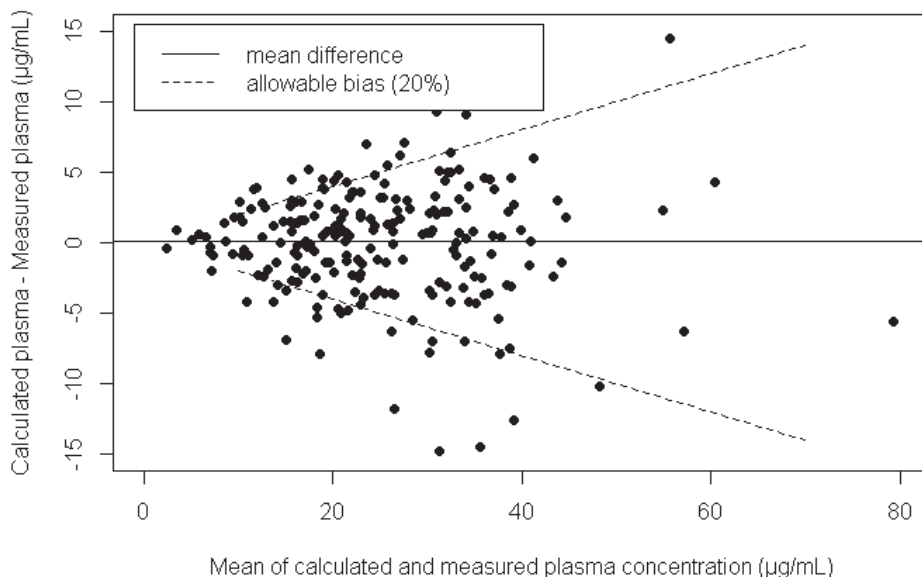
Figure 4. *Bland–Altman plot showing the difference between the calculated and measured pazopanib plasma concentration (n = 221). The mean difference between the two methods was 0.08 μg/ml.*
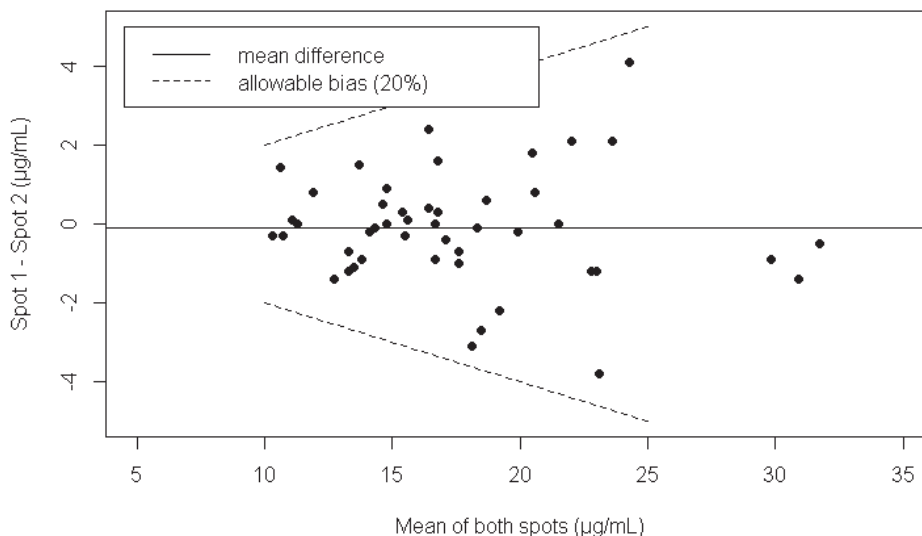
Figure 5. *Bland–Altman plot showing the difference between the measured pazopanib spots in the subset of samples of which two spots provided by the same patient at the same time were measured (n = 47). The mean difference between the two methods was -0.105 μg/ml.*
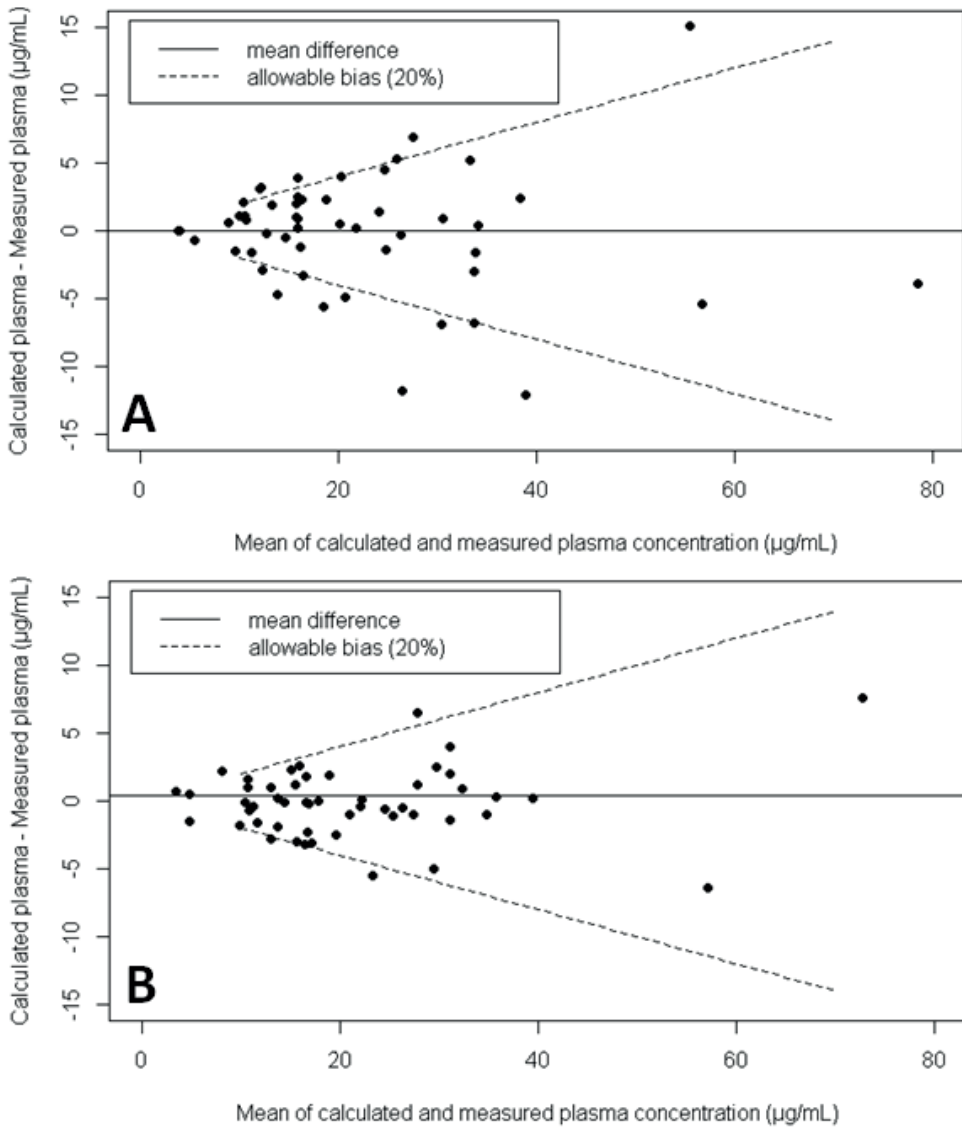
Figure 6. *Bland–Altman plots showing the difference between the measured pazopanib spots in the subset of samples (n = 51) which were measured after a 3 mm punch (A) and a 6 mm punch (B) from the DBS card. The mean difference was -0.09 and 0.44 µg/ml for the 3 and 6 mm punched samples, respectively.*

9

Our method was successfully developed to quantify pazopanib in DBS and validated in accordance with FDA and EMA guidelines on bioanalytical method validation and good laboratory practices.[16,17] With a run time of only 4 min, the developed method is suitable for routine analyses of patient samples. Moreover processed samples were shown to be stable for at least 168 days, therefore calibration standards can be reused several times, reducing the time needed to perform an analytical run.

Spot volume resulted in a small positive bias for large volumes and a small negative bias for small volumes (both within the predefined requirements). No clear mechanism for this effect has been reported. The same trend was found for the tyrosine kinase inhibitor vemurafenib[22] and other compounds such as everolimus, tacrolimus and sirolimus.[23]

Spot-to-spot carryover was shown to be only 6.4% of the LLOQ and will therefore have no relevant effect on the analytical outcome when applying this method.

The influence of spot homogeneity was assessed in the laboratory and showed a bias within ±3.5 and a CV of ≤4.6%. In practice however it is likely that this effect will be larger, as samples provided by patients will be less uniform than those made using a pipette.

During the DBS-specific validation experiments, hematocrit values from 35 to 50% were tested and the bias and variability were within predefined limits. Low hematocrit values resulted in a negative bias, while high hematocrit resulted in a positive bias. This might be explained by the higher viscosity with higher hematocrit and, consequently, less spreading on paper. The effect of hematocrit seems to be dependent on the analyte tested. For example, a trend similar to that of pazopanib was found for vemurafenib, everolimus and sirolimus, no clear trend was observed for tamoxifen, endoxifen, tacrolimus and an opposite trend was found for cyclosporine A.[22–24]

A good correlation was observed between the DBS concentration and the plasma concentration (R^2 = 0.872), with a slope of 0.709 and intercept of -0.182 (**Figure 2**). The lower DBS concentration probably results from pazopanib's high plasma protein binding causing a higher concentration in the plasma relative to blood cells.

Based on this weighted Deming fit, the plasma concentration could be back calculated using the formula: [pazopanib$_{calculated\ plasma}$] = ([pazopanib$_{DBS}$] + 0.182) / 0.709

(**Figure 3**). Correction for patient-specific hematocrit when calculating the plasma concentration, did not improve the correlation between the calculated and measured plasma concentrations compared with the empirical Deming regression formula. This suggests that even though hematocrit influences the analytical results (as seen in the DBS-specific validation tests) in the clinical setting it is not the most important factor driving the variability between the two methods.

Despite the good correlation between plasma and DBS samples, 20.8% of the calculated plasma concentrations deviated more than 20% from the measured plasma concentration (**Figure 4**). Taking into account the excellent analytical performance of the assay during the validation with the laboratory spots (Table 2) it is likely that the variability arises during the clinical spotting procedure.

This is supported by the results of the DBS samples measured in duplicate. As even in these samples, which were taken from the same patient at the same time, differences of up to 17.2% were observed (**Figure 5**). Spot quality, volume and (in)homogeneity are the likely factors that cause this variability. Since these samples were taken from the same patient at the same time, blood hematocrit could not explain this difference. Using a larger 6 mm punch resulted in a small reduction of the imprecision (**Figure 6**). But using the 6 mm punch would require patients to produce larger spots, leading to use of larger blood volumes and most likely to a larger number of samples smaller than the punch size.

Acknowledging the above, care should be taken to inspect the quality of the spot before measurement. Very large, very small or irregular spots should not be used, as parameters such as spot homogeneity and volume seemed more important than hematocrit during the clinical validation study. Careful instruction and training of patients in the sampling procedure should thus considered important when using this method, but a recent study in breast cancer patients treated with tamoxifen shows the feasibility of DBS self-sampling.[25]

In guiding pazopanib therapy it will be particularly important to identify patients above or below the PK target of ≥20 μg/mL. When the calculated pazopanib plasma concentration was used to identify patients below the PK target level of ≥20 μg/mL, the DBS method was in agreement with the plasma method in 91.4% of the cases. This makes

the DBS method acceptable for the proposed purpose of guiding pazopanib therapy, with relevant practical advantages over the plasma method. Furthermore in light of the intrapatient variability (CV) of pazopanib of 24.7%,[7] the discrepancy between the two analytical methods will have little effect on the clinical application. As patients with a C_{min} around the 20 µg/mL threshold (e.g., 15–25 µg/mL) would require repeated measurements of the pazopanib concentration, regardless of the analytical method used.

An earlier method for the quantification of pazopanib in DBS has been described,[26] when this method was used to compare calculated versus measured plasma pazopanib concentrations in paired samples, 92.6% of the samples were within the predefined deviation of ±25% in the Bland–Altman analysis. When applying these (wider) acceptance criteria to our current method a similar percentage of 88.2% was found. However the earlier method used the patient's hematocrit in calculating the plasma concentration. This is a significant disadvantage if the method is to be applied to patient self-sampling, as calculation of the pazopanib plasma level would still require a visit to the clinic to measure a patient's hematocrit. With the current method there was no need to use the patient's hematocrit and no such correction was used during our clinical validation study, making it more suited to a patient self-sampling approach. Given the well-established exposure–response relationship of pazopanib, a fast and minimally invasive DBS method might help implementation of an individualized dosing approach or TDM. Patients would be able to take DBS samples at home and send these at ambient temperatures (these were shown to be stable for at least 398 days) to the analytical laboratory. The pazopanib DBS concentration could then be measured before the next visit to the clinic and the plasma concentration could be calculated using [pazopanib$_{calculated\ plasma}$] = ([pazopanib$_{DBS}$] + 0.182)/0.709. Subsequently an assessment of the C_{min} could be made by the treating physician and a dose adjustment could be considered for patients with a low pazopanib exposure to optimize their treatment.

CONCLUSION

An LC–MS/MS method for the quantitative determination of pazopanib in DBS was developed and successfully validated in accordance with FDA and EMA guidelines and European Bioanalysis Forum recommendations for DBS method validation. The DBS

concentrations showed a good correlation with the plasma concentrations (R^2 of 0.872) and could be used to determine a calculated plasma concentration. The DBS method can be used for pharmacokinetically guided dosing of pazopanib therapy.

FUTURE PERSPECTIVE

The described method is suitable for the application to TDM of pazopanib, with relevant advantages over plasma quantification (e.g., patient friendly sampling and sample stability) and no need to correct for patient hematocrit. The availability of this assay facilitates further implementation of TDM of pazopanib and enables more personalized treatment with this drug. But further prospective clinical trials are needed to demonstrate the added value of an individualized dosing strategy for pazopanib based a measured drug concentration.

9

REFERENCES

1. Hamberg P, Verweij J, Sleijfer S. (Pre-)clinical pharmacology and activity of pazopanib, a novel multikinase angiogenesis inhibitor. Oncologist. 2010;15(6):539-47

2. Sternberg CN, Davis ID, Mardiak J, Szczylik C, Lee E, Wagstaff J, et al. Pazopanib in locally advanced or metastatic renal cell carcinoma: results of a randomized phase III trial. J Clin Oncol. 2010;28(6):1061-8

3. van der Graaf WT, Blay JY, Chawla SP, Kim DW, Bui-Nguyen B, Casali PG, et al. Pazopanib for metastatic soft-tissue sarcoma (PALETTE): a randomised, double-blind, placebo-controlled phase 3 trial. Lancet. 2012;379(9829):1879-86

4. Suttle AB, Ball HA, Molimard M, Hutson TE, Carpenter C, Rajagopalan D, et al. Relationships between pazopanib exposure and clinical safety and efficacy in patients with advanced renal cell carcinoma. Br J Cancer. 2014;111(10):1909-16

5. Hurwitz HI, Dowlati A, Saini S, Savage S, Suttle AB, Gibson DM, et al. Phase I trial of pazopanib in patients with advanced cancer. Clin Cancer Res. 2009;15(12):4220-7

6. Deng Y, Sychterz C, Suttle AB, Dar MM, Bershas D, Negash K, et al. Bioavailability, metabolism and disposition of oral pazopanib in patients with advanced cancer. Xenobiotica. 2013;43(5):443-53

7. de Wit D, van Erp NP, den Hartig J, Wolterbeek R, den Hollander-van Deursen M, Labots M, et al. Therapeutic drug monitoring to individualize the dosing of pazopanib: a pharmacokinetic feasibility study. Ther Drug Monit. 2015;37(3):331-8

8. Dziadosz M, Lessig R, Bartels H. HPLC-DAD protein kinase inhibitor analysis in human serum. J Chromatogr B Analyt Technol Biomed Life Sci. 2012;893-894:77-81

9. van Erp NP, de Wit D, Guchelaar HJ, Gelderblom H, Hessing TJ, Hartigh J. A validated assay for the simultaneous quantification of six tyrosine kinase inhibitors and two active metabolites in human serum using liquid chromatography coupled with tandem mass spectrometry. J Chromatogr B Analyt Technol Biomed Life Sci. 2013;937:33-43

10. Sparidans RW, Ahmed TT, Muilwijk EW, Welzen ME, Schellens JH, Beijnen JH. Liquid chromatography-tandem mass spectrometric assay for therapeutic drug monitoring of the tyrosine kinase inhibitor pazopanib in human plasma. J Chromatogr B Analyt Technol Biomed Life Sci. 2012;905:137-40

11. Minocha M, Khurana V, Mitra AK. Determination of pazopanib (GW-786034) in mouse plasma and brain tissue by liquid chromatography-tandem mass spectrometry (LC/MS-MS). J Chromatogr B Analyt Technol Biomed Life Sci. 2012;901:85-92

12. Wilhelm AJ, den Burger JC, Swart EL. Therapeutic drug monitoring by dried blood spot: progress to date and future directions. Clin Pharmacokinet. 2014;53(11):961-73

13. Jager NG, Rosing H, Schellens JH, Beijnen JH. Procedures and practices for the validation of bioanalytical methods using dried blood spots: a review. Bioanalysis. 2014;6(18):2481-514

14. Kromdijk W, Mulder JW, Rosing H, Smit PM, Beijnen JH, Huitema AD. Use of dried blood spots for the determination of plasma concentrations of nevirapine and efavirenz. J Antimicrob Chemother. 2012;67(5):1211-6

15. Jager NG, Rosing H, Schellens JH, Beijnen JH, Linn SC. Use of dried blood spots for the determination of serum concentrations of tamoxifen and endoxifen. Breast Cancer Res Treat. 2014;146(1):137-44

16. Guideline on bioanalytical method validation. European Medicines Agency, London, UK (2011). www.ema.europa.eu

17. Guidance for industry bioanalytical method validation, draft guidance, US Department of Health and Human Services, US FDA, Rockville, MD, USA (2013). www.fda.gov

18. Timmerman P, White S, Cobb Z, de Vries R, Thomas E, van Baar B, et al. Updates from the EBF DBS--microsampling consortium. Bioanalysis. 2012;4(16):1969-70

19. Timmerman P, White S, Cobb Z, de Vries R, Thomas E, van Baar B, et al. Update of the EBF recommendation for the use of DBS in regulated bioanalysis integrating the conclusions from the EBF DBS-microsampling consortium. Bioanalysis. 2013;5(17):2129-36

20. Verheijen RB, Bins S, Mathijssen RH, Lolkema M, van Doorn L, Schellens JH, et al. Individualized pazopanib dosing: a prospective feasibility study in cancer patients. Clin Cancer Res. 2016 July 28 [Epub ahead of print]

21. R Development Core Team (2011), R: A Language and Environment for Statistical Computing. Vienna, Austria: the R Foundation for Statistical Computing. ISBN: 3-900051-07-0. Available online at http://www.R-project.org/

22. Nijenhuis CM, Rosing H, Schellens JH, Beijnen JH. Quantifying vemurafenib in dried blood spots using high-performance LC-MS/MS. Bioanalysis. 2014;6(23):3215-24

23. Koster RA, Alffenaar JW, Greijdanus B, Uges DR. Fast LC-MS/MS analysis of tacrolimus, sirolimus, everolimus and cyclosporin A in dried blood spots and the influence of the hematocrit and immunosuppressant concentration on recovery. Talanta. 2013;115:47-54

24. Jager NG, Rosing H, Schellens JH, Beijnen JH. Determination of tamoxifen and endoxifen in dried blood spots using LC-MS/MS and the effect of coated DBS cards on recovery and matrix effects. Bioanalysis. 2014;6(22):2999-3009

25. Jager NG, Rosing H, Linn SC, Schellens JH, Beijnen JH. Dried Blood Spot Self-Sampling at Home for the Individualization of Tamoxifen Treatment: A Feasibility Study. Ther Drug Monit. 2015;37(6):833-6

26. de Wit D, den Hartigh J, Gelderblom H, Qian Y, den Hollander M, Verheul H, et al. Dried blood spot analysis for therapeutic drug monitoring of pazopanib. J Clin Pharmacol. 2015;55(12):1344-50

9

CHAPTER 10

Discussion

Genomic precision medicine

The first part of this thesis represents contemporary efforts to make anti-cancer treatment more precise. As mentioned in **Chapter 1**, many patients still do not benefit from systemic treatment or they experience excessive side effects. Internationally, there are many consortia that aim to find biomarkers that predict for treatment effect or for the occurrence of side effects. The ultimate goal in this quest is to prevent patients from being treated with ineffective drugs and to prevent patients from experiencing (unnecessary) heavy side effects. The Dutch Center for Personalized Cancer Treatment (CPCT) is an example of such a collaboration. The aim of the CPCT is to collect fresh frozen tumor biopsies on a large scale and to identify predictive biomarkers in the DNA of these biopsies.

CPCT studies

The backbone of the biopsy collection is the "CPCT-02" study (NCT01855477), in which patients that are planned to be treated with systemic anti-cancer treatment are included. After inclusion, these patients are biopsied from a – preferably metastatic – tumor lesion before start of the treatment. The fresh frozen biopsies are shipped to a central facility, where they are further processed, i.e. the percentage of tumor cells is determined and if that is sufficient (>30%), DNA is isolated from the macrodissected tumor cells. In case there is sufficient DNA (>500 ng), next-generation sequencing (NGS) is performed on it. Meanwhile, the clinical patient data is being collected in an electronic case record form (eCRF), from which the important clinical endpoints can be distracted. For the primary analyses, the DNA sequencing results and the clinical outcome are compared in order to identify somatic genetic alterations that can potentially serve as a predictive biomarker for the effectivity of a selected anti-cancer agent. In **Chapter 2**, a part of the logistical process of CPCT is outlined. It was already known that performing biopsies from metastatic lesions is a relatively safe procedure. However, we have also shown in this chapter that the central storage of fresh frozen biopsies from multiple clinical centers is feasible, which enabled us to set up a large biobank with high-quality tumor DNA from these biopsies. At start of the study, only three hospitals were affiliated to this initiative, being the Netherlands Cancer Institute, Amsterdam, the Erasmus MC Cancer Institute, Rotterdam,

and the UMC Utrecht. Once the process of biopsy collection and storage was set up in these centers, many other Dutch oncology centers have joined the CPCT, resulting in a unique collaboration that completely covers the Netherlands.

The main objective of the CPCT-02 is to identify somatic genetic aberrations predictive for treatment outcome. As the spectrum of genetic aberrations investigated is extremely large, especially with the continuous development of DNA sequencing techniques, and as the effects on treatment outcome might be subtle, large numbers of patients are required to have sufficient power for the analyses. Hence, it is estimated that no less than tens – or even hundreds – of patients are required for each analysis. As each administered drug exhibits a different working mechanism, they should be investigated separately. Therefore, it is fundamental that tumor tissue and patient characteristics are collected on a large scale, as is being done in CPCT. Currently, CPCT is focusing on performing high-throughput DNA sequencing, but since the biopsies are stored fresh frozen – and not formalin-fixed and paraffin-embedded (FFPE) – they can also be used for analyses on other platforms, such as for RNA sequencing or proteomics.

During the last years, when the CPCT was already initiated, several relevant findings have been reported. For example, the idea that genetic aberrations carry out their effects irrespective of tumor type has – at least partially – been refuted. For example, targeting mutated *BRAF* in colorectal cancer appeared to be ineffective,[1] whereas it had been found earlier that *BRAF* mutated melanoma responded very well to BRAF inhibition.[2] This effect was found to be caused by different activity of EGFR between the two tumor types, which results from the different embryological origin of the tissue.[3] Due to this context-dependency, it would be very helpful to discover what (histological) tumor types are susceptible to the investigated treatment. That way, patients can be recruited to specific trials based on the molecular characteristics of their tumor and the low number of patients can efficiently be allocated to the most informative trial. Unfortunately, even then the matter is probably much more complex than illustrated above. From *in vitro* studies, we have tried to identify genetic aberrations that are predictive for cisplatin response. We did so by comparing sensitivity analyses for genetic mutations in different cell lines from the Erasmus MC and from the public COSMIC database.[4] Strikingly, and unfortunately, these sensitivity analyses had very different – if not completely opposite –

10

results, which made it impossible to generate a predictive gene signature. Therefore, we were not able to set up a prospective clinical study to validate it. The irreproducibility of sensitivity analyses on cell lines was later confirmed on a larger scale, when results from the Cancer Genome Project (CGP) and the Cancer Cell line Encyclopedia (CCLE) were found to be highly discordant.[5] The authors conclude, justly, that experimental and analytic uniformity is lacking and should be optimized, especially when these experiments are to serve as the basis for further clinical research.[6]

As generating hypotheses for targeted anti-cancer treatment appears to be much more complex than expected, several initiatives have started giving targeted therapies to patients with other tumors than those for which the therapy has been registered. In a small set of patients, these targeted agents are aimed at the molecular aberrations, which they are known to effectively target in another cancer type, without anteriorly investigating the biological mechanism in a preclinical setting. The SHIVA trial[7] pioneered this type of research by randomizing almost 200 patients to either a targeted therapy against a proven molecular aberration or to treatment at the physician's choice. Regrettably, patients in the targeted therapy arm did not have better progression free survival (PFS) rates than those in the control arm. These results seem to provide an additional message that targeting molecular mechanisms, regardless of tumor type, is based on an oversimplified model of tumor biology. Additionally, 40% of the completely analyzed tumors did not harbor a mutation that was considered targetable by one of the drugs available to this initiative, which is most likely an illustration of the lack of adequate therapies to target all investigated molecular aberrations. In addition to this study, several other initiatives have been initiated to test the effectivity of targeted therapies outside their indication. Each target in the SHIVA trial was only represented by a small number of patients across several tumor types, which might have camouflaged successes in one of the subsets. The new trials are being performed on a much larger scale and, moreover, are designed to investigate the effect of each actionable aberration by itself. The CPCT, for example, has initiated a trial ("DRUP protocol") in which small patient cohorts are created to assess the effectivity of a drug per genetic aberration per tumor type. The data are then, more importantly, shared in an even larger collaboration, Global Alliance for Genomic Health (GA4GH).[8] Once the first results from these trials become available, we

will be able to see if the previous studies have just been too small or if we have a too simplistic view on tumor biology.

We already know that our current methods of (genetic) biomarker discovery are complicated by several other biological issues, of which the most complicated one appears to be tumor heterogeneity. Molecular tumor characteristics are subject to change at several levels: metastatic lesions can differ from each other and from the primary tumor, each lesion itself can contain multiple heterogeneous areas and the molecular characteristics can also change over time.[9] Although we know that heterogeneity can have both diagnostic and therapeutic implications on precision medicine, it remains unclear how to take it into account. For example, it is not known if the mutational profile in a single biopsy from a metastatic tumor lesion is representative for the mutational status of the tumor as a whole, if that abstraction of total tumor burden exists at all. Liquid biopsies, containing circulating tumor cells (CTCs) or DNA (ctDNA) that have been shed into the systemic circulation, have been proposed to cover that mutational status of the total tumor burden[10-12] and are less invasive to obtain than tumor biopsies. However, analyzing any circulating tumor material is still accompanied by a lot of diagnostic issues, such as capturing CTCs or determining what part of the ctDNA to sequence. Furthermore, it remains to be seen whether the hypothesis of circulating biomarkers being representative for all tumor burden is a valid one and – if existing – a clinically relevant one that can be used to direct the choice of therapy, as has only been described incidentally up till now.[13, 14] Despite its disadvantages, intratumoral molecular profiling remains the golden standard for assessing mutational status and only direct comparison between different platforms can show which platform is the most useful, especially since there are a lot of differences between the sequencing results of solid and liquid biopsies.[15]

Not only tumor material can be analyzed in multiple ways. While being key in the assessments of novel treatment strategies, the quantification of an intervention on clinical outcome is also not as straightforward as often presented. As quality of life is difficult to structurally assess, overall survival (OS) is regarded as the best clinical endpoint. However, it can take some time to reach that endpoint, especially in the less aggressive tumor types. In drug development, quick assessment of a drug's effectiveness is vital for efficient research and the use of OS would cause this early phase research to be very time-

10

consuming. Therefore, surrogate endpoints that are reached much quicker, such as progression free survival (PFS) or tumor response according to RECIST,[16] better suit this setting. In **Chapter 3**, we investigated another surrogate endpoint, the time to progression (TTP) ratio. The TTP ratio was found to be significantly correlated to OS and was even better than RECIST in predicting for OS in some patients in this study. Now that drug efficacy is being tested earlier during clinical research, the TTP ratio seems to be a valid alternative to be used as endpoint for that analyses.

Conclusions on genetic biomarker discovery

Genomic medicine has advanced greatly during the last two decades. In the 20th century, systemic cancer treatment almost exclusively consisted of (combined) chemotherapeutic regimens, which were generated much more with empirical than with biological research. Now that the increasing knowledge on tumor biology has found its way into the clinic, both in diagnostics and in therapeutics, a lot of different classes of drugs have taken the place of conventional chemotherapy in cancer treatment. Nevertheless, "old fashioned" chemotherapy remains the cornerstone of treatment for the majority of cancer types, which illustrates that we are still unable to fully understand what is happening inside (and around) tumor cells and how we can reverse all these proliferative processes. However, the substantial improvements achieved in cancer treatment over last decades cannot be neglected and future research on molecular biomarkers should be aimed at determining what type of diagnostic platform is superior, which can only be achieved by direct comparison of the available platforms and is likely to be different within the context of each tumor type. As these assessments require a lot of resources, e.g. tumor samples, their blood samples, clinical data, a network to collect all these and especially a lot of funding to finance it, small-scale initiatives by individual institutions should be regarded as obsolete. Only by combining (international) efforts the most fundamental questions in this field can be addressed in a scientifically proper manner and the CPCT is a prototype in that context, combining the resources from almost all Dutch oncology centers into an international network of similar collaborations.[8]

Pharmacokinetic precision medicine

In addition to the molecular characteristics of tumor cells, another main determinant of treatment outcome in humans is the amount of anti-tumor drug reaching the tumor sites. But the ideal way to determine how much drug reaches the tumor remains a black box. A generally accepted surrogate for drug exposure to the tumor is systemic exposure, which is evidently easier to sample and to monitor. For some anti-cancer agents, predominantly for tyrosine kinase inhibitors (TKIs), it has been found that systemic drug exposure is correlated to clinical outcome.[17, 18] Logically, the next step in improving clinical outcome is optimizing the exposure in patients that experience little effect due to low drug concentrations or in those that experience much toxicity due to high drug concentrations. Part of this mechanism is already incorporated in the way most anti-cancer drugs, especially the chemotherapeutic agents, are being dosed, i.e. based on body surface area (BSA). That way, big patients get higher doses and little patients small doses, which should ultimately lead to equal systemic drug concentrations. In **Chapter 4**, however, we argue that correcting doses for BSA is an outdated principle and cannot be justified by a scientific rationale. Unfortunately, the BSA-guided dose corrections have been implemented from the start of clinical oncology research and, hence, no empirical evidence is available for other – more simple and practical – dosing algorithms to be (at least) equal to it.

Most recently developed drugs, including TKIs, are being administered in a flat dose, which eliminates the false security of BSA guided dosing being accurate. There are still many other factors contributing to inter-individual variation (IIV) in drug exposure, as is illustrated by the large coefficient of variation (CV) for many TKIs, such as sorafenib. In **Chapter 5**, we have shown that the activity of the OATP1B membrane transporters contributes significantly to the pharmacokinetics of sorafenib's metabolite sorafenib-glucuronide (SG). By inhibiting OATP1B function with rifampin in sorafenib-treated patients, we were able to inhibit biliary secretion of SG, which caused SG to accumulate systemically. Although we predicted that this reduced SG secretion would lead to reduced enterohepatic circulation of sorafenib and consequently, to lower systemic sorafenib concentrations, we did not observe this effect in our study. However, to fully disprove this mechanism of reduced sorafenib exposure and thus of reduced sorafenib anti-cancer

10

effects, studies with prolonged OATP1B inhibition are needed. As this study did not take clinical outcome of the altered sorafenib PK into account, we have retrospectively analyzed a sorafenib-treated cohort of patients in **Chapter 6**. In that study, we assessed if genetic polymorphisms in the enzymes involved in the PK of sorafenib and its metabolites were associated with clinical outcome. We found that single nucleotide polymorphisms (SNPs) in *SLCO1B1*, which encodes for OATP1B1, is associated with the incidence of sorafenib-induced adverse events. This can biologically be explained by increased toxicity in case of reduced OATP1B1 function. Although we have not been able to directly assess the relation between SG accumulation and toxicity, the results from these two chapters are highly suggestive for a causal relation between the two. However, clinical implementation of structural *SLCO1B1* genotyping before commencing treatment with sorafenib is not likely in the near future. First, it is not known either if upfront sorafenib dose reductions in patients with an unfavorable pharmacogenetic profile results in less toxicity and – equally important – comparable anti-cancer effects. On that behalf, it would be interesting to see if patients with a genetic predisposition to sorafenib toxicity are more prone to other OATP1B inhibiting stimuli, such as comedication with clarithromycin or ramipril. Furthermore, as sorafenib does not frequently lead to catastrophic toxicity, such as in fluoropyrimidine-treated patients with a *DPYD* deficiency[19] or as in azathioprine-treated patients with a *TPMT* deficiency,[20] *OATP1B1* genotyping will to be cost-effective in sorafenib treated patients, whereas the other mentioned examples are.[21, 22]

Therapeutic drug monitoring (TDM)

For drugs with a large intrapatient variability in systemic exposure, determining only the optimal starting dose will probably not suffice to optimize treatment outcome. Systemic drug concentrations will have to be followed during treatment in order to verify that the exposure is still within the therapeutic window. For a TKI like imatinib, for instance, it has been found that the systemic exposure decreases with 30% within the first three months of treatment and stabilizes thereafter.[23] Being attributed to differential absorption between patients at first, it was later speculated[24] that the decrease could be caused by reduced alpha-1 acid glycoprotein (AGP) levels, which is an acute phase protein that was

thought to lower on treatment due to less tumor burden or fading surgical effects. In **Chapter 7**, however, we did not observe significant or clinically relevant changes in AGP. On the other hand, we confirmed that imatinib concentrations remarkably lowered after the first month of treatment, albeit less than the 30% decrease that was described earlier. By disproving this AGP-based theory, we have again lost sight of a possible biological rationale for the systemic imatinib exposure to decrease. This means that it is not possible to extrapolate measured (trough) concentrations at 1 month, used to determine the relation of PK to treatment effect,[18] to concentrations at other time points. In itself, that does not have to be a problem, if everyone were to use that same time point to measure imatinib trough concentrations. In reality, three retrospective studies have described a much higher incidence than the 25% (lowest quartile) of patients that have imatinib concentrations below the (assumed) target for efficacy.[25-27] In these studies, however, patients were sampled at random time points, mostly far beyond the third month of treatment, which logically results in a larger proportion of patients below the threshold. In a disturbing way, this illustrates the lack of uniformity between different studies that investigate TDM of imatinib in GIST patients. Based on the currently available evidence, we may conclude that patients with GIST that are being treated with imatinib have better progression free survival when their systemic trough concentration is above 1100 ng/mL after the first month of treatment, that there is currently no algorithm to predict at what concentration a patient's exposure will stabilize after the third month of treatment and that there is no clear evidence what trough concentration discriminates best for efficacy after the third treatment month. Regarding the latter conclusion, it would be interesting to have trough concentrations at different time points compared to clinical outcome, imatinib is given for years and as it might be beneficial to verify if there is sufficient imatinib exposure at a later time point, e.g. after 1 year. Possibly, a lower threshold might suffice at that moment, although that scenario seems to be unrealistic given the recent finding that prolonged adjuvant imatinib leads to better treatment outcome.[28] Additionally, tumor characteristics appear to play a role in the needed exposure as well: patients with a somatic *KIT* mutation in exon 9 benefit more from imatinib 800 mg daily than from 400 mg, whereas patients all other GIST subtypes benefited equally from both

10

doses.[29] It is therefore likely that patients with a *KIT* exon 9 mutations have a higher systemic exposure threshold for efficacy than others.

As for imatinib, a target trough concentration for pazopanib efficacy (of 20.5 µg/mL) has been distilled from early phase studies.[17] In those studies, 30% of patients did not reach the target concentration after four weeks of treatment. In **Chapter 8**, we therefore investigated if increasing the pazopanib dose in those patients would raise their trough concentrations above the set target. In more than half of the patients with a trough concentration below the target, we were able to raise that concentration above that target by increasing the dose. Now that PK-guided pazopanib dosing is proven feasible, subsequent studies should investigate the benefit that patients experience from correcting a (too) low systemic exposure. The problem of frequent outpatient visits for the blood draws to monitor pazopanib concentrations has been tackled in **Chapter 9**, where concentrations measured on dried blood spots (DBS) were proven to be similar to those measured from plasma samples.

Conclusions on pharmacokinetics

As said, there are two main pillars in pharmacokinetics: determining the correct starting dose and – if necessary – maintaining sufficient systemic exposure. Both serve the same goals of optimizing anti-cancer effects and reducing (long term) toxicity. Pretreatment dose adjustments are currently reserved for patients at high risk of toxicity, e.g. elderly patients and those with a poor performance status, significant comorbidity or poor renal or liver function. Pharmacogenetics or potential drug-drug interactions are, at least in oncology, rarely used to base a dose alteration upon. In the context of the other pillar, maintaining sufficient exposure, one can question the clinical importance of a precisely right starting dose, especially when the first drug monitoring is being performed quickly after treatment start. Hence, maintaining adequate systemic exposure seems of more importance. Although TDM is also infrequently applied in oncology, systemic drug exposure of many anti-cancer agents has been linked to treatment outcome, increasingly in a prospective setting.[30, 31] High-quality randomized trials are needed to prove that systemic exposure is indeed correlated to clinical outcome, but these trials are hard to perform, as patients are reluctant to enter such a trial, which necessitated the Sarcoma

Alliance for Research through Collaboration to terminate their phase III study on this subject. More surprisingly, physicians appear to be reluctant to follow up the dosing advice.[32] This seems to indicate that medical oncologists can be categorized as believers or non-believers, which makes it hard for the believers to perform the necessary research required for an honest evaluation of TDM. Therefore, studies to investigate TDM in oncology need to be set up in an innovative design. Example can be taken of the researchers that have explored the usefulness of concomitant prednisone during docetaxel treatment in prostate cancer, who have not randomized their patients to a treatment arm, but who have compared treatment outcome at two different hospitals with a different docetaxel treatment protocol (with and without concomitant prednisone).[33] This study design can also serve as a bridge between TDM believers and non-believers, who are already practicing according to their belief anyway.

10

REFERENCES

1. Kopetz S, Desai J, Chan E, Hecht JR, O'Dwyer PJ, Maru D, et al. Phase II Pilot Study of Vemurafenib in Patients With Metastatic BRAF-Mutated Colorectal Cancer. J Clin Oncol. 2015;33(34):4032-8

2. Chapman PB, Hauschild A, Robert C, Haanen JB, Ascierto P, Larkin J, et al. Improved survival with vemurafenib in melanoma with BRAF V600E mutation. N Engl J Med. 2011;364(26):2507-16

3. Prahallad A, Sun C, Huang S, Di Nicolantonio F, Salazar R, Zecchin D, et al. Unresponsiveness of colon cancer to BRAF(V600E) inhibition through feedback activation of EGFR. Nature. 2012;483(7387):100-3

4. Forbes SA, Beare D, Gunasekaran P, Leung K, Bindal N, Boutselakis H, et al. COSMIC: exploring the world's knowledge of somatic mutations in human cancer. Nucleic Acids Research. 2015;43(D1):D805-D11

5. Haibe-Kains B, El-Hachem N, Birkbak NJ, Jin AC, Beck AH, Aerts HJ, et al. Inconsistency in large pharmacogenomic studies. Nature. 2013;504(7480):389-93

6. Safikhani Z, El-Hachem N, Quevedo R, Smirnov P, Goldenberg A, Juul Birkbak N, et al. Assessment of pharmacogenomic agreement. F1000Res. 2016;5:825

7. Le Tourneau C, Delord JP, Goncalves A, Gavoille C, Dubot C, Isambert N, et al. Molecularly targeted therapy based on tumour molecular profiling versus conventional therapy for advanced cancer (SHIVA): a multicentre, open-label, proof-of-concept, randomised, controlled phase 2 trial. Lancet Oncol. 2015;16(13):1324-34

8. Siu LL, Lawler M, Haussler D, Knoppers BM, Lewin J, Vis DJ, et al. Facilitating a culture of responsible and effective sharing of cancer genome data. Nat Med. 2016;22(5):464-71

9. Gerlinger M, Rowan AJ, Horswell S, Larkin J, Endesfelder D, Gronroos E, et al. Intratumor heterogeneity and branched evolution revealed by multiregion sequencing. N Engl J Med. 2012;366(10):883-92

10. Brouwer A, De Laere B, Peeters D, Peeters M, Salgado R, Dirix L, et al. Evaluation and consequences of heterogeneity in the circulating tumor cell compartment. Oncotarget. 2016 March 9 [Epub ahead of print]

11. Cheng F, Su L, Qian C. Circulating tumor DNA: a promising biomarker in the liquid biopsy of cancer. Oncotarget. 2016 May 19 [Epub ahead of print]

12. Beije N, Jager A, Sleijfer S. Circulating tumor cell enumeration by the CellSearch system: The clinician's guide to breast cancer treatment? Cancer Treatment Reviews. 2015;41(2):144-50

13. Gautschi O, Aebi S, Heukamp LC. Successful AZD9291 Therapy Based on Circulating T790M. J Thorac Oncol. 2015;10(12):e122-3

14. Onstenk W, de Klaver W, de Wit R, Lolkema M, Foekens J, Sleijfer S. The use of circulating tumor cells in guiding treatment decisions for patients with metastatic castration-resistant prostate cancer. Cancer Treat Rev. 2016;46:42-50

15. Onstenk W, Sieuwerts AM, Mostert B, Lalmahomed Z, Bolt-de Vries JB, van Galen A, et al. Molecular characteristics of circulating tumor cells resemble the liver metastasis more closely than the primary tumor in metastatic colorectal cancer. Oncotarget. 2016 June 20 [Epub ahead of print]

16. Eisenhauer EA, Therasse P, Bogaerts J, Schwartz LH, Sargent D, Ford R, et al. New response evaluation criteria in solid tumours: revised RECIST guideline (version 1.1). Eur J Cancer. 2009;45(2):228-47

17. Suttle AB, Ball HA, Molimard M, Hutson TE, Carpenter C, Rajagopalan D, et al. Relationships between pazopanib exposure and clinical safety and efficacy in patients with advanced renal cell carcinoma. Br J Cancer. 2014;111(10):1909-16

18. Demetri GD, Wang Y, Wehrle E, Racine A, Nikolova Z, Blanke CD, et al. Imatinib plasma levels are correlated with clinical benefit in patients with unresectable/metastatic gastrointestinal stromal tumors. J Clin Oncol. 2009;27(19):3141-7

19. Lunenburg CATC, Henricks LM, Guchelaar H-J, Swen JJ, Deenen MJ, Schellens JHM, et al. Prospective DPYD genotyping to reduce the risk of fluoropyrimidine-induced severe toxicity: Ready for prime time. European Journal of Cancer. 2016;54:40-8

20. Lennard L. TPMT in the treatment of Crohn's disease with azathioprine. Gut. 2002;51(2):143-6

21. Deenen MJ, Meulendijks D, Cats A, Sechterberger MK, Severens JL, Boot H, et al. Upfront Genotyping of DPYD*2A to Individualize Fluoropyrimidine Therapy: A Safety and Cost Analysis. J Clin Oncol. 2016;34(3):227-34

22. Thompson AJ, Newman WG, Elliott RA, Roberts SA, Tricker K, Payne K. The Cost-Effectiveness of a Pharmacogenetic Test: A Trial-Based Evaluation of TPMT Genotyping for Azathioprine. Value in Health. 2014;17(1):22-33

23. Eechoute K, Fransson MN, Reyners AK, de Jong FA, Sparreboom A, van der Graaf WT, et al. A long-term prospective population pharmacokinetic study on imatinib plasma concentrations in GIST patients. Clin Cancer Res. 2012;18(20):5780-7

24. Chatelut E, Gandia P, Gotta V, Widmer N. Long-term prospective population PK study in GIST patients--letter. Clin Cancer Res. 2013;19(4):949

25. Yoo C, Ryu MH, Ryoo BY, Beck MY, Chang HM, Lee JL, et al. Changes in imatinib plasma trough level during long-term treatment of patients with advanced gastrointestinal stromal tumors: correlation between changes in covariates and imatinib exposure. Invest New Drugs. 2012;30(4):1703-8

26. Lankheet NA, Knapen LM, Schellens JH, Beijnen JH, Steeghs N, Huitema AD. Plasma concentrations of tyrosine kinase inhibitors imatinib, erlotinib, and sunitinib in routine clinical outpatient cancer care. Ther Drug Monit. 2014;36(3):326-34

27. Bouchet S, Poulette S, Titier K, Moore N, Lassalle R, Abouelfath A, et al. Relationship between imatinib trough concentration and outcomes in the treatment of advanced gastrointestinal stromal tumours in a real-life setting. Eur J Cancer. 2016;57:31-8

28. Joensuu H, Eriksson M, Sundby Hall K, Reichardt A, Hartmann JT, Pink D, et al. Adjuvant Imatinib for High-Risk GI Stromal Tumor: Analysis of a Randomized Trial. J Clin Oncol. 2016;34(3):244-50

29. Gastrointestinal Stromal Tumor Meta-Analysis G. Comparison of two doses of imatinib for the treatment of unresectable or metastatic gastrointestinal stromal tumors: a meta-analysis of 1,640 patients. J Clin Oncol. 2010;28(7):1247-53

30. Joerger M, von Pawel J, Kraff S, Fischer JR, Eberhardt W, Gauler TC, et al. Open-label, randomized study of individualized, pharmacokinetically (PK)-guided dosing of paclitaxel combined with carboplatin or cisplatin in patients with advanced non-small-cell lung cancer (NSCLC). Ann Oncol. 2016

31. Wilhelm M, Mueller L, Miller MC, Link K, Holdenrieder S, Bertsch T, et al. Prospective, Multicenter Study of 5-Fluorouracil Therapeutic Drug Monitoring in Metastatic Colorectal Cancer Treated in Routine Clinical Practice. Clin Colorectal Cancer. 2016

32. Gotta V, Widmer N, Decosterd LA, Chalandon Y, Heim D, Gregor M, et al. Clinical usefulness of therapeutic concentration monitoring for imatinib dosage individualization: results from a randomized controlled trial. Cancer Chemother Pharmacol. 2014;74(6):1307-19

33. Kongsted P, Svane IM, Lindberg H, Daugaard G, Sengelov L. Low-dose prednisolone in first-line docetaxel for patients with metastatic castration-resistant prostate cancer: is there a clinical benefit? Urol Oncol. 2015;33(11):494 e15-20

10

CHAPTER 11

Dutch summary
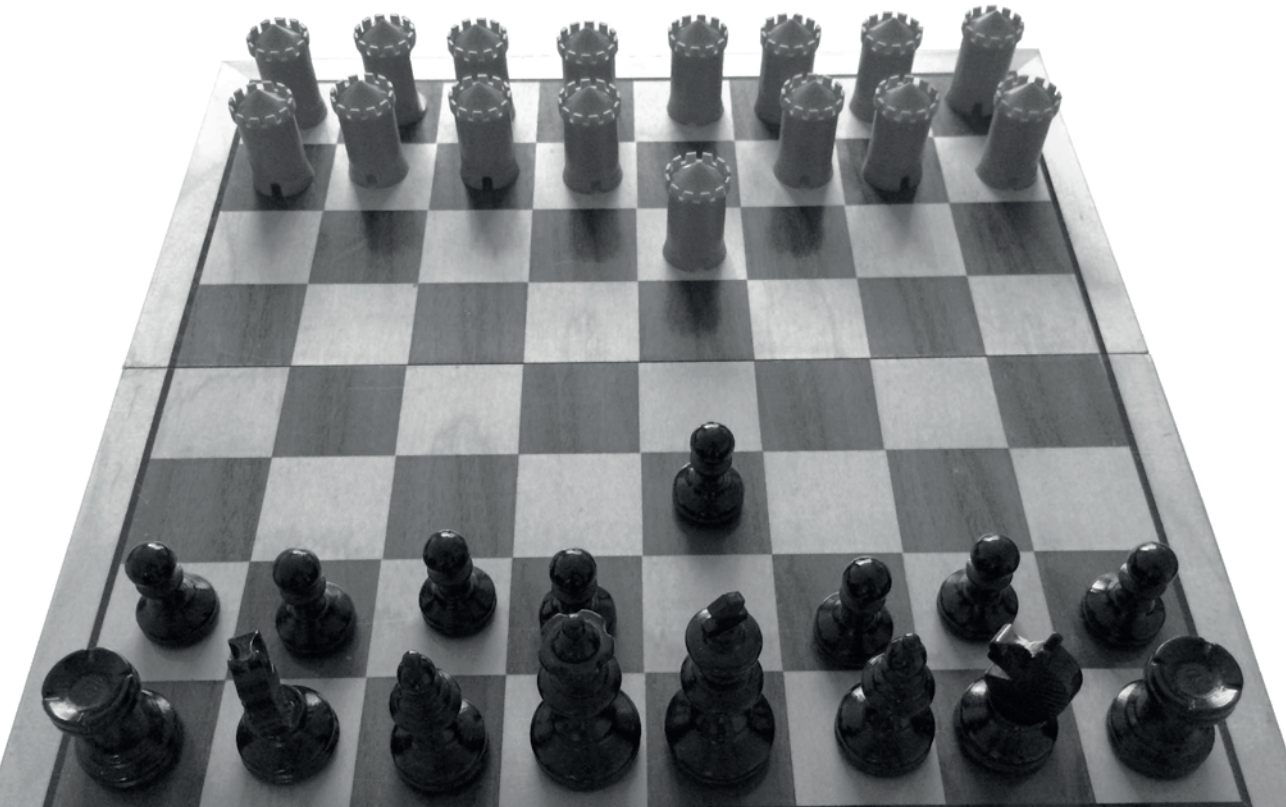
De afgelopen decennia heeft de medicamenteuze behandeling van kanker zich sterk ontwikkeld. Hoewel opereren in het overgrote deel van de gevallen vereist is voor genezing, zorgt de behandeling met medicijnen in toenemende mate voor een betere overleving. In de tweede helft van de 20^{e}e eeuw werden de eerste stappen naar een systemische behandeling van kanker gezet met de introductie van chemotherapie. Sindsdien heeft er veel onderzoek plaatsgevonden en is het inzicht in welke biologische mechanismen een rol spelen in tumoren sterk verbeterd. Dit heeft aan het einde van de vorige eeuw geresulteerd in de ontwikkeling van nieuwe geneesmiddelen voor de behandeling van kanker, zoals tyrosine kinase remmers (TKIs) en anti-hormonale middelen. Deze nieuwe middelen zijn gericht op het remmen van de signalen die aanzetten tot celdeling. Deze signalen zijn binnen een kankercel overactief en stimuleren daarmee ongeremde celdeling. Oorspronkelijk werd vermoed dat deze middelen door hun gerichte werkingsmechanismen een stuk minder giftig zouden zijn dan conventionele chemotherapieën, die hun effect op tumoren – en helaas ook op gezonde cellen – uitoefenen door de celdeling te remmen. De proliferatieve signalen, die door de nieuwe middelen worden geremd, blijken ook een rol te spelen in de fysiologie van gezonde cellen en het remmen daarvan leidt dus – net als bij chemotherapie – tot bijwerkingen. De uitdaging voor het hedendaagse onderzoek is om te ontdekken welke patiënten geen baat hebben van behandeling, omdat deze behandeling geen effect heeft of omdat de behandeling teveel bijwerkingen geeft. In dit proefschrift staan twee methoden beschreven om de medicamenteuze behandeling van kanker preciezer op de individuele patiënt af te stemmen: 1. op basis van genetische afwijkingen in de tumor en 2. op basis van de verdeling van het geneesmiddel in het lichaam. Dit laatste wordt ook wel farmacokinetiek genoemd.

Genetische afwijkingen in de tumor

Veel nieuwe behandelingen zijn al gericht op genetische afwijkingen binnen een tumorcel. Het medicijn imatinib is bijvoorbeeld alleen effectief bij gastro-intestinale stromaceltumoren (GIST) als die een mutatie in het *KIT*-gen bevatten. Datzelfde geldt voor een ander medicijn in dezelfde klasse van geneesmiddelen: vemurafenib, dat wordt toegepast bij melanomen met een zogenaamde *BRAF*-mutatie. Er zijn echter ook nog veel

anti-kanker geneesmiddelen waarvoor zo'n genetische biomarker nog niet ontdekt is. Om die reden werken vele ziekenhuizen in Nederland samen binnen het Center for Personalized Cancer Treatment (CPCT). Binnen het CPCT wordt in tumoren gekeken naar genetische afwijkingen die mogelijk de uitkomst van de medicamenteuze behandeling van kanker kunnen voorspellen. Voordat patiënten beginnen met die behandeling, wordt er een biopt uit de tumor genomen, bij voorkeur uit een uitzaaiing. Als er voldoende biopten zijn van patiënten die eenzelfde behandeling hebben gehad, wordt gekeken of de patiënten die goed op de behandeling reageerden een ander genetisch profiel van hun tumor hadden dan degenen die niet goed reageerden. Voordat de biopten op grote schaal verzameld en geanalyseerd kunnen worden, moet duidelijk zijn dat deze procedures veilig zijn en dat het verkregen tumormateriaal goed geanalyseerd kan worden. Uit een analyse na de eerste 500 biopsieprocedures blijkt dat dit het geval is, zoals staat beschreven in **Hoofdstuk 2** van dit proefschrift. Hiermee is de weg vrijgemaakt om op grote schaal tumorbiopten te verzamelen en inmiddels zijn er een groot aantal Nederlandse ziekenhuizen bij dit netwerk aangesloten.

Naast het vinden van (genetische) biomarkers voor de uitkomst van de behandeling, is de ontwikkeling van nieuwe geneesmiddelen een andere belangrijke pijler binnen het oncologische onderzoek. Om die ontwikkeling zo efficiënt mogelijk te laten verlopen, is het een uitdaging om zo vroeg mogelijk te zien hoe effectief een geneesmiddel is. In **Hoofdstuk 3** staat beschreven dat de verhouding tussen de natuurlijke groeisnelheid van een tumor en de duur van de behandeling een goede voorspeller is voor de effectiviteit (gemeten met 3D-beeldvorming) van behandeling met everolimus.

Farmacokinetiek

Naast kenmerken van de tumor, waarop een geneesmiddel kan aangrijpen, is het net zo belangrijk dat er voldoende geneesmiddel bij de tumor aankomt. Ten eerste is het belangrijk om een goede startdosering te kiezen, die afgestemd is op de individuele patiënt. Veel geneesmiddelen, met name chemotherapieën, worden nog gedoseerd op basis van lichaamsoppervlakte ('body-surface area'; kortweg BSA). BSA wordt berekend door middel van een formule, waarin lengte en gewicht worden meegenomen. In

11

Hoofdstuk 4 wordt uitgelegd waarom deze formule vaak geen toereikende correctie biedt voor de startdosis van geneesmiddelen binnen de oncologie. Wij menen dat een startdosis die in principe bij elke patiënt hetzelfde is, niet perse slechter hoeft te zijn dan doseren op basis van BSA.

Lengte en gewicht zijn niet de enige factoren die van invloed zijn op de farmacokinetiek van een geneesmiddel. Elk geneesmiddel wordt bijvoorbeeld actief in en uit de bloedbaan opgenomen door membraantransporters, die onder andere op levercellen, darmcellen en tumorcellen zitten. Om tot een patiëntgerichte dosering te komen moeten we dus beter rekening gaan houden met deze factoren. In **Hoofdstuk 5** is gekeken in welke mate de specifieke OATP1B transporteiwitten betrokken zijn bij de farmacokinetiek van het middel sorafenib. Hoewel dit onderzoek op cellijnen, muizen en patiënten is uitgevoerd, heeft dit onderzoek niet geheel in kaart kunnen brengen wat de daadwerkelijke consequenties van de veranderde farmacokinetiek op de klinische effecten van sorafenib zijn. Daarom is in **Hoofdstuk 6** onderzocht of patiënten met een genetische afwijking in deze transporter meer bijwerkingen van sorafenib hadden dan degenen met een normaal functionerend eiwit. Deze hypothese is inderdaad bevestigd: afwijkingen in het gen dat codeert voor OATP1B1 waren geassocieerd met het optreden van bijwerkingen.

Omdat de concentraties van het geneesmiddel in het bloed ook tijdens de behandeling kunnen veranderen, is het belangrijk om de concentraties periodiek te blijven controleren. Van imatinib is bijvoorbeeld bekend, dat de concentraties na drie maanden met 30% dalen. De oorzaak daarvan is vooralsnog onbekend. Hoewel anderen eerder hebben beweerd dat een gelijktijdige daling van de concentraties van het eiwit AGP in de bloedbaan de reden zou kunnen zijn, is in **Hoofdstuk 7** aangetoond dat hiervan niet zozeer sprake is. Verder onderzoek zal moeten uitwijzen of patiënten met een te lage blootstelling aan imatinib wellicht beter af zijn met een dosisverhoging. Datzelfde geldt ook voor patiënten die met pazopanib, wederom een ander middel in dezelfde klasse, behandeld worden. In **Hoofdstuk 8** staat beschreven dat relatief lage concentraties in het bloed veilig gecorrigeerd kunnen worden door de dosis geleidelijk te verhogen. Opnieuw zal vervolgonderzoek moeten uitwijzen of dit daadwerkelijk tot betere resultaten leidt. Door de concentraties te meten in bloed uit een vingerprik in plaats van uit een buis

bloed, zou het vervolgen van de geneesmiddelenconcentraties een stuk patiëntvriendelijker kunnen verlopen. Dat de metingen met een vingerprik dezelfde resultaten geven als met de standaard bloedafnames, hebben we aangetoond en staat beschreven in **Hoofdstuk 9**.

Conclusies

De ontwikkelingen binnen de oncologie hebben de laatste jaren een vlucht genomen. Toch blijft er nog veel ruimte voor verbetering. In dit proefschrift staan een aantal voorbeelden van het preciezer maken van de medicamenteuze behandeling door op zoek te gaan naar nieuwe (genetische) aangrijpingspunten in de tumor, of door de blootstelling aan het geneesmiddel te optimaliseren. Doordat de bestaande onderverdeling van tumoren op basis van celtype zal versplinteren, moet toekomstig onderzoek voor elk van deze subtype tumoren uitwijzen welk middel daar het beste tegen werkt en bij welke blootstelling dat het beste gebeurt.

11

APPENDICES

- **- Co-author affiliations**
- **- Dankwoord**
- **- Curriculum Vitae**
- **- List of Publications**
- **- PhD Portfolio**

CO-AUTHOR AFFILIATIONS

Co-author	Chapter	Affiliations
Aksana Vasilyeva	5	St. Jude Children's Research Hospital, TN, USA
Alex Sparreboom	5	Ohio State University, OH, USA
Alice A. Gibson	5	Ohio State University, OH, USA
Alwin D.R. Huitema	8, 9	NKI Amsterdam
Anne Lenting	6	Erasmus MC Rotterdam
Annette H. Bruggink	2	CPCT, UMC Utrecht
Astrid W. Oosten	7	Erasmus MC Rotterdam
Bas Thijssen	9	NKI Amsterdam
Christa G. Gadellaa - van Hooijdonk	2, 3	CPCT, UMC Utrecht
Edwin Cuppen	2	CPCT, Cancer Genomics Center, UMC Utrecht
Emile E. Voest	2, 3	CPCT, NKI Amsterdam
Erik van Werkhoven	2, 3	CPCT, NKI Amsterdam
Esther Oomen - de Hoop	6	Erasmus MC Rotterdam
Femke M. de Man	7	Erasmus MC Rotterdam
Ferry A.L.M. Eskens	5, 6	Erasmus MC Rotterdam
Fleur Weeber	2, 3	CPCT, NKI Amsterdam
Geert A. Cirkel	2, 3	CPCT, UMC Utrecht
Guoqing Du	5	St. Jude Children's Research Hospital, TN, USA
Hilde Rosing	9	NKI Amsterdam
Inge Ubink	3	UMC Utrecht
Isaac J. Nijman	2	CPCT, UMC Utrecht
Jacqueline S.L. Kloth	7	Erasmus MC Rotterdam
Jan H.M. Schellens	2, 3, 8, 9	CPCT, NKI Amsterdam, Utrecht University
Jos H. Beijnen	8, 9	NKI Amsterdam
Karel Eechoute	7	Erasmus MC Rotterdam
Leni van Doorn	5, 6, 8	Erasmus MC Rotterdam
Lianda Nan	9	NKI Amsterdam
Lie Li	5	St. Jude Children's Research Hospital, TN, USA
Maja J.A. de Jonge	2, 3	CPCT, Erasmus MC Rotterdam
Marco J. Koudijs	2	CPCT, UMC Utrecht

A

Co-author	Chapter	Affiliations
Marijn van Stralen	3	UMC Utrecht
Mark J. Ratain	4	The University of Chicago, IL, USA
Marlies H.G. Langenberg	2, 3, 8	CPCT, UMC Utrecht
Martijn P. Lolkema	2, 3, 8, 9	CPCT, Erasmus MC Rotterdam
Michel M. van den Heuvel	2	CPCT, NKI Amsterdam
Mitch A. Phelps	5	Ohio State University, OH, USA
Neeltje Steeghs	2, 3, 8, 9	CPCT, NKI Amsterdam
Paul Hamberg	5	St. Franciscus Gasthuis Rotterdam
Paul J. van Diest	2	CPCT, UMC Utrecht
Peter de Bruijn	5, 7	Erasmus MC Rotterdam
Remy B. Verheijen	8, 9	NKI Amsterdam
Rob J. de Knegt	2	CPCT, Erasmus MC Rotterdam
Ron H.J. Mathijssen	2, 4, 5, 6, 7, 8, 9	CPCT, Erasmus MC Rotterdam
Ron H.N. van Schaik	6	Erasmus MC Rotterdam
Samira el Bouazzaoui	6	Erasmus MC Rotterdam
Sharyn D. Baker	5	Ohio State University, OH, USA
Shuiying Hu	5	Ohio State University, OH, USA
Stefan M. Willems	2, 3	CPCT, UMC Utrecht
Stefan Sleijfer	2, 3, 7	CPCT, Cancer Genomics Center, Erasmus MC Rotterdam
Wouter B. Veldhuis	2, 3	CPCT, UMC Utrecht

DANKWOORD

Aan het tot stand komen van dit proefschrift hebben zoveel mensen bijgedragen, dat dit hoofdstuk niet toereikend is om iedereen daar persoonlijk voor te bedanken. Toch zal ik proberen dat zo volledig mogelijk te doen, te beginnen bij alle patiënten die hebben deelgenomen aan de hier beschreven studies. Hun bereidheid om dit belangeloos te doen is het fundament van klinisch wetenschappelijk onderzoek.

Mijn beide promotoren ben ik niet minder dank verschuldigd. Prof. dr. Sleijfer, Stefan, ik vind het wonderbaarlijk hoe je mij hebt kunnen begeleiden naast al je andere werkzaamheden. Je drukke agenda deed niets af aan de vakkundige manier waarop je me – altijd op korte termijn – niet alleen van opbouwende kritiek voorzag, maar ook de nodige sturing hebt gegeven bij het uitvoeren van de CPCT-studies. De hartelijke woorden, die je altijd graag voor me over had, zal ik nog lang meenemen. Prof. dr. Mathijssen, Ron, jij blijft me altijd verbazen met de persoonlijke manier waarop je alle promovendi begeleidt en met de oneindige gedrevenheid waarmee je je doelen nastreeft. Ik vind het bijzonder hoe je deze hele nieuwe groep succesvol hebt opgebouwd. De ontwikkeling die ik in Rotterdam heb doorgemaakt is grotendeels te danken aan de ruimte en het vertrouwen, die je me daarvoor hebt gegeven. In het bijzonder ben ik jullie beiden enorm dankbaar voor jullie actieve betrokkenheid in het afgelopen jaar.

Prof. dr. Huitema, Prof. dr. Van Schaik en Prof. dr. Voest, dank dat jullie dit manuscript hebben willen beoordelen als leescommissie. Prof. dr. Aerts, Prof. dr. Van Gelder, Prof. dr. Gelderblom en Prof. dr. Schellens, dank dat jullie bereid zijn om in de oppositie plaats te nemen.

Dr. Lolkema, Martijn, mijn 'slakkenfenotype' sloot niet altijd aan bij de manier waarop jij dingen graag geregeld ziet. Toch hebben we – sinds je mij bij mijn eerste wetenschappelijke stappen binnen de interne oncologie begeleidde - samen een aantal mooie projecten uitgevoerd. Uit het feit dat je me naar Rotterdam gevolgd bent, maak ik op dat je mijn vertragende invloed stiekem bent gaan waarderen. Dank voor je begeleiding tijdens de afgelopen jaren.

A

Dr. Eskens, Ferry, onze grote plannen voor wetenschappelijke samenwerking bleken niet allemaal te realiseren. Alsnog heb je een groot aandeel bij een aantal hoofdstukken in dit proefschrift. Daarnaast heb je mijn klinische activiteiten de afgelopen jaren gesuperviseerd en heb je mij geholpen om de medische wetenschap in die klinische context te leren plaatsen. Dank voor je enorme betrokkenheid.

Dear Sharyn and Alex, many thanks for supervising and coordinating the rifampin study and especially for the stay in Memphis. You've really introduced me into the fundamental part of science. Alice, Shuiying and Aksana, thank you for taking me through all the different experiments and for looking after me during the two weeks I was at your lab.

Christa en Geert, jullie hebben je als eerste gewaagd aan de logistiek van de CPCT-studies en jullie inspanningen zijn essentieel geweest voor alles wat er nu binnen het CPCT gebeurt. Christa, de 'bioptenpaper' is grotendeels door jouw inspanningen tot stand gekomen. Dank voor al jullie moeite die in deze projecten is gaan zitten. Fleur, het was mooi om samen de tweede generatie CPCT-promovendi te vormen bij alle (niet-wetenschappelijke) CPCT-activiteiten. Succes met de laatste loodjes.

Remy Verheijen, dank voor de prettige samenwerking bij de laatste twee hoofdstukken. Kers op de taart was de samenwerking tijdens de derde helft bij de laatste ESMO. Succes met het afronden van je eigen proefschrift.

Hoewel er uiteindelijk weinig next-generation sequencing resultaten in dit proefschrift terug te vinden is, ben ik veel dank verschuldigd aan allen die hebben geprobeerd om mij daar iets over bij te brengen. Marco, Annelies en vooral Ies , jullie stonden altijd klaar in Utrecht om de gapende hiaten in mijn kennis geduldig te vullen. Veel dank daarvoor. Daniel, onze regelmatige discussies over de resultaten van onder meer de CPCT-01 hebben helaas (nog) niet geleid tot iets publicabels, maar hopelijk troost het je dat ik er in ieder geval een hoop van geleerd heb. Jozien Helleman, John Martens en Erik Wiemer, jullie hebben veel met mij om de tafel gezeten om een mooie klinische studie (de CPCT-04) op te zetten, die helaas nooit van de grond is gekomen. Dat er nooit meer een CPCT-

studie met rugnummer 04 zal spelen, beschouw ik als terecht respect naar de inspanningen die jullie in dit project hebben gestoken.

Bij het verzamelen van alle (klinische) data heb ik de nodige hulp gehad uit meerdere windrichtingen. Vooral tijdens de eerste jaren van mijn promotietraject was ik kind aan huis bij het CTC van het Erasmus MC. Hoewel vrijwel iedereen van het CTC een bijdrage heeft geleverd, wil ik Willeke Bolle, Susan Marinissen, Nelly van der Meer, Robert Oostrum, René Vernhout, en Patricia de Vos in het bijzonder danken. Gea van der Hout, Lakshmi Mani, Jennifer Samson en Wendy Vorstenbosch, jullie hebben allemaal veel werk op de afdeling verricht voor de in dit proefschrift beschreven studies, waarvoor ik jullie erg dankbaar ben. Alle stafleden en fellows van het Erasmus MC, bedankt voor jullie actieve betrokkenheid bij het benaderen van patiënten voor de studies. De mensen op alle verschillende secretariaten (G4, D3, Balie B, behandelcentra, B0zuid) bedankt voor jullie hulp bij de planning, in het bijzonder Willy Bierwith, José de Lange en Eline van Munster. Marianne Keessen en Ida van Belle, jullie hebben veel betekend voor de logistieke processen binnen het CPCT en dus ook voor het tot stand komen van dit proefschrift, veel dank daarvoor. Erik van Werkhoven en Henk Botma, dank voor jullie geduld bij het verwerken en aanleveren van de klinische CPCT-data. Nicolle Besselink en Jan Beekhuis, dank voor jullie gastvrijheid in Utrecht als ik weer eens samples kwam brengen of halen. Esther Oomen – de Hoop, dank voor je hulp en opbouwende kritiek bij het stroomlijnen van vrijwel alle statistische analyses binnen het PK-lab. Samira, jij hebt je ontfermd over alle samples die ik aanleverde voor de PG analyses. Veel dank voor je snelle reacties.

Uiteraard hoort iedereen van het PK-lab ("Translationele Farmacologie") ook in dit dankwoord thuis. Peter, alleen de metingen van midazolam en imatinib benaderen niet hoeveel farmacologische kennis van jou in dit proefschrift verwerkt zit. Dank voor alle sturing op dat gebied. Inge en Mei, jullie ook bedankt voor het werk dat jullie in alle analyses hebben zitten. Vooral van de momenten van bespiegeling op Be-462 heb ik de afgelopen jaren genoten. Patricia, we hebben nooit samengewerkt, maar wel vier jaar lang schuin achter elkaar gezeten. Bedankt voor alle gezelligheid. Bimla en Robert, dank voor jullie noeste arbeid op B0zuid. Het was altijd fijn om even bij jullie te buurten. Jacqueline,

A

194 | Appendices

dank dat je me hebt ingewerkt op de Daniel, zoals bij het opstellen van de AGP-studie, maar vooral bij de verplichte rondleiding langs het dakterras. Van onze discussies over de zin van de wetenschap en van andere zaken heb ik (meestal op dat dakterras) genoten. Annemieke en Lisette, jullie hebben me de weg gewezen op de centrum locatie. Hoewel de kamer soms wat aan de warme kant was, was het leuk om daar samen met jullie te zitten. Helaas hebben jullie inmiddels allemaal de oncologie verlaten, maar hopelijk vinden we later nog een andere manier om weer samen te werken. Roelof, dank voor je positieve inbreng op het lab de afgelopen jaren. De bourgondische derde helften (ESMO in Wenen tijdens Oktoberfest...) waren altijd een waar genoegen. Als je nog een keer wat over de sora-rifa wil weten, dan weet je me te vinden. Leni, zowel aan de sorafenib- als aan de pazopanib-studies heb jij een grote bijdrage geleverd. Dank dat je mij op weg hebt geholpen bij de klinische uitvoering van die studies. Veel succes en plezier bij de volgende stappen die je binnen de wetenschap aan het maken bent. Astrid en Evelien, een bezoek aan/van jullie hoorde bij een werkdag op de Daniel en dat heeft zeker bijgedragen aan het werkplezier daar. Bodine, Emma, Femke, Florence, Koen, Stijn en Peric, jullie zijn in de loop van de tijd het lab binnen gedruppeld. Het is jammer om straks niet meer dagelijks met jullie op het lab te zitten. Allemaal veel succes en vooral plezier de komende jaren. Hopelijk houden jullie me een beetje op de hoogte van de ontwikkelingen. Pim, Anne en Edwin, ik heb jullie mogen begeleiden bij het schrijven van jullie masterscripties, die allemaal tot een (naderende) publicatie hebben geleid. Jullie hebben me regelmatig nieuwe dingen geleerd, maar het was vooral leuk om met jullie samen te werken. Edwin, heel gaaf dat je nu doorgaat met de onderzoekslijn waar je je masterscriptie mee begon. Esther, Jaco, Nick en Wendy, dank dat jullie me geadopteerd hebben in tijden van eenzaamheid aan de overkant van de gang. Het was altijd prettig om tijdens of na de lunch even met jullie over de zin van het leven te kunnen praten.

Bijzondere dank gaat uit naar mijn paranimfen. Bart, onze studententijd stond bol van de onsuccesvolle avonturen: (licht) roeien, WECO, zanglessen, voetballen, etc. Gelukkig hebben we er wel veel plezier aan beleefd. Nadat we (gelijktijdig) afstudeerden is het allemaal wat serieuzer geworden en nu mogen we ook bijna tegelijk ons proefschrift verdedigen over bijna hetzelfde onderwerp. Dat maakt het mooi om jou als paranimf

naast me te hebben. Misschien hebben we in de wetenschap dan eindelijk iets gevonden wat we wel samen kunnen. Arjan, ik vind het geweldig dat jij ook naast me staat bij de verdediging. Vroeger stonden we vaak samen op de voetbal- of tennisbaan, wat voor mij als 2 jaar oudere broer niet altijd even goed voor mijn zelfvertrouwen was. Toen je later nog wel eens een zinnetje uit mijn schoolverslagen wilde overnemen voor die van jezelf, had ik weer even de illusie om je grote broer te kunnen spelen. Inmiddels ben je me weer ouderwets links en rechts aan het inhalen met al je opleidingen en met je eigen promotietraject. Hoewel ik me daar eigenlijk boos om zou moeten maken, ben ik vooral hartstikke trots op wat je allemaal aan het klaarspelen bent. Dounia, jij bent natuurlijk stiekem de motor achter Arjan en het is hartstikke mooi dat jij inmiddels een onderdeel van de familie bent.

Ma van Stuijvenberg en de hele schoonfamilie, dank voor de warme manier waarop ik zo snel welkom ben geheten binnen jullie familie. Ik kijk uit naar de jaren die nog komen.

Lieve pa en ma, aan jullie heb ik te danken dat ik hier überhaupt sta. Mam, jij was misschien wel de grootste drijfveer om toch geneeskunde te gaan doen. Pa, jouw onvermoeibare pogingen om me warm te maken voor de wetenschap lijken nu (hoewel *On the origin of species* nog altijd ongelezen in de kast staat) pas eindelijk tot me door te dringen. Ik ben jullie enorm dankbaar voor jullie grenzeloze steun en voor alles wat ik aan jullie te danken heb. Daarbovenop heb ik het laatste half jaar nog meer bewondering voor jullie beiden gekregen. Ik hoop nog heel lang van jullie te kunnen genieten.

Lieve Andrieske, ongeveer aan het begin van mijn promotietraject leerden wij elkaar kennen. Vanaf toen was al duidelijk dat wij bij elkaar horen en dat gevoel is sindsdien alleen nog maar sterker geworden. Ik ben enorm blij dat wij de rest van ons leven aan elkaar vast zitten en dat we komend jaar gaan trouwen. Onze toekomst samen gaat alleen nog maar mooier worden.

A

CURRICULUM VITAE

Sander Bins was born on June 21st 1987 in Voorburg, the Netherlands. After graduating from the Stedelijk Gymnasium Leiden in 2005, he studied medicine at Utrecht University. In 2011, he obtained his MD degree. For a period of four months he was employed at the department of Medical Oncology at the University Medical Center Utrecht, where he was involved in educating undergraduate medical students and in a research collaboration with the departments of Neurology and Neurosurgery. From January 2012 until December 2012, he worked as a resident at the department of Internal Medicine at the Ziekenhuis Gelderse Vallei, Ede. Next, he started his PhD program in 2013 at the department of Medical Oncology at the Erasmus MC Cancer Institute, Rotterdam. Being supervised by prof. dr. S. Sleijfer and prof. dr. A.H.J. Mathijssen, he studied intratumoral genetic aberrations within the Center for Personalized Cancer Treatment (CPCT), and pharmacokinetics of anti-cancer drugs at the laboratory of Translational Pharmacology. Starting in 2017, he will begin his medical specialist training at the Ziekenhuis Gelderse Vallei Ede to become internist, supervised by dr. R. Heijligenberg and prof. dr. H.A.H. Kaasjager.

A

LIST OF PUBLICATIONS

Bins S, Koster TD, de Heij AH, de Vries AC, van Pelt AB, Aarts MC, Rovers MM, van der Heijden GJ. No evidence for diagnostic value of Mallampati score in patients suspected of having obstructive sleep apnea syndrome. Otolaryngol Head Neck Surg. 2011;145(2):199-203

Bins S, Schellens JH, Voest EE, Sleijfer S. Geneesmiddelenonderzoek in de oncologie; Vorderingen in het genoomtijdperk. Ned Tijdschr Geneeskd. 2014;158:A6801

Bins S, Ratain MJ, Mathijssen RH. Conventional dosing of anticancer agents: precisely wrong or just inaccurate? Clin Pharmacol Ther. 2014;95(4):361-4

Verheijen RB, **Bins S**, Thijssen B, Rosing H, Nan L, Schellens JH, Mathijssen RH, Lolkema MP, Beijnen JH, Steeghs N, Huitema AD. Development and clinical validation of an LC-MS/MS method for the quantification of pazopanib in DBS. Bioanalysis. 2016;8(2):123-34

Cirkel GA, Weeber F, **Bins S**, Gadellaa-van Hooijdonk CG, van Werkhoven E, Willems SM, van Stralen M, Veldhuis WB, Ubink I, Steeghs N, de Jonge MJ, Langenberg MH, Schellens JH, Sleijfer S, Lolkema MP, Voest EE. The time to progression ratio: a new individualized volumetric parameter for the early detection of clinical benefit of targeted therapies. Ann Oncol. 2016 Aug;27(8):1638-43

Bins S, Lenting A, El Bouazzaoui S, van Doorn L, Oomen-de Hoop E, Eskens FA, van Schaik RH, Mathijssen RH. Polymorphisms in SLCO1B1 and UGT1A1 are associated with sorafenib-induced toxicity. Pharmacogenomics. 2016 Sep;17(14):1483-90

Bins S, Eechoute K, Kloth JS, de Man FM, Oosten AW, de Bruijn P, Sleijfer S, Mathijssen RH. Prospective Analysis in GIST Patients on the Role of Alpha-1 Acid Glycoprotein in Imatinib Exposure. Clin Pharmacokinet. 2016 Jul 26 [Epub ahead of print]

A

Verheijen RB*, **Bins S***, Mathijssen RH, Lolkema M, van Doorn L, Schellens JH, Beijnen JH, Langenberg MH, Huitema AD, Steeghs N. Individualized pazopanib dosing: a prospective feasibility study in cancer patients. Clin Cancer Res. 2016;22(23):5738-46
*Authors contributed equally

Yu H, van Erp N, **Bins S**, Mathijssen RH, Schellens JH, Beijnen JH, Steeghs N, Huitema AD. Development of a Pharmacokinetic Model to Describe the Complex Pharmacokinetics of Pazopanib in Cancer Patients. Clin Pharmacokinet. 2016 Aug 17 [Epub ahead of print]

Van Doorn L, Veelenturf S, Binkhorst L, **Bins S**, Mathijssen R. Capecitabine and the Risk of Fingerprint Loss. JAMA Oncol. 2016 Aug 25 [Epub ahead of print]

Bins S*, Cirkel GA*, Gadellaa-van Hooijdonk CG*, Weeber F, Nijman IJ, Bruggink AH, van Diest PJ, Willems SM, Veldhuis WB, van den Heuvel MM, de Knegt RJ, Koudijs MJ, van Werkhoven E, Mathijssen RH, Cuppen E, Sleijfer S, Schellens JH, Voest EE, Langenberg MH, de Jonge MJ, Steeghs N, Lolkema MP. Implementation of a Multicenter Biobanking Collaboration for Next-Generation Sequencing-Based Biomarker Discovery Based on Fresh Frozen Pretreatment Tumor Tissue Biopsies. Oncologist. 2016 Sep 23 [Epub ahead of print]
*Authors contributed equally

Nieuweboer AJM, de Graan AM, Hamberg P, **Bins S**, van Soest RJ, van Alphen RJ, Bergman AM, Beeker A, van Halteren H, ten Tije A, Zuetenhorst H, van der Meer N, Chitu D, de Wit R, Mathijssen RHJ. Effects of budesonide on cabazitaxel pharmacokinetics and cabazitaxel-induced diarrhea: A randomized, open-label multicenter phase II study. Clin Cancer Res. 2016 Oct 04 [Epub ahead of print]

PHD PORTFOLIO

1. PhD training	Year	Workload	
		Hours	**ECTS**
General courses			
- BROK course	2013		1
Specific courses (e.g. Research school, Medical Training)			
- CPO minicourse in methodology	2013	8	0.5
- Basic and Translational Oncology (MOLMED)	2013		1.8
- Molecular Diagnostics (MOLMED)	2013		1
- 'Integrity in Research' (Medical Ethics)	2013		2
- Genetics for Dummies (MOLMED)	2014		0.5
- Survival Analysis Course (MOLMED)	2014		1
- English Biomedical Writing and Communication (MOLMED)	2015		3
- Statistics (NIHES)	2015		5.7
- NONMEM course	2015	24	2
Seminars and workshops			
- Training OpenClinica	2013	8	0.5
- Seminar Spotlight on Individualized Medicine	2013	4	0.25
- Pharmacogenetics workshop	2014	4	0.25
- Photoshop and Illustrator CS 6 workshop	2014		0.3
- MS Excel: Advanced workshop	2014		0.4
Presentations			
- Translational Pharmacology meetings, Erasmus MC	2013-2016		2
- CPCT meetings	2013-2016		2
- NVFG symposium	2014		0.5
- CPCT symposium	2014-2016		1,5
- Young Oncologists Evening, Erasmus MC	2015		0.5
- Wengen op de Wadden	2015		0.5
- 1st International Workshop on Dose Optimization Strategies for Targeted Drugs – Focus on Oncolytics	2015		0.5
- Annual Ethics for Medics Congress	2015		0.5
- Scientific meeting, Medical Oncology, Erasmus MC	2015		0.5
- European Cancer Congress	2015		0.5
- FIGON Dutch Medicine Days	2015		0.5
- 14th International Congress of TDM & Clinical Toxicology	2015		0.5
- ASCO	2016		0.5
- JNI Bridge Meeting	2016		0.5
- ESMO	2016		0.5
- ESMO Immunology	2016		0.5
(Inter)national conferences			
- CGC kick-off meeting	2013	8	0.5

A

- NVKFB spring meeting	2013- 2016	32	2
- PhD-day Erasmus Medical Center	2013	8	0.5
- CPCT symposium	2013-2015	24	1.5
- STO annual meeting	2013	8	0.5
- Continuum Oncologie	2014, 2015	16	1
- Daniel 100 symposium	2014	12	1
- 1st International Workshop on Dose Optimization Strategies for Targeted Drugs – Focus on Oncolytics	2015	16	1
- ESMO	2015	24	2
- FIGON Dutch Medicine Days	2015	8	0.5
- ASCO	2016	24	2
- ESMO	2016	24	2
- ESMO immuno-oncology	2016	24	2
Other			
- IKNL netwerkdagen	2013	16	1
- Scientific meeting, Medical Oncology, Erasmus MC	2013- 2016	16	1
- Internship Pharmaceutical Sciences, Memphis	2015	80	5
- Wengen op de Wadden	2015	40	3

2. Teaching			
Lecturing			
- Lecture "Early phase research in oncology"	2015		0.5
Supervising practicals and excursions, tutoring			
- Tutoring first year students	2013		1.5
- Tutoring "klinische begeleiding beroepspraktijk"	2014	10	1
Supervising Master's thesis			
- Pim Laven	2015		1
- Anne Lenting	2015		1
- Edwin Basak	2016		1
Other			
- Deel BKO	2016	16	1